Development and validation of *in vitro* and *in silico* tests to predict compounds' toxicity

Inaugural dissertation

for the attainment of the title of doctor
in the Faculty of Mathematics and Natural Sciences
at the Heinrich Heine University Düsseldorf

presented by

Linda Chiappalupi
from Terni, Italy

Düsseldorf, August 2024

From the Department/Institute of Quantitative und Theoretische Biologie (QTB)
of Heinrich Heine University Düsseldorf

Printed by permission of the Faculty of Mathematics and Natural Sciences of Heinrich Heine University Düsseldorf

Examiners:

1. Prof. Dr. Oliver Ebenhöh

2. Prof. Dr. Matias Zurbriggen

Date of the oral defense: April 16th, 2025

Declaration of originality:

I hereby declare that the present thesis represents my own work, it was performed without outside help and no other sources of information have been used than those indicated. All informations that were gathered from released or unreleased sources were marked definetly as such.

Date: August 10th 2024 Signature

Content

ABSTRACT

The primary objective of this project is to develop and validate a method to predict compounds' toxicity using both *in vitro* and *in silico* models to deselect compounds with a high probability of producing significant adverse effects in the early stages of drug discovery, contributing to improve chances of success of the entire process.

Initially, the effect of parent compounds was assessed by testing 28 drugs in seven cell lines (HepG2, HK-2, MRC-5, Neuro2a, T98G, H9c2, and Jurkat), representing various body systems, including liver, kidney, lung, CNS, heart, and immune system. Compounds' cytotoxicity was assessed by measuring cells' viability by detecting ATP, an indicator of metabolically active cells. Overall, the results were compliant with the known drugs' toxicity found in previous studies and with the toxicity outcomes of the drugs in clinics.

Secondly, toxicity related to metabolites deriving from parent compounds was investigated. As the liver is the main organ for drugs' metabolism, HepaRG, a human metabolically competent liver cell line, was used to test the cytotoxicity of 7 drugs (diclofenac, acetaminophen, troglitazone, fialuridine, amiodarone, nefazodone, and simvastatin). HepaRG cells were cultured in different configurations—monolayer, sandwich, and spheroids—to compare the toxic outcomes in 2D and 3D systems. The study found that HepaRG spheroids (3D), which more closely mimic *in vivo* conditions, exhibited higher cytotoxicity than cells cultured in 2D systems (monolayer and sandwich), demonstrating that 3D cultures may provide a more accurate model for toxicity testing.

To further explore species-specific differences in drugs' metabolism, which can affect toxicity, cytotoxicity tests were performed in primary rat and pig hepatocytes, and the results were compared to those previously found in the human model HepaRG. Our findings showed that overall, in the short-term assessment, drugs induced comparable hepatotoxic effects across human and animal species. However, in the long-term assessments, HepaRG spheroids were clearly more sensitive to drugs' toxicity than rat and pig primary hepatocytes. This finding highlights that, often, animal models do not adequately replicate human metabolism and thus do not represent the ideal model to study human toxicity.

With the aim to identify metabolites responsible for toxicity, the drug nefazodone was used as a case study, and the parent compound, along with its main metabolites, NFZ-OH and NFZ-TD, were singularly tested in HepG2 and HepaRG. Our hepatotoxicity test showed, for the first time, that NFZ-OH exerts a toxic effect comparable to that of nefazodone parent compound, whereas NFZ-TD was non-toxic.

The project also introduced the use of hollow fiber bioreactors (HFS), a dynamic system able to faithfully replicate the pharmacokinetic/pharmacodynamic (PK/PD) profile of drugs *in vivo*. This system

represents a valuable model for studying the long-term hepatotoxic effects of drugs more accurately than static models previously used. Preliminary studies were designed to ensure the stability of cells within the HFS and compatibility with the drug, setting the basis for future chronic toxicity assessments.

Alongside the *in vitro* studies, two *in silico* approaches were employed for drug toxicity prediction. The first, DEREK Nexus, is a software that is able to predict the potential toxicity of drugs based on the detection of structural alerts in chemicals. While DEREK Nexus successfully predicted the hepatotoxicity of several drugs, confirming our *in vitro* findings, it failed to predict hepatotoxicity of amply documented hepatotoxic drugs such as nefazodone and fialuridine, highlighting the need for experimental validation of its predictions.

The second *in silico* approach, developed at Heinrich Heine University, used deep learning methods to simulate interactions between drugs and human liver enzymes, predicting potential impacts on liver toxicity. The model successfully identified high-affinity interactions between a subset of drugs, including amiodarone, nefazodone, astemizole, troglitazone, and trazodone, and key enzymes involved in lipid and bile acid metabolism. These interactions align with known drug-induced liver injuries (DILI), including conditions like steatosis, cholestasis, bile acid disorders, and non-alcoholic steatohepatitis. By analyzing specific drug-target interactions, this approach not only validates toxic effects observed *in vitro* but also provides insights into possible new mechanisms of toxicity.

Overall, this project shows that the integration of *in vitro* and *in silico* methods for more accurate and comprehensive toxicity predictions represents a strategic tool to increase success in early drug discovery, therefore expanding the therapeutic arsenal for treatments of patients.

ABBREVIATIONS

2D	Two-dimensions
3D	Three-dimensions
5-FU	5-FluoroUracil
5-HT2A	5-hydroxy-tryptamine receptor type 2A
ADMET	absorption, distribution, metabolism, excretion and toxicity
ALP	Alkaline Phosphatase
ALT	Alanine transaminase
AST	Aspartate aminotransferase
ATP	Adenosine triphosphate
AZT	Azidothymidine
BSEP	Bile Salts Export Pump
CCA	Cell Culture Analogue
CNS	Central Nervous System
CYP450	Cytochromes P450
DILI	Drug-induced Liver Injury
DNA	Deoxyribonucleic acid
ECM	Extracellular matrix
ELISA	Enzyme-linked immunosorbent assay
GABA	Gamma-aminobutyric acid
GSTs	Glutathione S-transferases
hERG	Human Ether-à-go-go-Related Gene
HSC	Human Stellate Cells
HTS	High throughput screening
IC_{50}	Half-maximal inhibitory concentration
LC_{50}	Half-maximal lethal concentration
LD_0	Maximal non-lethal dose
LD_{50}	Half-maximal inhibitory dose
LDH	Lactate dehydrogenase
MDR3	Multidrug resistance protein 3
MMP	Matrix metalloproteinases

MRP3	Multidrug-resistance protein 3
MRP4	Multidrug-resistance protein 4
MTT	3-[4,5-dimethylthiazol-2-yl]-2,5 diphenyl tetrazolium bromide
NAD^+	Nicotinamide adenine dinucleotide (oxidized form)
NADH	Nicotinamide adenine dinucleotide hydrogen (reduced form)
NADPH	Nicotinamide Adenine Dinucleotide Phosphate Hydrogen
NAFDL	Non-alcoholic fatty liver disease
NASH	Non-alcoholic steatohepatitis
NATs	N-acetyil transferases
NBE	New biological entity
NCE	New chemical entity
NTCP	Na/bile acid cotransporter
OAT1-2	Organic anion transporter 1-2
OXPHOS	Oxidative phosphorylation
PD	Pharmacodynamic
PGS	Poly (glycerol sebacate)
PK	Pharmacokinetics
PLGA	Poly(dl-lactic-co-glycolide)
QSAR	Quantitative structure-activity relationship
ROS	Reactive oxygen species
SAR	Structure activity relationship
SOD	Superoxide dismutase
SULTs	Sulfotransferases
TC_{50}	Half-maximal toxic concentration
TD_{50}	Half-maximal toxic dose
TI	Therapeutic index
TIMP	Tissue inhibitors of metalloproteinases
UGTs	UDP-glucuronosyltransferases
ULN	Upper limit normal
VEGF	Vascular endothelial growth factor

INTRODUCTION

1. Evolution of toxicology throughout history

Toxicology is defined as a multidisciplinary science that studies the adverse effects of toxic agents on biological systems, as well as the symptoms deriving from toxicant exposure, the mechanisms that underlie their toxicity, and the investigation of poisoning treatments.

The term "toxicology" derives from the fusion of the ancient Greek words *toxikon*, which means poison, and *logia*, which means science. Hence, a more traditional and straightforward definition of toxicology is the "science of poisons."

Toxic agents normally refer to chemicals, like drugs, although they could refer to physical agents, like radiation, or biological agents, like bacterial toxins.

Toxicology originated in the Renaissance era with Paracelsus who is considered the father founder of this science. His famous sentence "*Omnia venenum sunt: nec sine veneno quicquam existit. Dosis sola facit, ut venenum non fit -All things are poison, and nothing is without poison; only the dose makes that a thing is no poison – "*introduced for the first time in history a fundamental concept of toxicology: the dose makes the poison. In other words, any substance at sufficiently high doses can become toxic and harmful to living organisms. Indeed, any medicine we benefit from in everyday life can become harmful if administered at very high doses. Paracelsus was also the pioneer of experimental medicine, stating the essential need for animal testing to study both the toxic and beneficial effects of chemicals.

An outstanding figure in the field of toxicology was Matheu Orfila, a Spanish physician who published several treatises on the poisoning effect of substances found in the mineral, vegetable, and animal kingdom and their potential use in medicine. He used animal models, and human tissues from autopsies to elaborate a method for poisons detection (Michaleas SN et al., 2022).

Along with Orfila, Claude Bernard, a French medical doctor and author of "Lessons on the effects of toxic substances and drug," described the toxicological effects of opium, atropine, curare, and other neuroactive compounds and studied for the first time the effects of carbon monoxide in the human body (Griffin JP, 1993).

At the beginning of the 20th century, Paul Elrich introduced arsenic-based compounds to treat syphilis, and shortly after, he discovered their acute and chronic toxicological properties.

The work of all these scientists over history remarkably contributed to the development and evolution of modern toxicology.

From the second half of the 20th century, the introduction of chemicals in agriculture, farms, factories, and particularly the rising pharmaceutical industry, with the development of new medicines introduced

to the market, brought the population more and more into contact with xenobiotics. Consequently, cases of poisoning increased dramatically.

The widespread use of DDT (dichlorodiphenyltrichloroethane), a synthetic compound with potent insecticide properties, revolutionized the agriculture world in 1950. However, its success only lasted a few decades due to the severe adverse effects on humans as an endocrine-disrupting agent and its harmful impact on the environment. DDT-related risks led to its ban in 1972 (Beard J. et al., 2006).

The Minamata disease, a human neurological syndrome discovered in 1956, was revealed to be caused by mercury poisoning. For three decades, dimethylmercury, a waste product of the chemical industry, was discarded in Minamata Bay (Japan), entering the food chain through seafood consumption by the Minamata inhabitants. This environmental disaster caused over 2000 victims among the inhabitants of the Minamata area at the time (Eto K, 2000; Harata M, 1995).

Thalidomide, an anti-nausea drug commercialized at the beginning of the fifties, is probably the most ancient example of drug withdrawal from the market due to toxicity. The drug, initially prescribed to pregnant women, was associated with newborns with severe congenital abnormalities. Later, thalidomide's proved teratogenicity led to its withdrawal in 1961 (Lenz W, 1988; Hayes AN et al., 2009).

Numerous cases of toxicity have been reported throughout history. Chemicals were discovered to be responsible for human and animal poisoning, environmental disasters, or post-marketing adverse effects that led to drug withdrawals. The ones listed above only represent a few of the most famous examples.

Since the last century, all these toxicity cases and the consequent increasing research in the field of chemicals' harmful effects have shaped the history of modern toxicology and set the necessity to establish monitoring bodies and guidelines to control compounds' safety, above all in the pharmaceutical industry, in addition to food and chemical sectors.

In this scenario, many regulatory organs were instituted worldwide: EMA, established in 1995 with the aim to ensure efficacy and safety of medicines across Europe; the FDA (Food and Drug Administration), founded in the US since 1906 to protect the public health by controlling security and quality of drugs, biological products, food and cosmetics; the EPA (Environmental Protection Agency) and the NIEHS (National Institution of Environmental Health Science), responsible for regulating and conducting research on impact of environmental pollutants to human health. Along with those agencies, principal professional organizations like the SOT (Society of Toxicology) in the US, EUROTOX in Europe, and IUTOX (International Union of Toxicology) work in cooperation to advance and disseminate globally the knowledge in toxicology science. In 1990, the International Council of Harmonization (ICH) was created with the mission of unifying the actions of regulatory authorities and pharma industries worldwide with respect to the technical requirements of therapeutic agents for human use during the drug development process.

2. Toxicology in drug discovery

The development of a new therapeutic agent is a cumbersome, hugely costly, and long-lasting process that typically starts from the identification of hit compounds against a specific target to the final approval of the drug by the regulatory authorities (e.g., FDA, EMA) and its launch into the market. Other approaches for hit identification involve high throughput tests of compound libraries, using whole cells or non-specific assays, followed by the discovery of the compound's mechanism of action.

It has been estimated that the whole process requires an average of 12-15 years and an investment of around $2.6 billion (DiMasi et al., 2016). This amount has increased by 15% since 2022, as shown in a study conducted in the top 20 biopharma industries worldwide (Deloitte Report, 2023).

Conventionally, the first step of the drug discovery pipeline involves target identification and validation, where a biological molecular structure is accurately selected once it is demonstrated to have a pivotal role in the disease`s pathogenesis or progression and its modulation is proven to be effective for disease elimination. A high percentage of failures occurring at clinical stages were found to be related to an incorrect target selection, making this step crucial in the early stage of drug discovery and essential to avoid enormous capital and time-wasting (Hay et al., 2014).

Following the target selection, libraries of thousands of compounds are tested via high throughput screening (HTS) assays to select the molecules that most efficiently bind to the target. The selected compounds at this stage, referred to as hits, are considered the starting point in drug discovery. Hits are then retested to confirm their interaction with the target, and then biological *in vitro* tests are performed to define their affinity and potency. The most potent compounds enter thereafter the hit-to-lead phase, where they are characterized in terms of selectivity, off-target activity, and druggability through an initial structure-activity relationship (SAR) study. The aim here is to identify the most promising molecules that will constitute the group of lead compounds. Starting from the selected lead structures, SAR and structure-based design studies are used as tools for analog synthesis. Analogs are expected to exhibit superior potency, affinity, and physiochemical properties such as solubility and stability and possibly a lower off-target effect. During this stage, called lead optimization, ADMET properties are investigated, and the most attractive compounds identified here will be used for *in vivo* studies in the preclinical phase conducted in animal models (Keseru et al., 2006). The welfare of animals used in the preclinical phase is highly regulated by guidelines of the competent authorities such as the FDA and EMA that guarantee compliance to the 3R rule: Reduction (reduce the number of animals used for the experiments), Refinement (ensure the least pain and stress to the animal), Replacement (replace animal testing with a suitable alternative *in vitro* and/ or *in silico* assay).

Typically, the preclinical phase includes several types of studies: pharmacokinetics (PK), pharmacodynamics (PD), ADME, and toxicology studies. The main objective of the preclinical stage studies is to develop the drug formulation, test it in terms of PK and PD parameters, and finally, define

the correct dose for the First In Human (FIH) administration, which allows to proceed to the clinical phase. Besides understanding the interactions between the drug candidate and the body systems via PK and PD studies, toxicology testing in animal models is required for drug safety prediction in humans. These studies focus on the identification of tissues where toxicity occurs and comprehend *in vivo* and *in vitro* experiments concerning short-term (acute) and long-term (chronic) toxicity. While acute toxicity is evaluated after a single dose administration, chronic effects are analyzed after multiple dosage applications over a long period of time, set according to the drug and the animal model selected. Toxicity related to a new chemical entity needs to be exhaustively defined before compounds advance to clinical trials, where the first human tests will be performed.

During Phase I studies of clinical trials, single or multiple ascending doses of drug candidates are administered to a small group of healthy volunteers for PK and safety assessments. In the course of Phase II and Phase III, dose, efficacy, and toxicity studies are evaluated in patients. The main objective of Phase II trials is to examine efficacy and safety in patients, especially those with comorbidities, compared to Phase I, where drug candidates were tested in healthy volunteers. Phase II trials are crucial intermediaries where different doses and administration regimens can be tested, with the aim of selecting the best treatment condition to ensure therapeutic efficacy and an acceptable therapeutic index in Phase III studies. Data collected in Phase II will be used to design Phase III trials, where the effectiveness of the drug candidates will be confirmed, and the side effects will be monitored in a larger population of patients.

If the selected drug candidates succeed in the three clinical trial phases, they are reviewed by the regulatory bodies (e.g., FDA, EMA) for approval and finally launched into the market.

3. Principal reasons for failure in drug discovery

Drug discovery is a complex and multifaceted process, often marked by a high failure rate.

To launch a new drug into the market, up to 10.000 compounds may need to be tested. From the initial screening, approximately 10-20 normally enter the preclinical phase, and from here, only a few progress to clinical trials (Takebe T et al., 2018). Nevertheless, it is estimated that 90% of candidates reaching clinical phases will fail at this stage, making the entire journey extremely arduous (Sun D et al., 2022).

According to recent reports, lack of efficacy and lack of safety are the two principal attritions in drug discovery (Kiriiri, G.K et al., 2020; Harrison RK, 2016; Fogel DB, 2018; Hwang TJ et al., 2016). Particularly, toxicity issues account for 24% of total failures, with lack of efficacy being the first cause of 52% of total failures (Harrison RK, 2016). Strategic, commercial, and operational issues represent only minor concerns of failure (Fig.1).

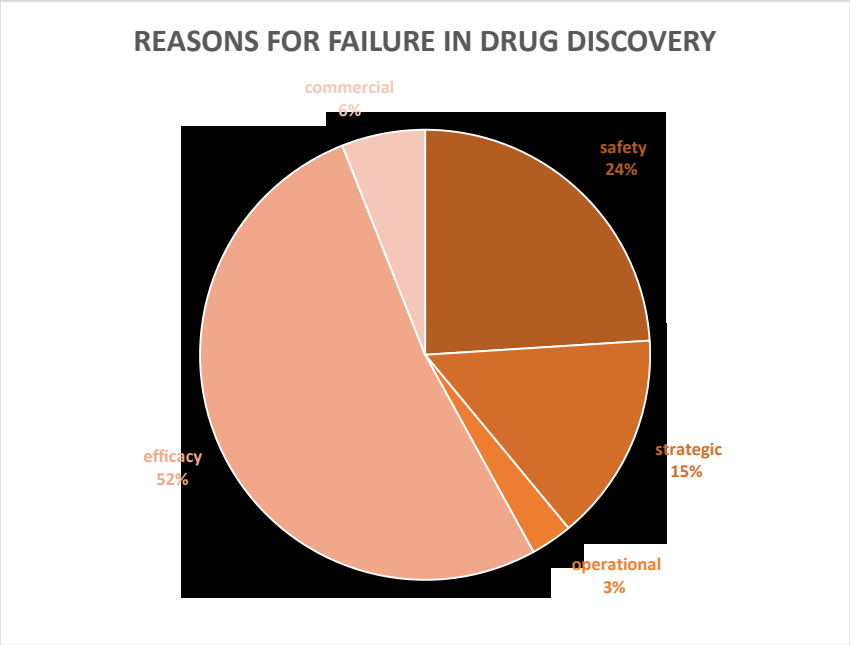

Fig.1. Causes of failure in drug discovery (Harrison RK, 2016).

A study conducted in 2014 by Cook D et al. analyzed 142 projects interrupted between 2005 and 2010 at AstraZeneca with the scope to identify the reasons for their failure (Cook D et al., 2014). All the projects selected were projects from preclinical to clinical phase II. According to this study, lack of safety was the primary cause of the project's closure in the preclinical phase and in clinical Phase I, with a percentage of 82% and 62%, while in Phase IIa and Phase IIb, toxicity issues were responsible for the 35% and 12% of projects terminations, respectively.

On the other hand, efficacy concerns accounted for only 6% of closures of pre-clinical projects and 15% of compounds' termination in Phase I. However, insufficient efficacy was the main reason for failure at later stages, leading to the closure of 57% of projects in Phase IIa and 88% in Phase IIb (Cook D et al., 2014).

The study by Cook D et al. highlights the critical challenges in drug development, emphasizing the significant role of safety and efficacy in the progression of pharmaceutical projects. These insights are crucial for the pharmaceutical industry to refine strategies for successful drug development and align with findings from other notable research in the field (Harrison RK, 2016; Watkins PB, 2011).

Although this study referred specifically to a single pharmaceutical company in a limited timeframe, it highlighted important insights that could help to better understand toxicity reasons leading to failure and thereby help to optimize the drug discovery process.

There are many reasons leading to lack of efficacy in drug discovery. One of the major issues is the poor translatability of preclinical, experimental animal models to clinical trials in humans. Many times, in fact, animal models of disease, isolated animal tissue, or animal cell lines do not efficiently replicate outcomes in human clinical trials due to species-specific differences (Olson H et al., 2000).

Another reason for inadequate efficacy is associated with the pharmacokinetics properties of the drug candidate. Compounds with unsuitable bioavailability or metabolism properties or poor distribution to the target tissue often fail to replicate promising results observed in *in vitro* experiments against the selected target.

Reduced drug efficacy can also occur when the pathogenesis mechanism, or the target, is not well-known. When these elements are not fully understood, developing effective and selective agents could be very challenging (Hingorani AD et al., 2019).

Additionally, insufficient efficacy could be related to dose problems. Often, the maximal dose tolerated in healthy tissues is not sufficient to achieve the desired therapeutic effects in diseased tissues (Sun D et al., 2022). Therefore, increasing the dose could expose the patient to the risk of toxicity. Indeed, the success of candidates depends on a precarious balance between effectiveness and toxicity that defines the benefit/risk ratio of each drug.

Toxicity is the second leading cause that hinders success in drug discovery. Often, toxicity issues cause candidates to terminate at the late stages of drug discovery, when compounds have already undergone clinical trials, and sometimes even after approval or commercialization (Fogel DB, 2018). When such discontinuations occur, all the efforts and resources invested to progress the candidates to the final phases are wasted. This highlights the importance of early and comprehensive toxicity screening to mitigate risks and reduce late-stage failures.

While efficacy properties are extensively screened in early drug discovery, safety tests are only conducted starting from the preclinical phase, both in *in vitro* and *in vivo* animal models. If the candidate accomplishes all the required safety features in animals, then toxicity will be tested in humans during clinical trials. However, the greatest percentage of compounds fail in this stage because of adverse events in humans that were not detected in animal models (Sun d et al., 2022). The key reason for this discrepancy is the inter-species difference between human and animal models, which affects the safety profile of drugs. Variations in the physiological architecture of tissues and organs' functioning account for the different pharmacodynamic effects between humans and animals, which could lead to interactions with unexpected or not predicted targets, leading ultimately to toxicity.

Also, metabolic differences between humans and animals can indeed lead to the formation of harmful compounds in humans that are not produced in animal models (Olson H et al., 2000; Clark M and Steger-Hartmann T, 2018). This discrepancy constitutes a significant challenge, as it may result in the underestimation of potential risks when translating findings from animals to humans.

Such findings indicate the importance of developing more predictive models and testing methods to determine therapeutic efficacy and adverse effects that can better simulate the human *in vivo* environment and its responses to new compounds.

4. Impact of toxicological issues in failure of compounds in drug discovery

Toxicity issues, being the second major cause of attrition in drug discovery, have been extensively analyzed with the aim of identifying the most critical factors in research and development and possibly improving the success rate of drug candidates.

Many are the safety concerns leading to compounds' discontinuation in drug discovery. Several studies highlighted the critical impact of hepatotoxicity, cardiotoxicity, and neurotoxicity as primary factors leading to clinical trial termination. According to a study conducted on 79 drug candidates that were interrupted in clinical phases (Watkins PB, 2011), safety concerns occurring in the liver, cardiovascular, and nervous systems represented the three major causes equally contributing to failure in clinical trials (Fig. 2).

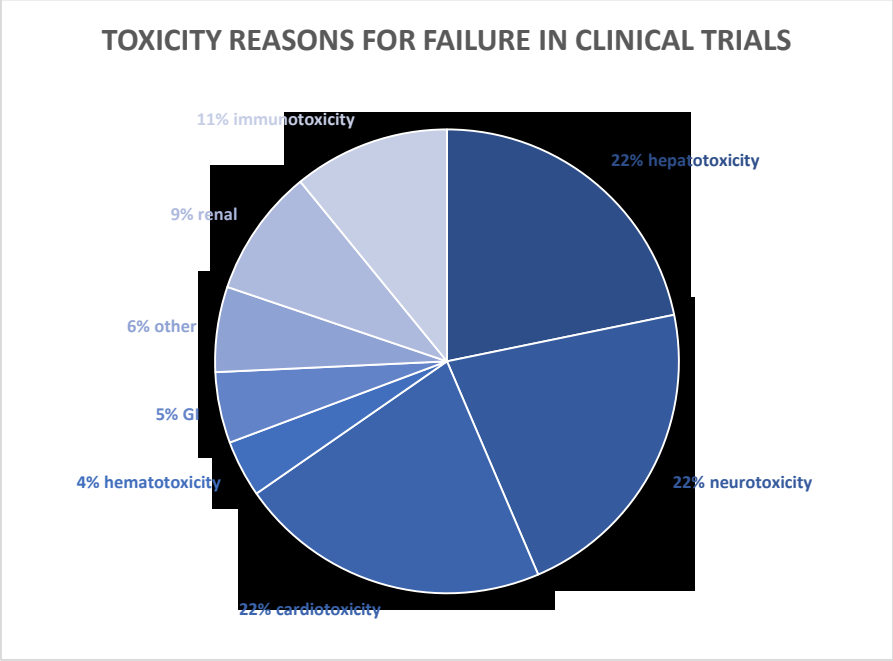

Fig. 2. Toxicity reasons for compound discontinuation in clinical phases I, II, and III (Watkins PB, 2011).

Other studies conducted years later confirmed the same outcomes, highlighting that hepatotoxicity, cardiotoxicity, and neurotoxicity are the three main reasons for projects' interruption in preclinical and clinical studies (Stevens JL and Baker TK, 2009; Cook D et al., 2014). The consistency of these results over time suggests that despite advancements in drug design and screening, toxicity remains a major hurdle.

Among cardiotoxicity issues, disturbances of cardiac electric activity such as prolongation of QT interval, ventricular tachycardia, and torsade de pointes represent major causes of potentially lethal arrhythmias that led to compounds drop in clinical trials or in the post-marketing phase (Herrmann, J, 2020).

Some inhibitors of VEGF developed for cancer therapy were discontinued in clinical trials due to toxic effects such as arrhythmias following prolongation of the QC interval as well as for hearth failure and thromboembolism (Van Heeckeren WJ et al., 2006; Dobbin SJH et al., 2021; Snider KL and Maitland ML, 2009). Some compounds belonging to the class of peroxisome proliferator-activated receptors (PPARs) agonists did not reach the market because of cardiovascular events developed in clinical trials (Nissen SE et al., 2005). Additionally, cardiotoxicity remains a serious concern in the post-approval phase, causing several drug withdrawals. Antihistaminic agents like terfenadine and astemizole, as well as cisapride, the antipsychotic drug thioridazine, and the antibiotic grepafloxacin, represent only a few examples of drugs withdrawn from the market following life-threatening cardiotoxicity issues (Gottlieb S, 1999; Ashworth L, 1997; Quigley EM, 2011; Haddad PM and Anderson IM, 2002; Cowling T and Farrah K, 2019).

Neurotoxicity, another leading cause of failure in clinical trials, manifested in multiple ways following candidates' administration. In general, principal neurotoxic effects included seizures, cognitive impairment, speech disturbances, encephalopathies, neurological degeneration, and many others. Several agents, either small molecules or biopharmaceutical products, induced severe adverse effects in the central nervous system, leading to termination in clinical phases. An anti-CD-28 monoclonal antibody-induced cytokine storm after infusion in clinical trials led to cerebral edema and intracranial pressure elevation (Suntharalingam G. et al., 2006). A fatty acid amide hydrolase inhibitor provoked cerebral hemorrhage and necrosis after administration, leading to the death of one volunteer (Kaur R et al., 2016). The monoclonal antibody pembrolizumab, approved for various cancer treatments, was associated with encephalitis in clinical trials (Feng S et al., 2017). Although, in general, well tolerated, IDH1 inhibitors, lately developed for specific cancer treatments, were often associated with neurological adverse events (Miller JJ, 2022).

Hepatotoxicity remains a significant challenge in the development of new pharmaceuticals, with a range of toxic liver effects observed in clinical trials leading to the discontinuation of some compounds. For instance, fialuridine, an antiviral drug developed to treat Hepatitis B infections, was halted in clinical phase II following severe liver failure that caused five deaths and two liver transplantations (Manning FJ, Swartz M, 1995).

In 2005, the clinical studies conducted for aplaviroc, an anti-HIV agent, were terminated after two weeks because some patients developed hyperbilirubinemia and severe hepatic cytolysis (Nichols WG et al., 2007).

During a Phase I study of an anti-inflammatory compound with an inhibitory effect against microsomal prostaglandin synthase 1 (MPGES1), four women developed severe signs of liver failure. After recognizing the significant liver damage induced by the compound, the investigation was terminated (Marumoto A et al., 2013).

Severe cases of drug-induced liver injuries (DILI) reported after commercialization led to the termination of several medications. Some of the most notorious examples include the fluoroquinolone trovafloxacin, the antidiabetic agent troglitazone, the antidepressant nefazodone, along with the anti-inflammatory lumiracoxib and the anticoagulant ximelagatran (Choi S, 2003; Graham DJ et al., 2003; Murphy EJ et al., 2003; Kaden T et al., 2023; Shi S and Klotz U, 2008). These and many other cases of discontinued drugs highlight the unpredictable nature of DILI, often occurring as an idiosyncratic event that can manifest after a drug has been marketed.

DILI has always been a bottleneck among toxicity reasons for failure in drug discovery. A study analyzing drugs withdrawn from the market between 1975 and 2007 reported that 32% of drugs were discontinued for hepatic adverse events (Stevens JL and Baker TK, 2009). Figure 3 depicts the impact of different toxicity concerns that led to drug withdrawals between 1953 and 2013 (Onakpoya IJ et al., 2016).

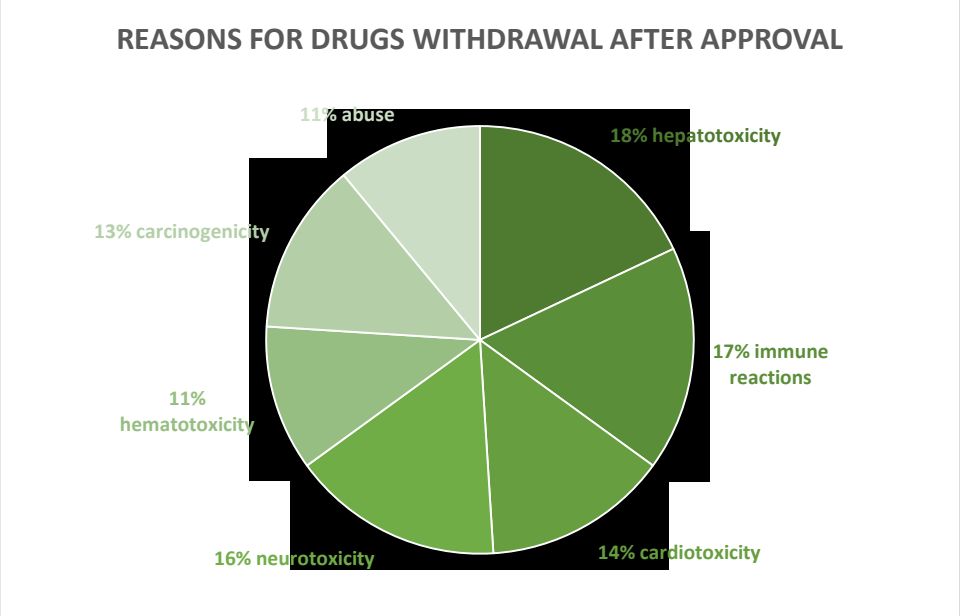

Fig. 3. Reasons for compound withdrawals in the post-marketing phase (Onakpoya IJ et al., 2016).

The study of Onakpoya et al., conducted on 462 drugs, confirmed and expanded the results of previous research, providing a broader outcome by including a larger dataset of drugs and a more extended timespan. Indeed, several studies were previously conducted to review and analyze toxicity issues related to drug withdrawals. Remarkably, hepatotoxicity resulted overall a leading reason for medicinal product discontinuation, followed by cardiovascular adverse events (Fung M et al., 2001; Siramshetty

VB et al., 2016; Babai S et al., 2016; Björnsson ES, 2015; Reuben A et al., 2010; Lasser KE et al., 2002; Stevens JL and Baker TK, 2009).

5. Drug-induced liver injury (DILI)

The essential role of the liver in the metabolism and excretion of xenobiotics -substances foreign to the body, such as drugs and chemicals- makes this organ highly vulnerable to damage. Toxic effects in the liver caused by drugs are referred to as drug-induced liver injuries (DILI). DILI incidence is estimated to be 14 to 19 cases per 100.000 people, with jaundice constituting 30% of cases (Björnsson ES et al., 2013; Sgro C et al., 2002). DILI is a challenging problem in clinics, causing more than 50% of the total cases of acute liver failure in the western world (Reuben A et al., 2010; Wei G et al., 2007). It is worth noting that paracetamol overdose is responsible for more than half of the total cases of acute liver failure and about 20% of liver transplantations in the US (Yoon E et al., 2016).

5a. Liver: the target system

The liver is the largest organ of the human body, with a cone shape and a weight of approximately 1.5 Kg in adult humans. It is involved in numerous vital metabolic reactions; indeed, it is estimated that more than 500 functions are performed by the liver (Naruse K et al., 2007). This organ is situated in the upper right-hand portion of the abdominal cavity, beneath the diaphragm, and on top of the stomach. The liver is constituted by four lobes: right, left, caudate, and quadrate, and it is perfused by two large blood vessels: the hepatic artery, delivering oxygen from the aorta, and the portal vein, delivering blood enriched with nutrients deriving from the gastrointestinal tract, spleen, and pancreas. Another fundamental vessel connected to the liver is the vena cava inferior, which collects and transports oxygen-poor blood from the liver and other organs to the heart, situated in the part of the body below the abdomen (Fig. 4).

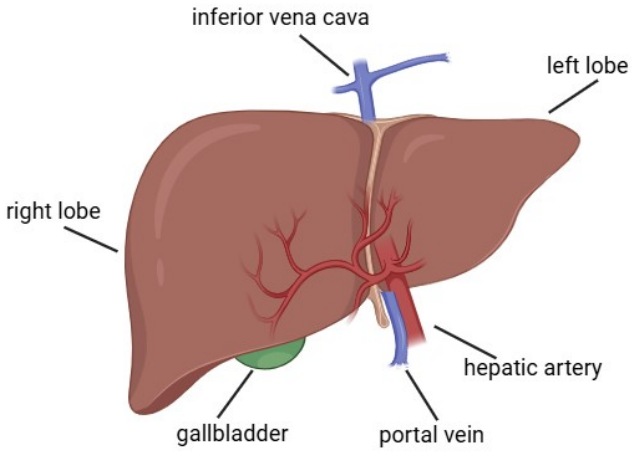

Fig.4. Anatomic structure of the liver. Two principal blood vessels perfuse the liver: the hepatic artery and the portal vein, along with the inferior vena cava are shown, as well as the liver connection with the gallbladder. Image created with BioRender.com.

The hepatic artery and portal vein subdivide in the liver into smaller and smaller branches to form capillaries, known as hepatic sinusoids, which supply the lobules, the smallest functional autonomous unit of the liver. Each lobule is made of millions of hepatocytes closely interconnected by a rich capillary network of sinusoids. While the hepatic artery and portal vein represent the inlet flow, the vena cava inferior constitutes the outlet flow.

A third system is present in every lobule, formed by the bile ducts, with the function of bile transporters. The bile, produced by liver cells and conveyed into the bile ducts in growing vessels, is concentrated in the gallbladder and finally poured into the small intestine to promote the digestion of dietary lipids. Altogether, the intrahepatic ramifications of the portal vein, hepatic artery, and bile ducts form the triad of vessels, typically located peripherally at each corner of the lobule (Fig. 5).

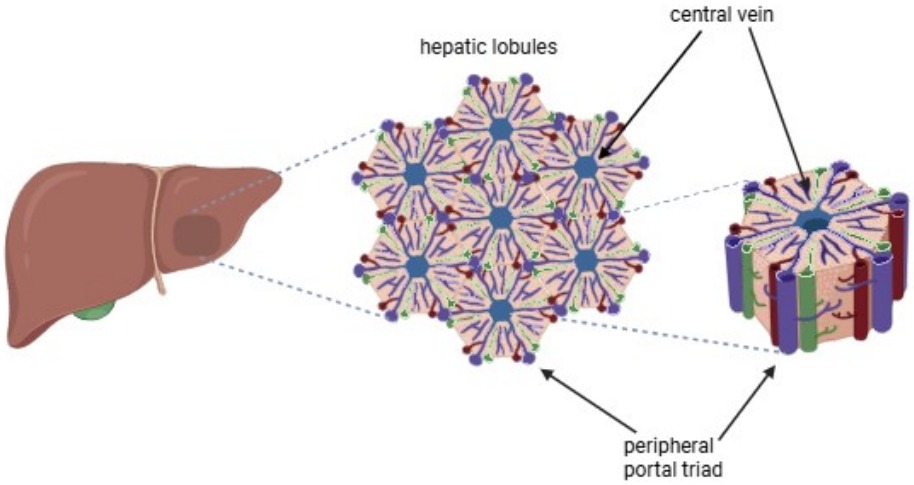

Fig.5. Schematic structure of the lobule. Inlet flows come from the hepatic artery and portal vein (blue and green vessels in the corner of the lobule), which, along with bile ducts (in green), form the triad of vessels. The centrilobular vein forming the outlet flow is also represented (Lorente S et al., 2020). Image reproduced with BioRender.com.

The liver's architecture is designed to facilitate the vital process of blood mixing. The assembly of lobules forms a porous medium through which oxygenated blood from the hepatic artery and deoxygenated blood from the portal vein can interweave. This intricate arrangement allows for the efficient exchange of substances between blood and liver cells. The positioning of lobules ensures that blood from both sources comes into close contact with liver cells, optimizing the organ's ability to regulate metabolism and remove toxins from the bloodstream.

Approximately 60% of the total cell population in the liver are parenchymal hepatocytes, cells highly specialized in metabolism and secretion, characterized by three surfaces: sinusoidal, canalicular, and

lateral. The polarity of hepatocytes is unique. Adjacent hepatocytes form with their canalicular surfaces, capillary-sized canaliculi; the sinusoidal surfaces are directed towards the endothelial cells, which form the sinusoids, and the lateral surfaces are engaged in cell-cell interactions forming basal domains connected with the extracellular matrix (Müsch A, 2013; Treyer A and Müsch A, 2013).

The remaining 40% of total liver cells consist of non-parenchymal cells, including endothelial cells, forming the largest part of this population, Kupffer cells, and stellate cells. Sinusoidal endothelial cells form the endothelium of the liver's fenestrated sinusoids. The endothelium of sinusoids is characterized by loose junctions that generate fenestrae, relatively large spaces where blood can easily flow into Disse's spaces and come into contact with hepatocytes.

Kupffer cells, the liver macrophages, reside in the lumen of sinusoids in contact with endothelial cells. They represent the first line of defense of the liver against infections and circulating toxins.

Although forming only 5% of the hepatic cell population, stellate cells, also known as Ito cells, are cells specialized in the accumulation of lipid and liposoluble vitamins such as vitamin A. Additionally, they produce components of the extracellular matrix (e.g., collagen and laminin) and are primarily involved in fibrosis development upon liver injury (Kamm DR and McCommis KS et al., 2022).

5b. Principal liver functions

The liver is a highly specialized tissue predisposed to multiple functions. The main ones include metabolism, bile secretion, reserve function, and synthesis.

The liver plays a crucial role in maintaining the body's metabolic balance. This organ regulates glucose homeostasis through glycogenolysis, glycogen synthesis, and gluconeogenesis. The excess of circulating glucose accumulates as glycogen in the liver, which is broken down in case of glucose reduction in blood. Additionally, in case of glucose depletion, gluconeogenesis can be activated from amino acid, lactate, and glycerol.

Another important function of the liver is exerted in lipid metabolism. Fatty acids from digestion are captured by the liver, where they are oxidized to produce energy or accumulated as triacylglycerols in the formation of lipoproteins.

Additionally, the liver is responsible for the amino acid catabolism, incorporating the nitrogen portion of these molecules into urea, which is formed for excretion.

Besides metabolic functions, the liver is also involved in fundamental synthetic processes. It plays a central role in the synthesis of serum proteins, with albumin being the most abundant one. Albumin's critical functions include maintaining oncotic pressure, which is essential for the distribution and balance of fluid in the body, and binding various substances, including drugs, thereby facilitating their transport

and metabolism. Furthermore, the liver synthesizes binding proteins that are crucial for the storage and transport of trace elements and vitamins, such as copper, iron, and vitamin A. Ultimately, the liver's role in the synthesis of coagulation factors, such as Factor VIII, underscores its importance in hemostasis.

As mentioned, bile is the principal product secreted by the liver. This liquid, a physiological solution containing bilirubin, bile acids, electrolytes, phospholipids, and cholesterol, is fundamental for the emulsion of dietary lipids and their absorption in the small intestine.

Additionally, the liver's reserve function is also well recognized, as glycogen, liposoluble vitamins, triglycerides, and iron accumulate here.

Remarkably, the liver is the primary body site where detoxification of xenobiotics, including drugs, environmental contaminants, and toxins, takes place. The liver is the first organ to encounter chemicals absorbed from the gastrointestinal tract into the systemic circulation, which makes this body system particularly vulnerable to their toxicity.

The delicate interplay between all the liver's metabolic pathways ensures the energy supply to vital organs and maintains the health state. Indeed, liver dysfunctions always reflect the alteration of fundamental body functions, resulting in malabsorption of nutrients, development of edema or ascites, blood clotting diseases, and metabolic disorders.

5c. Metabolism and detoxification of drugs

Metabolic transformation of drugs is essential for their elimination from the body and to terminate their pharmacological effect. In general, biotransformation reactions transform drugs into more hydro soluble molecules, easily eliminated by the body. Most xenobiotics are lipophilic substances, and as such, they are easily absorbed from the intestinal tract and conveyed to the liver. Inside the hepatocytes, these substances are converted into polar metabolites, then exported into the blood circulation or to bile through specific transporter proteins located on the hepatocytes' membrane for their excretion through the kidneys or the intestine.

Hepatic biotransformation of drugs typically includes Phase I and Phase II reactions. In some cases, Phase III reactions may also follow.

Phase I reactions are also known as the modification or functionalization reactions as they involve the introduction or exposure of specific chemical moieties in the molecules such as -OH, -CO_2H, NH_2, or -SH (Penner N et al., 2012). They include oxidation, hydrolysis, oxidative deamination, and reduction reactions mostly catalyzed by the enzymes of the CYP450 family primarily situated in the endoplasmic reticulum of the hepatocytes. The majority of CYP450 reactions are oxidations carried out using molecular oxygen O_2 and NADH or NADPH as cofactors (Guengerich FP, 2018). The principal CYP450

isoforms involved in drugs' metabolism are: CYP3A4, CYP2D6, CYP2B6, CYP2C8, CYP2C9, CYP2C19, CYP1A2 AND CYP2E1. Other major enzymes involved in Phase I reactions are flavin-containing monooxygenases (FMOs), monoamine oxidases (MAOs), xanthine oxidase (XO), alcohol dehydrogenase (ALDH), and aldehyde oxidase (AO) (Table 1).

Drug Metabolism Enzyme	Major Enzyme Isoform	Localization in Human Liver	Biotransformation Reaction
Cytochrome P450	CYP1A2, CYP2B6, CYP2C8, CYP2C9, CYPC19, CYP2D6, CYP3A4/5	Microsomes	Oxidation
Aldheyde oxidase; Xantine oxidase	AO, XO	Cytosol	Oxidation
Alcohol dehydrogenase	ALDH1 ALDH2	Cytosol	Oxidation
Uridine 5' -diphospho glucuronosyltransferase	UGT1A1, UGT1A3, UGT1A4, UGT1A6, UGT1A9, UGT2B7, UGT2B10, UGT2B15	Microsomes	Conjugation
Sulfotransferases	SULT1A1, SULT1A3, SULT1E1, SULT2A1, SULT1B1	Cytosol	Conjugation
Aldo-keto reductases	AKR1A1, AKR1B1, AKR1C1, AKR1D1	Cytosol, microsome	Reduction
FMOs	FMO3, FMO4, FMO5	Microsomes	Oxidation
MAO	MAO-A, MOA-B	Cytosol	Oxidation
N-acetyltransferases	NAT1, NAT2	Cytosol, mitochondria	Conjugation
Methyl transferases	COMT, PNMT	Cytosol, microsomes	Conjugation
Glutathione S - transferase	GST A1-1, M1-1, P1-1	Cytosol	Conjugation
amino acid conjugation enzymes	Acyl-CoA synthetase, Amino acid N-acyltransferase	Cytosol, microsomes, mitochondria	Conjugation

Table 1. Enzymes of drug metabolism, biotransformation reactions, and localization in human liver (Penner N et al., 2012).

Phase II reactions involve conjugations of the initial drug molecule or the activated drug from Phase I reactions with endogenous substrates (e.g., glucuronic acid, glycine, glutathione, glutamic) in order to render the product hydrosoluble and pharmacologically inert. Phase II reactions include glucuronidation, sulfonation, acetylation, amino acid conjugation, methylation, and GSH conjugation. They are catalyzed primarily by specific transferases such as UGTs (Uridine di-phospho glucuronosyltransferase), SULTs

(sulfotransferases), GST (glutathione S-transferase), NATs (N-acetyl transferase), amino acid conjugation enzymes and methyltransferases (Table 1).

Lately, Phase III reactions are included in drug metabolism, which refers to the transporter-mediated elimination of drugs and their metabolites through the liver, intestine, and lung cells (Almazroo OA et al., 2017). In the liver, Phase III reactions are those operated by membrane transporters transferring products of drug metabolism outside the hepatocyte or into the bile excretion system.

The expression of metabolizing enzymes and transporters is under genetic control, and there may be significant differences in metabolic capacity in relation to race and slow or rapid metabolizer status, leading to unexpected sensitivity or resistance to drugs among different individuals (Williams DP and Park BK, 2003). Also, the different expressions of metabolizing enzymes between human and animal species account for different drug effects observed between species and often for different adverse effects.

Moreover, the activity of these enzymes in an individual can be increased or decreased by the action of co-administered drugs and other substances that behave as enzymatic inductors or inhibitors. For instance, rifampicin and carbamazepine are well-known inducers of the isoform CYP3A4 (Bolleddula J et al., 2022; Fuhr LM et al., 2021). On the other hand, ketoconazole and omeprazole are known for their inhibitory activity against the same isoform (Deodhar M et al., 2020; Shirasaka Y et al., 2013). These represent just a few examples of drugs affecting CYP activity, which must be considered when drugs are co-administered. Indeed, enzyme inhibition and induction represent the major mechanism underling drug-drug interactions.

As mentioned, xenobiotics' metabolism, operated by the liver, serves to detoxify and eliminate drugs from the body. However, biotransformation can often potentiate drugs' pharmacological activity or, alternatively, activate toxicity. The drug-induced liver injury occurs when a drug or its metabolites cause hepatocyte toxicity, leading to liver damage that manifests in various forms, ranging from mild and transitory symptoms to chronic and severe life-threatening pathologies.

6. Types and mechanisms of DILI

DILI is a major cause of hepatic-related morbidity and mortality and a leading cause of drug withdrawals from the market (Garcia-Cortes M et al., 2020).

Two different types of drug-induced liver injury are overall recognized: direct and idiosyncratic. Direct DILI is due to the intrinsic toxic properties of the drug; it is characterized by dose-dependent symptoms, and it is often predictable. It generally has a short onset, typically a few days after drug administration (Hoofnagle JH and Björnsson ES, 2019).

On the other hand, idiosyncratic DILI is unpredictable, and it is caused by medications not intrinsically toxic, with a wide-ranging onset from days to years after drug administration. Despite its rarity, with an incidence rate of 1-50 cases per 100.000 exposures, idiosyncratic DILI remains a challenge due to its unpredictable nature and potential severity (Björnsson ES et al., 2013; Chalasani N et al., 2015).

Some authors include indirect hepatotoxicity as a third type of DILI, including, in this category, exacerbation or induction of liver damage due to a preexisting pathology or individual predisposition (Hoofnagle JH, Björnsson ES, 2019). This type of DILI is quite rare but much more frequent than idiosyncratic reactions, and it is also predictable in some cases.

The three types of DILI are characterized by different phenotypic manifestations.

6a. Direct DILI

The most frequent clinical manifestation of direct DILI consists of temporary elevation of liver enzymes in serum like alanine amino transferase (ALT), aspartate transferase (AST), and alkaline phosphatase (ALP) which normalize upon dose reduction or discontinuation. Normally, no jaundice is present, and other symptoms are minimal. Sometimes, serum enzyme elevation can resolve spontaneously in a process called adaptation (Watkins PB, 2005). The common pattern of direct liver injury is acute hepatic necrosis, occurring soon after the drug administration, most frequently after a single high dose or at overdose. Generally, necrosis is not accompanied by inflammation, but in severe cases, liver failure can occur and be fatal. The typical example of severe drug-induced acute hepatic necrosis is that of paracetamol. Paracetamol's misuse represents the primary cause of acute liver failure in the western world, being responsible for more than 50% of the total cases (Larson AM et al., 2005). Additionally, other drugs such as amiodarone, aspirin, and antitumor agents were found to be associated with acute hepatic necrosis (Pye M et al., 1988; Laster J and Satoskar R, 2014; Mudd TW and Guddati AK, 2021).

Intrinsic DILI is typically initiated by a direct effect of the drug or its metabolites. Compounds can directly attack mitochondria, acting as uncoupling agents and damaging the electron transport chain

(Varga ZV et al., 2015). Other drugs (e.g., chlorpromazine) acting as surfactants cause alterations of the hepatocyte's plasma membrane, leading to cell death (Morgan K et al., 2019).

Most frequently, the mechanism of hepatotoxicity involves the metabolic bioactivation of drugs. Often, reactive metabolites produced in the liver can bind covalently proteins or DNA, inactivating fundamental cell functions and causing damage and cell death. Reactive metabolites can also produce ROS with consequent oxidative stress and lipid peroxidation, which are responsible for the alteration of membrane integrity. Mitochondria dysfunction represents one of the primary mechanisms of DILI, which can be caused mainly by OXPHOS (Oxidative Phosphorylation and Electron Transport Chain) impairment, mitochondria membrane disruption, or impairment of fatty acid oxidation. In some cases, drugs can induce mitochondrial permeability transition pore opening through various mechanisms, leading to cell necrosis or apoptosis (Mihajlovic M, Vinken M, 2022). Alternatively, reactive compounds interfering with the OXPHOS chain can affect the ATP synthesis process, causing ATP depletion, thereby leading to cell death (Fromenty B and Pessayre D, 1995; Terada H, 1990).

Hepatocytes' damage can also occur following impairment of beta-oxidation of fatty acids, resulting in intracellular accumulation of triglycerides or fatty acids forming micro- or macro vesicles, a typical feature of steatosis disease (Fromenty B, 2019; Amacher DE, 2014). Several drugs, including amiodarone, acetaminophen, valproic acid, troglitazone, and tetracycline, can induce steatosis by inhibition of beta-oxidation enzymes (Fromenty B, 2019; Fromenty B et al., 1990; Aires CCP et al., 2010; Fulgencio J.P et al., 1996; Szalowska E et al., 2014).

Lactic acidosis accompanied by microvesicular steatosis is another common sign of direct liver injury induced by drugs such as aspirin, intravenous tetracycline, and linezolid (Kishor K et al., 2015; Simon TG et al., 2024; Patel V and Sanyal AJ, 2013). The mechanism of pathogenesis involves mitochondria damage with consequent impairment of aerobic metabolism. This leads to acidosis deriving from the overproduction of lactate deriving from the activation of anaerobic metabolism, along with lipid accumulation in vesicles inside the cells.

The alkylating agents' busulfan and cyclophosphamide used in the hematopoietic stem cells transplantation regimen as well as the monoclonal antibody approved for acute leukemia gemtuzumab-ozogamicin, were reported for hepatotoxicity caused by sinusoidal obstruction syndrome, a potentially life-threatening condition characterized by obstruction of sinusoids (McKoy JM et al., 2006; Jain R et al., 2017; Pramod G et al., 2020). The initial damage and subsequent loss of endothelial cells forming the sinusoids lead to inflammation, edema, and fibrin deposition within the venules' lumen, causing partial or total occlusion, hindering blood flow, and ultimately causing liver injury.

6b. Idiosyncratic DILI

The great majority of DILI cases are of idiosyncratic origin (Meunier L and Larrey D, 2019). In contrast to direct DILI, idiosyncratic DILI relies not only on the intrinsic properties of the drug but also on the susceptibility of the individual due to its genetic predisposition and other factors (Uetrecht J, 2019). For this reason, idiosyncratic DILI is individual-specific and, therefore, very challenging to predict. Also, the late onset, typically weeks or months after continuous treatment, makes idiosyncratic DILI even more difficult to recognize and to do differential diagnosis.

According to several studies, it has been established that idiosyncratic DILI has an immunological mechanism (Fontana RJ, 2013; Liu W et al., 2021; Utrecht J, 2019;). Specifically, the production of new antigens, typically modified cellular proteins or macromolecules originating from the drug or drug metabolites' binding, will induce, in susceptible individuals, an innate immune response followed by an adaptive response (Williams DP Park BK, 2003; Boelsterli UA and Lee KK, 2014; Uetrecht J and Naisbitt DJ, 2013; Fontana RJ, 2013). The activation of macrophages will stimulate T-cells and promote the adaptive immune response (Mosedale M and Watkins PB, 2017). The association of idiosyncratic DILI with specific HLA genotypes strongly supports the immune-mediated theory (Daly AK and Day CP, 2012), and the time needed for lymphocytes' activation and sufficient proliferation to mediate the immunological event could explain the prolonged latency before symptoms' occurrence. While most idiosyncratic DILI are immune-mediated, there are few exceptions suggesting that further mechanisms are involved in this type of DILI (Clay KD et al., 2006; Orman ES et al., 2011).

Conventionally, idiosyncratic DILI are divided into hepatocellular, cholestatic, and mixed, based on the induced imbalance of liver enzymes (Danan G. and Benichou C, 1993; Brennan PN et al., 2021). The most frequent clinical manifestation of idiosyncratic DILI is hepatocellular hepatitis, resembling signs and symptoms of those of viral hepatitis, with significant serum ALT elevation (5 times or more the Upper Limit of Normal-ULN), inflammation and cellular (eosinophils) infiltration. This type causes 11-15% of cases of acute liver failure in the western world (Reuben A et al., 2010; Wei G et al., 2007). The evolution of hepatocellular hepatitis into chronic hepatitis is rare. However, it can occur if the drug is continued for a long period of time. In such cases, autoantibodies are produced. Several drugs like isoniazid, nitrofurantoin, and diclofenac were reported to cause hepatocellular liver injury by idiosyncrasy mechanism (Schmeltzer PA et al., 2015; Metushi I et al., 2016).

Cholestatic hepatotoxicity, a condition characterized by the obstruction of bile flow, can lead to various symptoms and complications. The elevation of alkaline phosphatase (ALP) levels, typically not exceeding twice the upper limit of normal (ULN), is one of the diagnostic markers for this condition. The underlying cause is often the damage to the bile ducts, which can result from certain medications. A drug often associated with cholestatic hepatitis is the commonly prescribed antibiotic amoxicillin-

clavulanic acid (Beraldo DO et al., 2013). While symptoms like jaundice and itching are common, severe cases may lead to complete bile duct disruption.

The mixed pattern of liver injury is characterized by both histological signs of cholestasis as well as hepatocellular damage. Notorious prescribed drugs associated with mixed hepatotoxicity include antibiotics of fluoroquinolones and macrolides families and the anti-epileptic phenytoin and carbamazepine (Chalasani N et al., 2015; Orman ES et al., 2011; Martinez MA et al., 2015; Chalasani N et al., 2022). Typically, the mixed type of idiosyncratic DILI has a benign prognosis, and it rarely evolves into liver failure.

It is worth noting that, overall, antibiotics and antiepileptics account for more than 60% of the total cases of idiosyncratic DILI (Kaplowitz N, 2005; Chalasani N et al., 2015).

6c. Indirect DILI

Indirect DILI is a condition not due to the intrinsic properties of the drug nor to its immunogenicity. Indirect DILI encompasses liver conditions triggered by a secondary effect of the drugs. For instance, fatty liver disease can result from drugs affecting triglycerides accumulation, like lomitapide, or from the insulin-resistance induced by chronic administration of glucocorticoids (Alonso R et al., 2019; Rahimi L et al., 2020). Acute hepatitis can occur following anticancer therapy with drugs like imatinib or iplimumab (Aliberti S et al., 2009; Kleiner DE and Berman D, 2012). There is evidence that therapy with tumor necrosis factor antagonists is associated with marked hepatocellular injury triggered by an autoimmune mechanism (Ghabril M et al., 2013).

Differently from idiosyncratic reactions, which are individual-specific and drug-specific, indirect DILI is a common reaction regarding an entire class of medications.

6d. Spectrum of pathologies deriving from DILI

DILI encompasses a wide range of hepatic manifestations, from asymptomatic conditions to severe liver pathologies, including acute/chronic liver failure, steatosis, hepatitis, vascular damage, cholestasis, and others. Although most injuries resulting from the toxic drug's effect occur in hepatocytes, other liver cells can be involved, including cholangiocytes, stellate cells, and endothelial cells. Depending on the cell type affected, different pathologies can originate (Fig.6, Suh JI, 2020).

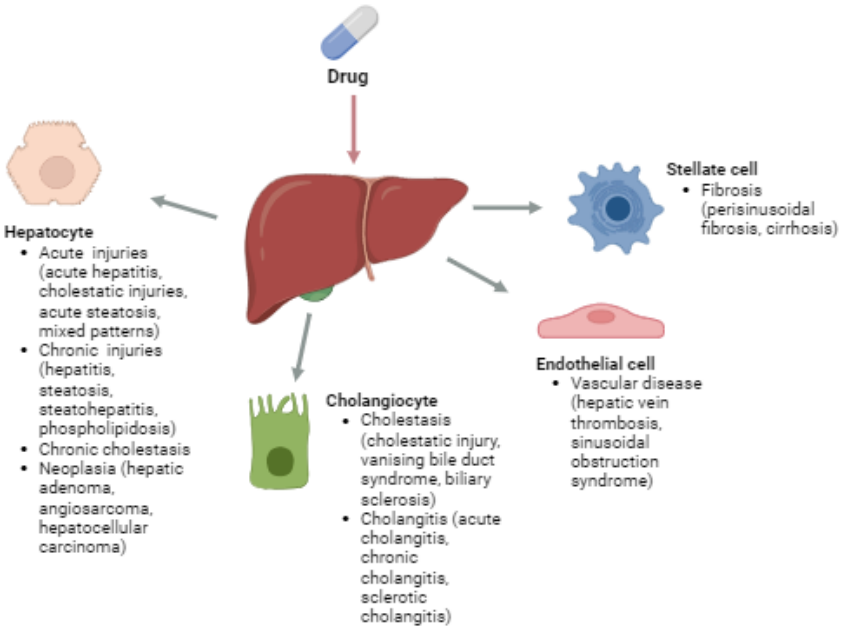

Fig. 6. Spectrum of DILI. Drugs can cause several liver diseases ranging from asymptomatic conditions to fatal liver failures. Depending on the liver cell type involved in DILI (hepatocytes, stellate cells, cholangiocytes, endothelial cells), different pathologies can manifest (Suh JI, 2020).

A common classification of DILI is based on the disease's onset. Typically, acute liver injuries are referred to as those recovering within six months. However, if the pathology persists for more than six months, it is defined as chronic DILI (Suh JI, 2020).

Liver failure represents the most common manifestation of DILI, accounting for approximately 50% of the total liver failure cases requiring transplantation (Larrey D, 1995).

Acute liver failure results from severe and rapid damage of the hepatocytes. Paracetamol is the first cause of acute liver failure, followed by other prescription drugs and herbal supplements, the latter representing the second major cause (Stravitz RT and Lee WM, 2019). Direct toxicity (toxic paracetamol by-products) or immune-mediated mechanisms (idiosyncratic DILI) induce hepatocellular necrosis or apoptosis, impairing the liver's vital functions. Although acute liver failure has, in general, a favorable prognosis after treatment discontinuation, in some cases, it can progress into chronic failure necessitating transplantation or be fatal.

Cholestasis is a condition characterized by bile stagnation in the liver following a marked reduction of bile flow due to hepatocytes' function impairment. The sudden decrease in bile flow within the liver can lead to the accumulation of bile acids and toxins within the hepatocytes. Some drugs can induce cholestasis by direct inhibition of bile acids transporters (e.g., BSEP, MDR3, MRP3, MRP4) or indirectly by dysregulating the transporters' expression or localization within the hepatocyte (Yang K et al., 2013). In some cases, DILI can cause a chronic form of cholestatic hepatitis, which persists for a

prolonged period after discontinuation of the drug. This condition can lead to irreversible liver damage and progression to liver cirrhosis.

Steatosis, or fatty liver disease, is the consequence of lipids accumulation within the hepatocytes in micro- or macro vesicles. Drugs like corticosteroids, amiodarone, methotrexate, and tamoxifen were associated with steatosis (Amacher DE and Chalasani N et al., 2014). The principal mechanism involved in the pathogenesis of fatty liver disease relies on beta-oxidation and oxidative phosphorylation impairment in hepatic mitochondria. The reduced capacity of fatty acid breakdown induced by prolonged exposure to steatogenic drugs leads to fatty acid accumulation and ultimately to ATP depletion. In some instances, steatosis, if accompanied by inflammation and cell damage, can progress into non-alcoholic steatohepatitis (NASH), characterized by lobular hepatitis, inflammatory cell infiltration, and ultimately collagen deposition (Amacher DE and Chalasani N et al., 2014).

If endothelial liver cells are injured, pathologies like sinusoidal obstruction syndrome or vascular thrombosis can occur. As mentioned, the impairment of blood flow, oxygen delivery, and nutrient supply to hepatocytes results in ischemic injury or necrosis.

The prolonged use of drugs such as minocycline, methyldopa, infliximab, and phenytoin was associated with cases of autoimmune hepatitis, a disease involving the attack of liver cells by the immune system, causing inflammation and liver damage. Although the exact cause of autoimmune hepatitis is not fully understood, it is believed to involve a combination of genetic, environmental, and immunological factors (Harmon EG et al., 2018; Czaja AJ, 2011; Jenkins A et al., 2021).

Hepatic fibrosis is the liver response to persistent insults, including chronic drug exposure. The deposition of collagen and other extracellular matrix proteins is the initial event of fibrosis, resulting in the alteration of the liver tissue and, thereby, of its vital functionality (Mormone E et al., 2011). A key process in hepatic fibrosis initiation is the activation of stellate cells and their consequent transformation into myofibroblast-like phenotype. These transformed cells exhibit an increased secretion of collagen and other ECM proteins, which contributes to fibrosis progression (Garbuzenko DV, 2022).

7. Strategies for DILI identifications in drug discovery

Toxicity evaluation of compounds is a critical step in drug discovery. Determining accurate toxicity in the initial phases of the process is necessary to prevent failures in clinical trials. Given that hepatotoxicity represents a leading cause of attrition, the prediction of liver adverse effects during the early development of novel agents is fundamental to prevent late-stage attritions and severe adverse reactions in the post-marketing phase.

In general, toxicological studies can be carried out using different models: *in vitro*, like cell cultures or subcellular fraction; *in vivo*, using animal experimental models; *ex vivo*, in tissues or organs directly

isolated from animals and *in silico*, with the aid of computational provisional tools or mathematic models. Finally, epidemiological studies conducted in clinical trials represent the in vivo evaluation of toxicological effects in humans. Each of the above-mentioned models belongs to a specific step of the drug development process. However, whereas efficacy and potency are extensively studied in early drug discovery, in this phase, few tests for toxicity evaluation are performed, like genotoxicity tests performed in bacteria strains. Toxicity evaluation of compounds is primarily assessed in animal models starting from the preclinical phase.

Several studies highlight the poor capability of animal models in predicting human toxicity. Indeed, animal models often fail to detect adverse reactions of compounds in humans, which progressing in clinical trials could expose volunteers and patients to unknown toxic effects (Dirven H et al., 2021; Van Norman GA, 2019). A comparative study conducted by Olson et al. in 2000, which collected data from 150 compounds, showed that rodent and non-rodent preclinical models only detected approximately 50% of the total human liver injuries induced by these drugs (Olson et al., 2000). Another study, analyzing the capability of animal models to identify toxicity causes for withdrawals of 43 drugs, reported that preclinical tests were able to detect only 19% of 93 severe adverse reactions (van Meer PJ et al., 2012). Remarkably, there are several examples of drugs that caused serious toxicological problems in humans that were found to be safe in animal models. A striking case was that of thalidomide, which caused numerous cases of phocomelia, while its teratogenicity had not been found in tests performed on different animal species (Brook CG et al., 1977; Cuthbert R and Speirs AL, 1963). The TGN1412 antibody caused acute severe complications during Phase I studies. During Phase II, the antiviral drug fialuridine induced severe liver failure that led to 5 deaths and two liver transplantations (Suntharalingam G et al., 2006; Attarwala H, 2010; Manning FJ and Swartz M, 1995). However, all these serious adverse effects were not previously detected during preclinical testing. This stresses the necessity of having a system that can effectively detect the toxicity of NCE in the human species.

Recent advancements have seen a shift from traditional animal models to more refined human *in vitro* cell-based models, which offer multi-parametric endpoints for better prediction of human toxicity (Walker PA et al.,2020).

Being hepatotoxicity the major concern among toxicity issues, often causing termination of projects in drug discovery, pharmaceutical industries along with academia are directing hepatotoxicity research towards the development of *in vitro* systems capable of resembling the *in vivo* human liver microenvironment to achieve a more reliable toxicity prediction.

The examination of the most common *in vitro* systems developed so far is important to analyze their advantages and disadvantages, and it will help to understand the progressive evolution towards the most sophisticated and reliable ones.

7a. In vitro systems for toxicity detection of compounds

Monolayer cultures, constituting the conventional 2D cellular model, are widely used in cell biology and drug discovery. Typically, in such systems, cells are grown on a flat plastic surface, like a flask, and adhere to it, forming a single cell layer. Monolayer cultures provide a simplified and easy system for studying basic cellular processes, including cell proliferation, differentiation, and response to external stimuli. In such systems, cells are in contact with a homogeneous environment with uniform exposure to nutrients and other soluble factors present in the culture medium, ensuring uniform cells proliferation. On the other hand, the homogeneous access to oxygen and nutrients does not resemble their natural gradient *in vivo*. For their ease of use and relatively low-cost, monolayer cultures are widely applied in high-throughput screening assays, allowing rapid evaluation of numerous compounds or different experimental conditions. Indeed, monolayer cultures are often used in drugs' screening for toxicity during the preclinical phase, providing a useful model for the evaluation of compounds' effects on cellular proliferation, apoptosis, or other cellular endpoints. Despite the many advantages offered, monolayer cultures have limitations. In such systems, cells are flattened; therefore, their three-dimensional morphology and polarity are lost. This leads to a less physiological growth environment with limited intercellular interactions. Monolayer cultures also lack interactions with the extracellular matrix (ECM) components, which are crucial to regulating several functions. Components of ECM, like integrins and proteoglycans, are key signaling mediators, thereby affecting cell proliferation and cell fate. Additionally, ECM, acting as a reservoir for growth factors, drives cellular differentiation (Chen SS et al., 2007), and it is the essential substrate for cell migration (Kim SH et al., 2011).

Ultimately, the bidimensionality of monolayer systems limits cells' growth and cells' diffusion, which should be achieved instead in a three-dimensional space (Charwat V and Egger D, 2018). For these limitations, monolayer cultures do not fully recapitulate the complex *in vivo* microenvironment and tissue architecture. Therefore, cellular responses to drugs and external stimuli can be biased in such systems.

In an attempt to reduce the limits of monolayer cultures and to better simulate cellular behaviour *in vivo*, several strategies have been used, and more sophisticated cellular systems have been developed, thanks to the advanced *in vitro* techniques currently available.

For instance, the sandwich culture technique, introduced for the first time in 1989, is a bidimensional system where cells are seeded between two layers of extracellular matrix (e.g., collagen, Matrigel, fibronectin). In such systems, cells retain their natural morphology and polarity (Dunn JC et al., 1989). Originally developed to culture rat hepatocytes, which struggled to survive in conventional 2D monolayers, the sandwich configuration allows for relatively long-term cultivation. Moreover, it facilitates essential interactions between cells and their surrounding matrix, improving signalling and functionality.

Sandwich systems are particularly suitable for hepatocytes culture. The polarity of the hepatocyte plays a crucial role in the correct functionality of the liver tissue, as the metabolic and secreting functions of the liver rely on the polarized epithelium of the hepatocyte. Indeed, concerning the lobule architecture, hepatocytes form with their apical membrane, the bile canaliculi network, and with their basal membrane, the sinusoid network. Hepatocytes cultured in sandwich configuration retain their polarity expressing specific transporters in each of those membranes, representing, therefore, a reliable tool to study liver functionality and response to drugs' insults (Bi YA et al., 2006; Ziegerer C et al., 2016; Yang K et al., 2016). Moreover, these systems provide culture for extended periods compared to monolayer systems, allowing drugs-toxicity assessments at longer times.

Another remarkable application of sandwich culture was its use in the establishment of hippocampus neuronal cultures that enabled the visualization of neurites' interactions (Brewer GJ and Cotman CW, 1989).

Although sandwich culture mimics more closely than 2D monolayer the *in vivo* environment, it still has some bottlenecks. The major limitation of this system is the cellular de-differentiation that results in a reduced functional capacity and sensitivity to the effect of drugs, already seen after 24 h of culture (Bell CC et al., 2018). Indeed, studies showed altered protein expression already after two weeks of culture.

Moreover, poor cell-cell interaction constitutes another important limitation of these cultures, which is responsible for altering cell behaviour and impaired ability to respond to stimuli (Duval K et al., 2017).

Sandwich cultures can be considered pseudo-3D systems as they do not completely simulate the complex *in vivo* system. Therefore, to enhance predictability in drug discovery, more advanced three-dimensional culture systems have been developed.

Cells' growth and interaction in three-dimensional models allow to recapitulate more closely the *in vivo* microenvironment. For this reason, such systems gained lately more and more importance in cell biology and drug discovery, representing a bridge between *in vitro* and *in vivo* models, and their use has increased to study physiology, pathology, and tissue response to drugs (Urzì O et al., 2023; Langhans SA, 2018). Compared to bidimensional systems, 3D cultures offer increased cell-cell interaction and cell-ECM interactions, which are established while cells retain their spatial organization and polarity, better mimicking the *in vivo* architecture of a tissue. The three-dimensionality affects proteins and receptor organization on the cell's surface, thereby influencing cell signalling, communication, and processes (Wanigasekara J et al., 2023). Additionally, in 3D systems, a gradient of oxygen and nutrients is spontaneously generated, as the access to them is reduced proportionally towards the inner part of the culture (Griffith LG and Swartz MA, 2006).

Several strategies have been developed for three-dimensional cultures, some of them involving scaffolds, whereas others are scaffolds-free, like cell aggregates (e.g., spheroids). In general, hydrogels are used as scaffolds, which are made of collagen, fibronectin, hyaluronic acid, Matrigel®, and other

proteins of the natural ECM. Also, biodegradable polymers have been included, like poly(dl-lactic-co-glycolide) (PLGA) and poly(glycerol sebacate) (PGS) as a scaffold for 3D cultures (Cardoso BD et al., 2023). Besides the mechanical support function for cells, the ECM acts as a repository for grow factors, hormones, and active mediators promoting cell proliferation and differentiation, and influencing several biological behaviours (Cukierman E et al., 2001). It has been described how the presence of ECM in 3D cultures not only increases specific gene expressions that are not expressed in 2D cultures but also induces cells' deposit and remodelling of their own ECM as it happens *in vivo* (Frantz C et al., 2010).

Moreover, the mechanical properties of the ECM are key in cell migration occurring through mechanotransduction, a process starting with the mechanical stimulation of integrins and ion channels-mediated pathways, leading to control of nuclear transcription (Saraswathibhatla A et al., 2023).

The introduction in the last decades of the electrospinning technique (Xue J et al., 2019) allowed the manufacturing 3D scaffolds for cell culture made of tightly woven nanofibers that faithfully mimic the structure of the natural ECM, providing an ideal environment for cell culture (e.g., BioSpun™). The specific porosity and uniformity of these membranes ensure that cells retain their correct three-dimensional morphology, which is crucial to display the natural organization of the membrane's receptors. This is essential to simulate the real drug-target interaction and the consequent cell response.

Spheroids are the simplest three-dimensional model for cell culture, introduced for the first time by Sutherland et al. in 1970 to study survival after radiation of solid tumour cultures (Sutherland RM et al., 1970). Spheroids are self-aggregation of one or multiple cell types, typically generated under centrifugal force in low-attachment plates, characterized by the absence of a support scaffold. Another method for spheroids formation is the hanging drop technique, where a drop of cell suspension is pipetted into a plate lid. By inverting the lid, the superficial tension and the gravity force promote cells' aggregation. In the method called liquid overlay, cell aggregation is induced by continuous rotation using a shaker (Białkowska K et al., 2020).

In the formation of spheroids, cadherins, and integrins are the proteins that play a major role. Particularly, three stages in spheroids formation have been identified. The first involves the formation of loose aggregation through ECM fibers, allowing anchorage of integrins; the second, in which enhanced cell aggregation is mediated by upregulated E-cadherins; and the last, consisting in the establishment of strong homophilic interactions between E-cadherins, responsible for the increasing compactness and transition from irregular to round-shape spheroids (Lin RZ et al., 2006).

Spheroids represent the most common model for *in vitro* tumour as they accurately emulate the key feature of the tumour tissue, characterised by highly proliferating cells in the outer layer and hypoxic, necrotic tissue in the inner space (Nunes AS et al., 2019). Therefore, spheroids find large applications as tumour models in cancer research to study tumour microenvironment signalling, and factors

implicated in drug penetration and accumulation, which ultimately serve to assess the antitumor efficacy of drugs for screening and development of new therapies (Pinto B et al., 2020).

For their relatively simple creation, handling, and reasonable costs, spheroids offer the advantage of being amenable for high throughput screening of compounds' toxicity in drug discovery.

More complex than spheroids are organoids, 3D *in vitro* models mimicking structures and function of specific *in vivo* tissues. They derive from stem cells, like embryonal, adult, or induced pluripotent stem cells subjected to directed growth conditions (McCauley HA and Wells JM, 2017; Spence JR et al., 2010; Takasato M et al., 2015). The peculiarity of such models is the self-organization, the ability to auto-organize, forming complex 3D structures containing several differentiated cell types recapitulating the functional characteristics of specific organs (Lewis A et al., 2021). Organoids are increasingly being used in drug discovery to test the potency and toxicity of compounds as their physiological similarity with *in vivo* models provides a relevant and accurate prediction of drug-response and insights into the mechanism of action (Matsui T and Shinozawa T, 2021).

Conventional 3D systems described so far, like organoids and spheroids, are static models as they are in contact with a static medium but do not include systems that recapitulate blood flow like in *in vivo* conditions. Such systems do not consider, therefore, nutrients, oxygen, and waste fluctuations over time, nor do drug concentration changes. Furthermore, they do not consider shear stress, which can affect cell functions in several ways. Cells cultured under continuous flow are subjected to a mechanic force that can stimulate cells, affecting ion channels activation, gene expression, and polarization, therefore accelerating proliferation, protein expression, differentiation, and cell signalling (Fois CAM et al., 2021; Huang Y et al., 2021; Chistiakov DA et al., 2017; Espina JA et al., 2023; Tsaryk R et al., 2022). As static models do not provide vascular perfusion, interstitial flow, and circulation of immune cells, ADME of drugs is not accurately reproduced, and therefore, neither is their PK/PD profile. Hence, testing the efficacy and toxicity of drugs can lead to erroneous outcomes (Ingber DE, 2022).

To address the limitations of static 3D models and make them more capable of resembling the physiology of the human body, dynamic cell culture systems have been developed in the last decades. One of the most revolutionary 3D dynamic culture models is the organ-on-a-chip, developed thanks to the cooperation between cell biology and bioengineering studies.

The first idea of a microscale organ traces back to 2004 when Shuler and colleagues developed the cell culture analogue (CCA), a microscale device consisting of multiple chambers with mammalian cells communicating through a network of channels, which can be considered the precursor of the current organ-on-a-chip (Sin A et al., 2004; Viravaidya K et al., 2004).

The term organ-on-a-chip was introduced later by Dr. Donald Ingber, the Founding Director of the Wyss Institute at Harvard University (Boston), who developed a microdevice to recreate tissue-tissue interfaces essential for the organ function, as such, the human lung (Huh D et al., 2010).

Organ-on-a-chip are microfluidic devices providing miniature tissues cultured in a plastic support, that can recapitulate physiological and pathological functions of a human organ. Typically, mammalian cells are cultured within chambers interconnected by micro-channels where media is continuously flowing, reproducing the circulatory system. Such technology, in contrast to the traditional static models, which use a single cell type, provides connection and communication between different cell types, to recapitulate the complexity of the entire organ, which is the result of several functions specifically carried out by a heterogeneous population of diverse cell types (Mertz DR et al., 2018). Organ-on-a-chip systems provide precisely a controlled cellular microenvironment through the simulation of nutrients and oxygen gradients, continuous perfusion shear stress, and mechanical cues, leading to longer cell viability compared to that of static 3D models (Białkowska K et al., 2020).

Organ-on-a-chip are used to model the functionality of several body systems including lung, heart, liver, kidney, bones, skin, brain and intestine (Huh D et al., 2010; Zhang YS et al., 2016; Ho C et al., 2016; Jang KJ et al., 2013; Mansoorifar A et al., 2021; Zoio P et al., 2022; Bang S et al., 2019; Xiang Y et al., 2020). Additionally, interconnecting different organs-on-a-chip, multi-organ- or even body-on-a-chip have been recently developed to study multiple organs interplay in physiological processes or in the pathogenesis and progression of diseases, such as the metastatization process in cancer (Park SE et al., 2019; Esch MB et al., 2014; Sung JH et al., 2019).

Organ-on-a-chip finds several applications in research besides the faithful reproduction of organ physiology. Indeed, they are used to model human disorders, reproduce interactions between different organs, and study human response to drugs, chemicals, or pathogens. Interestingly, the accurate mimicry of the liver tissues achieved by the co-culture in the liver chip of primary human hepatocytes, sinusoidal endothelial cells, and Kupffer cells allowed to reproduce liver-specific functions, like Phase I and II reactions, accurately replicating PK parameters found in *in vivo* human tests (Sarkar U et al., 2015). A liver chip was used to demonstrate drug-drug interactions by its capability to modulate CYP3A4 enzymes under the effect of different agents (Long TJ et al., 2016). Ultimately, an outstanding application of liver chips is in the evaluation of drugs' hepatotoxicity. By the microscale reconstruction of the sinusoid circulation, drugs' transportation through the liver endothelium can be simulated, as well as their metabolism (Lee PJ et al., 2007). Additionally, species-specific liver toxicities were revealed by using hepatocytes isolated from dogs, rats, and humans, highlighting the potential of such *in vitro* systems to overcome the limitations of preclinical animal models in hepatotoxicity prediction (Jang KJ et al., 2019). According to a recent survey, the replacement of animal models with *in vitro* organ-on-a-chip for DILI identification could bring significant economic benefit to pharmaceutical companies and would also align with ethical requirements related to the use of animal models in drug discovery research (Ewart L et al., 2022).

Despite 3D cell culture systems offer a more physiologically relevant environment for studying complex biological processes, they do have challenges. They often lack reproducibility due to the intrinsic

variability within each 3D structure, which can lead to difficult standardization of testing and difficult interpretation of results (Khafaga AF et al., 2022). On the other hand, the simplicity of 2D cultures facilitates the achievement of reproducible results and easy standardization, although they are far from emulating the *in vivo* tissue. Furthermore, 3D cultures often require more resources, both in terms of time and cost, and they necessitate higher expertise than their 2D counterparts. However, the potential of 3D cultures to fill the gap between *in vitro* and *in vivo* testing in drug discovery continues to drive research in this field.

7a.i. Cell type selection for toxicity assessments

Primary cells are considered the gold standard for ADME and toxicity studies, as they retain the characteristics of the real tissues; therefore, their responses to drugs and chemicals closely mimic those observed *in vivo* (Richter M et al., 2021; Eglen R and Reisine, 2011). Unlike tumour cell lines, when primary cells are subjected to toxic drugs, they undergo apoptosis or necrosis, depending on the damage. However, primary cells undergo dedifferentiation when cultured *in vitro,* losing their characteristic functionality (Hu C and Li L, 2015; Heslop JA et al., 2017). Therefore, cell lines commonly used often derive from cancer phenotypes, ensuring in this manner unlimited replicability, high reproducibility of results, and easier handling (Gillooly JF, et al., 2012). However, some drawbacks need to be considered. For example, due to their tumor derivation, processes of cell death are here altered and, therefore, can jeopardise the toxicity outcomes (Wilding JL and Bodmer WF, 2014; Mirabelli P et al., 2019; Kaur G and Dufour JM, 2012).

Moreover, another important factor that must be considered, especially when liver toxicity is studied, is the different metabolic capacities expressed by different cell types. For instance, the hepatoma cell line HepG2, despite the advantage of unlimited proliferation over numerous passages, does not accomplish the metabolic requirements for the accurate detection of drugs' toxicity (Yokoyama Y et al., 2018). HepG2 express indeed a very low biotransformation capacity compared to primary hepatocytes; thereby, drugs are not adequately activated or detoxified, and this can affect the toxicity outcomes (Westerink WM and Schoonen WG, 2007, a, and b). A good compromise is reached with the HepaRG, an engineered cancer cell line, expressing the great majority of liver metabolizing enzymes and at the same time with the indefinite proliferative features of cancer cells (Guo L et al., 2011; Seo et al., 2019), allowing in this way to have in a single cell type both the principal advantages of primary hepatocytes and cancer-derived liver cell lines.

Given the poor translatability of toxicity outcomes across different species, the choice of the species where the assays are going to be performed also plays a crucial role. For example, if the final goal is liver toxicity evaluation in human species, then human hepatocytes-based models are usually preferred

to animal hepatocytes' models, like mice and rats, although rodent-based models are still commonly used.

7a.ii. Assays and parameters for drugs cytotoxicity evaluation

The capacity of a compound to induce cell damage by impairment of fundamental structures or living functions is referred to as basal cytotoxicity, a concept introduced by Dr. Biorn Ekwall, a distinguished Swedish toxicologist who made a fundamental contribution to the history of cellular toxicology. In 1983, he formulated the basal cytotoxicity concept based on the observation that 80% of a battery of compounds showed the same toxicity *in vitro* and *in vivo* (Ekwall B, 1983), suggesting the idea of basal cytotoxicity as the agents provoked a similar lethality by interfering with essential functions, common to diverse cell types.

Ekwall demonstrated for the first time the reliability of cellular *in vitro* tests in the assessment of toxicity of chemical compounds in humans. Specifically, Ekwall undertook an outstanding project, the MEIC (Multicentre Evaluation of In Vitro Cytotoxicity Programme, 1989-1999), involving 100 laboratories worldwide, in which 61 different *in vitro* toxicity tests were used to determine the concordance with LC_{50} and IC_{50} of 50 compounds found in humans (Bondesson I et al., 1989; Ekwall B et al., 1990). The novelty of this work relied on the use, for the first time, of lethal and sublethal compounds' blood concentration in humans as reference values for test comparison. Through this work, Ekwall provided experimental evidence that *in vitro* toxicity testing is are valuable tool to extrapolate *in vivo* toxicity outcomes in humans (Clemedson C et al. 1998). This started a new era in the experimental field of toxicology, which has led to the evolution of the numerous refined *in vitro* assays we have today for drug toxicity prediction.

Overall, three principal steps can be identified in the cytotoxicity process, common to every cell type: initial injury, mitochondrial injury, and cell death (Vinken M and Blaauboer BJ, 2016). Therefore, in the evaluation of a compound's toxicity, if there are no tissue-specific toxicity insights, it is recommendable to prior proceed by assessing general toxicity tests. Such general assays can address initial cell injury, mitochondria dysfunction, including ROS-mediated mitochondria damage, and cell death by apoptosis or necrosis.

One of the most common effects of initial injury, which can be triggered by different mechanisms (e.g., phospholipid double-layer damage, channel proteins, or transporter impairment), is the plasma membrane disruption. As a result of damage to the plasma membrane, the release of cellular components, including enzymes or metabolic products, occurs, compromising the compartmentalization of cellular functions and, ultimately, cell homeostasis.

Some assays developed to assess membrane injury are based on the detection of enzymes' leakage in the extracellular media, like lactate dehydrogenase (LDH) or proteases, constitutively present in all cell

types. Some examples of such assays include the LDH leakage assay and the protease activity assay. The first one relies on the quantification of the LDH, the enzyme necessary for the biotransformation pyruvate-lactate. In the conversion lactate-pyruvate catalysed by LDH, NAD^+ is reduced in NADH. The LDH released in the extracellular media can be indirectly quantified by detecting the NADH consumption in a coupled reaction, where the substrate, a tetrazolium salt, is converted to a red formazan product, detectable by measuring absorbance at 490 nm (Korzeniewski C and Callewaert DM, 1983).

Similarly, the proteases released can be quantified by measuring their activity. The protease activity assay is based on the ability of constitutive cellular proteases to convert an uncoloured substrate into a fluorescent product. The fluorescence quantification is used to correlate the number of viable cells (Niles AL et al., 2007).

Additionally, the Trypan blue exclusion assay is a very common, simple, and low-cost assay that selectively discriminates cells with integer membranes. It is based on the capability of the dye trypan blue to penetrate only cells with damaged membranes, therefore staining intracellular proteins. As a result, alive cells are visualized as white, whereas dead cells are blue (Piccinini F et al., 2017).

Several cytotoxicity assays were developed to address mitochondria dysfunction, which is a critical factor in cellular health. Indeed, mitochondria represent the energy factory of the cell, where beta-oxidation and oxidative phosphorylation take place thanks to a controlled interplay of enzyme-guided reactions for the final production of ATP, essential for cell vitality. Therefore, compounds interfering with mitochondria functions can cause damage generally associated with impairment of energy metabolism, leading to a marked reduction of ATP production. Additionally, compounds can damage mitochondria with different mechanisms by altering the mitochondrial membrane potential, compromising the mitochondria transition pore, or uncoupling the electron transport chain, leading to ROS formation (Vuda M and Kamath A, 2016).

The MTT assay, considered one of the most valuable *in vitro* viability tests, relies on the ability of metabolically active cells to reduce tetrazolium salts, like the MTT substrate (3-(4,5-dimethylthiazol-2-yl)-2,5-diphenyl-2H-tetrazolium bromide) into the blue-coloured formazan products (Mosmann T, 1983). Although this reaction is primarily catalysed by a mitochondrial reductase, other organelles' enzymes can perform it. Thus, the MTT assay is more considered a general cell viability test rather than a specific mitochondrial functionality test.

Similarly, the Resazurin assay, also known as the trade name of Alamar blue™, is a colorimetric assay based on the reduction of the substrate resazurin into resofurin, a fluorescent and soluble product (Page B et al., 1993). The fluorescence released gives an estimation of the number of living cells. However, it is worth noting that the assay reflects the overall metabolic activity rather than just mitochondrial function, as the reaction is operated by mitochondrial and cytosolic enzymes. Therefore, the results should be interpreted as a general picture of cell functionality.

Assays developed to monitor ATP content in cells offer one of the most robust tools to estimate viable and metabolically active cells, being ATP, the primary energy-carrying molecule for cells' functions. The great majority of such assays rely on the firefly luciferin–luciferase system for ATP detection. The principle of this assay is the oxidation of the natural substrate luciferin by the enzyme luciferase, which gives the oxidized product with the emission of light (Fig. 7).

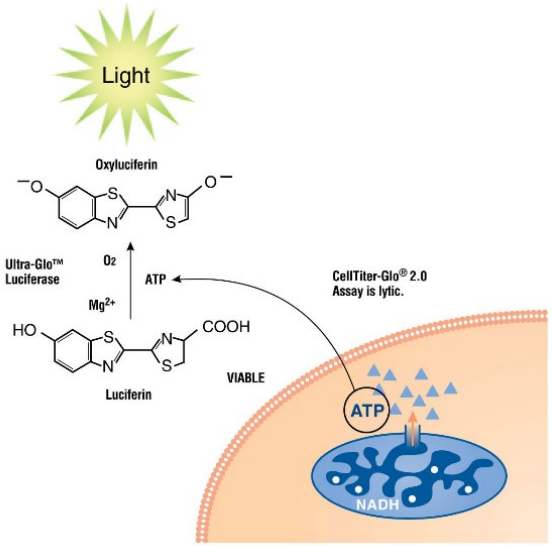

Fig.7. Schematic representation of the ATP-content assay principle (e.g., CellTiter-Glo®, Promega). ATP is necessary as it is consumed during the oxidation of the Luciferin substrate into oxyluciferin product, operated by the Luciferase enzyme. As cells are the source of ATP, the luminescence signal is proportional to the number of viable cells. Source: CellTiter-Glo® Luminescence Assay, Promega Corporation.

As this reaction requires ATP, its consumption is proportional to the bioluminescent signal, which indirectly quantifies the intracellular ATP (Riss TL et al., 2013; Lomakina GY et al., 2015). Assays for ATP detection are considered among the most reliable in measuring cell viability as these biomarkers undergo a rapid decrease in damaged cells, where metabolic pathways are compromised. Additionally, as ATP is primarily produced in mitochondria, this assay is a valuable evaluation of mitochondria integrity and functionality (Lanza IR and Nair KS, 2010). Furthermore, the high sensitivity, reproducibility, stability of the signal that could remain stable up to 5 h, and the low background noise represent remarkable advantages, making such an assay one of the most used in determining cell viability. Another advantage is its applicability for high throughput screening due to its agility, simple handling, and absence of incubation time, unlike other *in vitro* tests (Niles AL et al., 2008; Cali JJ et al., 2008). Finally, it is worth noting that such assay can be used to determine cell viability in 3D systems, like spheroids, 3D scaffold-based cultures, or microtissues, and lately, innovative ATP-based methods have been advanced to measure ATP in living cells and animals (Kijanska M and Kelm J, 2016;

Morciano G et al., 2017). This represents an added value, given the increasing use of three-dimensional models in research.

However, some limitations of the ATP content assays need to be mentioned. These include the high cost and the low stability of luciferase to certain compounds or culture conditions. Also, the requirement of cell lysis makes the assay an end-point test. Additionally, as a consequence of cell lysis, ATPases released in the media can degrade ATP molecules, affecting the results (Cali JJ et al., 2008).

The introduction of engineered and more stable luciferases to chemicals and temperature, as well as the inclusion of ATPase inhibitors within assays working solutions, overcame many of those limitations, making the current versions of ATP-content assays extremely reliable and sensitive (Hall MP et al., 1998; Kitayama A et al., 2003; Koksharov MI and Ugarova NN, 2012).

In addition to cell viability tests, other *in vitro* tests have been developed to specifically determine mitochondrial damage and dysfunction. Among these, we find mitochondrial membrane potential assays and those measuring oxidative stress by quantification of intracellular ROS. Assays based on ROS detection include direct methods, which quantify superoxide radicals or lipid peroxidation, or indirect methods based on measurement of the activity of ROS- neutralizing enzymes, like superoxide dismutase (SOD), catalase and glutathione peroxidase (Sakamuru S et al., 2016; Hadwan MH, 2018; Ahmed AY et al., 2021).

Healthy mitochondria display a membrane potential characterized by a negative charge. However, when mitochondria are damaged, the incorrect ion distribution across their membrane alters the potential. Assays developed to detect altered mitochondria membrane potential rely on the use of cationic fluorescent dyes, which accumulate within the mitochondria matrix, thereby giving the damage estimation through the fluorescent signal (Perry SW et al., 2011).

General ROS species and superoxide radicals can be detected using molecular probes, which can permeate cells and can be oxidized by reactive oxygen species into fluorescent-colored products, detectable by spectrophotometry. Although they constitute valuable assays for ROS detection, the principal limit is the artifact generation as such probes can react with other intracellular oxidant rather than solely ROS or superoxide radicals (Kalyanaraman B et al., 2011; Chen, X et al., 2010). More precise techniques to determine cellular oxidative stress are based on measuring the activity of enzymes involved in redox reactions like catalase, SOD, and glutathione peroxidase. These methods are colorimetric assays based on the use of enzyme-specific substrates transformed into colored detectable products (Beers RF Jr and Sizer IW, 1952; Nebot C et al., 1993; Hadwan MH, 2018).

General toxicity induced by compounds can be detected using cell death assays. These assays can differentiate between apoptosis and necrosis, the principal forms of cell death. The annexin V staining assay, for example, is used to detect early phases of apoptosis. This test exploits the high affinity of the protein annexin V for phosphatidylserine (PS) residues, which are exposed outside the plasma

membrane during apoptosis initiation (Mariño G and Kroemer G, 2013). Annexin V can be fluorescently labeled and used in this way to detect apoptotic cells after binding the exposed PS residues (Vermes I et al., 1995). Other widely used methods for apoptosis assessment rely on quantification of caspase-3 (CAS-3) activity, as this enzyme plays a key role in the apoptotic pathway. Such methods are based on the measurement of specific substrates cleaved by CAS-3 (Pérez-López AM et al., 2016; Savitsky AP et al., 2012). Although this is an overall accepted method for apoptosis detection, it has been described that such substrates' specificity is not restricted to CAS-3 and that other enzymes like caspase-6 and -7 can also induce apoptosis without the involvement of CAS-3 (Liang Y et al., 2001). Therefore, it is recommended to use multiple assays to ensure the activation of a specific caspase in apoptosis activation.

An alternative method for apoptosis identification is the TUNEL (terminal deoxynucleotidyl transferase biotin-dUTP nick end labeling) assay, which detects DNA fragmentation, a typical indicator of apoptotic cells. In this assay, labeled 2-deoxyuridine 5-triphosphate (dUTPs) nucleotides are bonded to hydroxyl ends of DNA, marking DNA strand breaks (Kyrylkova K et al., 2012). Although very sensitive, the TUNEL assay is very costly, so alternative low-cost tests are preferred in certain applications, such as propidium iodide (PI) staining, used to identify necrotic cells due to its inability to permeate intact cell membranes.

Altogether, the described assays provide a comprehensive view of general mechanisms of cell damage that can occur in any cell type, which is crucial for understanding the general toxicity of compounds and to further investigate the mechanism of toxicity concerning specific tissues.

7a.iii. Liver-specific assays for DILI

General toxicity tests are often end-point assessments, so they do not provide information regarding initial or progressive cell damage as they measure irreparable events such as membrane disruption, mitochondria impairment, or cell death. General toxicity evaluation has the advantage of being applicable to any cell type, but for its nature, it lacks specificity. Therefore, specific methods have been developed to provide tissue-specific toxicity. For instance, specific tests were generated to detect liver-specific injuries. The liver is the organ majorly insulted by drugs and chemicals due to its fundamental role in xenobiotic metabolism. Among the main ones, we find specific tests for cholestasis, steatosis, and fibrosis detection.

Cholestasis is a condition characterized by impairment of bile flow from the liver to the intestine with consequent accumulation of bile acids inside or outside the liver (intrahepatic cholestasis or extrahepatic cholestasis). Dysfunction or alteration of the expression of bile acid transporters, mainly localized in the canalicular membrane of the hepatocytes, results in the accumulation of toxic bile acids, leading to liver injury (Pauli-Magnus C and Meier PJ, 2005). Principal causes of cholestasis are genetic disorders

causing defective expression of bile acid transporters, pre-existing liver diseases, and medications (Shaffer EA, 2002; Velayudham LS and Farrell GC, 2003; Zollner G and Trauner M, 2008). Several commercial drugs, including amoxicillin-clavulanic acid, erythromycin, nitrofurantoin, chlorpromazine, estrogens, and amiodarone, have been directly associated with cholestatic diseases deriving from bile acid transporters' inhibition or indirectly, by altering their expression or functionality (Padda MS et al., 2011; Sundaram V, Björnsson ES et al., 2017; Yang K et al., 2013). Assays to assess cholestasis are based on the use of specific fluorescent or labeled substrates for the principal bile acid transporters (e.g., BSEP, MRP2-3, NTCP, OAT1-2) to evaluate their functionality (Jazaeri F et al., 2021; Jackson JP and Brouwer KR, 2019).

Steatosis, also known as fatty liver disease, is a condition characterized by the accumulation of lipids in liver cells, mainly triglycerides. This disease results principally from the impairment of fatty acid metabolism within the hepatocytes, which leads to intracellular accumulation in the form of micro or macrovesicles and ultimately interferes with normal liver tissue functionality. Besides alcohol consumption, considered the leading cause of steatosis, genetic factors, other disorders such as insulin resistance, and drugs are involved in steatosis. If not treated, NAFLD can progress into a condition of severe inflammation called non-alcoholic steatohepatitis (NASH) (Cobbina E and Akhlaghi F, 2017). Several drugs have been reported to be associated with NAFLD and NASH, such as amiodarone, glucocorticoids, methotrexate, tamoxifen, nonsteroidal anti-inflammatory drugs, paracetamol, estrogens (Kolaric TO et al., 2021). Therefore, in DILI evaluation, it becomes crucial to test compounds for steatosis. Different *in vitro* assays are available to determine steatosis induced by compounds and chemicals. The most used ones are colorimetric assays based on neutral triglycerides and lipid stainings such as Oil Red-O or fluorescent dyes, which selectively detect lipid droplets like Nile staining (Mehlem A et al., 2013; Stellavato A et al., 2018; Martinez V and Henary M, 2016).

In general, fibrosis consists of the substitution of the functioning parenchymal tissue with fibrotic tissue. In the liver, a perpetual insult caused by chronic diseases could promote fibrosis, impairing the physiological activities of the liver. This process is typically initiated by transformed stellate cells (HSC), which pass from a quiescent state into fibroblast-like cells, which start depositing components of the ECM (Kamm DR and McCommis KS, 2022; Yang F et al., 2021). Subsequently, HSC acquire contractility, Kupffer cells are activated, and ECM materials are accumulated in the Disse space (Yang F et al., 2021; Roehlen N et al., 2020). In severe cases, this status can become irreversible, progressing to cirrhosis (Ginès P et al., 2021). Fibrotic tissue in the liver is characterized by the abundance of collagen I, III, and IV and other proteins, mainly including fibronectin, elastin, and laminin, due to enhanced secretion and inhibition of metalloproteinases activity (Bataller R and Brenner DA, 2005). Several *in vitro* tests for liver fibrosis evaluation have been developed. Some of them, such as Sirius Red (SR) or Picrosirius Red (PSR) assays, are commonly used and rely on the red staining of collagen fibers visible under light or fluorescence microscopy (Rittié, L, 2017). Other tests are based on the

quantification of hydroxyproline, an amino acid highly present within the collagen protein (Langrock T and Hoffmann R, 2019). Also, specific collagen types can be identified through immunostaining or ELISA tests (Bielajew BJ et al., 2020). Such methods are more accurate, although quite costly and time-consuming. Other techniques for liver fibrosis detection include the evaluation of metalloproteinase (MMPs) activity or tissue-inhibitor metalloproteinase (TIMP) blockage (Hawkes SP et al., 2010).

7b. Pragmatic strategy for early hepatotoxicity assessment of compounds

When hepatotoxicity assessment concerns novel compounds whose toxic effect has never been explored before, a pragmatic approach consists of evaluating firstly a general cytotoxicity, then once this is verified, proceed with the evaluation of liver-specific toxicity.

The selection of the appropriate cell type and culture format is key to achieving a reliable cytotoxicity evaluation, and this is strictly dependent on the purpose of the investigation. Although primary cells are considered the gold standard as they retain the characteristics of the *in vivo* tissue, they do not represent the optimal cell type for an initial cytotoxicity assessment. Cell lines are preferable in such cases, as they offer several advantages compared to primary cells, like higher stability, high proliferation rate, easy handling, and reproducibility of results. For instance, *in vitro* liver cytotoxicity screenings in drug discovery are mainly carried out with the tumor-derived HepG2 or HepaRG cell lines, while for organ-specific tests, primary cells, such as primary hepatocytes, are considered more valuable tools (Vinken M and Hengstler JG, 2018).

Concerning the species, although rodent cell lines are still widely used, human cell lines are, in general, highly preferable as they more closely replicate human *in vivo* physiology and response to drugs.

Selecting the appropriate culture format is also crucial for an accurate cytotoxicity assessment. There are many different systems available nowadays for cell culture, all of them with their advantages and disadvantages. While conventional monolayer cultures are reliable and widely used for cytotoxicity detection, they lack the complexity of the *in vivo* environment. More sophisticated 3D systems, such as spheroids, scaffold-based 3D cultures, organoids, or organ-on-a-chip, offer a more physiologically relevant model. Some of them, like organoids and organ-on-a-chip, however, are not amenable for HTS and, therefore, are not accessible for general cytotoxicity assessments. Lately, 96 well plates providing inserts of ECM membranes or where it is possible to generate spheroids represent a valuable solution, offering an *in vivo*-like system compatible with the HTS plate format.

Lastly, selecting adequate test conditions is fundamental to achieving reliable results. If a general cytotoxicity screening of a set of novel compounds has to be performed, the use of 96 plates allows simultaneous testing of several compounds in multiple concentrations, reducing resources and time needed. Normally, it is advisable to start testing a broader range of concentrations in a preliminary

experiment to then narrow down the compounds' concentrations to establish a reasonable range for the expected effects. For initial cytotoxicity assessments, the recommended exposure time to drugs is between 24h and 72h, and at least three repeats for each measurement are recommended.

Additionally, other parameters need to be considered, such as the medium composition, which can affect the readout, and the compounds' solubility (Tabernilla A et al., 2021). Indeed, as many drugs are insoluble in cell media, they require prior solubilization in organic solvents. DMSO is one of the principal solvents used for its high solubilizing capacity and for its compatibility with biological systems. However, some studies showed that DMSO, at certain concentrations, can damage cells (Sangweni NF et al., 2021). Therefore, when organic solvents such as DMSO are used, it is necessary that a proper control, consisting of media supplied with the used DMSO concentration, is included as a negative control. Obviously, positive control is also required. In general, in the case of cytotoxicity assessments, a positive control is represented by a well-known toxic drug, inducing strong cell mortality in the tested cell type. For instance, tamoxifen is the typical drug used as a positive control in assays assessing hepatocyte viability, owing to its proven high toxic profile in liver cells (Petinari L et al., 2004).

After deciding the most appropriate cell type, system, and experimental conditions, one should proceed with the adequate assay selection: general or specific, depending on the purpose of the study.

Typically, the first step involves general cytotoxicity evaluation, followed by organ-specific toxicity studies. As previously mentioned, reliable general cytotoxicity assays include ATP-content assays as well as LDH activity and MTT assays, which provide a comprehensive view of cell viability, making them appropriate for initial screenings. Specifically, ATP-based assays measure the energy content within the cell, reflecting its metabolic state. LDH activity assays indicate the cell membrane integrity by detecting the released lactate dehydrogenase from damaged cells. Finally, MTT assays identify metabolically active cells based on mitochondrial functioning.

Each one of these cytotoxicity tests generates a dose-response outcome to evaluate compounds' toxicity. The dose, defined as the quantity of a therapeutic agent administered at one time, is the principal parameter used. As a result, toxicity is expressed via toxicological indexes that estimate the substance concentration at which toxicity occurs. As such, the most common indexes are LD_{50} (Median Lethal Dose), the drug's dose killing 50% of the tested population of living organisms; LC_{50} (Median Lethal Concentration), the drug's concentration killing 50% of the population; LD_0 (Lethal Dose zero), the drug's dose at which no individual in the population is expected to die. If the assay endpoint is not the lethality event but a specific toxic event, TD_{50} (Toxic Median Dose) and TC_{50} (Toxic Median Concentration) are used. TD_{50} and TC_{50} are defined respectively as the drug dose or drug concentration at which toxicity occurs in 50% of cases.

The major indicator of a drug`s safety in toxicology is the therapeutic Index. By definition, the therapeutic index (TI) is the ratio between the lethal dose (LD_{50}) and the therapeutic dose (ED_{50}, the effective dose of a drug producing a biological response in 50% of the tested population). It is a quantitative measure used both in preclinical and clinical trials to estimate the margin of safety of a pharmaceutical agent. The higher the TI, the safer the drug is.

After general cytotoxicity has been verified, more targeted studies are performed to address the mechanism of toxicity and pathogenesis of specific organ-related diseases. In the case of the liver, tests revealing drugs-induced cholestasis, steatosis, or fibrosis, as those mentioned in the previous section of this report, may be used.

7c. Conditions for toxicity assessment of drugs in the present study

Several cell lines to study toxicity in different organs have been selected in the present study, each one representative of a different human organ. For instance, the HepaRG cell line was selected to study the toxicity of the liver, and other cell lines were chosen to assess toxicity in other organs, such as the lungs, kidneys, heart, CNS, and immune system. All of them are human-derived cell lines.

In the case of hepatotoxicity assessment, we also added rat and pig hepatocytes for comparison to possibly highlight species-specific differences. Finally, in the case of hepatotoxicity evaluation, we used monolayer, sandwich, and 3D spheroids as different *in vitro* formats to analyze the advantages and drawbacks, as well as the different sensitivity to drugs.

Concerning our *in vitro* models, conventional monolayer cultures were chosen to confirm the known toxicity of a set of drugs within the cell lines. Additionally, liver toxicity evaluation was performed in sandwich and spheroids formats. As the liver is the most affected organ by the toxicity of drugs, comparing conventional systems, such as monolayer, to more sophisticated *in vitro* cultures that better reflect the *in vivo* liver microenvironment, like sandwich and spheroids, could provide a more realistic prediction of toxicity. Moreover, despite their complexity, sandwich and spheroid formats remain compatible with high-throughput screening (HTS) platforms, such as 96-well plates, facilitating their integration into early drug discovery processes. Indeed, the aim of this project is to develop and validate an *in vitro* reliable screening procedure to evaluate compounds' toxicity during the initial stages of drug development to accurately drive the advancements towards safer and more promising candidates.

Three-dimensional systems like organoids and organ-on-a-chip are considered even more representative of the *in vivo* tissue. However, they are not amenable to medium-high throughput screening (Ingber DE, 2022), and therefore, they do not represent a suitable model for the purpose of this study. Nonetheless, in the specific case of organ-on-a-chip, it must be mentioned that polydimethylsiloxane polymers (PDMS), the principal material used for their manufacturing, absorbs hydrophobic drugs, limiting its

use in drug discovery (Toepke MW and Beebe DJ, 2006). Similarly, despite the promising development recently of higher throughput organ-on-a-chip, the issue related to the material still constitutes a major limitation of these devices in drug discovery research (Azizgolshani H et al., 2021; Bircsak KM et al., 2021).

Several specific assays are very useful in determining the initiation or progression of organ-specific pathologies. However, in this study, we needed a broader test to detect cell viability in response to drug exposure. Such an assay would provide a global view of cellular safety status without exploring the mechanism of cell death and not necessarily discriminating the type of cell damage, which could represent a further and important step in elucidating the mechanism of toxicity. Therefore, an ATP-content assay was selected to evaluate cells' viability in our study for its high sensitivity, reproducibility, and stability and because it is an indirect measure of mitochondria damage, which is one leading mechanism of drugs' toxicity (Massart J et al., 2018). More importantly, this test, for its rapidity and easy handling, could be applicable in HTS, which is the final goal of the toxicity prediction procedure provided here.

8. *In silico* tools for toxicity evaluation

The introduction of Artificial Intelligence (AI) in the last couple of decades has extremely affected the pharmaceutical industry by advancing and accelerating the conventional drug development process. The advent of deep learning tools, along with the rapidity of data interpretation, contributed to the more rapid and less costly identification of promising NCE (new chemical entities) or NBE (new biological entities) with high safety profiles (Nag et al., 2022).

Lately, machine learning models have found valuable applications in predicting potential toxicity, providing a cost-effective and time-efficient alternative to *in vivo* animal testing. Many of these innovative approaches aim to enhance the predictability of drug-induced liver injury (DILI), making hepatotoxicity the primary cause of failure in clinical trials, thereby improving the safety profile of new compounds before reaching clinical trials. It's a concerted effort to bridge the gap between preclinical studies and human outcomes, ensuring a higher success rate in drug development and safer therapeutic options for patients.

Advancements in predictive toxicology based on machine learning models are helping researchers identify potential toxicity earlier in the drug discovery. Computational methods, including quantitative structure-activity relationship (QSAR), along with ADME models, have been increasingly used in toxicity predictions (Wang MWH et al., 2021). The shift from *in vivo* to *in silico* studies observed in the last years offers the advantage of successful predictions with decreased animal and human testing aligning with ethical research practices.

Typically, computational models developed for drug safety assessment can be divided into three main categories: qualitative classification, quantitative regression, and read-across (Yang H et al., 2018). Qualitative models are used at the beginning of drug safety assessment to understand only if a compound is toxic or not, whereas quantitative regression models address the extent of toxicity, and read-across assessments are used to identify specific toxicity endpoints based on comparing outcomes associated with experimental toxicity findings (Yang H et al., 2018).

Building a machine learning model involves four main steps: data collection, data description, model building, and model evaluation (Yang H et al., 2018). Creating a high-quality experimental dataset is key to building a valuable *in silico* prediction model. Data are collected through several databases in which chemical structures are associated with toxic effects, target interactions or biological pathways. Some examples include TOXNET (Fowler S and Schnall JG, 2014), ACToR (Judson R et al., 2008), DSSTox (Williams-DeVane CR et al., 2009), PubChem (Richard AM et al., 2006), KEGG (Kanehisa M and Goto S, 2000), SuperToxic (Schmidt et al., 2009), ToxBank (Kohonen P et al., 2013), admetSAR (Cheng et al., 2012b).

The second step, the data description, is done by representing chemical structures through numeric features such as molecular descriptors or molecular fingerprints (Winter R et al., 2018; Bajusz D et al., 2017). In this way, data can be processed and used to build a computational model for toxicity prediction, which is finally evaluated. There are several publicly available tools that are used singularly or in combination to build a computational predictive model, such as Scikit-learn (Pedregosa et al., 2011) and WEKA (Frank E et al., 2004).

Finally, the model has to be evaluated. The evaluation of a model aims to determine its accuracy, sensitivity, and specificity by estimating specific parameters that compare the values provided by the model to those of experimental findings.

Other computational methods for toxicity prediction of chemicals are based on the identification of Structural Alerts (SAs), chemical substructures responsible for toxicity. The pioneer in such a field was the scientist Ashby, who first demonstrated a strict association between certain mutations occurring in *Salmonella* and specific chemical patterns (Ashby J and Tennant RW, 1988). Nowadays, SAs are identified through software tools such as SARpy, MoSS, Gaston, and Derek Nexus (Yang H et al., 2017) and stored in web servers such as ToxAlerts and SApredictor (Hua Y et al., 2022).

Currently, many computational tools have been developed to determine organ-specific toxicity. One example is VenomPred, developed by Galati S. et al. in 2022.

As liver injury still represents a major cause of attrition in drug discovery, several *in silico* models are applied for DILI determination, offering the advantage of predicting hepatotoxicity with high accuracy, reduced time, and, more importantly, without the necessity to synthesize products for experimental testing, thereby reducing costs enormously. However, independently from the type of model used, a common feature limiting their performance is the accessibility to high-quality data (Hewitt M and Przybylak K et al., 2016; Di Zeo-Sánchez DE et al., 2022; Ellison C et al., 2022).

In addition to the described tools, investigative toxicology has recently gained importance as a field to minimize the risk of toxicity in drug development (Fig.8, Beilmann M et al., 2019). This field of study uses advanced techniques to perform prospective analysis, aiming to predict compounds' toxicity before *in vivo* trials are carried out and retrospective analysis based on already-known clinical toxicity findings (Pognan et al., 2023). The goal is to discard the most toxic compounds in early drug discovery and direct the compounds' selection towards the most promising and successful ones from the safety point of view.

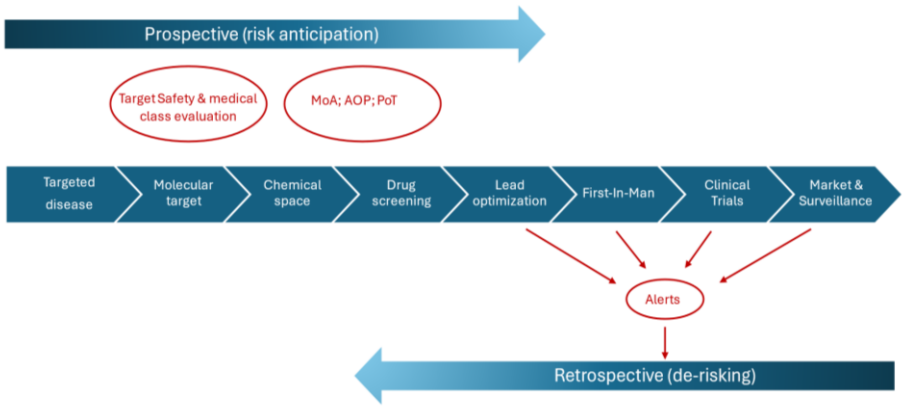

Fig.8. Investigative toxicology: goals and approaches in drug discovery and development (Beilmann M et al., 2019). MoA= mode of action; AOP= adverse outcome pathways; PoT= pathways of toxicity.

However, the creation of a high-quality data set, essential to assess meaningful toxicological evaluations, constitutes the major limit of all the described approaches, hindering their progress and effectiveness. Access to high-quality data relies not only on the quantity of collected data but also on their diversity and relevance. Despite the abundance of data nowadays available online, building robust models remains yet challenging as data availability can be limited, especially for emerging chemicals, and the quality of existing data may vary.

Additionally, while *in silico* methods for toxicity predictions offer several advantages, they have some disadvantages that need to be considered. These models often rely on computational algorithms based on chemical structures and physical properties of the molecules but do not consider the complexity of biological systems, thus lacking the mechanistic understanding responsible for the biological mechanism of toxicity. Therefore, these models may not always accurately predict the *in vivo* toxicity of compounds.

In this scenario, we believe that the integration of a reliable *in vitro* screening tool along with *in silico* methods for early detection of compounds' toxicity is key to enhancing the success of novel drugs. Such tools can streamline the drug development process by identifying potential toxic compounds and preventing failures in clinical stages, thereby minimizing time and money investments in research and, more importantly, reducing human and animal testing with potential adverse effects.

AIM OF THE STUDY

The present study is within the scope of the INNOTARGETS project, a European Union's Horizon 2020 research and innovation program under the Marie Skłodowska-Curie action. The focus of INNOTARGETS is to identify innovative targets in multi-drug resistant (MDR) bacteria for the development of novel antimicrobials overcoming the limitations of current drugs.

Within the INNOTARGETS project, a crucial step in the development of novel agents is the toxicity assessment. The high attrition rates in drug discovery due to adverse effects not predicted by traditional animal models require urgent alternative and innovative methodologies to accurately predict the adverse effects of compounds in humans.

Nowadays, toxicology research is moving towards the development of more and more sophisticated *in vitro* and *in silico* models to reliably predict toxicity and reduce reliance on animal models, aligning with the ethical 3R principle of replacement, reduction, and refinement.

The aim of the present study is to develop and validate *in vitro* and *in silico* approaches for toxicity prediction of novel compounds in humans that are suitable for compounds' screening in early drug discovery. We started by testing the general toxicity of drugs in human cell lines, each one used as a model of a different organ, to then focus our study on hepatotoxicity prediction. The liver, being the primary organ involved in drug metabolism, is indeed principally affected by toxicity exerted by the parent drug and eventually by the production of toxic metabolites. Within the hepatotoxicity evaluation, we aim to emphasize the selection of appropriate *in vitro* systems and species-specific effects, remarking toxicity discrepancies between 2D and 3D systems as well as between humans and animal hepatocytes-based models, such as rat and pig hepatocytes.

The other goal of the study is to develop *in silico* tools for toxicity prediction and for the elucidation of the mechanism of compounds' toxicity. The use of machine learning tools could streamline the screening process, providing precious insights by predicting adverse effects of compounds based on their chemical structure or by predicting the formation of toxic metabolites without the need for synthesis and experimental testing. On the other hand, *in vitro* testing is more time-consuming and expensive compared to *in silico* assessment, but it is necessary to refine computational tools by generating experimental data on toxicity.

We believe that the integration of *in vitro* and *in silico* methodologies for toxicity prediction could have a synergistic effect, providing a valuable tool applicable at the early stages of drug discovery potentially revolutionizing the process. It will guide the Go/No-Go decision by anticipating toxic compounds, thereby preventing their advancement in clinical trials. The combination of *in vitro* and *in silico* tools could reduce toxicity issues, ultimately enhancing the efficiency and success of drug discovery.

MATERIALS AND METHODS

1. Drug compounds

All drug compounds tested in the experimental part of this project were commercially available drugs or withdrawn drugs. The complete list of the compounds includes 5-aminobenzimidazole, 5-FluoroUracil, Acetaminophen, Acyclovir, Amiodarone hydrochloride, Amphotericin B, Astemizole, Bleomycin sulfate, Bortezomib, Ciprofloxacin, Clozapine, Colistin Sodium methane sulfonate, cyclophosphamide monohydrate, Dexamethasone, Diclofenac Sodium salt, Doxorubicin hydrochloride, Erythromycin, Fialuridine, Imipramine hydrochloride, Isoniazid, Nefazodone hydrochloride, Nefazodone's metabolite M7, Nefazodone's metabolite M8, Nitrofurantoin, Rapamycin, Simvastatin, Tamoxifen, Trazodone hydrochloride, Troglitazone, Valproic acid sodium salt, Vancomycin hydrochloride, Zidovudine. All the compounds were purchased from Sigma Aldrich except for Bleomycin sulfate (European Pharmacopoeia Reference Standard), Bortezomib (EMD Millipore Corp., USA), Nefazodone's metabolite NFZ-OH (TRC, Toronto Research and Chemicals Inc.) and Nefazodone's metabolite NFZ-TD (TRC, Toronto Research and Chemicals Inc.), Vancomycin hydrochloride (European Pharmacopoeia Reference Standard).

2. Monolayer cultures of tissue-specific cell lines

To test compounds' cytotoxicity in different body tissues the following cell lines were selected: HepG2 (human hepatocellular carcinoma, ATCC HB-8065™), HK-2 (normal human adult male kidney, ATCC CRL-2190™), MRC-5 (human lung fibroblast, ATCC® CCL-171), T98G (human glioblastoma multiforme, ATCC CRL-1690™), Neuro-2a (mouse neuroblasts, ATCC CCL-131™), H9c2 (rat cardiomyocyte, ATCC CRL-1446 ™), Jurkat Clone E6-1 (human acute leukemia T-lymphocyte, ATCC TIB-152 ™). All cell lines were obtained from the American Type Culture Collection (ATCC).

2a. HepG2 culture

Cryopreserved HepG2 were thawed and maintained in culture following the vendor's instructions. Specifically, after thawing cells were seeded in a flask and cultured in MEM medium (Gibco™) completed with 10% heat-inactivated Fetal Bovine Serum (Gibco™), 1mM Sodium Pyruvate solution (Sigma), 1% MEM Non-Essential Amino Acid solution (100X, Sigma), 1% penicillin-streptomycin (100X, Sigma). Cells were maintained in a humidified incubator with 5% CO_2 at 37°C and cultured until passage 6 or 7 before starting the cytotoxicity assay. Medium was renewed three times a week. For the cytotoxicity assay, HepG2 were seeded in a monolayer in 96 well, transparent flat bottom plate, at a concentration of 35,000 cells per well.

2b. HK-2 culture

Cryopreserved HK-2 cells were thawed and maintained in culture following the vendor's instructions. Specifically, after thawing, cells were seeded in a flask and cultured in Keratinocyte Serum-Free Medium (K-SFM, Gibco™ kit catalog number 17005-042) completed with 0.05 mg/mL of Bovine Pituitary Extract (BPE) and five ng/mL of Human recombinant Epidermal Growth Factor (EGF). Cells were maintained in a humidified incubator with 5% CO_2 at 37°C for two weeks before starting the cytotoxicity assay. Medium was renewed three times a week. For the cytotoxicity assay, HK-2 were seeded in a monolayer in 96 well, transparent flat bottom plate, at a concentration of 8,000 cells per well.

2c. MRC-5 culture

Cryopreserved MRC-5 cells were thawed and maintained in culture following the vendor's instructions. Specifically, after thawing cells were seeded in a flask and cultured in MEM medium (Gibco™) completed with 10% heat-inactivated Fetal Bovine Serum (Gibco™), 1mM Sodium Pyruvate solution (Sigma), 1% MEM Non-Essential Amino Acid solution (100X, Sigma), 1% penicillin-streptomycin (100X, Sigma). Cells were maintained in a humidified incubator with 5% CO_2 at 37°C for three weeks before starting the cytotoxicity assay. Medium was renewed three times a week. For the cytotoxicity assay, MRC-5 were seeded in a monolayer in 96 well, transparent flat bottom plate, at a concentration of 7,000 cells per well.

2d. T98G culture

Cryopreserved T98G were thawed and maintained in culture following the vendor's instructions. Specifically, after thawing cells were seeded in a flask and cultured in MEM medium (Gibco™) completed with 10% heat-inactivated Fetal Bovine Serum (Gibco™), 1mM Sodium Pyruvate solution (Sigma), 1% MEM Non-Essential Amino Acid solution (100X, Sigma), 1% penicillin-streptomycin (100X, Sigma). Cells were maintained in a humidified incubator with 5% CO_2 at 37°C for three weeks before starting the cytotoxicity assay. Medium was renewed three times a week. For the cytotoxicity assay, T98G were seeded in a monolayer in 96 well, transparent flat bottom plate, at a concentration of 10,000 cells per well.

2e. Neuro2a culture

Cryopreserved Neuro2a were thawed and maintained in culture following the vendor's instructions. Specifically, after thawing cells were seeded in a flask and cultured in MEM medium (Gibco™) completed with 10% heat-inactivated Fetal Bovine Serum (Gibco™), 1mM Sodium Pyruvate solution (Sigma), 1% MEM Non-Essential Amino Acid solution (100X, Sigma), 1% penicillin-streptomycin (100X, Sigma). Cells were maintained in a humidified incubator with 5% CO_2 at 37°C for three weeks before starting the cytotoxicity assay. Medium was renewed three times a week. For the cytotoxicity assay, Neuro2a were seeded in a monolayer in 96 well, transparent flat bottom plate, at a concentration of 5,000 cells per well.

2f. H9c2 culture

Cryopreserved H9c2 cells were thawed and maintained in culture following the vendor's instructions. Specifically, after thawing, cells were seeded in a flask and cultured in DMEM medium w/Glutamax (Gibco™) completed with 10% heat-inactivated Fetal Bovine Serum (Gibco™), 1mM Sodium Pyruvate solution (Sigma), 1% penicillin-streptomycin (100X, Sigma). Cells were maintained in a humidified incubator with 5% CO_2 at 37°C for at least three weeks before starting the cytotoxicity assay. Medium was renewed three times a week. For the cytotoxicity assay, H9c2 were seeded in a monolayer in 96 well, transparent flat bottom plate, at a concentration of 5,000 cells per well.

2g. Jurkat clone E6-1 culture

Cryopreserved Jurkat were thawed and maintained in culture following the vendor's instructions. Specifically, after thawing, cells were seeded in a flask and cultured in suspension in IMDM medium (Gibco™) completed with 10% heat-inactivated Fetal Bovine Serum (Gibco™) and 1% penicillin-streptomycin (100X, Sigma). Cells were maintained in a humidified incubator with 5% CO_2 at 37°C for at least three weeks before starting the cytotoxicity assay. Medium was renewed three times a week. For the cytotoxicity assay, Jurkat were seeded in a monolayer in 96 well, transparent flat bottom plate, at a concentration of 40,000 cells per well.

3. Exposure of tissue-specific cell lines to Drugs

Twenty-four hours after seeding in 96 well plates, each cell line cultured in a monolayer was exposed to increasing concentrations of each test compound. In total, six concentrations per drug were assayed, ranging from the Cmax (the therapeutic maximal drug concentration in human plasma) as the lowest to 32-fold Cmax as the highest. Drugs' values of Cmax were found in published literature (see Tab. 1 in

the “Results and Discussion” section). Mother solutions of compounds were prepared by dissolving each drug in 100% DMSO in order to have 200X the highest concentration (32-fold Cmax). The other test concentrations were made starting from the mother solution and preparing 2-fold serial dilutions in 100% DMSO.

DMSO solution, at the final concentration of 0.5% v/v (DMSO/media), was used as negative control. Tamoxifen, 200 μM final concentration, was used as positive control of toxicity.

Drug concentrations tested in all cell lines are provided in Table 1.

HepG2 test compounds	**Abbreviation**	**Test concentrations (μM)**
Diclofenac	DCF	500, 250, 125, 62.5, 31.3, 15.65
Acetaminophen	ACP	4000, 2000, 1000, 500, 250, 125
Troglitazone	TRG	200, 100, 50, 25, 12.5, 6.3
Fialuridine	FLD	60, 30, 15, 7.5, 3.75, 1.87
Amiodarone	AMI	300, 150, 75, 37.5, 18.75, 9.37
Nefazodone	NFZ	200, 100, 50, 25, 12.5, 6.3
Simvastatin	SIM	0.66, 0.32, 0.16, 0.08, 0.04, 0.02
Tamoxifen (ctr +)	TMX	200
Dimethyl sulfoxide (ctr -)	DMSO	0.5% (v/v)

HK-2 test compounds	**Abbreviation**	**Test concentrations (μM)**
Colistin	COL	200,100, 50, 25, 12.5, 6.3
Cyclophosphamide	CPM	200,100, 50, 25, 12.5, 6.3
Rapamycin	RAP	200, 100, 50, 25, 12.5, 6.3
Amphotericin B	AMB	100, 50, 25, 12.5, 6.3, 3.1
Doxorubicin	DOX	400, 200, 100, 50, 25, 12.5
Vancomycin	VAN	400, 200, 100, 50, 25, 12.5
Dexamethasone	DEX	400, 200, 100, 50, 25, 12.5
Tamoxifen (ctr +)	TMX	200
Dimethyl sulfoxide (ctr -)	DMSO	0.5%

MRC-5 test compounds	**Abbreviation**	**Test concentrations (μM)**
Bleomycin	BLM	200,100, 50, 25, 12.5, 6.3
Cyclophosphamide	CPM	2000, 1000, 500, 250, 125, 63.5
Amiodarone	AMI	200,100, 50, 25, 12.5, 6.3
Methotrexate	MET	1, 0.5, 0.25, 0.12, 0.06, 0.03
Doxorubicin	DOX	100, 50, 25, 12.5, 6.3,3.1
Nitrofurantoin	NIT	200, 100, 50, 25, 12.5, 6.3
Amphotericin B	AMB	100, 50, 25, 12.5, 6.3, 3.1
Tamoxifen (ctr +)	TMX	200
Dimethyl sulfoxide (ctr -)	DMSO	0.5%

T98G/Neuro2a test compounds	**Abbreviation**	**Test concentrations (μM)**
Valproate	VAL	8000, 4000, 2000, 1000, 500, 250
Imipramin	IMI	200, 100, 50, 25, 12.5,6.3
Paclitaxel	PAX	4, 2, 1, 0.5, 0.25, 0.12
Bortezomib	BOR	0.2, 0.1, 0.05, 0.025, 0.012, 0.006
Isoniazid	ISO	8000, 4000, 2000, 1000, 500, 250
Amiodarone	AMI	40, 20, 10, 5, 2.5, 1.25
Ciprofloxacin	CIP	200, 100, 50, 25, 12.5, 6.3
Tamoxifen (ctr +)	TMX	200
Dimethyl sulfoxide (ctr -)	DMSO	0.5%

H9c2 test compounds	Abbreviation	Test concentrations (µM)
Doxorubicin	DOX	100, 50, 25, 12.5, 6.3, 3.1
Amiodarone	AMI	100, 50, 25, 12.5, 6.3, 3.1
5-F Uracile	5FU	800, 400, 200, 100, 50, 25
Zidovudin	AZT	100, 50, 25, 12.5, 6.3, 3.1
Trazodone	TRZ	300, 150, 75, 37.5, 18.8, 9.4
Diclofenac	DIC	400, 200, 100, 50, 25, 12.5
Astemizole	AST	20, 10, 5, 2.5, 1.2, 0.6
Tamoxifen (ctr +)	TMX	200
Dimethyl sulfoxide (ctr -)	DMSO	0.5%

Jurkat test compounds	Abbreviation	Test concentrations (µM)
Doxorubicin	DOX	8, 4, 2, 1, 0.5, 0.25
5Fluorouracil	5FU	160, 80, 40, 20, 10, 5
Aciclovir	ACI	160, 80, 40, 20, 10, 5
Dexamethasone	DEX	80, 40, 20, 10, 5, 2.5
Rapamycin	RAP	4, 2, 1, 0.5, 0.25, 0.12
Ciprofloxacin	CIP	800, 400, 200, 100, 50, 25
Erythromycin	ERT	400, 200, 100, 50, 25, 12.5
Tamoxifen (ctr +)	TMX	200
Dimethyl sulfoxide (ctr -)	DMSO	0.5%

Table 1. The table shows the drugs that were used to evaluate the cytotoxic effects on different cell lines. The right column indicates the final concentrations (µM) of the drugs that were applied to the cells. Each drug was tested in six different concentrations.

To expose cells to the drugs, 1 µL of each drug solution (200X) was added from the drugs' mother plate to 199 µL of media contained in each well where cells were seeded previously. In this way, the overall DMSO concentration per well was 0.5% v/v. To test acute toxicity, cell cultures with added drugs were then incubated with for 48h, and then cytotoxicity assay was performed.

4. Cytotoxicity assay

Cell viability assessment was performed in HepG2, HK-2, MRC-5, T98G, Neuro2a, H9c2, and Jurkat cell lines by evaluating cellular ATP content using the CellTiter-Glo® Luminescent Cell Viability Assay (Promega), following manufacturer's instructions. Briefly, the medium was renewed, and an equal volume to that of the media of CellTiter-Glo® reagent was added to each well. The plates were put in an orbital shaker for 2.5 minutes to allow the mixing of the reagent and to induce cell lysis. Finally, plates were incubated at RT in the dark for 10 minutes, and then the luminescence signal was measured and recorded using BioTek Synergy H1 Plate Reader. Relative light units (RLUs) of luminescence signal

were proportional to the ATP released by lysed cells and served, therefore, as a parameter of cells' viability.

5. Data analysis

At least three independent experiments were conducted to assess the compounds' toxicity in each cell line. Raw data of luminescence signal were analyzed by generating mean and standard error of the mean, SEM (GraphPad Prism 8.3.0; GraphPad Software, San Diego, CA). Each value, subtracted from the blank (luminescence signal from wells with medium only), was then divided by the control (luminescence signal of cells treated with 0.5% DMSO only) and expressed as a percentage of viable cells with respect to the control. LC_{50} values were calculated using non-linear regression analysis with a sigmoidal dose-response model (GraphPad Prism 8.3.0; GraphPad Software, San Diego, CA).

Comparison between culture systems was performed using two-way ANOVA followed by Tukey's multiple comparison test or Sidak's multiple comparison test (GraphPad Prism 8.3.0; GraphPad Software, San Diego, CA). $p<0.05$ was considered statistically significant.

6. HepaRG monolayer cell culture (2D)

Cryopreserved differentiated HepaRG were purchased from Gibco™ (Thermo Fisher Scientific). After thawing, cells were seeded in monolayer in transparent flat bottom 96 well plates coated with Collagen I, Rat tail (Gibco™). A solution of 0.05 mg/mL of Collagen I, Rat Tail, was used for the coating. Cells were seeded at a density of 70,000 cells/well and maintained in William's E media (Gibco™) supplemented with 10% heat-inactivated Fetal Bovine Serum (Gibco™), 1% penicillin-streptomycin (100X, Sigma-Aldrich), five µg/mL of insulin (insulin solution from bovine pancreas, Sigma-Aldrich Chemie, Germany), 0.1 µM dexamethasone (Sigma-Aldrich), Glutamax™ (100X, Gibco™). Cells were maintained in culture for six days, renewing the media every two days. For the cytotoxicity assay, drugs were added on day 7.

7. HepaRG sandwich culture (SW)

To establish HepaRG sandwich culture, HepaRG cells were seeded between a layer of Collagen Type I Rat Tail (Gibco™, BD 354236) and Matrigel® (Sigma) matrixes. Ninety-six-well plates for cell culture were coated with collagen solution of 0.05 mg/mL one day prior to cells' seeding and stored at 4 °C.

Collagen I Rat Tail solution 0.05 mg/mL was prepared as follows:

- A solution of acetic acid 0.02 N was prepared by adding 572 µL of concentrated acetic acid (SIGMA 49199-50ML-F) to 500mL of Milli-Q water.
- The solution was sterilized by filtration with a Millipore filter of 0.22 µm cutoff.
- 8.33 mL of Collagen I Rat Tail solution to 491.67 mL of the filtered acetic acid water solution in order to reach a final concentration of 0,05 mg/ml.
- 70 µL/well of collagen I solution were dispensed.
- The plate was incubated at RT for 1h.
- Then, collagen solution was aspirated, and each well was washed three times with 100 µL/well of sterile room temperature PBS 1X solution.

The next day, HepaRG cells, cultured in a flask to confluency, were trypsinized and counted. The number of viable cells was obtained with Trypan blue exclusion method (Trypan Blue Solution, 0.4%, Gibco™) using the automated cell counter Countess™ II Automated Cell Counter (Invitrogen). Then, cells were seeded in the collagen-coated plate at a density of 70,000 cells/well. After 4h, necessary for the initial cells' attachment, the medium was aspirated, and 100 µL/well of iced cold Matrigel® solution were added.

Matrigel® solution was prepared by adding Matrigel® Matrix (Sigma; concentration variable, reported in each bottle) to an iced-cold medium (to avoid Matrigel® coagulation) to reach a final concentration of Matrigel® solution equal to 0.5 mg/mL. One hundred µL/well of Matrigel® solution were dispensed. HepaRG sandwich culture was incubated at 37°C, 5% CO_2.

8. HepaRG spheroid culture (3D)

Cryopreserved HepaRG (Gibco™) vial was thawed quickly in a 37ºC water bath. Upon thawing, cells were transferred into a 15 mL centrifuge tube containing 9 mL of HepaRG complete media (see section 6 in Materials and Methods, "HepaRG monolayer cell culture"). The tube was centrifuged at 500 x g for 3 minutes, and then the supernatant was discarded. The cell pellet was gently re-suspended in 5 mL of HepaRG complete media. Cell counting was performed with Trypan Blue using a Countess™ II Automated Cell Counter.

Cell suspension was prepared to contain 1,500 cells/200 µL of media. Using a multichannel pipette, 200 µL of the cell suspension was added into each well of Nunclon™ Sphera™ super low attachment U-bottom 96-well microplates. Then, plates were centrifuged at 200 x g for 2 minutes to allow cells to pool at the bottom of each well. Then, plates were transferred to an incubator (37ºC, 5% CO_2, humidified) and allowed to aggregate in complete HepaRG media. Media was renewed every two days by discarding half the volume (100 µL) of old media and adding another half (100 µL) of fresh media. This procedure allowed the aspiration of spheroids to be avoided while renewing media as they grow in suspension.

9. Rat Primary Hepatocytes monolayer cultures

Rat (Sprague-Dawley) Cryopreserved Hepatocytes, Plateable Male, were purchased from Thermo Fisher Scientific (cat. N. RTCP10) and cultured following the manufacturer's instructions. Briefly, cryopreserved rat primary hepatocytes (RPH) were thawed in a 37°C water bath and transferred in 9 mL of complete media consisting of William's E medium 500 mL supplemented with Hepatocyte Thawing and Plating Supplement Pack (Thermo Fisher, CM3000, containing Prequalified fetal bovine Serum, dexamethasone, cocktail solution of fetal bovine serum, penicillin-streptomycin, human recombinant insulin, HEPES). Resuspended cells were centrifuged at 55 x g for 3 min at RT, and then the supernatant was discarded. The cell pellet was resuspended in 3-4 mL of complete media, and then cells were counted. The percentage of viable cells after thawing was assessed with trypan blue exclusion test as described before (see section 7 in Materials and Methods, "HepaRG sandwich culture "). Then, cells were seeded with a density of 70,000 cells/well in collagen-coated 96 well plates. For the coating, a 0.05 mg/mL solution of Collagen I Rat Tail (Gibco™, rat tail collagen I) was used. Collagen I Rat Tail solution was prepared as described before (see section 7 in Materials and Methods, "HepaRG sandwich culture "). Monolayer cultures were incubated at 37°C, 5% CO_2, for two days before adding test compounds. Media was renewed every two days.

10. Rat Primary Hepatocytes sandwich cultures

To establish rat primary hepatocytes (RPH) sandwich culture, RPH were seeded between a layer of Collagen Type I Rat Tail (Gibco™, BD 354236) and Matrigel® (Sigma) matrixes as follows. Ninety-six-well plates for cell culture were coated with collagen solution of 0.05 mg/mL one day prior to cells seeding and stored at 4 °C. Collagen I Rat Tail solution was prepared as described before (see section 7 in Materials and Methods, "HepaRG sandwich culture ").

After thawing, RPH were counted with Trypan blue exclusion method (Trypan Blue Solution, 0.4%, Gibco™) using the automated cell counter Countess™ II Automated Cell Counter (Invitrogen). Then RPH were seeded in monolayer as described in the previous section at a density of 70,000 cells/well in plates previously coated with Collagen I Rat tail solution. Cells were incubated at 37°C, 5% CO_2 for 4-5 h, until attachment to the bottom of the plates was reached. After incubation, the medium was aspirated, and 100 µL/well of iced cold Matrigel® solution were added.

Matrigel® solution was prepared by adding iced cold Matrigel® Matrix (Sigma; concentration variable, reported in each bottle) to iced-cold medium (to avoid Matrigel coagulation) to reach a final concentration of Matrigel® solution equal to 0.5 mg/mL. One hundred µL/well of Matrigel solution were dispensed. RPH sandwich cultures were incubated at 37°C; 5% CO_2.

11. Rat Primary Hepatocytes spheroids cultures

Rat (Sprague-Dawley) Cryopreserved Hepatocytes in a 37ºC water bath. Upon thawing, the cells were transferred into a 15 mL centrifuge tube containing 9 mL of complete media (see section "Rat Primary Hepatocytes monolayer cultures" in "Materials and Methods"). The tube was centrifuged at 500 x g for 3 minutes, and then the supernatant was discarded. The cell pellet was gently re-suspended in 5 mL of RPH complete media. Cell counting was performed with Trypan Blue using a Countess™ II Automated Cell Counter.

Cell suspension was prepared to contain 1,500 cells/200 µL media. Using a multichannel pipette, 200 µL of the cell suspension were added into each well of Nunclon™ Sphera™ super low attachment U-bottom 96-well microplates. Then, plates were centrifuged at 200 x g for 2 minutes to allow cells to pool at the bottom of each well. Then, plates were transferred to an incubator (37ºC, 5% CO_2, humidified) and allowed to aggregate in RPH complete media. Media was renewed every two days by discarding half the volume (100 µL) of old media and adding another half (100 µL) of fresh media. This procedure allowed to avoid aspiration of spheroids while renewing media, as they grow in suspension.

12. Isolation of pig hepatocytes

Two separate hepatocytes' isolations were performed during the secondment at IRTA-CReSA. The first one was carried out starting from an adult pig's liver; the second one started from two piglets' livers. After resection, the livers were aseptically weighted. Then, perfusion was applied in sterile conditions with an ice-cold complete medium (DMEM supplemented with 10% FBS, Penicillin, Streptomycin, L-glutamine, and sodium pyruvate) using a 20 mL syringe directly inserted into the portal vein multiple times.

After perfusion, the liver was transferred into a sterile beaker filled with an iced-cold complete medium for transportation to the laboratory. All the reagents and solutions were prepared before starting the isolation process as follows:

Perfusion Buffer 1 (PB1): PBS 500 mL; BSA 0.2 mg/mL; EDTA 0.5 mM

Perfusion Buffer 2 (PB2): DMEM 250 mL; BSA 0.2 mg/mL

Digestion Buffer (DG): DMEM 250 mL; BSA 0.2 mg/mL; Collagenase A (100mg, dissolved directly in the medium); DNAse I (100 mg, dissolved directly by adding media)

Complete media/Plating media1: DMEM+ 10% FBS+ Pen/strep+ L-glutamine+ Sodium pyruvate

Plating media2: William's medium E, supplemented with 100 mU/mL penicillin, 100 µg/mL streptomycin and 10% fetal bovine serum, dexamethasone 1µM, insulin 10 µg/mL.

Red Blood Cells (RBC) Lysis Buffer 10X: 8.02 g NH4Cl; 0.84 g NaHCO3; sterile Milli-Q water up to 100 ml. Diluted 1:10 with sterile Milli-Q water.

The liver was first washed multiple times with Perfusion Buffer 1(PB1) and then with Perfusion Buffer 2 (PB2) by inserting a syringe directly in the portal vein. A volume of 250 mL of PB1 and PB2 was used each time for the washing steps.

The liver specimens were diced into small pieces (cubes about 0.5 cm in size) using a sterile scalpel and forceps. Digestion buffer (DB) was then added to the minced tissue in a ratio of 1:4 (50 ml of DB were added to digest approximately 200 g of the liver specimen), and the mixture was incubated at RT for 1 h to allow the complete digestion of the tissue. After incubation, the liver pieces were pressed with the back part of a sterile syringe to mince the digested tissue. Then, the mixture was filtered with a sterile mesh of 250 µM to discard debris and collected in a 50 mL falcon tube.

The mixture was filtered through a 100 µM cell strainer first and with a 70 µM cell strainer second. After each filtration, the suspension was centrifuged at 75 x g, 5 min, 4°C; the supernatant was discarded, and the pellet was resuspended in complete media. As the amount of red blood cells (RBC) was visibly very high, an extra step was added at this point in the second isolation performed. Here, the suspension was centrifuged at 200 x g for 5 min, 4°C, and the supernatant was discarded. The pellet was resuspended with a minimal amount of RBC lysis buffer and incubated in a 37 °C bath for 5 min. After incubation, sterile PBS was added to inactivate the RBC lysis buffer process. Cells were centrifuged again at 200 x g for 5 min at RT, and the supernatant was discarded.

The entire pellet was resuspended partially with Plating Media 1 and partially with Plating Media 2. However, it was impossible to count the cells before seeding due to the high amount of debris still present in the suspension. For plating, all the flasks and plates used were previously coated with a solution of collagen I (Collagen I Rat tail, A10483-01, Gibco™) to improve the hepatocytes' attachment and proliferation. Cultures were incubated in a humidified incubator with 5% CO_2 at 37 °C.

13. Pig primary hepatocytes monolayer culture

In order to define the optimal growing conditions of isolated PPH, two different media were used to maintain monolayer cultures for comparison. The first one consisted of William's Medium E basal medium, no phenol red, supplemented with GlutaMAX™ and HepaRG™ Thaw, Plate & General Purpose Medium Supplement (HPRG 770, Gibco™). The second consisted of DMEM (Dulbecco Modified Eagle's Medium, Gibco™) supplemented with 10% inactivated FBS, 1% Penicillin-Streptomycin, L-glutamine, and Sodium pyruvate. All cultures were maintained in a humidified incubator with 5% CO_2 at 37 °C. Monolayer cultures were performed in 96 well plates (96 wells, white

cell culture microplate, transparent bottom, Greiner bio-one) and flasks. Medium was renewed three times a week.

14. Pig Primary Hepatocytes sandwich cultures

To establish pig primary hepatocytes (PPH) sandwich culture, PPHs were seeded between a layer of Collagen Type I Rat Tail (Gibco, BD 354236) and Matrigel® (Sigma) matrixes as follows. Ninety-six-well plates for cell culture were coated with collagen solution of 0.05 mg/mL one day prior to cells seeding and stored at 4 °C. Collagen I Rat Tail solution was prepared as described before (see section 7 in Materials and Methods, "HepaRG sandwich culture ").

After isolation, PPHs were counted manually with Trypan Blue exclusion method (Trypan Blue Solution, 0.4%, Gibco). Then, PPHs were seeded in complete DMEM in monolayer as described in the previous section at a density of 70,000 cells/well, in plates previously coated with Collagen I Rat tail solution. Cells were incubated at 37°C, 5% CO_2 for 4-5 h, until attachment to the bottom of the plates was reached. After incubation, the medium was aspirated, and 100 µL/well of iced cold Matrigel® solution were added.

Matrigel® solution was prepared by adding Matrigel® Matrix (Sigma; concentration variable, reported in each bottle) to an iced-cold medium (to avoid Matrigel coagulation) to reach a final concentration of solution equal to 0.5 mg/mL. One hundred µL/well of Matrigel® solution were dispensed. PPH sandwich cultures were incubated at 37°C; 5% CO_2.

15. Pig primary hepatocytes spheroid culture

For the spheroids generation, PPH were counted and seeded in a concentration of 1500 cells per well in a ULA (ultra-low attachment) 96 well plate (Nunclon Sphera, 96U, Thermo Scientific). A total volume of 200 µL/well was used for seeding. Then, cells were centrifuged at 200 x g for 3 minutes to allow cells to group at the bottom of the wells and incubated overnight in a humidified incubator with 5% CO_2 at 37 °C. The medium was renewed every two days by removing 100 µL/well of the old medium and replacing it with the same volume of fresh medium. Spheroids cultures were maintained for one week; after this time, they were used for drug cytotoxicity assays. Images were taken with an optical microscope (Nikon Eclipse, Ti series, Japan), and the diameter was analyzed with NIS-Elements 3.0.

16. Immunofluorescence assay

For the immunofluorescence assay, PPHs were seeded in monolayer in a 96-well, white, transparent bottom cell culture microplate in two different concentrations, 4000 and 8000 cells/well, and incubated

overnight at 37 °C, in a humidified incubator with 5% CO_2. The next day, the medium was removed. Cells were incubated 10 min at RT with formaldehyde 4% (pre-warmed at 37 °C) for fixation. After incubation, formaldehyde was removed, and cells were washed three times with PBS 1X. Next, 0.1% solution of TritonX-100 (in PBS 1X) was added to the fixed cells and incubated for 15 min at RT for the permeabilization step. Then, cells were washed three times with PBS 1X and blocked by adding a solution of BSA 3% (prepared in PBS 1X). For this step, cells were incubated 1h at RT. Then, cells were incubated overnight, at 4 °C, with a goat anti-pig albumin (Goat anti-pig albumin A100-110 Bethyl Labs), as the primary antibody, diluted 1:200. The next day, cells were washed 5 times with PBS 1X, then a rabbit anti-goat, FITC conjugated (Rabbit Anti Goat IgG- FITC, 31509 Invitrogen) diluted 1:50 and HOECHST 33342 diluted 1:5000, were added and incubated 1h, RT, in the dark. Visualization of the positive cells was done by fluorescence microscope (Nikon eclipse, Ti series, Japan), and images were taken with Motic Images Plus 3.0.

17. Drugs' exposure of 2D, SW and 3D cultures of HepaRG, RPH and PPH

Twenty-four hours after cells' seeding in 96 well plates, monolayer, sandwich, or spheroids cultures were exposed to increasing concentrations of each test compound. HepaRG monolayer and sandwich cultures were maintained for 6 days before adding drugs, whereas RPH and PPH monolayer and sandwich were maintained for 2 days before adding compounds. All spheroids cultures were maintained for 6 days prior to drugs' exposure to allow mature spheroids' formation.

In total, six concentrations per drug were assayed, ranging from the Cmax (the therapeutic maximal drug concentration in human plasma) as the lowest to 32-fold Cmax as the highest. Drugs' values of Cmax were found in published literature (see Tab. 1 in "Results and Discussion," section 1).

Mother solutions of compounds were prepared by dissolving each drug in 100% DMSO in order to have a final concentration of 200X the highest drug's concentration. The other test concentrations were made starting from the mother solution and preparing 2-fold serial dilutions in 100% DMSO. Drug concentrations tested in all cell lines are provided in Table 2.

Test compounds in HepaRG, RPH, PPH	Abbreviation	Test concentrations (µM)
Diclofenac	DCF	500, 250, 125, 62.5, 31.3, 15.65
Acetaminophen	ACP	4000, 2000, 1000, 500, 250, 125
Troglitazone	TRG	200, 100, 50, 25, 12.5, 6.3
Fialuridine	FLD	60, 30, 15, 7.5, 3.75, 1.87
Amiodarone	AMI	300, 150, 75, 37.5, 18.75, 9.37
Nefazodone	NFZ	200, 100, 50, 25, 12.5, 6.3
Simvastatin	SIM	0.66, 0.32, 0.16, 0.08, 0.04, 0.02
Tamoxifen (ctr +)	TMX	200
Dimethyl sulfoxide (ctr -)	DMSO	0.5% (v/v)

Table 2. The table shows the drugs used to evaluate the cytotoxic effects at 48h and 14 days in HepaRG, RPH, and PPH cultured, each one in monolayer, sandwich, and spheroids formats. The right column indicates the final concentrations (µM) of the drugs applied to the cells. Each drug was tested in six different concentrations.

To expose cells to the drugs, 1 µL of each drug solution (200 X) was added from the drugs' mother plate to 199 µL of media contained in each well where cells were seeded previously. In this way, the overall DMSO concentration per well was 0.5% v/v. DMSO solution, at the final concentration of 0.5% v/v (DMSO/media), was used as negative control. Tamoxifen 200 µM final concentration, was used as positive control of toxicity.

To test acute toxicity, cell cultures with added drugs were incubated for 48h, and then cytotoxicity assay was performed. To test long-term toxicity, cells were maintained in culture for 2 weeks, and drugs were added following the procedure mentioned above every other day by renewing the media every time. On day 14, cytotoxicity assay was performed.

18. Cytotoxicity assay

Cell viability assessment was performed in HepaRG, RPH, and PPH cultured in monolayer, sandwich format, and spheroids by evaluating cellular ATP content using the CellTiter-Glo® Luminescent Cell Viability Assay (Promega), following the manufacturer's instructions. Briefly, the medium was renewed, and an equal volume to that of the media of CellTiter-Glo® reagent was added to each well. Plates were put in an orbital shaker for 2.5 minutes to mix the reagent and to induce cell lysis. Finally, plates were incubated at RT in the dark for 10 minutes, then luminescence signal was measured using BioTek Synergy H1 Plate Reader and recorded. Relative light units (RLUs) of luminescence signal were proportional to the ATP released by lysed cells and served, therefore, as a parameter of cells' viability.

19. Data analysis

At least three independent experiments were conducted to assess compounds' toxicity in each cell line. Raw data of luminescence signal were analyzed by generating mean and standard error of the mean, SEM (GraphPad Prism 8.3.0; GraphPad Software, San Diego, CA). Each value, subtracted from the blank (luminescence signal from wells with medium only), was then divided by the control (luminescence signal of cells treated with 0.5% DMSO only) and expressed as a percentage of viable cells with respect to the control. LC_{50} values were calculated using non-linear regression analysis with a sigmoidal dose-response model (GraphPad Prism 8.3.0; GraphPad Software, San Diego, CA).

Comparison between culture systems was performed using two-way ANOVA followed by Tukey's multiple comparison test or Sidak's multiple comparison test (GraphPad Prism 8.3.0; GraphPad Software, San Diego, CA). $p<0.05$ was considered statistically significant.

20. Reactions and metabolites generation in the *in silico* model assessment

To generate Phase-I and II reactions, we first provided SMARTS (SMiles ARbitrary Target Specification) IDs in the RDKit python package, each one referring to a specific moiety of a molecule. Then, the moieties provided were matched with the substrates' molecules to test, introduced as SMARTS as well.

In each reaction, reactants and products are defined as SMARTS notation. Each reactant is converted to one or more products.

The reaction was performed by matching patterns (IDs) defined in the reactions that are found in the selected substrate. If present, the defined pattern will be highlighted in the displayed molecule of the substrate (Fig. 1). Then, when the reaction is run, the system will generate and visualize all the plausible metabolism products.

An example is given in Fig.1. Here, the reaction performed, named "aromatic hydroxylation," consists of the introduction of OH groups into aromatic rings. In the example reported, the drug diclofenac was chosen as substrate (reactant). In this case, the system generates 18 products, some of which do not exist in reality.

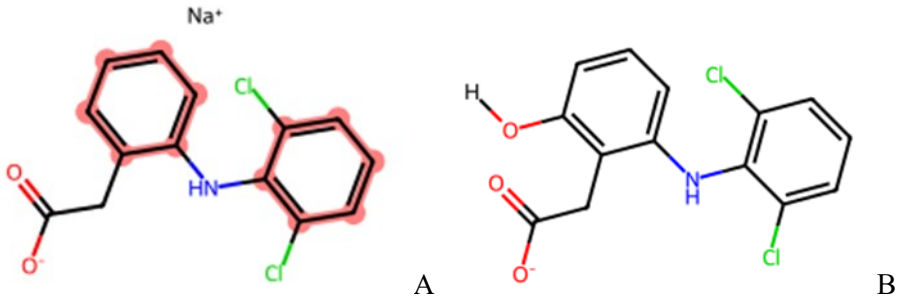

Fig.1. Aromatic hydroxylation reaction performed on Diclofenac. The matched patterns defined by the reaction are highlighted (A). One of the products, the hydroxylated Diclofenac, is shown (B).

RDKit generated around 2000 predicted products from 29 drugs undergoing Phase I reactions. Metabolites from Phase II reactions are not generated yet. Then, products were "filtered" based on valid smiles (complying with chemical criteria) and real compounds by comparison with the PubChem database.

21. KM prediction and Data analysis

All the simulations of compound-target proteins were performed by the KM prediction tool, a deep-learning system that enables to predict the Michaelis-Menten constant, Km, assigning it to each compound-target pair.

The list of hepatic proteins to test, including both enzymes and transporters, was selected in Uniprot. UniProt IDs were used in the KM prediction tool to refer to the respective hepatic protein. The 29 parent drugs and their metabolites, previously generated and filtered, were uploaded in KM prediction, provided as SMILES (Simplified Molecular-Input Line-Entry System), along with the total proteins, to run the interactions. The total entries generated were filtered to select only interactions with Km≤10μM and then listed from the lowest to the highest Km values.

Data were analyzed by dividing all the entries by target, identifying for each protein the correspondent substrate/s and Km.

Protein clustering was carried out by uploading each protein ID (Uniprot IDs) in the eggNOG-mapper.

Protein-protein network analysis was performed using String Version 11.5. to identify the proteins involved in each clustered pathway.

RESULTS AND DISCUSSION

One of the major causes of failure in the drug development process is related to safety concerns arising in clinical trials or drug withdrawals during the post-marketing phase. Principal human adverse reactions are predominantly associated with the liver, heart, kidney, and central nervous system (Cook et al., 2014; Olson et al., 2000; Sacks et al., 2014).

Most frequently, drug-induced liver injuries (DILI) represent the cause of such failure (Onakpoya IJ et al., 2016; Fisher K et al., 2015; Watkins PB, 2011).
As drug-related toxicity cannot be exhaustively predicted with animal models, an innovative, reliable alternative is needed. The intent of this project is to develop a method where *in vitro* and *in silico* approaches are integrated to accurately predict the toxicity of a drug.

1. Compounds and cell line selection

To validate the method object of this study, marketed compounds were accurately selected based on cytotoxicity data reported in scientific literature.
The goal of this project is to demonstrate the robustness of the method in toxicity prediction. As such, for its validation, approved drugs were used, as their adverse reactions have already been demonstrated and largely described. Once the model is validated and its solidity is demonstrated, it could be applied to examine the toxicity of innovative compounds investigated during the early stages of drug discovery.

To encompass as many drugs' adverse effects as possible, 28 marketed compounds were chosen, belonging to several medical classes, including antibacterial, antifungals, anticancer, anti-inflammatory, antiarrhythmic, antidepressant, immunosuppressant, antiviral, anticonvulsants, antipyretic, anti-cholesterol.

Drug selection relied on two main criteria: the severity of toxic reactions and the onset of these effects.

To accomplish the first criterion, we selected drugs with different known adverse effects in each body system, ranging from low-medium to high-toxic compounds, to simulate all possible cases of toxicity.

To completely describe drug-related toxicity, timing of occurrence is the other fundamental parameter that needs to be considered. In fact, some medicinal products evoke adverse effects right after a single, relatively potent dose administration. Indeed, the so-called acute toxic reactions are generally characterized by rapid onset, severe clinical symptoms, and unpredictability. By contrast, sometimes, patients exposed to repeated administrations at therapeutic doses over a long period of time do not show

any adverse effects at the beginning. However, adverse effects could occur in the long term, leading to chronic toxicity.

Therefore, to address the second criterion, the present study included both drugs associated with acute and chronic toxicity.

In this manner, it is possible to cover all possible cases of toxicity triggered by drugs and demonstrate that the method proposed here is reliable.

Taking advantage of the fact that the compounds tested in this study are approved drugs, I referred to the US FDA Toxicity Knowledge Base and EMA pharmacovigilance reports, searching for those that meet the criteria previously mentioned.

For accurate control of medicinal products' safety, FDA guidelines require the medicines exhibiting adverse events to be assigned to one of three different lists: Box Warning, Warning and Precautions, and Adverse Reactions, according to the severity of toxicity (FDA, 2011, Guidance for Industry warning and precautions, contraindications and box warning sections of labeling for Human Prescription Drug and Biological Products). Life-threatening agents or drugs' adverse events leading to patient hospitalization are labeled as Box Warnings while Warning and Precaution labels are applicable to those drugs with clinically significant adverse reactions but not life-threatening. Finally, the Adverse Reactions label is assigned to compounds with fewer toxicity concerns (Code of Federal Regulations). Withdrawn drugs are also remarked within this classification.

Pharmacovigilance reports are continuously updated by the EMA to warrant the safety of approved drugs in the post-marketing phase. It is possible to access those reports to be aware of any toxicity alerts related to commercialized medicines.

For the selection of the compounds panel to test in this study, I referred to both the FDA classification and EMA reports. High toxic compounds were elected among the Black Box warning labeled drugs list, while drugs included in the Warning and Precaution and Adverse Reactions lists were selected as medium-low toxic compounds.

In addition, few withdrawn drugs were included in this study as representatives of acute severe-toxicity inducers in specific organ *in vitro* models. Conversely, few compounds with ambiguous or not proven toxicity were also included as examples of safe drugs.

The complete list of drugs investigated in the present study is shown in Table 1, along with the corresponding medical class, the Cmax in the human species, and the related toxic reactions.

Drug	Therapeutic class	Cmax	Toxic effects	References
5-Fluorouracil (5FU)	Chemotherapic	6.23 µg/mL	Cardiotoxicity, acute coronary syndrome/myocardial infarction	Casale F et al., 2004; Sara JD et al., 2018; Lamberti M et al., 2014
Acetaminophen (ACP)	Antipyretic	12-14 µg/mL	Liver necrosis	Gold JR et al., 2023; Mingzhu Yan et al., 2018; Yoon E et al, 2016; Mazaleuskaya et al., 2015
Acyclovir (ACV)	Antiviral	0.45-0.52 µg/mL	nausea, vomiting, abdominal pain and rush	Taylor M and Gerriets V, 2023; Gnann JW Jr, et al., 1983; Yorulmaz A et al., 2016
Amiodarone (AMI)	Antiarrhythmic	1.4 µg/mL	DILI; pulmonary, cardiac, and thyroid gland toxicity	Meng X et al., 2001; Stravitz RT, et al., 2003; Ramachandran A et al., 2018; Wolkove N, Baltzan M, 2009; Barrett B, Bauer AJ, 2021
AmphotericinB (AMB)	Antifungal	0.7 mg/kg	Acute Kidney Injuries	Deray G, 2002; Tragiannidis A et al., 2021; Noor A, Preuss CV, 2023
Astemizole (AST)	Antihistaminic	0.0036 mg/L	Cardiotoxicity, hERG channel inhibition	Asai T et al., 2021; Bishop RO, Gaudry PL, 1989; Lehmann DF et al., 2018
Bleomycin (BLE)	Anticancer	0.1-0.5 mU/mL	Lung pneumonitis and fibrosis	O'Sullivan JM et al., 2003; Hay J et al., 1991; Tomas Reinert et al., 2013 Taparra K et al., 2019; Oken MM et al., 1981
Bortezomib (BOR)	Antibiotic; Anticancer	20.4 ng/mL	Peripheral neuropathy	Moreau P et al., 2012; Tan CRC et al., 2019
Ciprofloxacin (CIP)	Antibiotic	1.26 µg/mL	Tendinopathies, peripheral neuropathy, and neuropsychiatric adverse effects	Sudo RT et al., 1990; Thai T et al., 2023
Colistin (COL)	Antibiotic	0.6-7.8 µg/mL	Nephrotoxicity	Zabidi MS et al., 2021; Gai Z et al., 2019
Cyclophosphamide (CYC)	Anticancer	49 µg/mL	Myelosuppression, Pneumonitis, pulmonary fibrosis, Nephrotoxicity (hemorrhagic cystitis and bladder fibrosis)	Yang L et al., 2015; Malik SW et al., 1996; Patel JM, 1990; Santos MLC et al., 2020.
Dexamethasone (DEX)	Antiinflammatory	0.097 µg/mL	Gastric disorders, fluid retention, electrolyte imbalances, weight gain, nausea, vomiting, acne, agitation, and depression	Harahap Y et al., 2009; Polderman JAW et al., 2019
Diclofenac (DCF)	Analgesic	17.7-17.9 µg/mL	Mitochondria impairment	Leuratti C et al., 2019; Xu JJ et al., 2008; Bort r et al., 1998
Doxorubicin (DOX)	Anticancer	630.4 ng/mL	Cardiotoxicity, nephrotoxicity, hepatotoxicity, neurotoxicity, lung toxicity	Barpe DR et al., 2010; Liston DR et al., 2017; Chatterjee K et al., 2010; Kaviyarasi Renu et al., 2022

Erythromycin (ERY)	Antibiotic	1.8 µg/mL	indigestion and abdominal pain; allergic reactions; arrhythmia.	National Center for Biotechnology Information (2024); Carter BL et al., 1987; Hancox JC et al., 2014; Jorro G et al., 1996.
Fialuridine (FLD)	Antiviral	0.24 µg/mL	Acute liver failure, Mitochondria damage, reactive oxygen species formation, lipid accumulation, apoptosis induction,	Bowsher RR et al., 1994 Hendriks DFG et al., 2019
Gentamycin (GEN)	Antibiotic	20 µg/mL	Nephrotoxicity, ototoxicity	Hodiamont CJ et al., 2022; Blunston MA et al., 2015
Imipramin (IMI)	Antidepressant	0.96-1.44 µg/mL	Central nervous system toxicity, sedation, confusion, dizziness; cardiac arrhythmia	Asadpour E and Sadeghnia H, 2012; Rohner TJ Jr and Sanford EJ, 1975; Khalid MM and Waseem M, 2024
Isoniazid (ISO)	Antituberculosis	3 µg/mL	Neurotoxicity, peripheral neuropathy, hepatotoxicity	Peloquin CA, 2002; Badrinath M, John S, 2022; Wang P et al., 2016
Nefazodone (NFZ)	Antidepressant	µg/mL	Severe acute liver failure, hepatitis, cholestasis	Garside et al., 2014; Aranda-Michel J et al., 1999; Lucena MI et al., 1999
Nitrofurantoin (NIT)	Antibacterial	0.8- 1.81 µg/mL	chronic pneumonitis and pulmonary fibrosis	Wijma RA et al., 2018; Milazzo E et al., 2021; Batzlaff C and Koroscil M, 2020
Rapamycin (RAP)	Immunosuppressant; Antibiotic	67.4±22.8 ng/L	Diabetes-like syndrome, thrombocytopenia, leukopenia, pulmonary and renal toxicity	Emoto C et al., 2013; Buhaescu I et al., 2006; Barlow AD et al., 2013
Simvastatin (SIM)	Anti-cholesterol	5.56 ±2.39µg/L	Muscle toxicity	Moon SJ et al., 2017; Jeeyavudeen MS et al., 2022; Di Stasi SL et al., 2010
Tamoxifen (TMX)	Anticancer	59.1-63.6 ng/ml	Genotoxicity, ROS formation, hepatotoxicity, retinopathy	Fuchs WS et al., 1996; Yang G et al., 2013
Trazodone (TRZ)	Antidepressant	1.48 µg/mL	arrhythmias	Kale P, Agrawal YK et al., 2015; Soe KK and Lee MY, 2019; Mohan G et al., 2023
Troglitazone (TRG)	Antidiabetic	2.8 µg/mL	Liver Failure; mitochondria dysfunction; cholestasis (BSEP inhibition)	Xu JJ et al., 2008; Dirven H et al., 2021; Gale EA, 2001 Masubuchi Y, 2006 Funk C et al., 2001; Dawson S et al., 2012
Valproic acid (VAL)	Antiepileptic	50-100 µg/mL	Encephalopathy, hepatotoxicity	Tseng YJ et al., 2020; Wu J et al., 2021; Kesterson JW et al., 1984
Vancomycin (VAN)	Antibacterial	10-40 µg/mL	nephrotoxicity	Rybak MJ., 2006; Bamgbola O, 2016

Zidovudine (AZT)	Anti-HIV	0.49 µg/mL	Anaemia, cell proliferation impairment	Morris DJ, 1994; Unadkat JD et al., 1990

Table 1. The panel of drugs investigated in the present study includes therapeutic function and putative mechanism/s of toxicity in the human body.

Amiodarone, one of the most commonly used antiarrhythmic agents, is associated with a high risk of DILI and pulmonary, cardiac, and thyroid gland toxicity. Typically, toxicity is associated with long-term treatments of amiodarone. However, cases of idiosyncratic reactions were reported after intravenous administration for emergency treatments of arrhythmias (Livertox, 2016; Wolkove N et al., 2009). For these reasons, the FDA introduced amiodarone to the list of black box warning-labeled drugs and recommended the use of this medicinal product only for life-threatening arrhythmia (Siddoway LA, 2003). The mechanism of amiodarone's toxicity is ascribed to the impairment of mitochondrial functions, membrane lipids peroxidation, and the damage of fatty acid catabolism (Stravitz RT et al., 2003; Ramachandran A et al., 2018). In the present study, amiodarone was selected to validate its cytotoxicity in liver, heart, and lung *in vitro* models.

Nefazodone is a serotonin and noradrenaline reuptake inhibitor introduced into the market in 1994 as an antidepressant (Goldberg RJ, 1995). Cases of fatal acute hepatotoxicity led to its withdrawal in 2003 in Europe, while in the US, it is still used to treat severe cases of depression that do not respond to other therapies (Spigset O et al., 2003; Choi S, 2003). The mechanism of nefazodone-induced hepatotoxicity remains controversial and might be triggered by toxic compounds derived from nefazodone's metabolism. The most plausible mechanism of nefazodone hepatotoxicity seems to be related to the OXPHOS enzymes' impairment in mitochondria along with ROS production (Silva AM et al., 2016). Acute hepatitis and cholestasis are the acute adverse events happening after a few weeks of nefazodone treatments, whereas serum levels of liver biomarkers like AST (aspartate aminotransferase) and ALT (alanine aminotransferase) can slightly exceed the normal thresholds. Cases of liver failure related to nefazodone's chronic treatments have an incidence of 1 per 250,000 (Voican CS et al., 2014).

Troglitazone is an anti-type II diabetes that was launched into the market in 1997. Only three years later, it was discontinued due to severe cases of hepatic injuries. Troglitazone was responsible for 90 cases of liver failure leading to death or liver transplantation (Gale EA, 2001). Reactive metabolites of troglitazone seem to trigger troglitazone`s toxic effect by binding cell macromolecules and causing mitochondria dysfunction (Masubuchi Y, 2006). Previous studies also described the inhibition of Bile Salts Export Pump (BSEP) in human hepatocytes by troglitazone with the consequent intracellular accumulation of bile acids, the initiation process of cholestasis (Funk C et al., 2001; Dawson S et al., 2012).

Both nefazodone and troglitazone are used in this study to investigate severe hepatotoxicity related to different mechanisms of action.

Trazodone is an antidepressant with a structure analogous to nefazodone. Trazodone exerts its pharmacological properties through the inhibition of serotonin receptors, particularly 5-HT2A, as well as through antihistaminic and antiadrenergic actions, including the blockade of alpha-1 adrenergic receptors. Cardiotoxicity is a significant concern associated with trazodone use, particularly in cases of overdose, where it can lead to severe and life-threatening arrhythmias. Studies by Soe KK and Lee MY (2019) and Mohan G et al. (2023) have reported cases of trazodone overdose resulting in arrhythmias. This adverse effect is believed to be mediated by the inhibition of hERG (human Ether-à-go-go-Related Gene) channels by trazodone (Lee S et al. 2016). In your study, trazodone was selected as a representative example of a high-risk drug, and its potential for cardiotoxicity was assessed in cardiomyocytes.

The antihistaminic agent astemizole, initially developed for allergic rhinitis, was banned worldwide in 1999 (Gottlieb S, 1999). Its off-target effect, the inhibition of voltage-dependent heart hERG channels, was found to be responsible for severe cardiotoxic effects (Asai T et al., 2021). *In vitro* myocardiocyte models were used in this study to confirm the cardiotoxicity of astemizole.

The non-steroidal anti-inflammatory drug diclofenac remains one of the most widely used drugs for inflammation and pain treatment. Cases of acute and chronic toxicity have been reported in the last decades, particularly liver damage related to the drug. While initially it was thought that the hepatotoxicity of diclofenac was linked to hypersensitivity phenomena, through the formation of adducts hepatic proteins-drug, subsequent studies have shown that the main mechanism of hepatotoxicity is due to specific metabolites of the drug (Pumford NR et al., 1993; Miyamoto et al., 1997). The main mechanism of diclofenac's toxicity is mitochondrial damage, resulting in cell ATP depletion. Although this effect is triggered by diclofenac parent compound, some metabolites have been identified as responsible for mitochondrial damage. Specifically, 5-OH diclofenac and N,5-(OH)2-diclofenac appear to be responsible for mitochondrial impairment due to NADPH consumption following redox interchange reactions between the two metabolites (Bort et al., 1998). In this study, diclofenac was used to validate its hepatotoxicity in short- and long-term assessments.

Doxorubicin is an antibiotic agent extracted from *Streptomyces peucetius* bacterium, widely used as an anti-neoplastic agent since the 60s. Doxorubicin belongs to the anthracycline family, and it is used to treat hematologic and several types of solid tumors. Despite its effectiveness, this agent is characterized by multi-organ toxicity, with cardiotoxicity being the most relevant one. Other toxic effects were observed in the kidneys, pulmonary tissue, liver, nervous system, and reproductive organs (Kaviyarasi Renu et al., 2022; Chatterjee K et al., 2010; Pugazhendhi A et al., 2018; Eisenbeis CF et al., 2001). The principal mechanism of doxorubicin toxicity is believed to be the promotion of oxidative stress caused

by ROS production overwhelming cells' antioxidant defenses, which in turn triggers mitochondria dysfunction, inflammation, and cell death (Oktay T et al., 2013; Mia Baxter-Holland and Crispin R Dass, 2018). Therefore, doxorubicin represents an interesting example of drug-induced toxicity in several body districts and was tested in the present study to assess cytotoxicity in cardiomyocytes, human kidney cells, human T-lymphocytes, and human lung fibroblasts.

Cyclophosphamide is an alkylating agent widely approved for clinical use in the treatment of various cancers, including lymphoma, leukemia, breast cancer, and ovarian. However, myelosuppression, pulmonary toxicity, and nephrotoxicity have been often associated with cyclophosphamide. Specifically, cyclophosphamide can cause interstitial pneumonitis, and its prolonged or high-dose exposure may lead to pulmonary fibrosis. (Malik SW et al., 1996; Patel JM, 1990; Kachel DL and Martin WJ 2nd, 1994). Nephrotoxic effects, particularly manifest as hemorrhagic cystitis and bladder fibrosis in chronic treatments. (Santos MLC et al., 2020). For these reasons, in this study, cyclophosphamide was tested for acute cytotoxicity in lung fibroblast and renal tubular human cell lines.

The antimetabolite 5-Fluorouracil is the third most common drug used for solid tumor treatment worldwide (Sara JD et al., 2018; Grem JL, 2000). Among chemotherapy drugs, 5-FU is recognized as the second most common agent causing cardiotoxicity after anthracyclines (e.g., doxorubicin) (Sara JD et al., 2018). Mechanisms of cardiotoxicity include autoimmune injury of the myocardium, endothelial impairment, thrombosis, as well as myocardial damage and induction to necrosis (Sorrentino et al., 2012). 5-FU also could cause gastrointestinal and skin toxicity as well as myelosuppression (Macdonald JS, 1999). Both 5-fluorouracil and doxorubicin were used to test cardiotoxicity by exposing cardiomyocytes to several concentrations of the compounds.

Rapamycin, also known as sirolimus, is a macrolide compound with strong immunosuppressive properties used to prevent rejection after transplantation. Rapamycin also shows important anti-proliferative functions, demonstrating the capacity to reduce cell proliferation and cancer progression (Blagosklonny MV, 2023); therefore, it is also used as an anti-neoplastic agent. Lately, important anti-age functions of rapamycin have been discovered. Indeed, it was demonstrated that the drug's capacity to delay the onset of age-related pathologies (Selvarani R et al., 2021). Besides typical side effects like anemia, leukopenia, thrombocytopenia, and hypercholesterolemia, there is evidence that rapamycin has detrimental effects on pancreatic β-cells and peripheral insulin sensitivity (Barlow AD et al., 2013). Also, pulmonary and renal toxicity were recognized as severe complications related to rapamycin treatments (Buhaescu I et al., 2006). In the present study, rapamycin has been tested in vitro in human T-lymphocytes to explore toxic effects on the immune system.

Amphotericin B is an antifungal medication approved for the treatment of serious systemic fungal infections such as aspergillosis, candidiasis, cryptococcosis, blastomycosis, and coccidioidomycosis. Amphotericin B belongs to the polyene class, and its mechanism of action includes the binding to

ergosterol, the principal constituent of fungi membrane, provoking the disruption of the osmotic integrity of the membrane in fungi (Ellis D, 2002). However, the high incidence of nephrotoxicity related to amphotericin B limits its use. The direct impairment of epithelial cells' membranes, along with vasoconstriction at the tubular level, can cause tubular damage and a dramatic reduction of the glomerular filtration rate (Deray G, 2002). Therefore, amphotericin B was assayed in the human tubular cell line to assess *in vitro* acute nephrotoxicity.

Colistin and vancomycin, similarly to amphotericin B, were included in the set of drugs tested on HK-2 cells, the *in vitro* model of human epithelial tubular cells used in this study, to evaluate acute nephrotoxicity. Vancomycin, being one of the most commonly used antibacterial agents in hospitalized patients, has been associated with cases of nephrotoxicity. These instances typically involve tubular cell impairment and nephritis. While nephrotoxicity associated with vancomycin's use is clinically significant, it tends to occur majorly with exceptionally high doses of the medication (Vora S, 2016; Barceló-Vidal J et al., 2018; Kan WC et al., 2022). Conversely, acute kidney injury is a significant issue associated with colistin therapy, as highlighted in previous studies (Deryke CA et al., 2010; Özkarakaş H et al., 2017). Due to concerns about nephrotoxicity, the use of colistin was largely abandoned in the 1970s. However, in recent years, colistin has regained importance due to the emergence of multidrug-resistant bacteria. As a result, it is now being used to treat infections caused by multidrug-resistant gram-negative bacteria, for whose few effective treatment options exist. Despite its nephrotoxic potential, colistin remains a valuable tool in combating these challenging infections.

Bortezomib is a first-in-class proteasome inhibitor introduced in the market as an antitumor agent for multiple myeloma and mantle cell lymphoma treatment (Richardson PG et al., 2003; Tan CRC et al., 2018). However, bortezomib-induced peripheral neurotoxicity often requires regimen adjustments, sometimes limiting its use (Tan CRC et al., 2018; Argyriou AA et al., 2014; Meregalli C, 2015). Bortezomib neurotoxicity was assayed in our study by exposing human glioblastoma and mouse neuroblasts to the drug.

Acetaminophen (paracetamol) is the most commonly prescribed antipyretic drug used also to treat moderate pain for its minor analgesic properties. Hepatotoxicity induced by acetaminophen is the most studied case of DILI worldwide. The mechanism of acetaminophen`s hepatotoxicity has been elucidated and fully described, and it is known to be triggered by the accumulation in the liver of NAPQI, its toxic metabolite. At therapeutic doses, acetaminophen is mainly metabolized and transformed into glucuronide and sulfate conjugates. Only a small percentage of the drug is converted into NAPQI, a reactive intermediate, which is quenched by GSH conjugation. However, when administered at overdoses, the GSH conjugation pathway becomes overwhelmed, and NAPQI accumulates inside the hepatocytes, causing liver damage and leading to acute liver failure. Moreover, it has been observed that other factors and processes contribute to hepatotoxicity induced by acetaminophen besides the formation of NAPQI. Mitochondria impairment, oxidative stress, DNA damage, and apoptosis were found to be

related and triggered by high doses of acetaminophen and may contribute to the different hepatocyte damage that is observed between human and animal species (Yamada N et al., 2020; Zheng J et al., 2021; Abdullah-Al-Shoeb M et al., 2020).

Acetaminophen represents a useful model for studying hepatotoxicity, as it has a high safety profile at therapeutic doses and severe toxicity at overdose, triggered by liver metabolism. In this study, acetaminophen was evaluated in human and animal hepatocytes to determine its dose-dependent toxicity and different outcomes between species.

Fialuridine is a nucleoside analog developed in 1993 as a potential therapy for hepatitis B and discontinued because of five fatal cases of acute liver failure and two liver transplantations that occurred during Phase II clinical trials (McKenzie R et al., 1995). This was surprising because the drug did not show any sign of liver toxicity in animal studies. It is believed that mitochondrial damage is the principal mechanism of fialuridine's toxicity due to the compound's incorporation into mitochondrial DNA, causing impaired DNA synthesis (Mihajlovic M, Vinken M., 2022). Later on, hepatotoxicity induced by chronic exposure to fialuridine was demonstrated (Hendriks DFG et al., 2019). We included fialuridine in our set of compounds to test its toxicity in liver models *in vitro*, not only because of its known liver toxicity but also as an example of chronic toxicity and to compare the different effects across human and animal species.

Isoniazid, a pharmaceutical agent used for the treatment of tuberculosis, is a potent antibiotic associated with risk of acute and chronic toxicity. Acute toxicity can manifest with seizures due to GABA depletion induced by the drug, while toxicity in the long term mainly consists of peripheral neuropathy and hepatotoxicity (Badrinath M, John S, 2022; Wang P et al., 2016). Isoniazid induces both the inactivation of pyridoxine species and the enzyme pyridoxine phosphokinase necessary to convert pyridoxin into its active form, leading to depletion of this cofactor, fundamental for nerve integrity and GABA synthesis. Therefore, isoniazid represents a useful case of a drug that can be used to verify its toxic effects on neuronal cells.

The antiepileptic drug valproate was also included in the set of compounds to test dose-related toxicity in neuronal cell lines. In fact, cases of valproate-induced toxicity mainly occur during the drug regimen's adjustment. At overdose, valproate can cause encephalopathy with or without edema, which is generally reversible (Rupasinghe J, Jasinarachchi M, 2011).

We also chose two antibiotics, gentamycin and ciprofloxacin, and the antidepressant imipramine as compounds with a safe profile to test in our *in vitro* model of neuronal cell lines. Gentamycin is a bactericidal antibiotic from the aminoglycoside class used to treat Gram-negative infections. The main adverse effects of gentamycin are nephrotoxicity and ototoxicity, which occur after prolonged and systemic exposure to the drug (Blunston MA et al., 2015). Ciprofloxacin is a fluoroquinolone antibiotic that can treat various bacterial infections, such as urinary tract infections, pneumonia, gonorrhea,

digestive tract infections, skin and joint infections, acute bronchitis, and others. Ciprofloxacin has, in general, a good tolerability profile, and it is used in this study as an example of a safe drug tested in human lymphocytes and lung fibroblasts. However, some rare cases of nephrotoxicity leading to acute renal failure have been reported (Hajji M et al., 2018).

Simvastatin, belonging to statins, is one of the most common cholesterol-lowering agents used worldwide. Adverse effects related to statins in general and simvastatin are rare events. Serum elevation of the typical liver injury biomarkers (AST, ALT) was occasionally reported in long-term therapy with simvastatin (0.1%), totally reversible after drug discontinuation (Björnsson ES, 2017). Fatal liver injuries were only associated with patients with previous severe liver diseases (e.g., cirrhosis). Sporadic cases of autoimmune hepatitis-like diseases were also reported to be associated with simvastatin (LiverTox: Clinical and Research Information on Drug-Induced Liver Injury, Updated 2021). Overall, simvastatin-induced liver injury is estimated to be 1 per 100 patients; therefore, this drug was inserted in this study as an example of a safe compound with no hepatotoxic effects (Gillett RC Jr and Norrell A, 2011).

The antibacterial drug nitrofurantoin has reemerged as a valuable option for combating antibiotic-resistant infections, owing to its effectiveness against strains such as vancomycin-resistant enterococci and clinical strains of Escherichia Coli (Ten Doesschate et al., 2022). Unlike many other antibiotics, nitrofurantoin has not elicited significant resistance development among bacteria. However, rare pulmonary toxicity occurs with nitrofurantoin administration, ranging from acute effects due to hypersensitivity reactions to chronic pneumonitis and pulmonary fibrosis (Milazzo E et al., 2021; Batzlaff C and Koroscil M, 2020). For this reason, nitrofurantoin was introduced in the set of compounds to test in our human lung fibroblast MRC5 cell line to assess lung toxicity.

Like nitrofurantoin, the drug bleomycin has been tested in MRC5 cells to address acute pulmonary toxicity. Bleomycin, a natural derivative with potent antitumor activity, is notorious for its pulmonary adverse effects triggered by DNA damage and induction of lipid peroxidation, leading to cytotoxicity (Hay J et al., 1991). These effects can manifest with mild respiratory symptoms to severe pulmonary toxicity, which can lead to fatal outcomes in up to 10% of patients (Ge V et al., 2018). Lung injuries represent a significant limitation of bleomycin therapy, particularly in cancer treatment regimens.

Drugs with a low toxicity profile were also included in this study to validate the reliability of our cell-based *in vitro* testing in discriminating different levels of toxicity. These drugs include erythromycin, dexamethasone, acyclovir, and zidovudine (AZT).

Erythromycin is a broad-spectrum antibiotic, frequently prescribed for its high tolerability and safety. Occasionally, minor side effects can occur, such as gastrointestinal disturbances and abdominal pain (Carter BL et al., 1987). Rare cases of erythromycin allergic reactions and arrhythmias were reported (Hancox JC et al., 2014; Jorro G et al., 1996).

The potent corticosteroid dexamethasone has a wide variety of uses in clinics. Dexamethasone is used to treat inflammation, hypersensitivity reactions, allergies, sclerosis, and respiratory pathologies like asthma and dermatitis. Lately, dexamethasone has also been recommended for severe COVID-19 patients (Agarwal A et al., 2020). Adverse effects related to dexamethasone therapy are only minor and include gastric disorders, fluid retention, electrolyte imbalances, weight gain, nausea, vomiting, acne, agitation, and depression (Polderman JAW et al., 2019).

Lastly, two antiviral medications were included in our cytotoxicity assessment: zidovudine (AZT) and acyclovir. Acting as nucleoside inhibitors, they inhibit viral DNA replication. Although zidovudine is selective for the HIV reverse transcriptase, it can interfere with specific human DNA polymerases, causing impairment of cell replication. Therefore, anemia represents a major adverse event (Morris DJ, 1994).

Acyclovir is mostly used to treat herpes simplex and varicella-zoster virus infections. It has a wide therapeutic window; indeed, cases of overdose were rarely reported. Minor adverse events like nausea, vomiting, abdominal pain, and rush were associated with acyclovir intravenous administration (Taylor M and Gerriets V, 2023; Gnann JW Jr et al., 1983; Yorulmaz A et al., 2016). Previous studies by Poluektova et al. (1996) and Wingard et al. (1983) have demonstrated selective T-cell toxicity induced by acyclovir in both mice and humans. Considering this existing knowledge, the present study aims to investigate the *in vitro* toxicity prediction of acyclovir in human T-lymphocytes.

Zidovudine is known to affect cardiac mitochondrial function, causing cardiotoxicity, mainly in long-term treatments (Varga ZV et al., 2015; Mak IT et al.,2009). Therefore, this agent was tested to confirm its cardiotoxicity *in vitro* in cardiomyocytes.

Representative cell lines of the body systems were selected to investigate toxicity *in vitro* in the liver, kidney, lungs, nervous system, heart, and immune system. Respectively, the following cell lines were chosen for each system: HepG2, HK-2, MRC-5, T98G, Neuro-2a, H9c2, and Jurkat.
The toxicity of test compounds was evaluated by quantifying viable cells after compound application to the culture. The endpoint used to determine drug toxicity was the measure of cells' viability through ATP detection. This biomarker, in fact, is representative of metabolically active cells. The amount of ATP released by the cells exposed to the drugs under investigation was compared to that released by untreated cells, representing our control.

Seven drugs were tested in each organ model at six increasing concentrations per drug, starting from the Cmax, the therapeutic maximal drug concentration in human plasma, which is considered the lowest. The values of Cmax related to each drug were found in published literature (Table 1). All the concentrations tested ranged from the Cmax, as the lowest, to 32-fold Cmax, as the highest.

The assumption underlying the comparison of blood or plasma concentrations and cell culture medium concentrations is that the distribution of drugs between plasma and cells *in vivo* is comparable to that between cell culture medium and cells *in vitro* (Vinken M and Hengstler JG, 2018).

2. Evaluation of parent drugs cytotoxicity in human tissue-specific cell lines

As drug toxicity can derive from the action of parent compounds, the first step of the project was to analyze the effect of unmodified drugs in all cell lines cultured in monolayer or suspension as a simple model to resemble the main human organs. For each cell line belonging to a different apparatus, seven commercial compounds were selected depending on the different types and levels of toxicity published. The HepG2 cell line was adopted to test hepatotoxicity. HepG2 are human hepatoma cells widely used in toxicity screening and liver metabolism studies. Their unlimited lifespan, stability, and ease of handling represent their principal advantages in performing *in vitro* tests. Furthermore, HepG2 express many features of differentiated hepatocytes like triglycerides, bile acids, glycogen, lipoprotein synthesis, and plasma protein secretion (Donato MY et al., 2015). Thus, HepG2 are considered a valuable model to assess DILI. However, the poor expression of certain drugs metabolizing enzymes of the phase I and II reactions constitutes their major limitation (Guo L et al., 2011; Rodriguez-Antona C et al., 2002).
HepG2 monolayer cultures were exposed to six serial concentrations of diclofenac, acetaminophen, troglitazone, fialuridine, amiodarone, nefazodone, and simvastatin. The dose-response curves of each drug are shown in Fig.1.

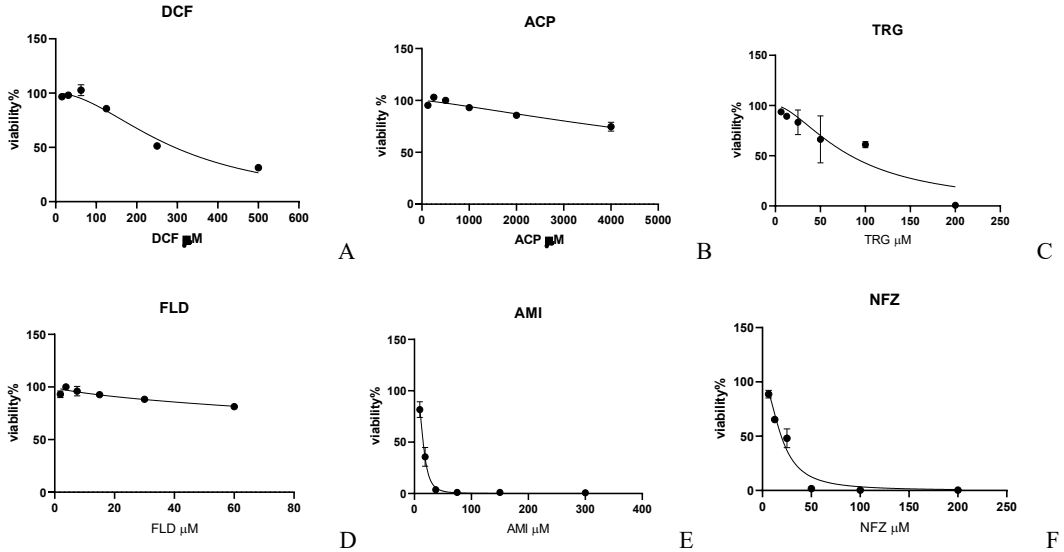

drugs	*LC_0 (μM)*	*LC_{50} (μM)*
DCF	30.5	**293.8**
ACP	175	**>4000**
TRG	<6.3	**83.8**
FLD	3.75	**>60**
AMI	<9.37	**15.3**
NFZ	<6.3	**19.2**
SIM	0.61	**>0.66**

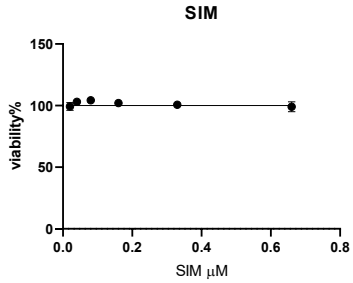

G H

Fig.1. Dose-viability curves of selected compounds in HepG2 monolayer cultures. Cells were treated with diclofenac (DCF), acetaminophen (ACP), troglitazone (TRG), fialuridine (FLD), amiodarone (AMI), nefazodone (NFZ) and simvastatin (SIM) for 48h. Drug concentration is indicated in μM. Cell viability was expressed in percentage relative to the control, represented by cells treated with DMSO only. Data are presented as mean ± SEM of three separate experiments. LC_{50} values reported in the table were calculated using non-linear regression analysis with a sigmoidal dose-response model (GraphPad Prism 8.3.0; GraphPad Software, San Diego, CA).

Based on cell viability after 48h of incubation with the drugs, nefazodone and amiodarone showed the highest toxicity with an LC_{50} of 19.2 μM and 15.3 μM, respectively (Table, Fig.1H). Simvastatin, fialuridine, and acetaminophen did not significantly affect cells' viability (Fig. 1B, 1D, 1G), while troglitazone and diclofenac showed a similar cytotoxic effect, increasing proportionally with the dose (Fig. 1A, 1C). Hepatotoxicity induced by amiodarone, nefazodone, troglitazone, and diclofenac was successfully reproduced by our HepG2 *in vitro* model. Indeed, liver injuries induced by these compounds are amply described (LiverTox: Clinical and Research Information on Drug-Induced Liver Injury, 2012; Buggey J et al., 2015; Babatin M et al., 2008; Stewart DE, 2002; Voican CS et al., 2014; Masubuchi Y, 2006; Funk C et al., 2001; Dawson S et al., 2012; Helfgott SM et al., 1990; Boelsterli UA, 2003; Scully LJ et al., 1993).

Conversely, the *in vitro* assessment did not show hepatotoxicity induced by acetaminophen. As already mentioned, liver damage induced by the antipyretic agent acetaminophen is very well known, and it is triggered by the toxic intermediate NAPQI, produced by acetaminophen metabolism operated by CYP2E1. The low toxicity observed in HepG2 is consistent with the fact that this cell line poorly expresses this isoform and, therefore, does not produce a sufficient amount of the toxic metabolite NAPQI (Kaplowitz N, 2004; Moyer AM et al., 2011; Guo L et al., 2011; Seo JE et al., 2019; Chen S et al., 2021).

HK-2 (Human Kidney-2), an immortalized proximal tubular cell line, was adopted as a model for a healthy human kidney. This cell line retains the phenotypic characteristic of differentiated proximal tubular cells with the advantage of indefinite growth (Ryan MJ et al., 1994). Therefore, HK-2 cells represented a valuable *in vitro* model of the human kidney system and were used in the present study to assess drug-related nephrotoxicity. For the toxicity test, this cell line was incubated with colistin,

cyclophosphamide, rapamycin, amphotericin B, doxorubicin, vancomycin, and dexamethasone. Dose-viability curves show the drugs' effects in HK-2 monolayer cultures (Fig. 2).

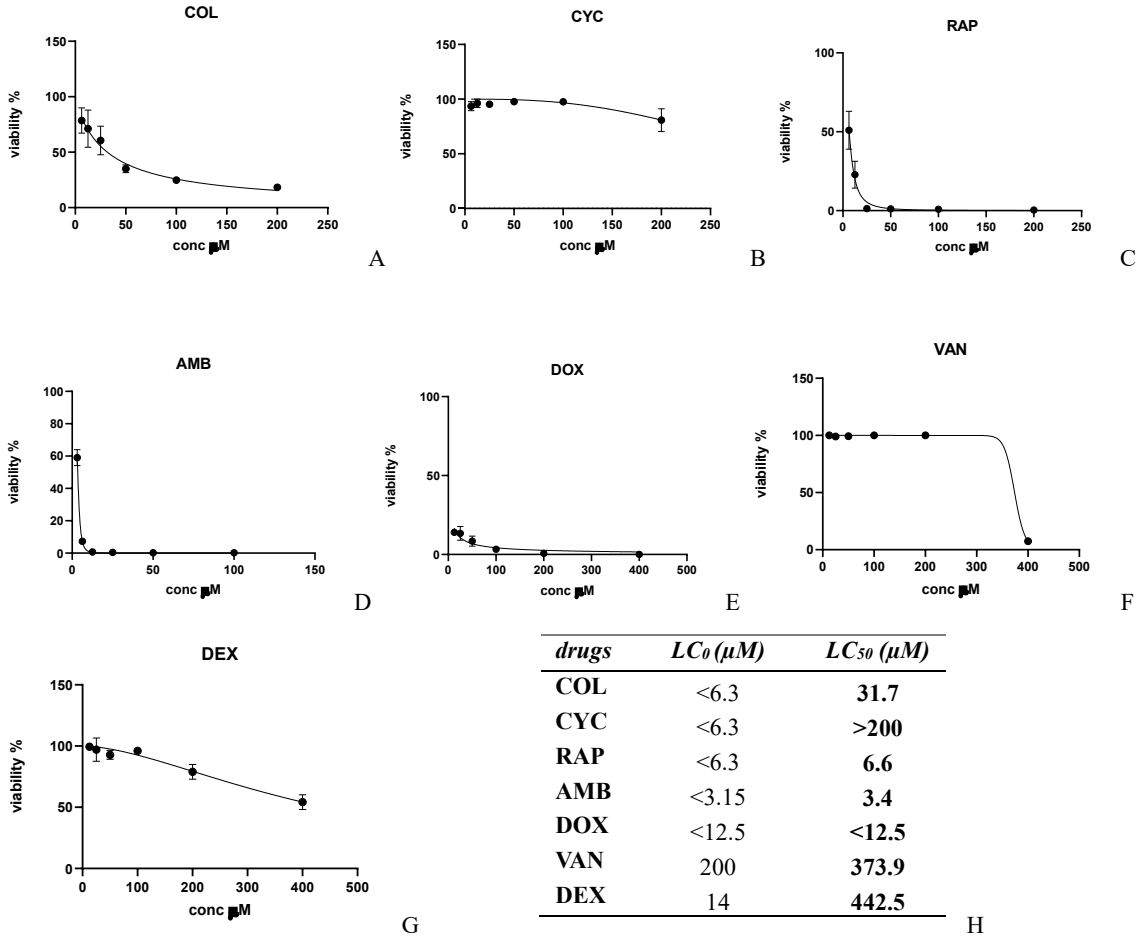

drugs	*LC0 (µM)*	*LC50 (µM)*
COL	<6.3	**31.7**
CYC	<6.3	**>200**
RAP	<6.3	**6.6**
AMB	<3.15	**3.4**
DOX	<12.5	**<12.5**
VAN	200	**373.9**
DEX	14	**442.5**

Fig.2. Dose-viability curves of selected compounds in HK-2 monolayer cultures. Cells were treated with colistin (COL), cyclophosphamide (CYC), rapamycin (RAP), amphotericin B (AMB), doxorubicin (DOX), vancomycin (VAN), and dexamethasone (DEX) for 48h. Drug concentration is indicated in µM. Cell viability was expressed in percentage relative to the control, represented by cells treated with DMSO only. Data are presented as mean ± SEM of three separate experiments. LC_{50} values reported in Table (H) were calculated using non-linear regression analysis with a sigmoidal dose-response model (GraphPad Prism 8.3.0; GraphPad Software, San Diego, CA).

All the compounds are known to induce acute kidney injury or nephrotoxicity, except for dexamethasone (Ordooei Javan A et al., 2015; Pike M, Saltiel E, et al., 2014; Fellström B, 2004; Deray G, 2002; Filippone EJ et al., 2017; Gupta S et al., 2021). For the latter, no toxicity at the therapeutic dose (12.5 µM) was confirmed in this study (Fig. 2G), as expected. At dexamethasone's highest concentration of 400 µM (32 times its therapeutic dose), cells' viability dropped to 50%. This result shows that compounds with safe profiles become toxic at overdoses, highlighting the fundamental principle of toxicology: "the dose makes the poison," introduced by Paracelsus.

High cytotoxicity was observed in HK-2 treated with amphotericin B, doxorubicin, and rapamycin, as shown by the dose-viability curves (Fig. 2D, 2E, 2C) and by their LC_{50} values (LC_{50} of 3.4, <12.5, 6.6 µM, respectively, Table in Fig.2H). As mentioned in the previous chapter, amphotericin B is known to induce tubular damage, impairing renal function (Deray G, 2002). Previous studies confirmed the toxic effects of amphotericin B in clinics, which had already been observed at a dose of 1 mg/kg/day (Eriksson U et al., 2001; Pasqualotto AC, 2008). Another study points out that amphotericin B dose should never exceed 3-4 mg/kg/day (Hamill RJ, 2013). For these doses, corresponding approximately to 15 µM and 60 µM, respectively, cells' viability in our assessment was zero, confirming the clinical findings in humans mentioned above.

The anti-tumor drug doxorubicin has a broader toxicity, exerted in various body systems, including kidneys. The mechanism is believed to be related to ROS production inducing membrane lipids peroxidation (Chiruvella V et al., 2020; Afsar T et al., 2020; Elsherbiny NM, El-Sherbiny M, 2014; Ayla S et al., 2011). The immunosuppressant rapamycin is known to induce acute renal failure in transplanted patients following tubular necrosis (Marti HP and Frey FJ, 2005; Lawsin L and Light JA, 2003; Buhaescu I et al., 2006). The present *in vitro* cytotoxicity assessment enabled the reproduction of toxicity of amphotericin B, doxorubicin, and rapamycin.

The chemotherapy drug cyclophosphamide, a well-known alkylating agent, is known to exert its action through DNA alkylation, causing high cell mortality. However, no severe cytotoxicity was detected in this study for cyclophosphamide, as shown in the dose-viability curve (Fig. 2C). At its highest dose, 200 µM, viability was slightly affected, remaining around 80% (Fig. 2C). This effect could be explained considering that the pharmacological effect of cyclophosphamide requires its transformation into the active compound by the CYP450 enzymes, mostly present in the liver, and only in the minority present in other body districts like intestine walls, lungs, kidney, and plasma (Clarke L and Waxman DJ, 1989).

Pulmonary acute toxicity was investigated in MRC-5, a cell line from a human fetal lung fibroblast. According to the dose-response curves, amphotericin B, doxorubicin, and amiodarone showed the highest toxicity outcomes (Fig. 3C, 3E, 3G), whereas cyclophosphamide and ciprofloxacin did not significantly induce cell mortality (Fig. 3B, 3D). Also, the drugs bleomycin and nitrofurantoin exerted dose-dependent mortality in the MRC-5 population (Fig.3).

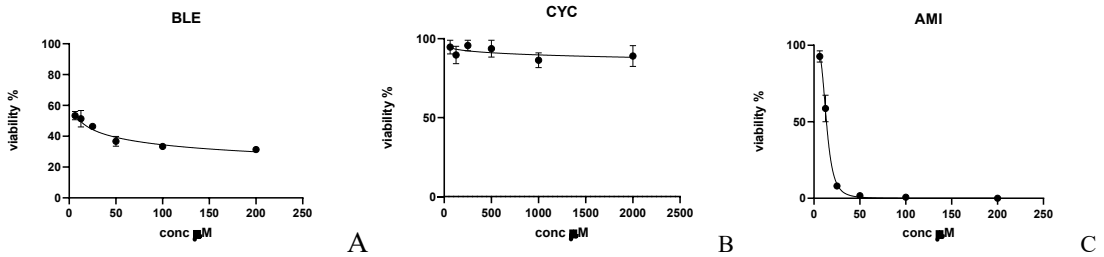

A B C

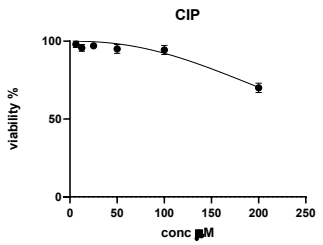

D

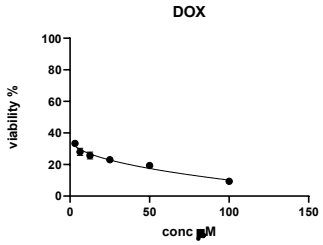

E

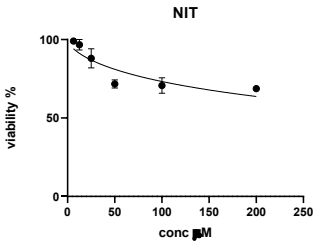

F

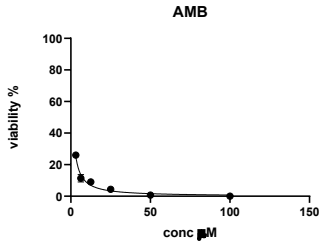

G

drugs	*LC_0 (µM)*	*LC_{50} (µM)*
BLE	<6.3	**11.8**
CYC	<63.5	**>2000**
AMI	<6.3	**13.6**
CIP	6.3	**>200**
DOX	<3.1	**<3.1**
NIT	6.3	**>200**
AMB	<3.1	**<3.1**

H

Fig.3. Dose-viability curves of selected compounds in MRC-5 monolayer cultures. Cells were treated with bleomycin (BLE), cyclophosphamide (CYC), amiodarone (AMI), ciprofloxacin (CIP), doxorubicin (DOX), nitrofurantoin (NIT) and amphotericin B (AMB) for 48h. Drug concentration is indicated in µM. Cell viability was expressed in percentage relative to the control, represented by cells treated with DMSO only. Data are presented as mean ± SEM of three separate experiments. LC_{50} values reported in Table (H) were calculated using non-linear regression analysis with a sigmoidal dose-response model (GraphPad Prism 8.3.0; GraphPad Software, San Diego, CA).

The high lethality exerted by doxorubicin is not surprising, given its potency as a chemotherapeutic agent. Acting as an intercalating DNA agent, doxorubicin induces necrosis and apoptosis in various organs, mainly the heart, brain, kidneys, and liver (Tacar O et al., 2013). Although pulmonary toxicity is not considered a primary site where adverse effects of doxorubicin are exerted, some studies reported dose-dependent damage of pulmonary tissue after doxorubicin administration (Eisenbeis CF et al., 2001). This effect was confirmed in our MRC-5 cell cultures. Indeed, at doxorubicin's lowest dose (3.1 µM), MRC-5 viability was already reduced to 40% (Fig. 3E).

Amphotericin B, primarily recognized for its nephrotoxicity, has been associated with cases of acute respiratory adverse events during drug infusion (Collazos et al., 2001). In our assessment, at the lowest concentration tested (3.1 µM), cells' viability was lower than 30%, and the entire cell population was killed after the single dose of 50 µM (Fig. 3G).

Pulmonary toxicity is recognized as one of the most severe adverse effects of amiodarone, occurring acutely after a few days of treatment or after years of chronic regimens (Wolkove N and Baltzan M, 2009; Papiris et al., 2010). Consistently with these findings, our assessment revealed a potent cytotoxic effect of a single dose of amiodarone on MRC-5 cells, evident as early as 48 hours.

As previously mentioned, cyclophosphamide, despite being a cytotoxic alkylating agent, does not exhibit toxicity in MRC-5 cells. This is likely due to the need for the drug to undergo transformation into its active metabolite in the liver to exert its effects. Similarly, ciprofloxacin, a commonly antibacterial agent used for treating respiratory infections, was included in our assessment to demonstrate its safety profile in our *in vitro* model using MRC-5 cells. Indeed, in our assessment, ciprofloxacin did not affect cell viability at increasing concentrations up to 100 μM, corresponding to 16 times its therapeutic doses (Terp DK and Rybak, MJ 1987) (Fig. 3D). However, when at ciprofloxacin 200 μM, MRC-5 viability decreased to approximately 65% (Fig. 3D).

Although pulmonary toxicity is rarely associated with nitrofurantoin, acute pulmonary adverse events have been reported in humans (Milazzo et al., 2021; Suliman et al., 2023; Pinerua and Hartnett, 1974). Lung injuries triggered by nitrofurantoin are typically associated with its chronic use (Weir M and Daly GJ, 2013; Holmberg L and Boman G, 1981). However, acute pulmonary reactions occur with a frequency of 1 in every 5000 patients (Holmberg L and Boman G, 1981; Kabbara WK and Kordahi MC, 2015; Huttner A et al., 2015). A recent case-report describes an acute pulmonary injury induced by nitrofurantoin at its therapeutic dose (Milazzo et al., 2021). Concordantly, our *in vitro* assessment indicates nitrofurantoin's acute effect slightly escalating with the dose (Fig. 3F).

Finally, the acute toxicity induced by bleomycin was clearly observed in MRC-5 cells, with an LC_{50} value close to its Cmax (Table 1 and Fig. 3). Importantly, this result underscores the low therapeutic index of this drug. Bleomycin-induced lung injury can manifest with varying onset and severity, underscoring the importance of considering such factors when establishing antitumor therapy based on this drug (Ghalamkari et al., 2022). A study conducted on 835 patients reported that 6.8% of them developed bleomycin-pulmonary toxicity, and 1% of the patients died (O'Sullivan JM et al., 2003). It is also reported that bleomycin pulmonary toxicity starts to occur at doses above 450.000 UI (Comis RL, 1992; Goldiner PL et al., 1978; Einhorn LH et al., 1989).

To investigate the impairment in the central nervous system induced by commercial medications, another set of compounds was tested in both T98G and Neuro2a cells. T98G is a human glioblastoma cell line. Despite not being neurons, T98G cells can still respond to neurotoxic insults and may exhibit some aspects of neurotoxicity. These cells express various signaling pathways relevant to neuronal function, making them a useful model for studying certain types of neurotoxicity. Neuro-2a are mouse neuroblasts isolated from brain tissue and were included in this assessment to compare neurotoxicity outcomes between species. Both cell lines were exposed to valproate, the antidepressant imipramine, the antibiotics gentamicin, isoniazid, and ciprofloxacin, and finally to bortezomib and amiodarone. Dose-viability curves show the acute effect of the drugs observed in the two species after a single dose administration (Fig. 4).

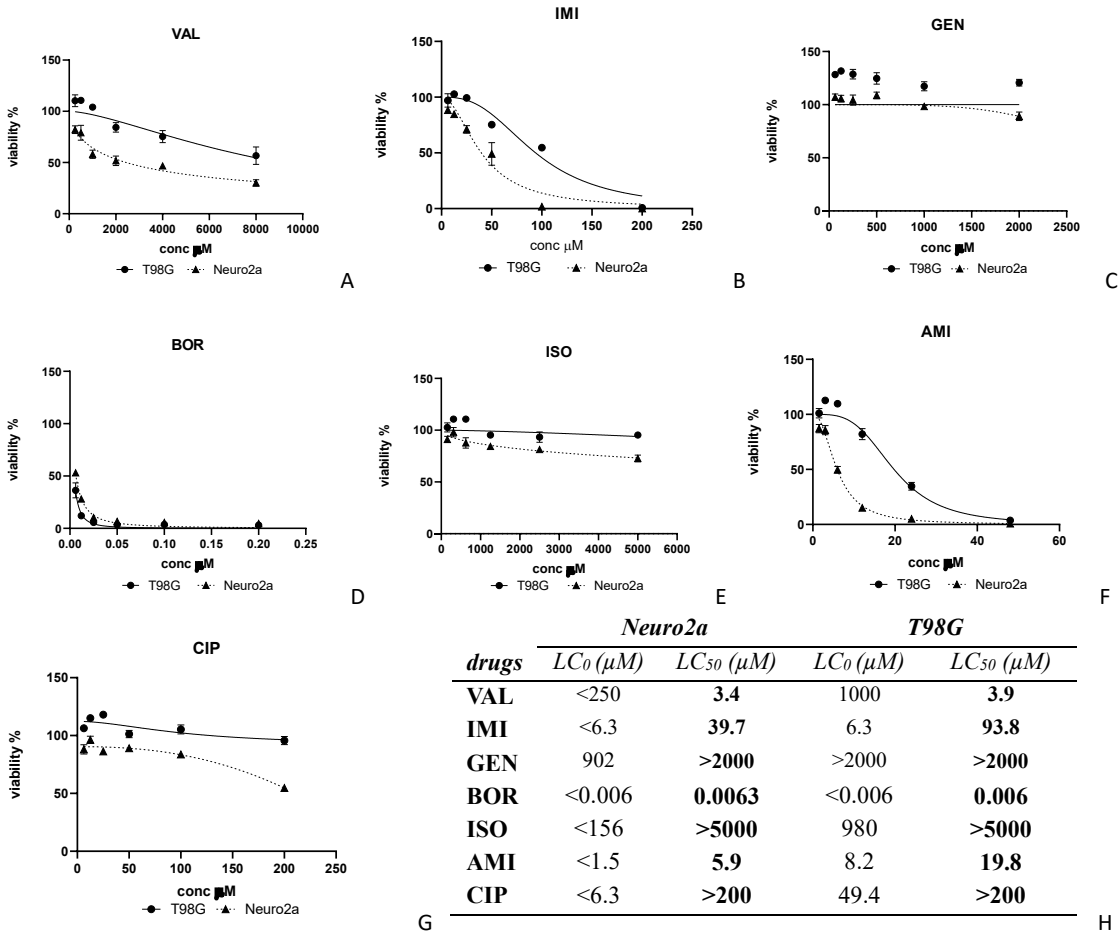

H

	Neuro2a		*T98G*	
drugs	*LC_0 (μM)*	*LC_{50} (μM)*	*LC_0 (μM)*	*LC_{50} (μM)*
VAL	<250	**3.4**	1000	**3.9**
IMI	<6.3	**39.7**	6.3	**93.8**
GEN	902	**>2000**	>2000	**>2000**
BOR	<0.006	**0.0063**	<0.006	**0.006**
ISO	<156	**>5000**	980	**>5000**
AMI	<1.5	**5.9**	8.2	**19.8**
CIP	<6.3	**>200**	49.4	**>200**

Fig.4. Dose-viability curves of selected compounds in T98G and Neuro2a monolayer cultures. Cells were treated with valproate (VAL), imipramine (IMI), gentamicin (GEN), bortezomib (BOR), isoniazid (ISO), amiodarone (AMI) and ciprofloxacin (CIP) for 48h. Drug concentration is indicated in μM. Cell viability was expressed in percentage relative to the control, represented by cells treated with DMSO only. Data are presented as mean ± SEM of three separate experiments. LC_{50} values (H) were calculated using non-linear regression analysis with a sigmoidal dose-response model (GraphPad Prism 8.3.0; GraphPad Software, San Diego, CA).

Gentamicin did not induce mortality in either T98G or Neuro2a cells (Fig. 4C). The results of this *in vitro* acute neurotoxicity assessment are consistent with previous findings where it is reported that ototoxicity is the major adverse effects of aminoglycosides, like gentamicin, while brain lesions were very rarely reported (Grill MF and Maganti RK, 2011).

Ciprofloxacin administration has been associated with peripheral neuropathy, cases of encephalopathy, and other neuropsychiatric events like seizures and confusion (Isaacson SH et al., 1993; Schwartz MT and Calvert JF, 1990; Refaeian A et al., 2023). However, toxicity in T98G and Neuro2a of ciprofloxacin was barely detected in our *in vitro* study (Fig.4G).

Similarly, the neurotoxic effects of the antitubercular drug isoniazid include peripheral neuropathy and seizure triggered by the depletion of GABA neurotransmitters in the central nervous system (Badrinath

M and John S, 2022). In our model, isoniazid did not induce mortality in T98G and slightly affected Neuro2a viability (Fig. 4E).

Among all, bortezomib showed the highest cytotoxicity, inducing cell death in 50% of both cells' populations already at its lowest dose (Fig. 4D). Bortezomib-induced peripheral neuropathy represents the major limit in its therapy. One of the principal mechanisms of neurotoxicity pathogenesis is proteasome inhibition, the mechanism of action of bortezomib, leading to impairment of the protein machinery that causes cell damage (Palanca A. et al., 2014).

Bortezomib-induced cytotoxicity was observed as an acute effect of the drug in our *in vitro* models, although cell toxicity is more prominent with chronic treatments.

The drugs valproate, imipramine, and amiodarone showed toxicity increasing proportionally with the dose (Fig. 4A, 4B, 4F). These drugs are, in general, well tolerated at therapeutic doses. However, at high doses, toxicity can occur. Imipramine, for its interaction with sodium ion channels, can induce alteration in neuronal electrical activity by giving abnormal EEGs (Fayez R and Gupta V, 2023).

Sedation is the primary side effect of valproate due to inhibition of GABA reuptake in neurons (Rahman M et al., 2023). Several studies reported that in cases of mild valproic acid poisoning, blood concentration was found between 100-450 mg/L, whereas in severe intoxications, blood concentration of the drug reached up to 1000 mg/L (Patel AR and Nagalli S, 2024; Manoguerra AS et al., 2008). Valproate's blood concentration of 1000 mg/L corresponds to a concentration of 6024 µM. Accordingly, in our study, valproate administered at 6000 µM reduced the viability of Neuro2a and T98G to 60% and 40%, respectively (Fig. 4A).

Although the mechanism of neurotoxicity of amiodarone is poorly understood, lipid intracellular accumulation, oxidative stress, and mitochondria dysfunction seem to trigger cell toxicity at amiodarone overdoses (Serviddio G et al., 2011).

Overall, Neuro2a showed higher susceptibility to amiodarone (LC_{50} =5.9 µM), imipramine (LC_{50} =39.8 µM), and valproate (LC_{50}>8000 µM) compared to the human T98G cells (amiodarone LC_{50}=19.8 µM; imipramine LC_{50}= 93.8 µM; valproate LC_{50}=2441 µM).

The higher sensitivity of Neuro2a cells compared to T98G to drug insults can be explained by the different characteristics of the two cell lines. T98G are tumor cells originating from the glia; therefore, they lack specific features of neurons like the typical electric activity and synapse formation (Stein GH, 1979; Pinevich AA et al., 2022). On the other hand, Neuro2a, deriving from neuronal tissue, expresses neurotransmitter receptors and ion channels found in neurons that make them relevant for neurotoxicity studies (LePage KT et al., 2005).

To test the potential cardiotoxicity of drugs, the H9c2 cell line was selected as an *in vitro* model. H9c2 cells are embryonic clone deriving from rat heart tissue, commonly used to study cardiac physiology and cardiotoxicity. H9c2 cells represent a valuable model in alternative to cardiomyocytes as they exhibit properties like spontaneous contractility and responsiveness to specific cardiac hormones and neurotransmitters (Kimes BW and Brandt BL, 1976; Louch WE et al., 2011). The embryonic derivation

of H9c2 gives the cells the advantage of high proliferation *in vitro* (Watkins SJ et al., 2011). On the other hand, they do not completely share features of primary differentiated cardiomyocytes.
The viability of H9c2 cells after single doses administrations of drugs is illustrated in Fig. 5.

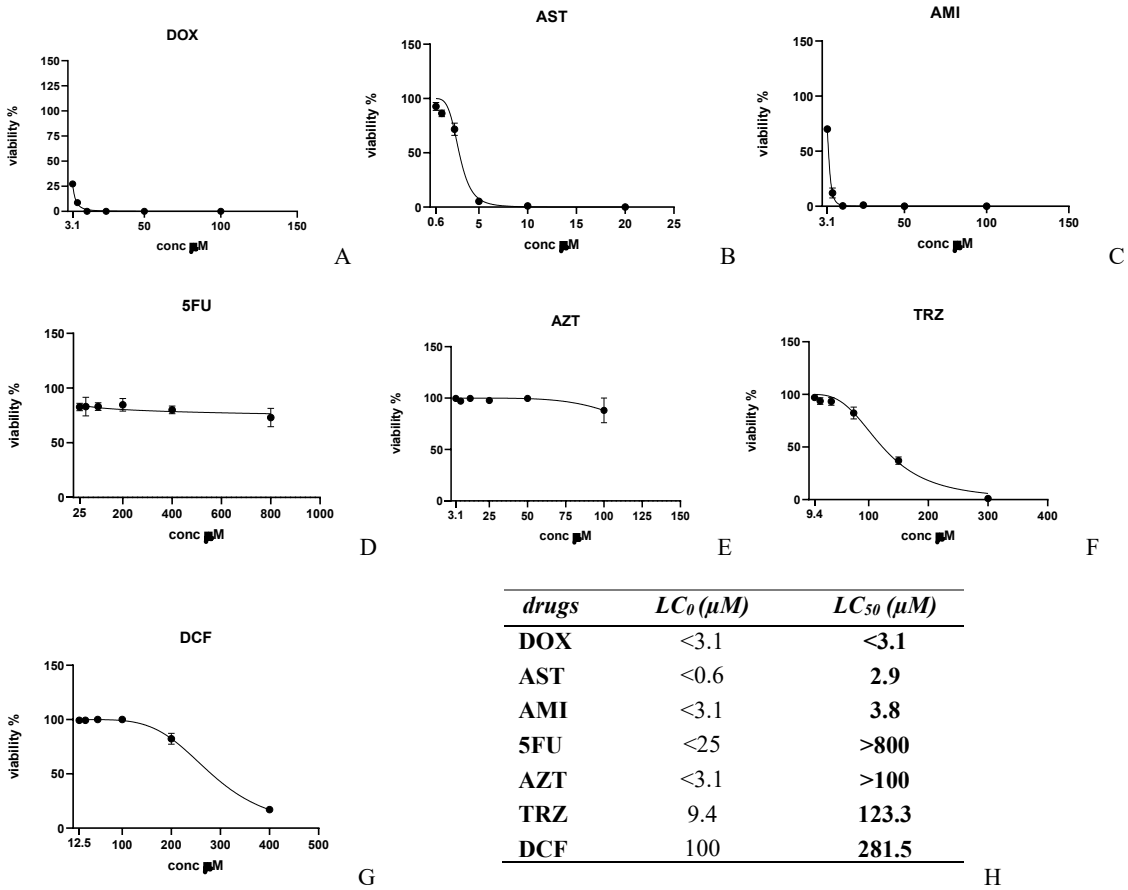

drugs	*LC_0 (µM)*	*LC_{50} (µM)*
DOX	<3.1	**<3.1**
AST	<0.6	**2.9**
AMI	<3.1	**3.8**
5FU	<25	**>800**
AZT	<3.1	**>100**
TRZ	9.4	**123.3**
DCF	100	**281.5**

H

Fig.5. Dose-viability curves of selected compounds in H9c2 monolayer cultures. Cells were treated with doxorubicin (DOX), astemizole (AST), amiodarone (AMI), 5-Fluororuracil (5FU), zidovudine (AZT), trazodone (TRZ) and diclofenac (DCF) for 48h. Drug concentration is indicated in µM. Cell viability was expressed in percentage relative to the control, represented by cells treated with DMSO only. Data are presented as mean ± SEM of three separate experiments. LC_{50} values reported in Table (H) were calculated using non-linear regression analysis with a sigmoidal dose-response model (GraphPad Prism 8.3.0; GraphPad Software, San Diego, CA).

After 48h of exposure, the antitumor agent doxorubicin, known for inducing severe cardiomyopathy (Wallace KB et al., 2020; Abdullah CS et al., 2019; Singal PK and Iliskovic N, 1998), resulted in the compound with highest toxicity followed by astemizole, a second-generation anti-histaminic drug, and the antiarrhythmic amiodarone.
The use of doxorubicin in cancer therapy is limited mainly for its well-known cardiac adverse effects. The mechanism of cardiomyocyte damage involves ROS production, lipid peroxidation, and mitochondria impairment, leading finally to heart failure, occurring in 10% of patients in therapy with

doxorubicin (Octavia Y et al., 2012). As reported in Fig. 5A, a marked reduction of cell viability was observed in our *in vitro* assessment as well as in other *in vitro* studies after two days of doxorubicin exposure (Louisse J et al., 2017).

Also, our cytotoxicity assessment on H9c2 cells confirmed the high acute toxicity of amiodarone and astemizole, consistent with findings reported in several studies (Hofmann et al., 2006; Varbiro et al., 2003; Smith SJ, 1994; Yun JS and Kim SY, 2015). The high lethality of these compounds is further demonstrated by their narrow therapeutic window, as indicated by their LC_{50} values being very close to their respective LC_0 values (see table in Fig. 5).

A marked reduction of cells' viability was observed only at high doses of diclofenac and trazodone. Indeed, the LC_{50} of these drugs (281.5 µM and 123.3 µM respectively) far exceed the respective values of Cmax (12.5 µM and 9.4 µM, refer to Table 1).

Previous studies confirmed, in fact, trazodone's and diclofenac's cytotoxicity at overdoses or chronic use of the drugs (Soe KK and Lee MY, 2019; Service JA and Waring WS, 2008; Moore N, 2020; Schmidt M et al., 2018).

Although cardiotoxicity is well recognized with the 5-fluorouracil therapy, this assessment showed only a slight decrease in H9c2 viability at 48h (Fig. 5D). 5-Fluorouracil is considered the second cause of cardiotoxicity, after anthracyclines (e.g., doxorubicin) in cancer therapy (Sara JD et al., 2018; Shiga T and Hiraide M, 2020). However, we did not observe significant effects on H9c2 viability in the acute exposure to the antiviral agent 5-Flurururacil, probably because cardiotoxicity occurs at repeated and long-term exposures to the drug (Fig. 5D).

Finally, AZT did not affect H9c2 viability at 48h in our test (Fig. 5E), despite dose-dependent cell death being described in heart tissue (Gao RY et al., 2010; Currie PF and Boon NA, 2003).

The last cell line investigated to assess the toxicity of parent compounds was Jurkat, derived from immortalized human T lymphocyte cells. Percentages of viable cells at increasing concentrations of drugs are shown in Fig. 6.

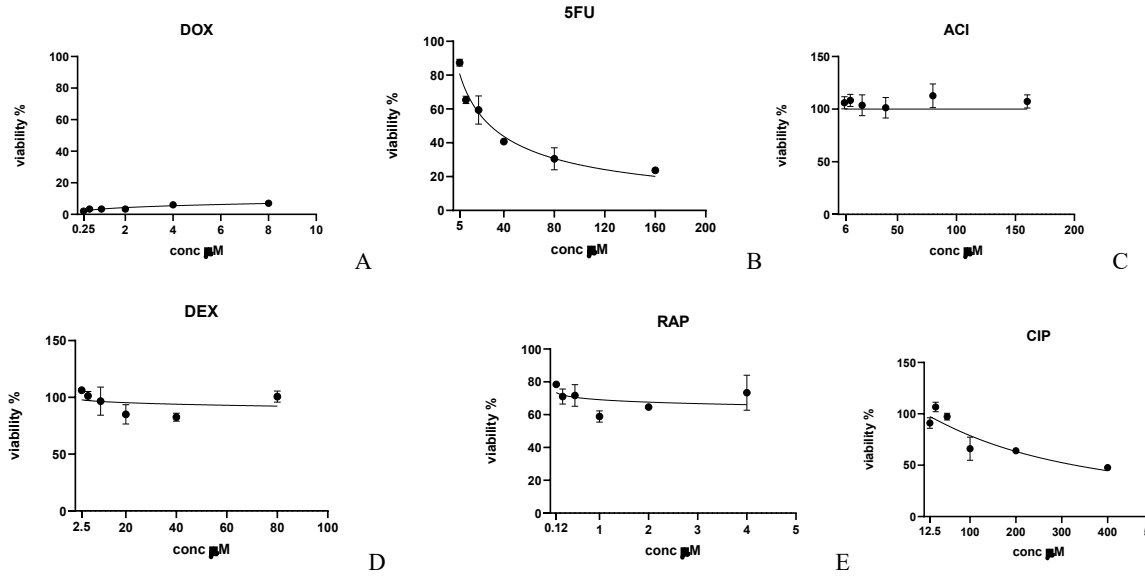

drugs	*LC_0 (µM)*	*LC_{50} (µM)*
DOX	<0.25	**<0.25**
5FU	<5	**29.5**
ACI	>150	**>150**
DEX	>80	**>80**
RAP	<0.12	**>4**
CIP	36.9	**328.9**
ERI	53.3	**318.8**

H

Fig.6. Dose-viability curves of selected compounds in Jurkat monolayer cultures. Cells were treated with doxorubicin (DOX), acyclovir (ACI), 5-fluorouracil (5FU), dexamethasone (DEX), rapamycin (RAP), ciprofloxacin (CIP) and erythromycin (ERI) for 48h. Drug concentration is indicated in µM. Cell viability was expressed in percentage relative to the control, represented by cells treated with DMSO only. Data are presented as mean ± SEM of three separate experiments. LC_{50} values reported in Table (H) were calculated using non-linear regression analysis with a sigmoidal dose-response model (GraphPad Prism 8.3.0; GraphPad Software, San Diego, CA).

Jurkat cells exhibited the highest susceptibility to doxorubicin, which induced the complete eradication of the cell population at its lowest dose of 0.25 µM (see Fig. 6A). This observation aligns with findings reported in the scientific literature, where doxorubicin has been shown to markedly reduce lymphocyte proliferation and induce apoptosis (Minderman H et al., 1991; Kalivendi SV et al., 2005).

On the contrary, acyclovir, dexamethasone, and rapamycin appear to be safer compounds in Jurkat cells, with their LC_{50} exceeding 32-fold their therapeutic concentration (the highest doses tested) (Fig. 6C, 6D, 6E). The drugs ciprofloxacin and erythromycin exhibited medium-low toxicity, inducing cell death in 50% of Jurkat's population at approximately 25 times their Cmax (refer to Table 1). In contrast, 5-fluorouracil demonstrated medium-high toxicity, with an LC_{50} value approximately 6 times its therapeutic dose. Taken together, these results align with previous studies where cytotoxicity induced by these drugs was investigated (Kobuchi S et al., 2017; Riesbeck K et al., 1998; Forsgren A et al., 1989; Wu L et al., 2007).

Overall, the tests performed in cell lines representatives of specific human tissues effectively replicated *in vitro* the acute toxic effects of the selected drugs described *in vivo*.

3. Liver toxicity assessment of drugs and their metabolites in human *in vitro* models

Only a few drugs are eliminated without undergoing any transformation after administration. Most of them undergo biotransformation before excretion. The liver is the principal organ where drugs' biotransformation occurs due to the presence of enzymes catalyzing Phase I and Phase II reactions.
Normally, this biotransformation is necessary to convert the parent drug into a (more) hydro-soluble form; sometimes, this conversion can activate the compound itself or generate toxic metabolites responsible for adverse effects. For this reason, the liver is normally the first organ where drug toxicity occurs.
In many cases, drugs' toxicological properties are due to hepatic metabolites (Baillie TA et al., 2007; Lammert C et al., 2010; Gómez-Lechón MJ et al., 2016; Uetrecht J, 2008). Therefore, from now on in this study, the liver was used as the key experimental system to assess the adverse effects of human drugs.
In the previous set of experiments, the toxicity of parent compounds was determined in several cell lines. In this section of the project, a subset of the investigated drugs was retested in liver *in vitro* models with the purpose of predicting toxicity related to parent drugs and their hepatic metabolites.
With the aim to develop a reliable *in vitro* model for hepatotoxicity prediction in humans, the cell line HepaRG was selected and cultured in three different systems: monolayer (referred to as 2D), sandwich (referred to as SW), and spheroids (referred as 3D) to compare sensitivity to toxicants' exposure across each cell culture model. Monolayer cultures were chosen as the simplest bidimensional system, whereas spheroids were chosen as a three-dimensional culture system. Sandwich cultures are considered bidimensional cultures as well, even though they exhibit some features of three-dimensional systems. Although they are constituted by a single cell layer, cells here are grown between two matrixes, resembling the interactions between cells and the extracellular environment occurring in the *in vivo* tissue.

Even though primary human hepatocytes remain the gold standard to emulate the hepatic tissue, HepaRG cells represent an optimal alternative as they retain the main phenotypic characteristics of primary hepatocytes. HepaRG, in fact, express liver metabolizing enzymes (e.g., the enzymes of the CYP450 family), transporters, and proteins at comparable levels to those of primary hepatocytes (Guillouzo A et al., 2007; Marion MJ et al., 2010; Anthérieu S et al., 2010). In addition, HepaRG cells are characterized by a strong proliferative activity and do not undergo the process of dedifferentiation, unlike primary cells (Aninat C et al., 2006). For these reasons, they can be grown for long periods of time and are currently being adopted as human liver models for long-term studies. The other important advantage of HepaRG is the absence of inter-donor variability, which is one of the critical aspects typical

of primary cells that very often causes a lack of reproducibility of results. Therefore, the HepaRG cell line was employed in this work as an accurate model for *in vitro* human liver culture.

To give a complete picture of the possible cases of drug toxicities, after exploring the effect of parent compounds, it is important to have a method that ensures the evaluation of adverse effects related to the drugs' metabolites. As already mentioned, HepaRG cells exhibit very similar metabolic capacities to those of primary hepatocytes. HepaRG's CYP450 enzymes are capable of detoxifying and transforming xenobiotics; therefore, they represent a precious tool for investigating liver injuries triggered by products of drugs' metabolism.

In this section of the study, a reduced set of drugs with different mechanisms of action and different proven toxicity in the liver was selected for cell treatment, consisting of diclofenac, acetaminophen, troglitazone, fialuridine, amiodarone, nefazodone and simvastatin (Fig. 8).

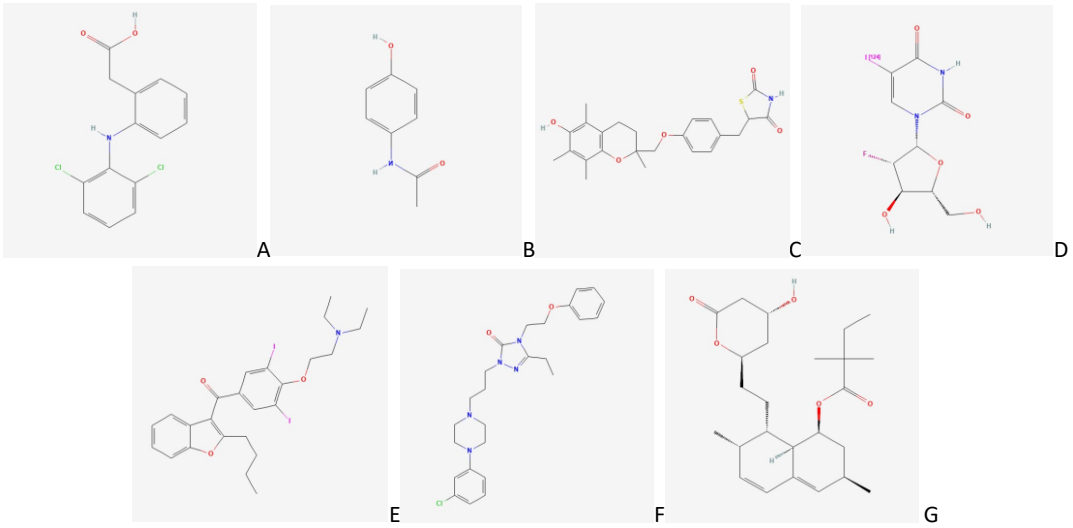

Figure 8. Chemical structures of the selected compounds tested in *in vitro* cultures of human and animal hepatocytes. diclofenac (A); acetaminophen (B); troglitazone (C); fialuridine (D); amiodarone (E); nefazodone (F); simvastatin (G). Source: PubChem website.

All of them were tested in six concentrations ranging from their Cmax (the highest blood concentration of the drug after administration at therapeutic dosage) as the lowest to 32-fold Cmax as the highest, in order to appreciate an evident toxic effect, if present. Values of Cmax were found in published literature (Table 1, section 1 in "Results and Discussion").

For an exhaustive prediction of hepatotoxicity, it was important to select a panel of compounds encompassing different levels and mechanisms of toxicity. For this reason, drugs like troglitazone and nefazodone were included in this study as examples of severe DILI. The widely documented cases of fatal liver acute injuries induced in the early 2000s their withdrawal from the market (Henney JE, 2000; Yokoi T, 2010; Edwards IR, 2003;).

Amiodarone represents another example of a highly hepatotoxic compound in this study. The long-term therapy with this antiarrhythmic drug was associated with severe liver injury (Calderon-Martinez E et al., 2023; Hussain N et al., 2013; Buggey J et al., 2015; Essrani R et al., 2020; Wu IJ et al., 2021).

The anti-inflammatory drug diclofenac was chosen to reproduce a medium-high acute hepatotoxicity. Compared to other NSAIDs, diclofenac was found to be one of the most frequently associated with DILI (Sriuttha P et al., 2018). Diclofenac is among the top ten drugs causing hepatotoxicity, with elevation of ALT being the major event occurring at chronic administration (O'Connor N et al., 2003; Laine L et al., 2009). However, serious liver damage requiring hospitalization is very rare and can occur either with early or late onset (Laine L et al., 2009).

The antipyretic drug acetaminophen was also included in the group of hepatotoxicants tested. Acetaminophen is safe if administered at therapeutic doses, but its hepatotoxic effect starts to develop if the dose exceeds 7.5 grams per day, about 2-fold the recommended daily dose in adults (Agrawal S, Khazaeni B, 2023). Acetaminophen is responsible every year in the US for 50% of the total cases of acute liver failure due to overdoses (Bunchorntavakul C, Reddy KR, 2013).

An interesting example of drug-induced chronic hepatotoxicity is the case of fialuridine that never achieved approval due to fatal liver failures that occurred in clinical trials and were not revealed previously, during the preclinical phase (Manning FJ and Swartz M, 1995; McKenzie R et al., 1995). Fialuridine was included in this study to assess chronic liver toxicity.

Simvastatin, whose related hepatotoxicity was occasionally reported, was finally comprised within the drugs set as representative of harmless or ambiguous hepatotoxic compounds.

3a. HepaRG 2D and 3D cultures as models for acute hepatotoxicity prediction

Drugs were administered in a single dose to the HepaRG monolayer, sandwich, and spheroids cultures to test their putative acute toxicity. Monolayer cultures of HepaRG were established by seeding cells on collagen-coated plates to improve cell attachment and stable growth. In sandwich cultures, HepaRG were seeded on a collagen layer and overlayed with Matrigel®. Hepatocytes are highly differentiated cells living in a well-coordinated and complex *in vivo* environment. However, after isolation, they often undergo dedifferentiation when cultured *in vitro*. Therefore, collagen and other matrixes are commonly used to reproduce the extracellular matrix component and maintain the cell phenotype and functionality of hepatocytes *in vitro* (De Hoyos-Vega JM et al., 2021).

Three-dimensional culture techniques have been developed over time to recreate the hepatocyte's microenvironment and further improve cells' function. In this section of the study, spheroids of HepaRG were generated as a three-dimensional model for toxicity testing. Spheroids were successfully created

by self-aggregation induced by centrifugation force and maintained for at least two weeks. Figure 9 shows the HepaRG spheroids' development over time.

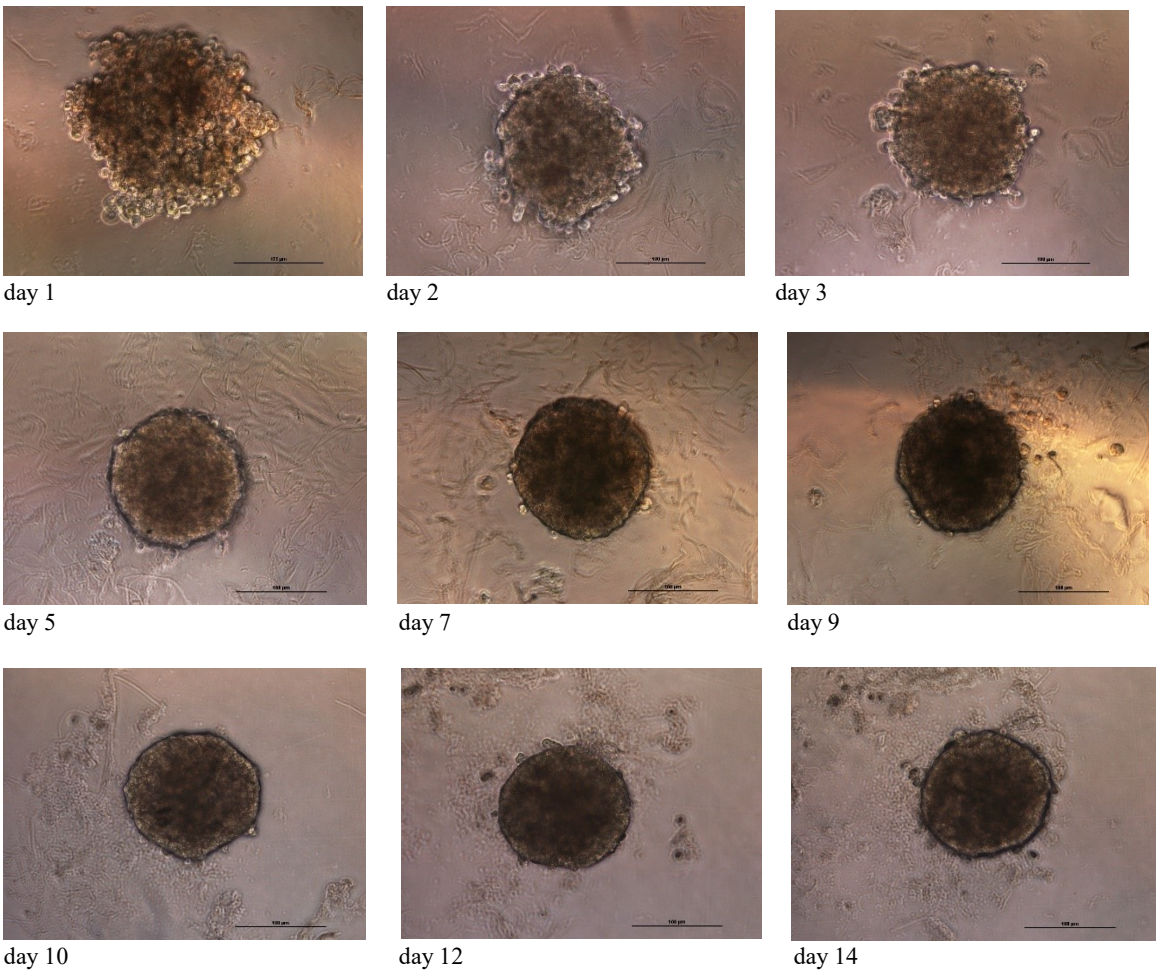

Figure 9. 3D HepaRG spheroids. HepaRG cells seeded at 1500 cells/well in ULA plates developed spheroids already on day 3 and were maintained in culture for 2 weeks. Scale bar=100 µm.

After two days, cell viability was assessed by detecting cells' ATP levels. ATP values were normalized to controls, treated only with the vehicle DMSO, the drug solvent.

Dose-response curves were generated by correlating each drug's concentration to the respective percentage of viable cells, directly proportional to the ATP released by alive cells (Fig. 10).

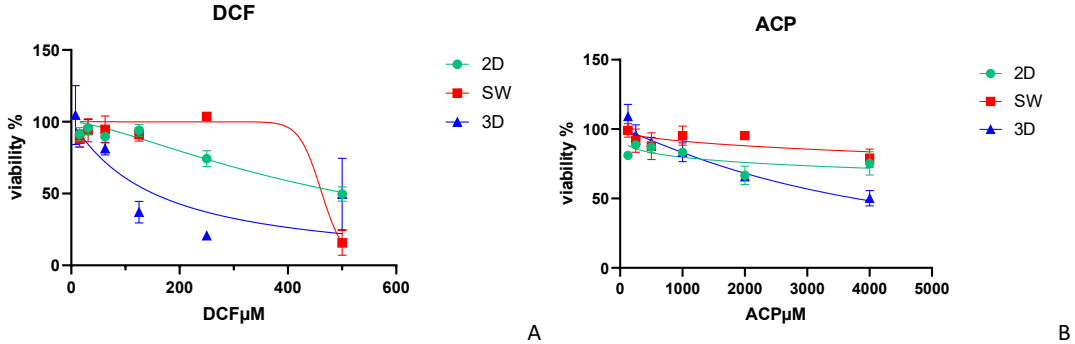

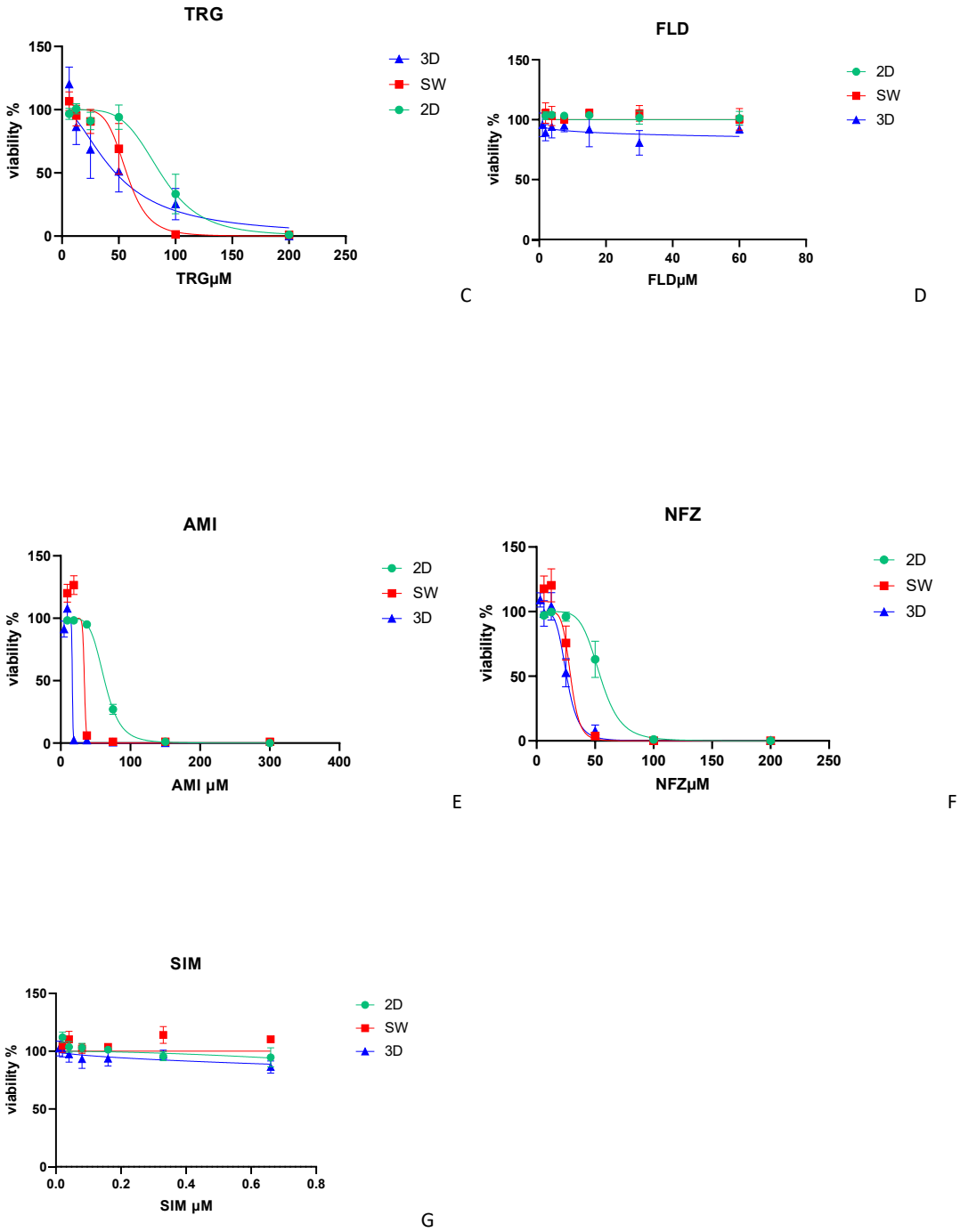

Figure 10. Acute hepatotoxicity of selected compounds on HepaRG cultures. Drug toxicity was compared between three different HepaRG systems: monolayer (2D, green), sandwich (sand, red) and spheroids (3D, blue). Cells were treated with diclofenac (DCF), acetaminophen (ACP), troglitazone (TRG), fialuridine (FLD), amiodarone (AMI), nefazodone (NFZ) and simvastatin (SIM) for 48h. Drug concentration is indicated in µM. Cell viability was expressed in percentage relative to the control, represented by cells treated with DMSO only. Three independent experiments were carried out for each HepaRG system. Data are presented as mean ± SEM. LC_{50} values were calculated using non-linear regression analysis with a sigmoidal dose-response model (GraphPad Prism 8.3.0; GraphPad Software, San Diego, CA). Comparison between systems was made using two-way ANOVA followed by Tukey's multiple comparison test (GraphPad Prism 8.3.0; GraphPad Software, San Diego, CA). $p<0.05$ was considered statistically significant.

The application of a single dose of drugs revealed that, after 48 hours, HepaRG spheroids resulted in general slightly more sensitive to compounds' toxicity compared to the two-dimensional cultures (monolayer and sandwich) (Fig. 10).

In fact, viability values related to spheroids (Fig. 10, blue) are lower than those of sandwich (Fig. 10, red) and monolayer cultures (Fig. 10, green).

In general, these results are in line with our expectations and confirm previous studies proving the higher sensitivity of 3D spheroids than 2D cultures in detecting compounds' hepatotoxicity (Li J et al., 2019). It is largely described in literature how the 3D asset is exceptionally capable to simulate the real tissue environment and to respond with high accuracy to external perturbations (Antoni D et al., 2015; Fitzgerald KA et al., 2015; Foglietta F et al., 2020; Kapałczyńska M et al., 2018; Habanjar O et al., 2021; Fang Y and Eglen RM, 2017). Spheroids are scaffold-free 3D systems that can be generated with different techniques (Białkowska K et al., 2020). An easy way to generate spheroids is to induce spontaneous adhesion between cells by applying centrifugation force (Białkowska K et al., 2020; Froehlich K et al., 2016). Differently from bidimensional systems, inside the spheroid, cells retain their natural morphology, and this is reflected in a more physiological orientation of surface proteins than that of 2D cultures, where cells are flattened (Białkowska K et al., 2020). In addition, the establishment of cell-cell interactions, which is poorly present in 2D cultures, increases cell communication and signaling (Langhans SA, 2018). Therefore, cells in a 3D environment behave differently from 2D systems and react differently to external insults, like xenobiotics, thus representing an appealing instrument to investigate liver toxicity and physiology.

Globally, amiodarone, troglitazone, and nefazodone were found to be the most toxic compounds within the set of drugs investigated. In fact, it can be easily deduced from the dose-response curves as these drugs exhibit toxicity with a similar trend, causing a deep decrease in HepaRG vitality at low concentrations (Fig. 10C, 10E, 10F). Indeed, amiodarone, troglitazone, and nefazodone are referred to as compounds responsible for severe DILI, being responsible for the generation of reactive metabolites, mitochondrial and lysosomal dysfunction, and bile acid cycle impairment. As a consequence, those drugs have often been reported as a cause of steatosis, steatohepatitis, cholestasis, and liver failure (Vorrink SU et al., 2018; Donato MT 2022; Ott LM et al., 2017; NIH.LiverTox, 2018; Walker PA et al., 2020; Sison-Young RL et al., 2017; Stewart DE, 2002).

Additionally, remarkable differences were observed between 3D and 2D systems. At amiodarone 18.75 µM cells' viability was significantly lower in spheroids than in sandwich and monolayer cultures ($p<0.0001$). Similarly, significantly higher cytotoxicity was observed in 3D spheroids than in 2D systems at diclofenac 125 µM ($p<0.0001$), nefazodone 50 µM and 25 µM ($p<0.001$), and acetaminophen 2000 µM ($p<0.01$).

On the other hand, fialuridine and simvastatin did not show any remarkable toxicity in any of the HepaRG formats (Fig. 10D, 10G). As expected, both drugs, even at their highest concentration, did not reduce HepaRG viability below 75% (Fig. 10D, 10G). Although their effect on viability was minor, it was still more visible in spheroids than in other bidimensional systems (Fig. 10D, 10G). According to previous findings, fialuridine's hepatotoxicity is only related to chronic therapy and not to a single-dose administration (Bell CC et al., 2018; Hendriks DFG et al., 2019). Simvastatin-related liver injury is ambiguous and very rarely reported. It normally requires an onset of 1-6 months, and, in most cases, full recovery is achieved after therapy discontinuation (LiverTox-Simvastatin, updated 2021).

Two fundamental parameters were considered to analyze drugs' toxicity: Lethal Concentration 50 (LC_{50}) and Lethal Concentration 0 (LC_0), representing respectively the compounds´ concentration killing 50% and 0% of the cell population. Even though in many studies, LC_{50} is the only parameter reported for toxicity evaluation, we believe that to ensure compound safety, it is also important to determine the maximal safe concentration (LC_0). In this manner, it is possible to define a "toxic window" by comparing the drug concentration that kills 50% of cells (LC_{50}) to the maximally effective dose without harmful effects (LC_0). It follows that the greater the gap between these two values, the safer the compound will be.

LC_{50} and LC_0 values, extrapolated from the dose-response curves, are listed in Table 2.

	HepaRG 2D		**HepaRG SW**		**HepaRG 3D**		
	LC_0	**LC_{50}**	**LC_0**	**LC_{50}**	**LC_0**	**LC_{50}**	**Cmax**
DCF	<15.7	511.2	<15.7	463.0	8.3	151.9	7.5
ACP	<125	>4000	125	>4000	191	3779	93-139
TRG	13	86.7	9.6	56.9	6.9	47.1	6.39
FLD	>60	>60	>60	>60	<0.95	>60	0.64
AMI	9.4	62.9	20.7	33.9	9	16.6	2
NFZ	12.5	54.4	17.3	29.1	5.6	25.7	4.3
SIM	0.16	>0.66	>0.66	>0.66	0.014	0.66	0.03

Table 2. Comparison of LC_0 and LC_{50} between three different HepaRG formats: 2D (monolayer), sandwich (SW), and 3D (spheroids) after 48 hours of drug exposure. Values are reported in µM. LC_{50} values were calculated using non-linear regression analysis with a sigmoidal dose-response model (GraphPad Prism 8.3.0; GraphPad Software, San Diego, CA). The right column reports the Cmax values of drugs.

Troglitazone, amiodarone, and nefazodone values of LC_{50} dropped, passing from bidimensional cultures to 3D spheroids (Table 2). Particularly, amiodarone's LC_{50} values decreased linearly from 62.9 µM in monolayer cultures to 33.9 µM in sandwich, down to 16.6 µM in spheroids. Troglitazone's LC_{50} was reduced from 86.7 µM (in 2D) and 56.9 µM (in SW) to 47.1 µM in spheroids (3D). Reduced values of LC_{50} were progressively found also for nefazodone when applied to monolayer, sandwich, and 3D spheroids. Particularly, the LC_{50} diminished from 54.4 µM 29.1 µM to 25.7 µM respectively (Table 2).

In a similar manner, the different sensitivity of cell systems is evident for the drug diclofenac. Indeed, comparable values of LC_{50} were found for 2D and sandwich cultures (511.2 µM and 463.0 µM, respectively), whereas LC_{50} found for spheroids was only 151.9 µM, four times less than those of bi-dimensional cultures (Tab. 2).

Ultimately, all these findings confirm that HepaRG 3D models are more sensitive than 2D models in detecting acute liver toxicity.

LC_0 values of the drugs tested in HepaRG spheroids were respectively: 8.3 µM (DCF), 191 µM (ACP), 6.9 µM (TRG), <0.95 µM (FLD), 9 µM (AMI), 5.6 µM (NFZ), 0.014 µM (SIM) (Table 2). Notably, such values are comparable to the drugs' Cmax *in vivo* in humans (Table 2). By definition, Cmax is the highest concentration of drug present in the blood when the drug is administered at the therapeutic dose, where no toxicity occurs. Analogously, in our experiment, LC_0 is the maximum drug concentration found *in vitro*, at which no toxicity is manifested in human cells. This represents a very relevant result because it demonstrates that when a drug is administered, the concentration found *in vivo* is comparable, with high accuracy, to the safe drug concentration found experimentally in our spheroids cultures. Thus, we can assess that HepaRG spheroids represent a reliable model for the detection of drugs' acute hepatotoxicity, expressed as LC_0.

The other important information that can be deduced from the results of this part of the study is the severity of the cytotoxic effect by comparing the LC_{50} and LC_0 values of each compound.

For instance, by examining the ratios LC_{50}/LC_0 of troglitazone, we found that these ratios were 6.6, 5.9, and 6.8 for monolayer, sandwich, and spheroids cultures, respectively. The same ratios were 6.7, 1.6, and 1.8 for amiodarone and 4.4, 1.7, and 4.6 for nefazodone. These values, all below 10, indicate that the drug concentration killing 50% of the cell population is of the same order of magnitude as the drug concentration that does not kill any cell. In other words, LC_{50} and LC_0 are very close values, so the toxic window for these compounds is very narrow. This implies that the toxicity of troglitazone, amiodarone, and nefazodone is highly dose-dependent; therefore, the doses ensuring their safety have to be very close to their Cmax.

By contrast, the safety range of fialuridine and simvastatin is large, as their LC_{50}/LC_0 ratios are comprised between 50 and 150. This means that in this case, toxicity is not strictly related to dose, and the product can be safely administered in a wide variety of doses.

The LC_{50}/LC_0 ratios of diclofenac and acetaminophen range between 12 and 30, suggesting that these drugs show borderline toxicity, proportionally increasing with the concentration applied.

In summary, the approach described here represents a valuable tool for acute DILI prediction. Three-dimensional culture systems, like spheroids, resulted in an excellent model to describe drug-related

hepatotoxicity, as they were more sensitive than sandwich and monolayer cultures to compounds' effects.

Moreover, the similarity between the experimental LC_0 values and the *in vivo* Cmax in humans of each drug demonstrates that the drugs' concentration found in human plasma at therapeutic dose was closely reproduced as LC_0 in our *in vitro* 3D model.

Ultimately, by analyzing the LC_{50}/LC_0 ratios of each compound, we estimated the toxic window associated with each compound and the possible doses that can be administered without harmful effects.

3b. HepaRG 2D and 3D cultures as models for long-term hepatotoxicity prediction

Multiple doses of the drugs were added to the HepaRG cultures for two weeks to test the chronic toxicity of the compounds. For this assessment, differentiated HepaRG were seeded and cultured both in sandwich configuration and 3D spheroids. Monolayer cultures were excluded in this set of experiments as they cannot provide stable long-term cultures as sandwich and spheroids models. In fact, typical hepatic and metabolic functions are down-regulated in hepatocytes grown in monolayers while they are maintained closely to physiological levels in sandwich configuration (Kim et al., 2010).

Comparative studies of HepaRG culture models demonstrated that 3D spheroids exhibit longer viability and higher expression of liver metabolizing enzymes than other models. More importantly, these characteristics and metabolic functions can be maintained for up to three weeks in HepaRG spheroids, while after the first week of culture, they start to decrease in bidimensional systems (Jinpeng L et al., 2019).

The possibility to maintain stable sandwich and spheroids cultures for a relatively long period of time allows their use in long-term testing to assess the chronic effect produced by multiple applications of compounds (Bell CC et al., 2016; Vorrink SU et al., 2017; Li J et al., 2019). In this section of the study, we compare the long-term drugs' toxicity between sandwich and spheroids models of HepaRG.

Drugs were added to the cultures starting from day 2 after seeding sandwich cultures. Drugs were added to spheroids starting from day 7 as this time was necessary to reach the mature spheroids' formation. Repeated treatments of drugs were performed on alternate days for two weeks (7 doses added in total). On day 14, cells' viability was evaluated through ATP detection. Results are presented in Fig.11.

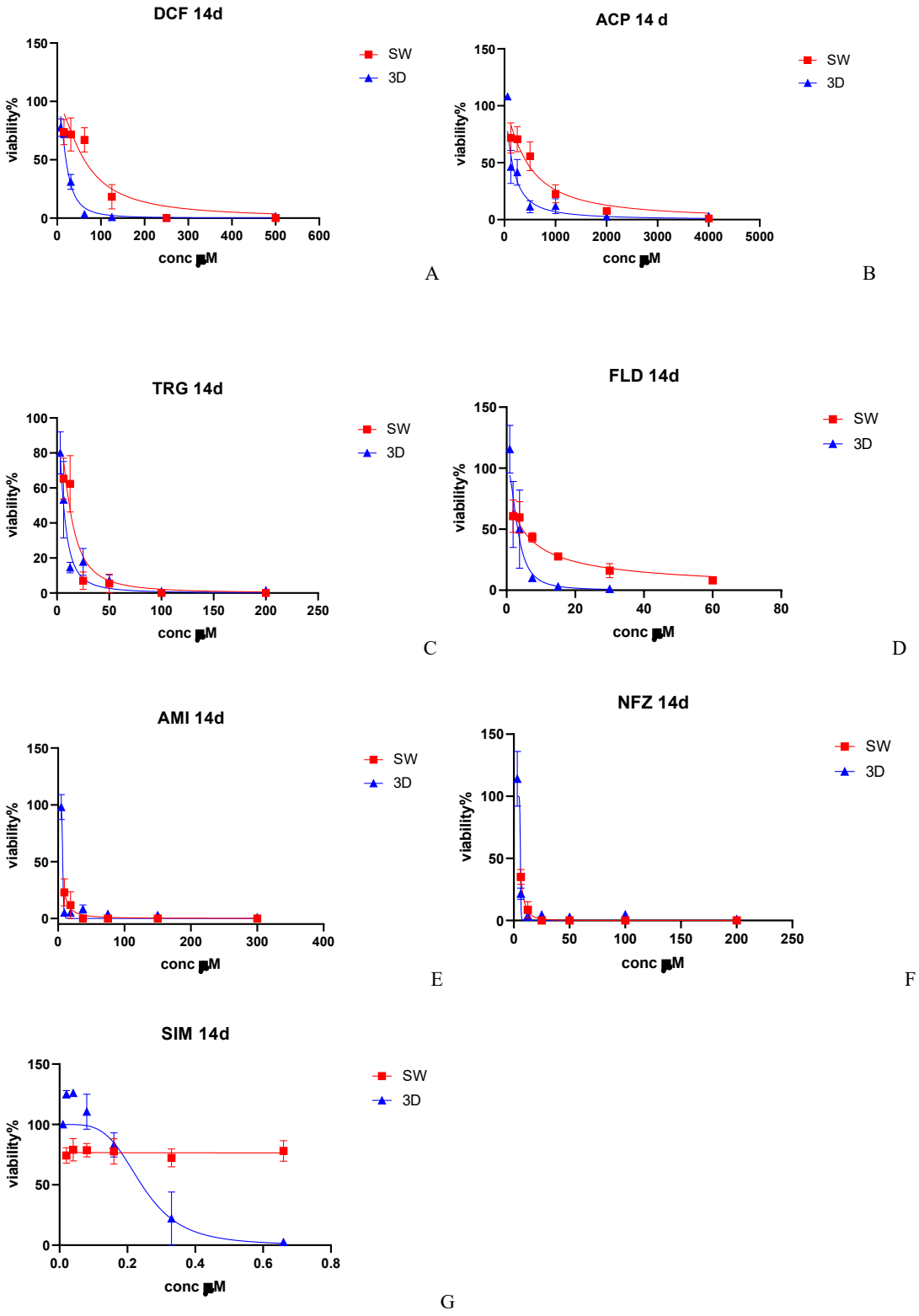

Figure 11. Long-term hepatotoxicity assessment of selected compounds in HepaRG cultures. Drug toxicity was compared between two different HepaRG systems: sandwich (SW, red) and spheroids (3D, blue). Cells were treated every other day for 14 days with diclofenac (DCF), acetaminophen (ACP), troglitazone (TRG), fialuridine (FLD), amiodarone (AMI), nefazodone (NFZ) and simvastatin (SIM). Drugs' concentration is indicated in µM. Cell viability was expressed in percentage relative to the control, represented by cells treated with DMSO only. Three independent experiments were carried out for each HepaRG system. Data are presented as mean ± SEM of three or more independent experiments. Comparison between systems was made using two-way ANOVA followed by Tukey's multiple comparison test (GraphPad Prism 8.3.0; GraphPad Software, San Diego, CA). $p<0.05$ was considered statistically significant.

Each graph, corresponding to a different drug, shows cell viability, expressed as the relative percentage of control, after repeated drug treatments of both HepaRG sandwich (Fig 11, red lines) and HepaRG 3D spheroids (Fig.11, blue lines).

In some of our previous experiments, the repeated applications of the positive control, DMSO 0.5%, caused a high rate of cell mortality in HepaRG spheroids. Thus, the impossibility of distinguishing between cell mortality caused by DMSO itself and drugs led to a misinterpretation of the results. To overcome this problem, when testing 3D spheroids, we reduced DMSO concentrations by half to have a final concentration of 0.25% DMSO in each well, which was harmless to spheroids.

Overall, compounds induced more evident cell mortality in HepaRG spheroids than in sandwich cultures, with the sole exception of the drugs amiodarone and nefazodone, whose toxicity was basically the same in both sandwich and spheroids systems (Fig 11E, 11F). Particularly, significantly different cytotoxic effects were observed between 2D and 3D cultures at diclofenac 62.5 µM and 31.3 µM; acetaminophen 500 µM; troglitazone 12.5 µM; amiodarone 9.4 µM and simvastatin 0.33 µM and 0.66 µM ($p< 0.05$). Remarkably, simvastatin, which appears to have a safe profile in sandwich cultures, induced high cell mortality in spheroids (Fig. 11G, $p<0.001$). Therefore, we can assess that, in general, HepaRG spheroids are more susceptible to compound-induced chronic toxicity than 2D sandwich formats. This result is in line with our previous experiment, where we observed higher hepatotoxicity at 48h in 3D spheroids than in 2D systems (see section 3a).

Amiodarone's liver injuries are primarily associated with the chronic administration of the drug. (Lv HJ and Zhao HW, 2020). As reported by several clinical cases, liver injuries can be reversible events such as transient elevation of liver enzymes or lead to very serious damages, like cirrhosis (Nagata T et al., 2023; Tsuda T et al., 2018). In previous studies, amiodarone's blood concentration found in patients who developed liver injuries ranged from 649 ng/mL (Nagata T et al., 2023) to 1.8 µg/mL (Tsuda, T et al., 2018). Such values correspond to amiodarone's molar concentration range of 0.9 µM-2.6 µM. Interestingly, in our assessment, LC_{50} of amiodarone found in HepaRG spheroids was 6.9 µM (Tab.3), and at concentrations lower than this, hepatotoxicity already started to occur (Fig. 11E). This result is compliant with the clinical outcomes described above, confirming the reliability of our *in vitro* assessment in determining long-term hepatotoxicity of amiodarone.

Severe cases of liver injuries were associated with chronic administration of nefazodone (Choi S, 2003; Lucena MI et al., 1999; Aranda-Michel J et al., 1999; Ehrentraut S et al., 2002; Schirren CA et al., 2000; Stewart DE, 2002). The three cases reported by Aranda-Michel J et al. described a hepatocellular pattern of liver damage at chronic administration of the drug. In two of them, liver injury required transplantation after 14-28 weeks of nefazodone therapy (Aranda-Michel J et al., 1999). Previous works reported that cases of liver failure were associated with nefazodone's therapeutic dose between 200 and 400 mg/day. In such cases, nefazodone's plasma concentration was found to be equal to or above 1

µg/mL (Barbhaiya RH et al., 1995; Dockens R et al., 1996), corresponding to a concentration of 2 µM. Remarkably, this concentration is very similar to the LC_{50} found in HepaRG spheroids in our 14-day assessment (5.9 µM, Tab.3) and quite different from the LC_{50} values found in PPH spheroids and RPH sandwich (17.8 µM and 22.4 µM respectively, Fig. 15H, 22H in chapter 4). This result shows the reliability of the proposed *in vitro* methods for toxicity prediction in humans, highlighting both the higher sensitivity of the human model (HepaRG) over animal models (PPH and RPH) and that of 3D systems compared to 2D systems.

Since the metabolic capacity of HepaRG is more elevated in spheroids than in sandwich systems, it can be hypothesized that the production of toxic metabolites is enhanced in 3D spheroids, causing such systems to have more consistent adverse reactions than in sandwich systems.

However, the difference in cell mortality observed between systems (SW and 3D) after repeated applications of amiodarone, nefazodone, and troglitazone is not as marked as that due to the single drugs' application. This effect is probably due to the strong toxicity and cell mortality induced by these drugs, even at low doses (Fig. 11C, 11E, 11F).

Cytotoxicity induced by the other drugs applied for two weeks showed a consistent increase compared to the toxicity measured at 48h after the single dose exposure (see section 3a).

As expected, the drugs diclofenac and acetaminophen provoked more marked mortality in the cell population treated for two weeks than in those treated for 48h (Fig. 10A, 10B and Fig.11A, 11B).

Notably, a consistent toxicity of fialuridine was observed in the chronic assessment, in contrast to its innocuous effect found at 48h (FLD 48h, Fig. 10D). Multiple doses of 30 µM and 60 µM applied to spheroid and sandwich HepaRG cultures, respectively, reduced cells viability to zero after 14 days of exposure (Fig. 11D) while the single administration of 60 µM, its highest dose, did not reveal significant reduction of cells viability at 48h (Fig. 10D). This result confirms the chronic toxicity of fialuridine already found in several studies (Bell CC et al., 2016; Bell CC et al., 2018; McKenzie R et al., 1995) and indicates that the proposed method is a reliable tool to detect both acute and chronic toxicity of drugs. As explained before, fialuridine was a very promising anti-hepatitis B compound whose failure was due to five fatal acute liver injuries, and two liver transplants occurred in clinical trials (Manning FJ, Swartz M,1995). Unfortunately, preclinical studies could not reveal the human-specific hepatotoxicity. Fialuridine is the exemplary case of a chronic hepatotoxicity inducer, as its effect can only be detected after repeated exposures to the drug and not after a single administration (McKenzie R et al., 1995). Recent *in vitro* studies have elucidated the mechanisms of chronic toxicity of fialuridine (Bell CC et al., 2018; Hendriks DFG et al., 2019).

To better evaluate the severity of drugs' effect on HepaRG, LC_0 and LC_{50} values were generated from the dose-response curves (Tab. 3).

	HepaRG SW		HepaRG 3D	
	LC_0	LC_{50}	LC_0	LC_{50}
DCF	<15.7	62.0	<7.8	20.1
ACP	<125	442.1	80.5	153.8
TRG	<6.3	11.9	<3.1	6.4
FLD	<1.87	4.6	0.9	3.2
AMI	<9.37	<9.37	4.8	6.9
NFZ	<6.3	<6.3	3.1	5.9
SIM	<0.02	>0.66	0.08	0.24

Table 3. LC_0 and LC_{50} values of compounds after two weeks of drug exposure (7 doses in total) found in HepaRG sandwich cultures (HepaRG SW) and spheroids (HepaRG 3D). LC_{50} values were calculated using non-linear regression analysis with a sigmoidal dose-response model (GraphPad Prism 8.3.0; GraphPad Software, San Diego, CA).

LC_{50} and LC_0 values clearly confirm the higher sensitivity to drugs of the 3D systems compared to that of the 2D sandwich in the chronic toxicity assessment. For example, acetaminophen's LC_{50} decreased approximately 4 times from sandwich to spheroids cultures. Likewise, diclofenac's LC_{50} was reduced by 3 times, and troglitazone's LC_{50} by 2 times approximately (Tab.3).

Remarkably, for all the compounds, the ratio LC_{50}/LC_0 ranged between 1 and 6, meaning that the drug concentration killing half of the cell population does not exceed by much the safe concentration. This result showed that chronic exposure to drugs increased drugs' toxicity, narrowing the range of doses that could produce beneficial effects without causing adverse reactions. Therefore, the chronic administration of drugs reduced the "therapeutic window," as demonstrated by the proposed method.

The duration of exposure has a significant impact on the lethal concentrations of compounds, as shown by the large discrepancy between the 48-hour and the 14-days values of LC_{50} and LC_0 found in spheroids cultures (Fig. 12).

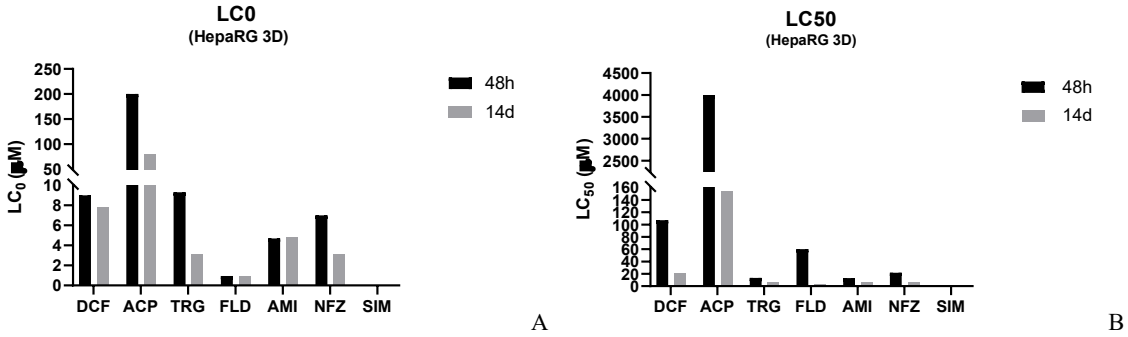

Figure 12. LC_0 (A) and LC_{50} (B) values compared between 48h (black columns) and 14 days (grey columns) of exposure in HepaRG spheroids. LC_0 and LC_{50}, respectively, the drug concentration killing 0% and 50% of the cell population, was calculated referring to dose-viability curves generated from three independent experiments where 3D spheroids of HepaRG were exposed to increasing drug concentrations.

Cells' exposure to diclofenac (LC_{50}=151.9µM at 48h and LC_{50}=20.1 µM at 14d), acetaminophen (LC_{50}= 3779 µM at 48h and LC_{50}=153.8 µM at 14d), fialuridine (LC_{50}>60 µM at 48h and LC_{50}=3.2 µM at 14d) and simvastatin (LC_{50}>0.66 µM at 48h and LC_{50}=0.24 µM at 14d) showed a major impact on spheroids at 14 days compared to 48h (Fig. 12). Conversely, a minor effect was seen for amiodarone, troglitazone, nefazodone which showed more similar values of LC_{50} at 48h and 14d of exposure (Fig. 12B). The same trend is visible for LC_0 values (Fig. 12A) except for fialuridine, which showed similar LC_0 in acute and chronic regimens.

In summary, the method here provided successfully replicated the long-term toxicity of drugs in liver cells *in vitro*, confirming that toxicity increases when drugs are given repeatedly. Indeed, the temporal factor is a very relevant parameter as it reveals the cumulative toxic effects of the substances over time.

Remarkably, the method was able to discriminate between the acute and chronic effects induced by specific therapeutic agents such as fialuridine and simvastatin. Finally, the proposed method was able to quantify the changes in the "therapeutic window" of drugs after repeated administrations.

4. Liver toxicity assessment of drugs and their metabolites in animal *in vitro* models

For a complete validation of the proposed *in vitro* method for toxicity prediction, we performed drugs' hepatotoxicity analysis in animal cell lines to compare the results with those observed in our human model, the liver cell line HepaRG, previously tested in this study.

Although animal models remain the consolidated strategy in preclinical trials, this approach often fails to translate into clinical success. Specifically, 90% of the drug candidates that pass preclinical tests turn out not successful in clinical trials, and a third of those fail due to safety issues (Sun D et al., 2022). Among all the adverse effects, DILI issues represent the most common cause of candidates' failure and post-approval withdrawal (Walker PA et al., 2020; Cook D et al., 2014).

The main reasons for such failure can be ascribed to inter-species differences between human and animal models, specifically regarding the metabolic profile, pharmacokinetics, and structures of drug targets, such as receptors and transporters (Dirven H et al., 2021; Olson et al., 2000; Mak IW et al., 2014).

As the liver is the organ where the majority of xenobiotic transformations occur, the different expression of metabolizing enzymes between human and animal species could affect drugs' metabolism and generate different products, such as toxic metabolites (Hammer H et al., 2021; Lewis DF et al., 1998; O'Brien PJ et al., 2004).

Previous studies have compared the expression of the principal CYP450 subfamilies involved in drugs' metabolism in both humans and the main species adopted in preclinical testing: mice, rats, donkeys, and dogs. They found that overall, the CYP2E1 was the only isoform conserved in all species, expressed at similar levels in animals and humans, while enzymes belonging to CYP1A, -2C, -2D, and -3A subclasses were differently expressed across species or expressed at low levels compared to humans

(Martignoni M et al., 2006). Hence, the lower expression or the reduced efficiency of a certain isoform in animals can reduce the efficiency of liver detoxification, leading to the accumulation of toxicants (Guengerich FP, 2006). On the other hand, the higher expression of metabolic enzymes in animals than in humans may incorrectly predict excessive toxicity during preclinical trials.

If the toxicity prediction is not concordant between species, the risk is the underestimation of adverse effects in humans.

To achieve our aim of developing a method that can efficiently predict adverse reactions in humans, it is important to demonstrate its specificity and demonstrate that it can produce different outcomes between animals and humans, as in reality.

Considering that regulatory guidelines require the use of at least a rodent and non-rodent species in the preclinical phase of drug discovery, we decided to investigate hepatotoxicity in rat and pig *in vitro* models, assisting the same requirement in our toxicological assessment.

4a. Acute and long-term toxicity evaluation in *in vitro* systems of rat primary hepatocytes

To analyze the hepatotoxicity of drugs in animal *in vitro* models, we started by performing acute and chronic toxicity tests in different systems of rat primary hepatocytes (RPH). For comparison to the human model HepaRG, we tested the same set of compounds in the same concentrations and conditions. Therefore, monolayer and sandwich cultures were established as bidimensional models, while spheroids represented our 3D model of rat primary hepatocytes. Analogously to HepaRG cultures, spheroids of rat hepatocytes were obtained by self-aggregation under the application of centrifugation force. Already on day 2 after seeding, the spheroids' morphology was visible, and on day 4, they were completely compact and mature. Spheroids retained a stable morphology up to day 7 of culture (Fig 13).

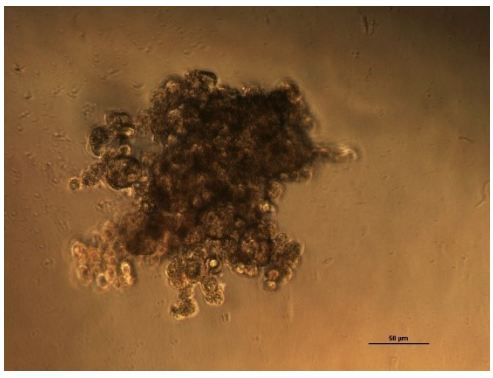

Day1

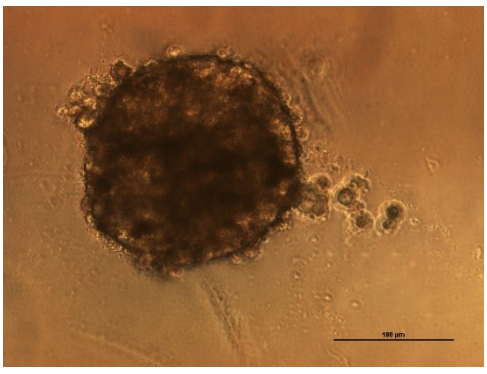

Day2

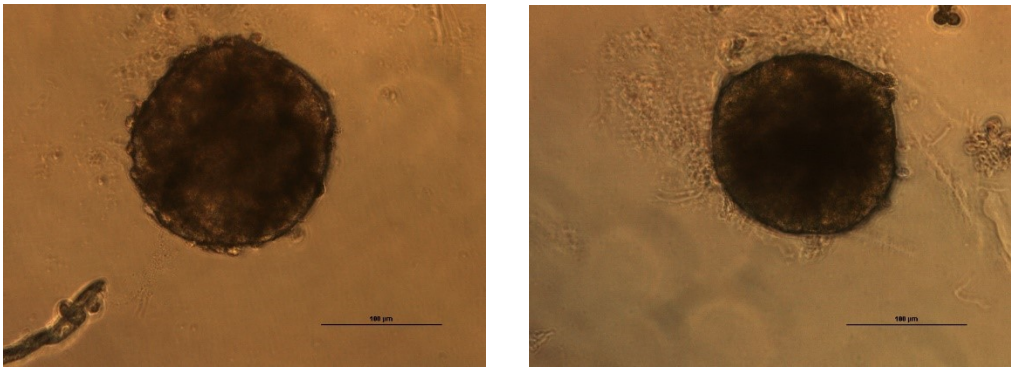

Day 4 Day 7

Figure 13. 3D spheroids of rat primary hepatocytes. Cells seeded at 1500 cells/well in ULA plates developed spheroids already at day 2 and were maintained in culture for 1 week. Day 1 scale bar =50 µm. Day 2, 4, 7 scale bars= 100 µm.

However, after day 7 of culture, they started to spontaneously disaggregate. Spheroids rely on strong cell-cell interactions to maintain their structure. If these interactions weaken due to factors like changes in cell viability or altered cell adhesion properties, spheroids may disintegrate. Over time, cell properties such as the production of adhesion molecules, surface receptors, and secreted factors can decrease, affecting spheroid stability (Efremov YM et al., 2021). Some cell types naturally form more robust spheroids than others. In addition, spheroids grown without an extracellular matrix (ECM) lack the structural support provided by ECM components. Consequently, they may be more prone to disaggregation (Shulman M, Nahmias Y., 2013).

As spheroid cultures of rat primary hepatocytes were found to be unreliable beyond one week, they were deemed unsuitable for assessing long-term toxicity. Consequently, results obtained from these cultures were not reported. Instead, long-term hepatotoxicity in rats was evaluated exclusively using sandwich cultures. This decision was made to ensure the accuracy and reliability of the long-term toxicity assessment, focusing on a culture system that could maintain viability and functionality over the 2 weeks period.

To test the acute effect, rat primary hepatocytes, cultured in the three formats (monolayer, sandwich, and spheroids), were treated once with the drugs (diclofenac, acetaminophen, troglitazone, fialuridine, amiodarone, nefazodone, and simvastatin) and incubated for 48h. Then, cell viability was determined by measuring the ATP content, which reflects the number of living cells. Results of cells' viability against increasing drugs concentrations were plotted (Fig. 14).

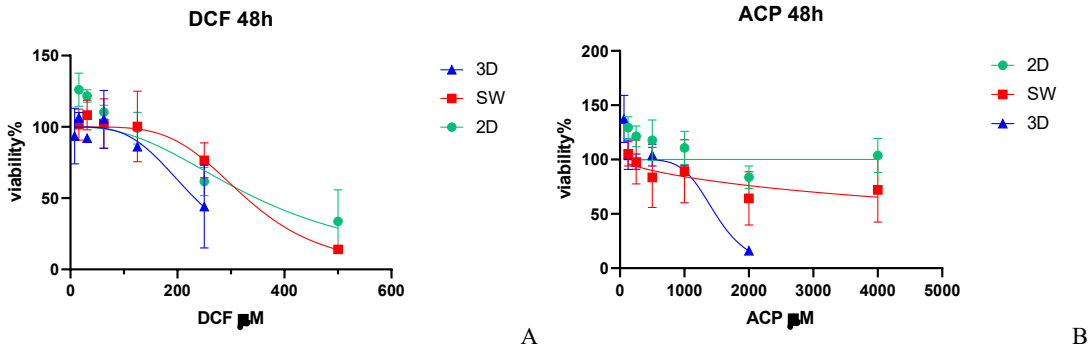

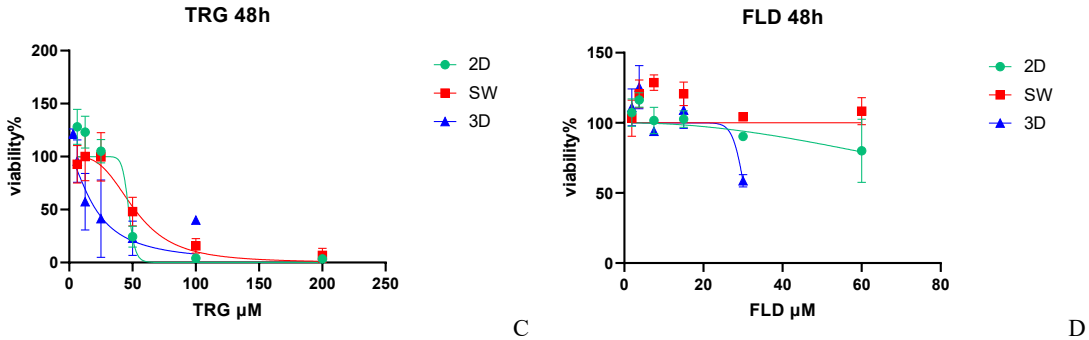

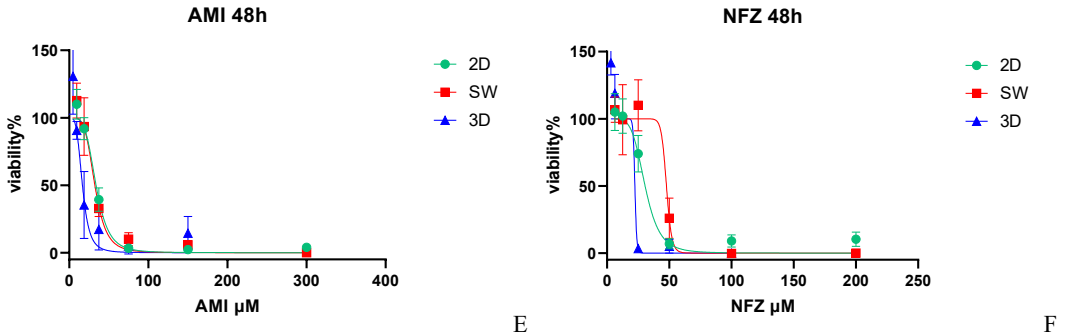

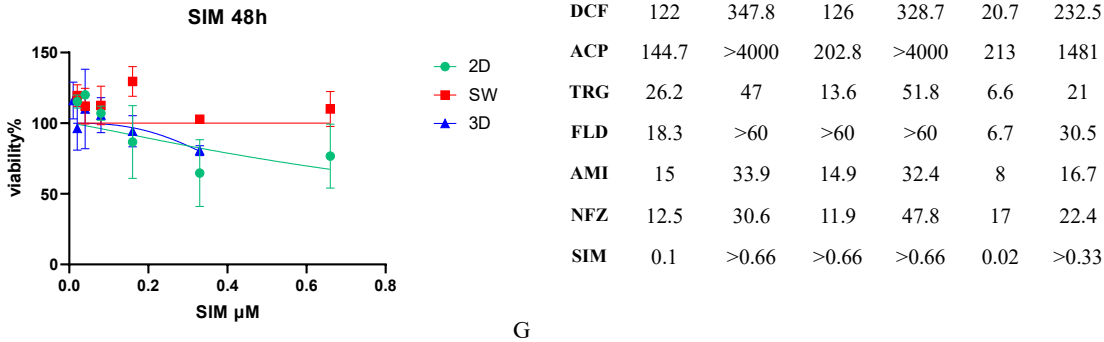

H

	RPH 2D		RPH SW		RPH 3D	
	LC_0	LC_{50}	LC_0	LC_{50}	LC_0	LC_{50}
DCF	122	347.8	126	328.7	20.7	232.5
ACP	144.7	>4000	202.8	>4000	213	1481
TRG	26.2	47	13.6	51.8	6.6	21
FLD	18.3	>60	>60	>60	6.7	30.5
AMI	15	33.9	14.9	32.4	8	16.7
NFZ	12.5	30.6	11.9	47.8	17	22.4
SIM	0.1	>0.66	>0.66	>0.66	0.02	>0.33

Figure 14. Acute hepatotoxicity assessment in rat primary hepatocyte systems (monolayer=2D; sandwich culture= SW; spheroids= 3D) of diclofenac (DCF), acetaminophen (ACP), troglitazone (TRG), fialuridine (FLD), amiodarone (AMI), nefazodone (NFZ) and simvastatin (SIM). Cell viability is expressed as a percentage of control (cells treated with DMSO only). Data are presented as mean ± SEM of three independent experiments. Table (h) reports LC0 and LC50 values, extrapolated from the dose-viability curves of each compound relative to RPH 2D, sand, and 3D systems exposed to a single drug dose. LC50 values were calculated using non-linear regression analysis with a sigmoidal dose-response model (GraphPad Prism 8.3.0; GraphPad Software, San Diego, CA). Comparison between systems was made using two-way ANOVA followed by Tukey's multiple comparison test (GraphPad Prism 8.3.0; GraphPad Software, San Diego, CA). $p<0.05$ was considered statistically significant.

Overall, the compounds troglitazone, amiodarone, and nefazodone showed the highest lethality in rat primary hepatocytes, in concordance with what was observed previously for the human HepaRG cells. Troglitazone, nefazodone, and amiodarone killed the total cell population at a concentration <100 μM (Fig.14C, 14E, 14F), whereas all the other compounds, even at their highest concentrations, did not induce the same effect. The strong cytotoxic effect of troglitazone, amiodarone, and nefazodone in rat hepatocytes is well documented.

To date, it is believed that the main cause of troglitazone's hepatotoxicity is a quinone metabolite formed by CYP3A1 in rat hepatocytes. This highly reactive metabolite is responsible for ROS generation and adducts formation with cellular proteins, impairing numerous cell function functions (Lauer B et al., 2009).

Studies conducted in rat hepatocytes revealed that the mechanism of amiodarone's hepatotoxicity is due to the inhibition of β-oxidation and respiration, leading to mitochondria dysfunction. The resulting ATP depletion and increasing reactive oxygen species with the following lipid peroxidation are responsible for triggering cell necrosis or apoptosis (Ruch RJ et al., 1991; Berson A et al., 1998; Spaniol M et al., 2001).

The mitochondrial toxicity of nefazodone has a similar mechanism to that of amiodarone. The inhibition of respiration in the mitochondria of rat hepatocytes can cause free radical formation and decreased energy production, resulting in cell death (Dykens JA et al., 2008). Moreover, nefazodone can also induce transient cholestasis in rats by inhibiting specific biliary transport systems (Kostrubsky SE et al., 2006).

All these findings are consistent with the high mortality induced by troglitazone, amiodarone, and nefazodone observed in our rat primary hepatocyte cultures (Fig. 14C, 14E, 14F).

The dose-viability curves also revealed that acetaminophen and diclofenac showed moderately high cytotoxicity, proportionally increasing with doses (Fig. 14A, 14B).

The dose-dependent acute toxicity of acetaminophen found in our experiment is principally due to NAPQI formation, an electrophile intermediate able to rapidly react with mitochondrial proteins, believed to be the major acetaminophen's toxic metabolite (Nelson SD, 1990). NAPQI- protein adducts trigger oxidative stress and mitochondria dysfunction, leading to cell necrosis (Ramachandran A, Jaeschke H, 2019). Many animal models, including rats, share with humans the same metabolic pathways of acetaminophen. Therefore, the mechanism of toxicity induced by acetaminophen in rats' hepatocytes that we observed in our study is similar to that observed in human hepatocytes. In fact, like humans, rats express the CYP2E1 isoform, responsible for NAPQI production, as well as sulfation and glucuronidation enzymes necessary for acetaminophen excretion (McGill MR, Jaeschke H 2013).

Diclofenac's toxicity is mainly related to mitochondria impairment, which causes ATP depletion inside the cell (Syed M et al., 2016; Ramachandran A et al., 2018). Although diclofenac can exert this toxic effect as a parent compound, other metabolites were found to trigger mitochondria damage (Syed M et al., 2016). A study revealed that the co-administration of diclofenac with CYP inhibitors significantly increased ATP production in rat and human hepatocytes, indicating that toxicity is induced by diclofenac's metabolites (Bort R et al., 1998). The same study showed a similar effect of diclofenac in freshly isolated rat hepatocytes to that of our study, highlighting the reliability of our results. The cell death rate increased with diclofenac exposure in a dose-dependent manner, and the LC_{50} in 2D systems was 300 μM, comparable to our value (347.8 μM, Fig. 14H).

Fialuridine and simvastatin mildly affected cells' viability. For both drugs, in fact, viability never went below 50% (Fig. 14D, 14G).

Although acute hepatotoxicity of fialuridine in rat *in vitro* models is poorly documented, the review of fialuridine preclinical trials conducted in several animal species, including rats, showed that no sign of hepatotoxicity was reported when the drug is administered at a single dose. Noteworthy, only mild elevation of ALT and AST were observed in some cases, and no change in liver morphology was visible (Institute of Medicine (US) Committee to Review the Fialuridine (FIAU/FIAC) Clinical Trials). These outcomes are in line with the low acute lethality of fialuridine observed in our systems of RPH.

The effect of simvastatin on rat liver cells is still debated. Some authors found that simvastatin induced oxidative stress, lipid peroxidation, and mitochondria depolarization in freshly isolated rat hepatocytes (Abdoli N et al., 2015). Conversely, another study showed that simvastatin had a protective effect against the pathogenesis of some liver diseases by inhibiting intracellular lipid accumulation in rats (Zhang Q et al., 2020). The low lethality of simvastatin in RPH that we observed after the single exposure to the drug may contribute to elucidating the toxic effect of this drug in rat liver cells (Fig. 14G).

Recent studies have also confirmed the reliability of the presented method in predicting drugs' toxicity in rat hepatocytes. Our 2D cultures of rat hepatocytes showed similar LC_{50} values for amiodarone, diclofenac, troglitazone, and acetaminophen as those reported in previous assessments performed in bidimensional systems under the same conditions (Noor F et al., 2009; Jemnitz K et al., 2008) (Fig. 14H). To our knowledge, however, LC_{50} of nefazodone, simvastatin, and fialuridine were never assessed before in *in vitro* rat liver cells; therefore, it was not possible to make a comparison with our data.

Among the three culture formats investigated, the acute toxicity elicited by the drugs, except for simvastatin, was more evident in 3D spheroids than in bidimensional monolayer and sandwich cultures, confirming the results found for the human HepaRG models (Fig. 10). This discrepancy was particularly evident for acetaminophen, and fialuridine (Fig. 14B, 14D). According to the dose-response curves, when cells were exposed to acetaminophen 2000 μM, viability was reduced to 16% in spheroids, whereas only to 65% in sandwich and to 84% in monolayer, showing that the drug's effect on 2D systems

was much less visible (Fig. 14B). The same conclusion is valid for the drug fialuridine. This drug, in fact, did not cause any significant acute toxicity in RPH monolayer and seems to exert even a beneficial effect on sandwich, where cell viability remained above 100% for any concentration applied (Fig. 14D). By contrast, when RPH spheroids were exposed to fialuridine 30 μM, cells viability was reduced by 50% (Fig. 14D). Indeed, significant differences in cells viability between 2D and 3D systems were observed at the concentration of fialuridine 30 μM, as well as at amiodarone 18.75 μM and nefazodone 25 μM ($p< 0.05$).

Unexpectedly, simvastatin exerted the highest lethality in the monolayer culture of RPH among the three systems investigated (Fig. 14G).

The higher sensitivity to drugs of the 3D RPH systems, compared to the 2Ds, can also be deduced by the analysis of the LC_{50} values shown in the table above (Fig. 14H). LC_{50}s of all compounds relative to spheroids cultures were lower than LC_{50}s of sandwich and monolayer cultures (Fig. 14H). Specifically, passing from 2D to 3D systems, LC_{50} of acetaminophen and troglitazone decreased approximately by 60%; LC_{50}s of fialuridine and amiodarone by 50%; nefazodone's LC_{50} by 45% and diclofenac's LC_{50} decreased by 35%. Simvastatin, which induced higher cell mortality in monolayer cultures than in spheroids, represented the sole exception (Fig. 14H).

LC_0 values showed a similar trend to that of LC_{50} values. For example, LC_0 values of acetaminophen, diclofenac, and simvastatin were much lower in 3D cultures than in 2D cultures, showing an 80% decrease. LC_0 of fialuridine and troglitazone decreased by 65% in 3D cultures, and amiodarone's LC_0 decreased by 45%. However, nefazodone's LC_0 values were similar in all the tested systems (Fig. 14H).

The marked reduction of the parameters LC_0 and LC_{50} that we observed in 3D spheroids, compared to 2D systems, clearly indicates the superior impact of xenobiotics on three-dimensional assets. As previously mentioned, the toxicity of drugs investigated here is mainly related to the production of harmful metabolites rather than to parent compounds. The higher capacity of metabolism expressed by 3D systems could explain why spheroids are more sensitive than 2D systems to the drugs (Bell CC et al., 2018). These findings demonstrate that the cells' response to the drugs depends on the system used and highlight the importance of choosing the appropriate model for drug toxicity testing.

To assess the long-term effects of the selected drugs in rat liver cells, sandwich cultures of rat primary hepatocytes were established and exposed to multiple doses of drugs every other day for 2 weeks. Then, viability was measured. As mentioned before, spheroids of rat hepatocytes started to disaggregate after the first week of culture. Consequently, they could not be utilized for assessing hepatotoxicity at 14-days. Therefore, the sandwich culture system was exclusively employed for this purpose, ensuring the viability and integrity of the cells throughout the duration of the experiment.

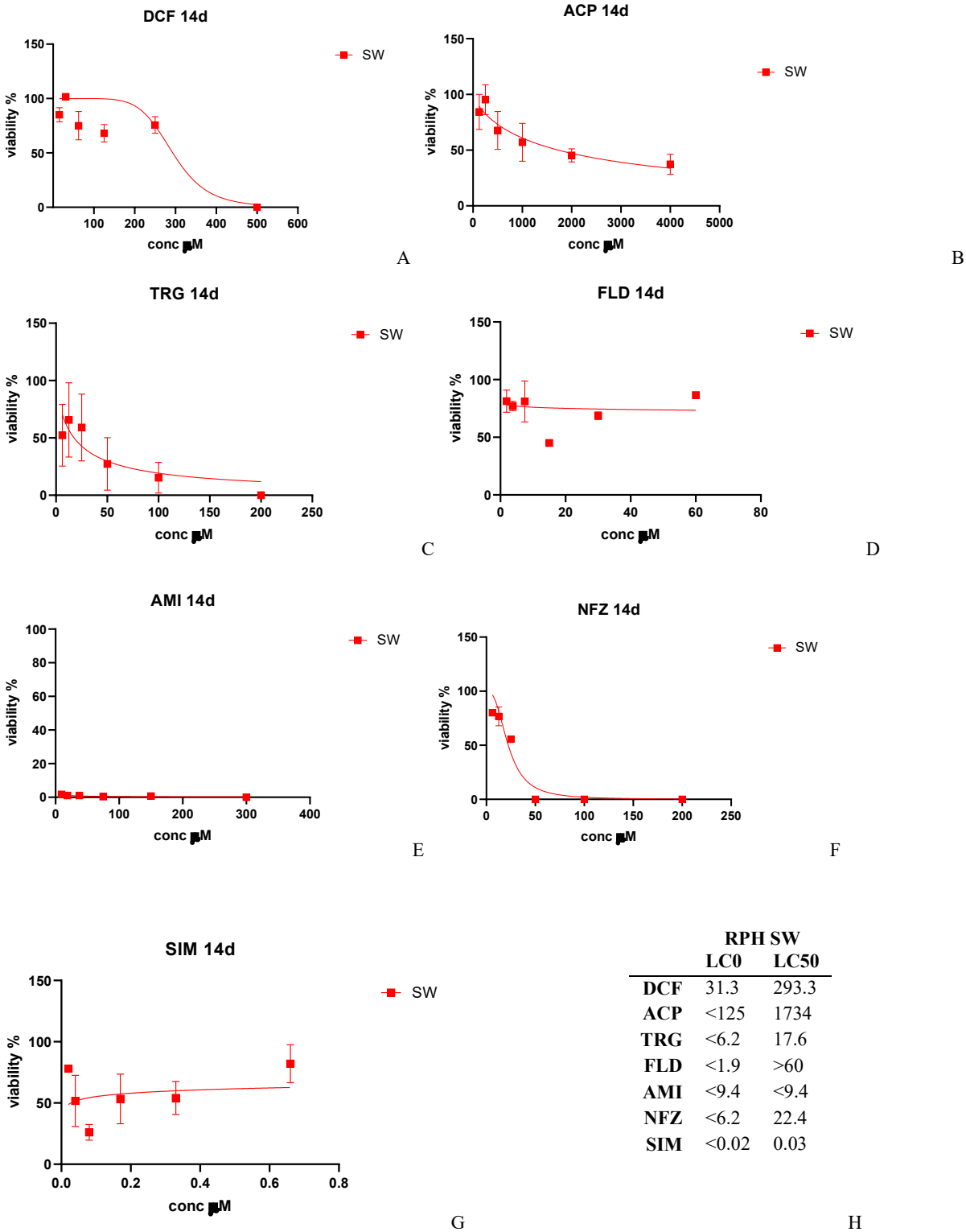

	RPH SW	
	LC0	LC50
DCF	31.3	293.3
ACP	<125	1734
TRG	<6.2	17.6
FLD	<1.9	>60
AMI	<9.4	<9.4
NFZ	<6.2	22.4
SIM	<0.02	0.03

Figure 15. Fourteen days' hepatotoxicity assessment in rat primary hepatocytes sandwich system (sandwich culture= SW) of Diclofenac (DCF), Acetaminophen (ACP), Troglitazone (TRG), Fialuridine (FLD), Amiodarone (AMI), Nefazodone (NFZ) and Simvastatin (SIM). Drug concentrations are expressed in µM. Cell viability is expressed as a percentage of control (cells treated with DMSO only). Data are presented as mean ± SEM of three independent experiments. Table (h) reports LC_0 and LC_{50} values, extrapolated from the dose-viability curves of each compound relative to RPH sandwich (SW) exposed to repeated drug doses for 2 weeks. LC_{50} values were calculated using non-linear regression analysis with a sigmoidal dose-response model (GraphPad Prism 8.3.0; GraphPad Software, San Diego, CA).

Exposing rat hepatocyte cultures to repeated drug doses for 2 weeks resulted in increasing cytotoxicity of compounds, as expected. Comparing cells viability of sandwich cultures at 48h and 14 days of drug exposure, a significant difference is seen for all the compounds except for fialuridine (Fig. 14D and 15D). This result is also supported by the LC_{50} values found for these drugs, which decreased markedly passing from short- to long-term exposures (Fig. 14H and 15H), especially for acetaminophen (from >4000 μM to 1734 μM), amiodarone (from 32.4 μM to <9.4 μM) and troglitazone (from 51.8 μM to 17.6 μM). However, the difference between short- and long-term exposure to the drug diclofenac was minor (Fig. 14A and 15A).

Overall, the long-term exposure to this set of compounds showed a similar outcome between our *in vitro* human model, HepaRG, and rat hepatocytes. All drugs induced a dose-dependent cytotoxic effect, increasing with the dose (Fig. 11 and Fig 15). However, although the trend was the same, rat hepatocytes were less sensitive than HepaRG to drugs' effects, as demonstrated by the LC_{50} values, which were lower in HepaRG than in rat sandwich (Tab. 3 and Fig. 15H).

Remarkably, there was a notable disparity in the response of rat hepatocytes compared to HepaRG cells when exposed to fialuridine. Specifically, the 14-days exposure to the drug resulted in high mortality of HepaRG cells, whereas it appeared to only have a minor effect on viability of rat sandwich culture (Fig. 11D and Fig. 15D). This finding highlights the differences between animal and human models and emphasizes the significance of considering the species-specific aspects in toxicity assessments, as animal models may not always accurately reflect the response observed in human species. In addition, to the best of our knowledge, no previous data regarding the cytotoxicity of fialuridine in in vitro rat hepatocyte models are available in the literature.

Overall, the toxicity prediction of compounds carried out in our *in vitro* models of RPH gave robust results in both short and long-term assessments. LC_{50} values obtained in this section of the study were comparable to LC_{50} values of previous studies conducted in similar conditions in rat hepatocytes (Kučera O et al., 2017; Wang K et al., 2002; Guo L et al., 2006; Kostrubsky SE et al., 2006; Gómez-Lechón MJ et al., 2003; Jurima-Romet M et al., 1994). Some discrepancies between values could be explained by the inter-donor variability of primary cells. Primary cells are always considered the "gold standard" in *in vitro* experiments, as they resemble *in vivo* tissues more closely than immortalized cell lines. On the other hand, as they are freshly isolated, their metabolic and physiologic characteristics may vary with the donor. This variation represents a limit and can significantly affect the results' reproducibility.

The comparison of LC_{50} values obtained from short- and long-term exposure of cells highlights the impact of multiple doses administered over 14 days on reducing cell viability compared to single-dose administration. This observation is critical in assessing the reliability of the proposed *in vitro* model for hepatotoxicity evaluation.

In your study, the LC_{50} and LC_0 values were found to be significantly lower in the 14-day assessments (Fig. 16, grey columns) compared to the 48-hour assessments (Fig. 16, black columns) across the drugs tested.

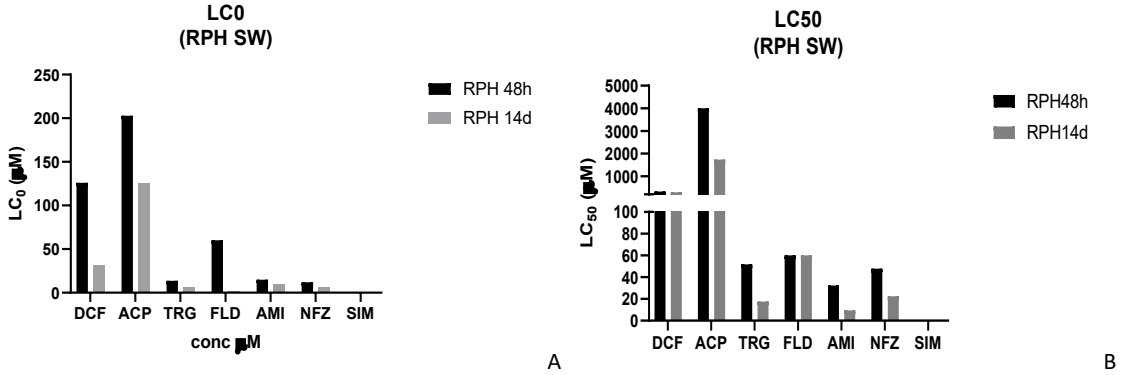

Fig. 16 LC_0 (a) and LC_{50} (b) comparison found at 48h (black columns) and 14 days (grey columns) of RPH exposure to drugs. LC_0 and LC_{50}, respectively, the drug concentration killing 0% and 50% of the cell population, was calculated referring to dose-viability curves generated from three independent experiments where sandwich cultures of RPH were exposed to increasing drug concentrations.

This indicates that prolonged exposure to drugs leads to a greater reduction in cell viability, highlighting the importance of considering the duration of exposure when evaluating hepatotoxicity.

However, it's noteworthy that fialuridine and simvastatin were exceptions to this trend, with comparable LC_{50} values found in both short and long-term experiments (Fig. 14H, 15H).

Overall, these results support the reliability of the proposed *in vitro* model for hepatotoxicity assessment, demonstrating its ability to capture the impact of prolonged drug exposure on cell viability. This information is critical for predicting the potential hepatotoxic effects of drugs over extended treatment durations.

4b. Acute and long-term toxicity evaluation in *in vitro* systems of pig primary hepatocytes (PPH)

Pig primary hepatocytes (PPH) represented in this study the non-rodent animal *in vitro* model used to investigate liver toxicity. In this manner, it was possible to compare two different animal models to our human liver model HepaRG.

As this study is part of the multidisciplinary project INNOTARGETS, I had the opportunity to isolate fresh pig hepatocytes during my secondment at IRTA-CReSA, an animal health research institute member of the INNOTARGETS Consortium. As mentioned, primary hepatocytes retain all the phenotypic characteristics of the real liver tissue, such as the metabolic activity of *in vivo* cells. Therefore, right after the isolation, PPH were plated and used for drugs' cytotoxicity assessments. Another fraction of the isolated cells was frozen for backups.

4b.i. Pig primary hepatocytes isolation and morphology changes

Primary pig hepatocytes (PPH) were isolated twice during the secondment. The first time started from an adult healthy pig (3 years old, liver weight: 836 g); the second time started from two healthy piglets (4 months old, liver weights: 310 g and 295 g). The protocol used for the hepatocyte's isolation was the same in both attempts except for an extra step added in the second one, consisting of erythrocytes separation to optimize the purity of the cell pellet. From the first attempt, we obtained a very low yield, probably due to erythrocytes' contamination.

From the second attempt, we successfully isolated a large number of viable cells from the sample using our optimized protocol. The final count was 50.35×10^6 cells, which corresponded to a viability of 82%. To enhance the adhesion and growth, cells were plated in flasks coated with collagen right after being isolated. In addition, some of the initial cell suspension was used to make backups that were cryopreserved in liquid nitrogen. Two different media were used in these cultures: DMEM and Williams' E, both completed with supplements (see materials and methods section) to determine the optimal growing conditions. Media was renewed every two days for the entire culturing time. We observed that the two different media did not affect cells doubling time differently over time.

The hepatocytes needed two days to recover completely from the isolation process (Fig 17A) and to assume the typical cuboid shape (Fig. 17C). After one week, they started growing in clusters (Fig 17B), and in 2 weeks, the confluency was reached (Fig 17C). PPH were maintained in culture for four weeks, during the latter of which, a substantial change in cell morphology was noticed (Fig 17D). Cells spontaneously switched from the typical hepatocyte-like shape (polygonal, binucleate cell morphology) (Fig. 17C) to an elongated spindle fibroblast-like shape (Fig.17D).

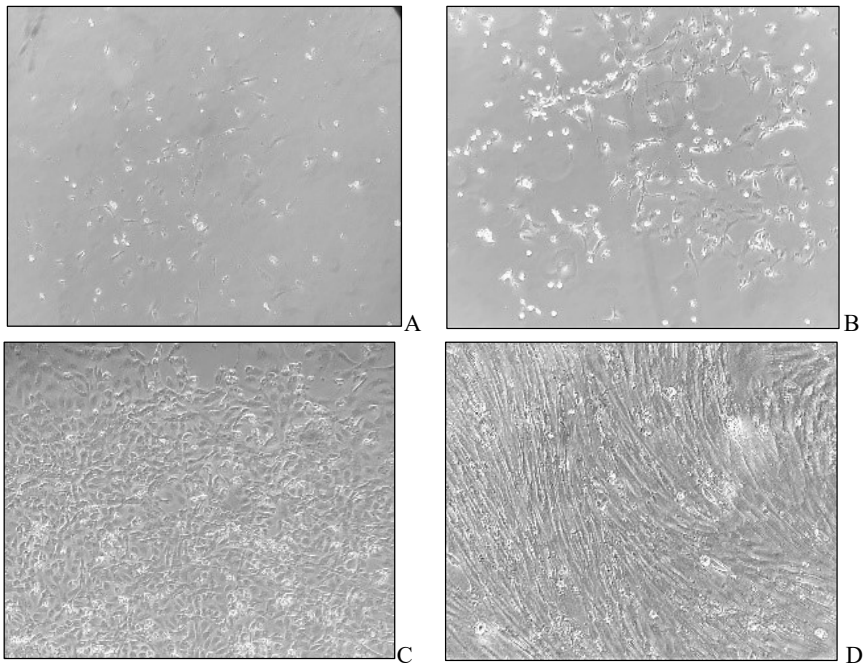

Figure 17. Primary pig hepatocyte (PPH) morphology during four weeks after isolation. Primary hepatocytes started to attach and showed their typical cuboidal morphology during the first week after isolation (A), then started to proliferate in clusters (B, week 2). After 100% confluency was reached on day 14 (C), PPH spontaneously changed their morphology in the last week of culture (D, week 4).

This effect is expected to be observed when culturing primary cells in monolayer. It is well known that primary mature hepatocytes, after isolation, undergo dedifferentiation, a process where the hepatocyte progressively loses liver-specific functions. Disruption of the tissue architecture during isolation results in loss of cell-cell and cell-extracellular matrix interactions as well as loss of cell polarity. Cell stress caused by the isolation and the adaptation to the new *in vitro* environment is considered responsible for genetic and phenotypic changes in the hepatocyte (Luttringer O et al., 2002; Fraczek et al., 2013). It has been described that hepatocytes' dedifferentiation is initiated by down or upregulation of numerous nuclear receptors and transcription factors, most of them belonging to LETFs (Liver-Enriched Transcription factors) resulting in a reduced expression of Phase I and II metabolic enzymes (e.g., CYP450, UGT, GST) and drugs' transporters (e.g., BSEP, NTCP) (Elaut G et al., 2006). Consequently, the metabolizing capacity of hepatocytes becomes highly compromised, and several other liver-specific functions decline.

These modifications also translate into important morphology changes that are visible just a few hours after isolation when hepatocytes assume a round shape due to loss of intercellular connections and polarity (Kaur I et al., 2023; Sugahara G et al., 2023). In general, it was described that about 12h after recovery, hepatocytes regain the typical polygonal shape and start to form bile canaliculi (Sugahara G et al., 2023). However, when dedifferentiation occurs, hepatocytes become flattened and start to acquire a fibroblast-like shape (Vinken M and Hengstler JG, 2018). The same transition was clearly seen in this study for our freshly isolated primary pig hepatocytes (Fig. 17D).

Ultimately, the massive deregulation at the genetic and functional level, along with the oxidative stress occurring during isolation, can lead to hepatocytes' death by apoptosis (Vinken et al. 2014). This is the main reason for the short lifespan of primary hepatocytes in 2D cultures, which represents a significant limit for their use in pharmacology and toxicology *in vitro* testing. However, several strategies were developed to reduce the dedifferentiation process and prevent early cell death by apoptosis. The more classical ones include the introduction of additives in cell culture media like hormones and growth factors (e.g., insulin, glucagon, dexamethasone, hydrocortisone) able to restore transcriptional factor-mediated pathways and promote the typical morphology of the hepatocyte (Luttringer O et al., 2002; Fraczek et al. 2013). Another strategy is the introduction of an extra layer of matrix, like Matrigel®, to establish sandwich culture configuration. This layer on top of cells provided essential interactions and was demonstrated to reduce apoptosis to some extent (Fraczek et al. 2013). In this way, it is possible to preserve *in vivo*-like conditions of hepatocytes for a longer time.

Although it is described that a significant percentage of primary hepatocytes' functionality is lost after freezing and thawing as well as after cell culture passaging (Baust JM et al., 2017; Stéphenne X et al., 2010; Chesné C et al., 1993), frozen PPH isolated in this study, completely recovered after thawing, showing the same trend as that of fresh isolated PPH in terms of doubling time and morphology, when culture in the same conditions (Fig. 18A, 18B).

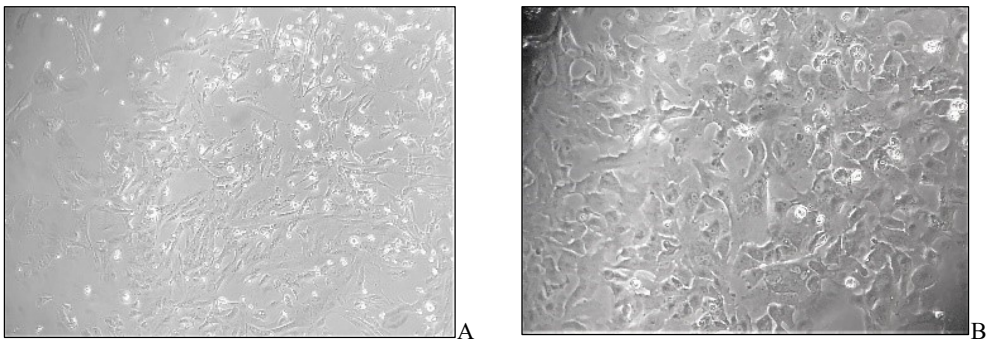
A B

Figure 18. Morphology of PPH 14 days after thawing**.** Magnification 10X (a) and 20X (b). PPH recovered the typical hepatocyte morphology during the first week after thawing, and after two weeks of culture, they started to become confluent.

PPH's morphology and confluence reached after two weeks in monolayer cultures (Fig. 18A and 18B) were comparable to those of freshly isolated cells immediately used for plating (Fig. 17C). The same result was obtained for cryopreserved PPH for longer than one year, allowing their use for further toxicity tests within our study. Viability of thawed cells was always above 80%, and attachment was always reached after 4-5 h from seeding in monolayer cultures using collagen-coated plates. Despite the high viability of thawed PPH, a high fraction of cells did not attach, suggesting that cell death was likely induced by apoptosis in response to stress stimuli accumulated during the initial isolation process or following cryopreservation and thawing, as indicated by previous studies (Ölander M et al., 2019).

4b.ii. Immunostain shows albumin production in isolated liver cells

Albumin is the most abundant protein present in the bloodstream, and it is synthesized by hepatocytes in the liver. Albumin plays a principal role in osmotic pressure's maintenance and in the transportation of both endogenous (e.g., hormones, unconjugated bilirubin, fatty acids) and exogenous substances (e.g., drugs) (Moman RN et al., 2024; Fanali G et al., 2011; Ascenzi P and Fasano M, 2009; Li Y et al., 2007; Roda A et al., 1982). Therefore, albumin represents a precious biomarker of liver functionality, and its biosynthesis was analyzed in this study in the isolated pig hepatocytes cultured in monolayer systems. To this aim, an antibody specifically directed against pig albumin was used to detect the protein expressed inside the isolated cells. As expected, a high yield of albumin was visible inside the cell cytoplasm, as shown by the green fluorescence in the image below (Fig.19B). This result characterized the isolated cells as metabolically active hepatocytes, allowing their use for drugs' toxicological testing.

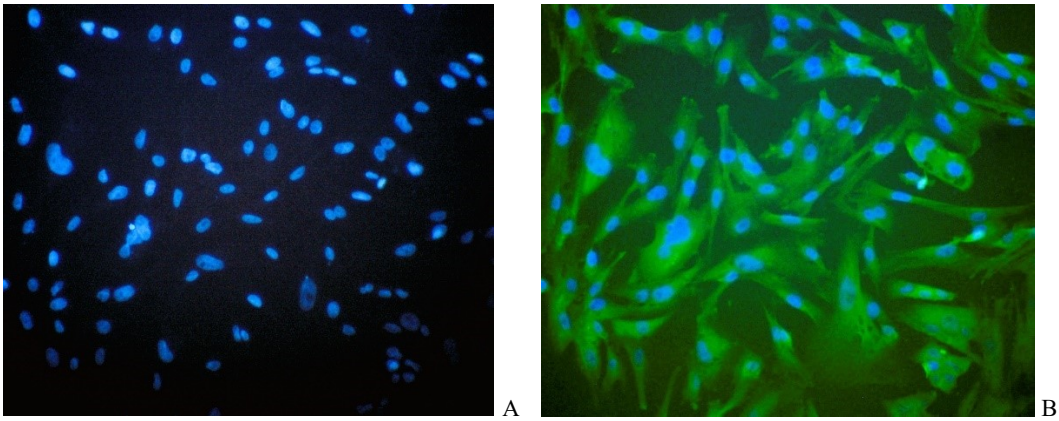

Figure 19. Albumin detection in PPH. Immunofluorescent staining imaging revealed the presence of a high yield of pig albumin inside the cytoplasm of isolated cells (green fluorescence, B). Isolated pig hepatocytes were stained with specific anti-pig Albumin antibodies revealed by anti-IgG-FITC (green). Nuclei, in blue, were counterstained with HOECST (A). The magnification of images is 20X.

4b.iii. Drugs hepatotoxicity evaluation in PPH culture systems

In order to set up a valuable method to predict drug-related hepatotoxicity, an important point of this study was to compare the effect of the selected compounds, known for their ability to induce different types and levels of toxicity in human and animal hepatocytes. Freshly isolated pig hepatocytes, characterized for their metabolic functionality, were therefore used as the other animal species, where drugs' hepatotoxicity was compared to that found in rat and human hepatocytes.

The cytotoxicity of selected drugs was previously assessed in HepaRG, and rat primary hepatocytes were cultured in monolayer, sandwich configuration, and three-dimensional spheroids. For comparison, the same compounds and culture systems were tested in PPH.

Monolayer, sandwich, and spheroids cultures were established with freshly isolated pig hepatocytes and were treated with one dose or multiple doses of each compound to test short and long-term effects, respectively. All systems were cultured for one week before adding compounds. This time was necessary for the cells to recover after isolation, to adopt the typical hepatocyte morphology, and to reach confluence in monolayer and sandwich cultures. Analogously, the same time was needed for the complete maturation of 3D spheroids (Fig 20). Spheroids were generated by self-aggregation of 1500 cells seeded in each well of ULA plates, induced only by gravity centrifugation. Surprisingly, after one day spheroids already showed a three-dimensional round shape. On day 7, spheroids became more compact and assumed a more homogenous morphology, which is typical of a mature spheroid (Fig.20).

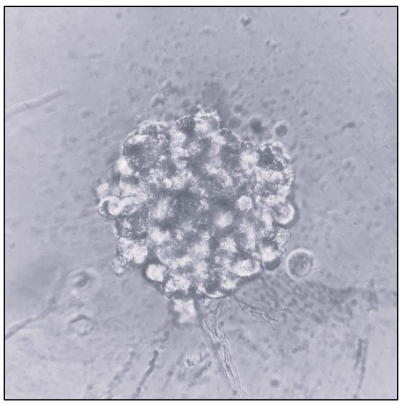

Figure 20. Morphology of a mature 3D-spheroid of pig primary hepatocytes at day 7 of culture. Magnification 20X.

To test acute cytotoxicity, six concentrations of the selected compounds, including diclofenac, acetaminophen, troglitazone, fialuridine, amiodarone, nefazodone, and simvastatin, were administered once to monolayer (2D), sandwich (SW) and mature spheroids (3D) cultures of PPH. Cell viability, expressed as a percentage of viable cells, was measured 48h after incubation with the drugs. The results of the cytotoxicity assay are shown in Fig. 21. Each graph shows cells' viability in percentage versus increasing concentrations of compounds in the three PPH culture systems.

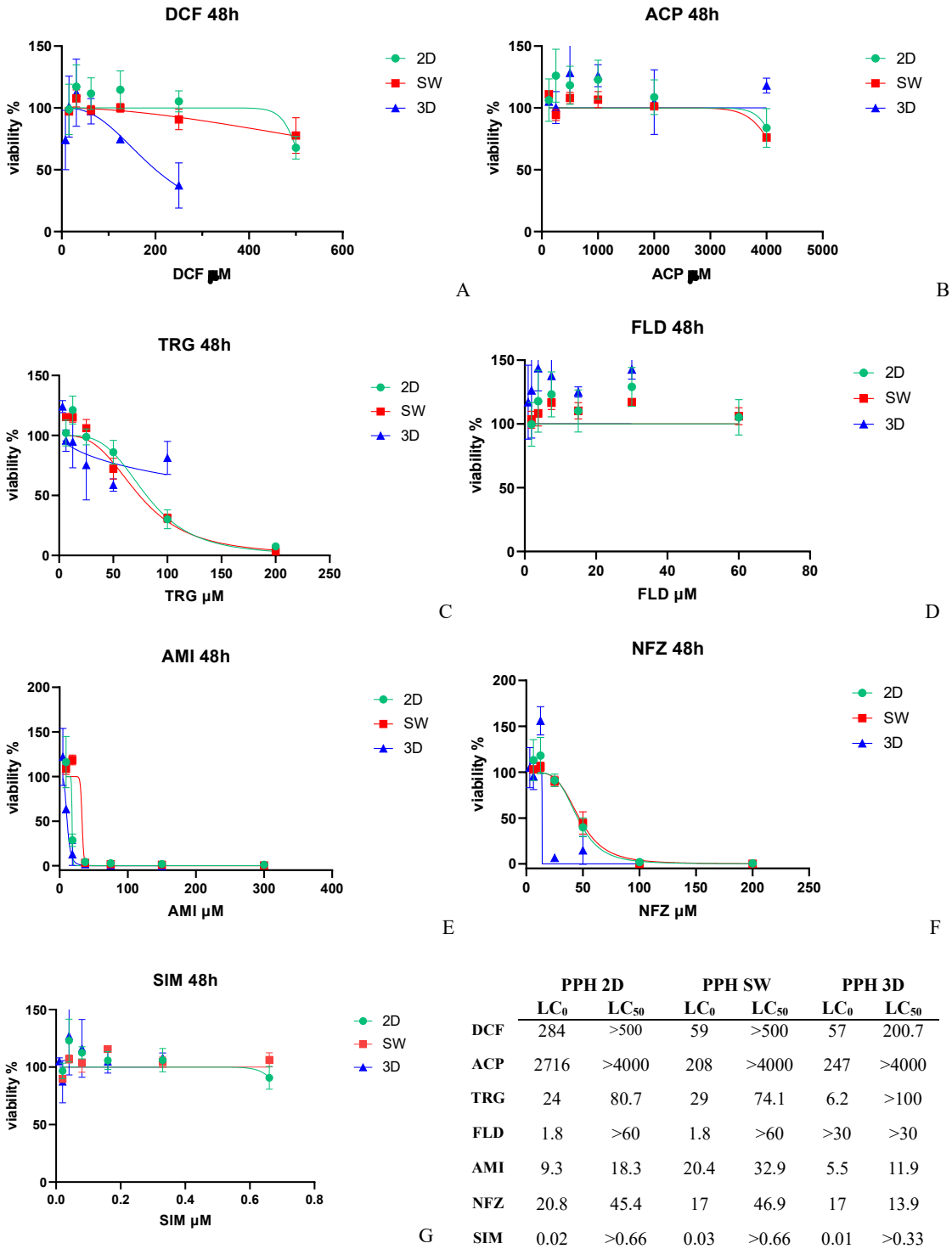

	PPH 2D		PPH SW		PPH 3D	
	LC_0	LC_{50}	LC_0	LC_{50}	LC_0	LC_{50}
DCF	284	>500	59	>500	57	200.7
ACP	2716	>4000	208	>4000	247	>4000
TRG	24	80.7	29	74.1	6.2	>100
FLD	1.8	>60	1.8	>60	>30	>30
AMI	9.3	18.3	20.4	32.9	5.5	11.9
NFZ	20.8	45.4	17	46.9	17	13.9
SIM	0.02	>0.66	0.03	>0.66	0.01	>0.33

H

Figure 21. Viability percentage of PPH monolayer (2D), sandwich (SW), and spheroids (3D) cultures after 48h of drug exposure. Drugs abbreviations: DCF= Diclofenac; ACP= Acetaminophen; TRG= Troglitazone; FLD= Fialuridine; AMI= Amiodarone; NFZ= Nefazodone; SIM= Simvastatin. X-axis: drug concentrations, µM. Y-axes: Cell viability is expressed as a percentage of control cells (cells treated with DMSO only). Data are presented as mean ± SEM of three independent experiments. Table (H) reports LC0 and LC50 values, extrapolated from the dose-viability curves of each compound relative to PPH 2D, SW, and 3D systems exposed to a single drug administration. LC50 values were calculated using non-linear regression analysis with a sigmoidal dose-response model (GraphPad Prism 8.3.0; GraphPad Software, San Diego, CA).

From the analysis of the dose-response curves, the three systems show, in general, the same sensitivity to drugs' lethality after the single administration (Fig. 21). In fact, except for diclofenac and to a lesser

extent for nefazodone, we do not see significant discrepancies of cells' viability between monolayer, sandwich, and spheroids within each drug application (Fig. 21A, 21F). This result is also confirmed by LC_{50} values reported in the table above (Fig. 21H). Indeed, for each compound LC_{50} values are comparable between the three systems. However, according to our previous findings, 3D models of rat and human hepatocytes demonstrated higher susceptibility to drug toxicity than bidimensional systems. Conversely, spheroids of PPH showed, in general, a similar susceptibility to drugs to that of 2D systems. Diclofenac and minorly nefazodone represented the sole exceptions, with PPH spheroids showing higher sensitivity than sandwich and monolayer cultures (Fig. 21A and 21F). Indeed, significant differences in cells' viability between 2D and 3D systems were observed at diclofenac's concentration of 250 μM and nefazodone's 25 μM ($p<0.05$). Moreover, PPH spheroids were outright less sensitive than monolayer and sandwich to lethality induced by fialuridine and acetaminophen (Fig 21D and 21B).

Overall, this result is quite unexpected since, for the drugs investigated, metabolites are the main responsible for toxicity. Therefore, 3D systems should be more sensitive to drugs, given their metabolic capacity, which is higher than that of 2D systems. There are two possible reasons to explain this effect: the first is that after a single dose of the drug, the amount of toxic metabolites produced does not reach a sufficient threshold to induce cell death; the second is that pig hepatocytes express different metabolizing enzymes than other species (e.g., humans and rats), so toxicity is no longer triggered by the same metabolites produced in rats and humans. Both cases imply a different metabolic activity between the species considered in terms of velocity in the first case and pathways in the second.

In line with the results of HepaRG and RPH, within the acute toxicity assessment, fialuridine and simvastatin can be considered the safest compounds among the drugs tested in this study as they did not cause any cells' viability decrease in PPH, even at high doses (Fig.21D and 21G).

Acetaminophen did not cause significant cell damage in PPH at doses up to 2000 μM, as the cell's viability remained above 100% in all systems. However, at 4000 μM, the highest dose tested, acetaminophen started to induce cell death in sandwich and monolayer cultures but not in spheroids (Fig. 21B). This is surprising since acetaminophen's toxicity is mainly attributed to its reactive metabolite NAPQI. We expected that spheroids, which have a more active metabolism than 2D systems, would be more susceptible to the effects of toxic metabolites like NAPQI. Although acetaminophen is metabolized similarly to humans in pigs, some differences in the proportions of metabolites occur. A recent study revealed that in pigs, NAPQI is only a minor product of acetaminophen metabolism (Dargue R et al., 2020a). This could account for the low toxicity of the drug observed in our PPH spheroids.

The drug troglitazone showed a peculiar effect in our PPH cultures. We found that while in monolayer and sandwich cultures, cells' viability decreased proportionally with the increasing drug concentration, in spheroids, the same effect occurred only when the concentration applied was minor or equal to 50 μM (Fig. 21C). When cells were exposed to troglitazone 100 μM cell viability was unexpectedly higher

(Fig. 21C). A plausible explanation could be that a side metabolic pathway, only expressed in 3D systems, is able to convert troglitazone into non-toxic metabolites when troglitazone's concentration reaches a certain threshold. However, previous experiments were not concordant with our results, as it was reported that troglitazone caused cell death in pig hepatocytes after acute exposure to 100 µM (Kostrubsky VE et al., 2000).

Overall, amiodarone and nefazodone showed the highest acute toxicity in PPH (Fig. 21E, 21F). This can be easily inferred from the dose-response curved pattern (Fig 21E and 21F) and from the analysis of LC_0 and LC_{50} values. Within each system, nefazodone's and amiodarone's LC_{50}/LC_0 ratios ranged between 1-3, meaning that for these compounds, LC_0 values are very close to the respective LC_{50} values (Fig.21H). For compounds with such a narrow therapeutic index, the risk of toxicity is very high, as doses allowed for a therapeutic action without adverse effects are very limited.

For the long-term cytotoxicity assessment, drugs were given to PPH sandwich and spheroids cultures repeatedly for 14 days. A marked rise in cell death rate was observed for every drug in both PPH sandwich and spheroids cultures compared to the single dose administration (Fig.21, Fig.22).

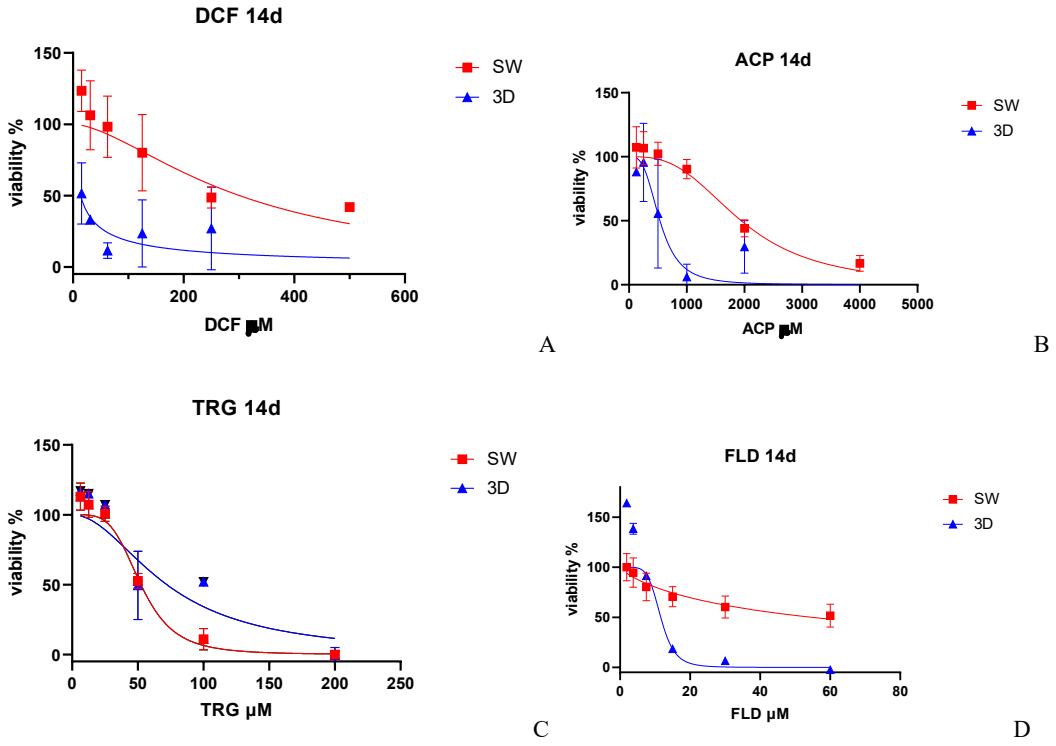

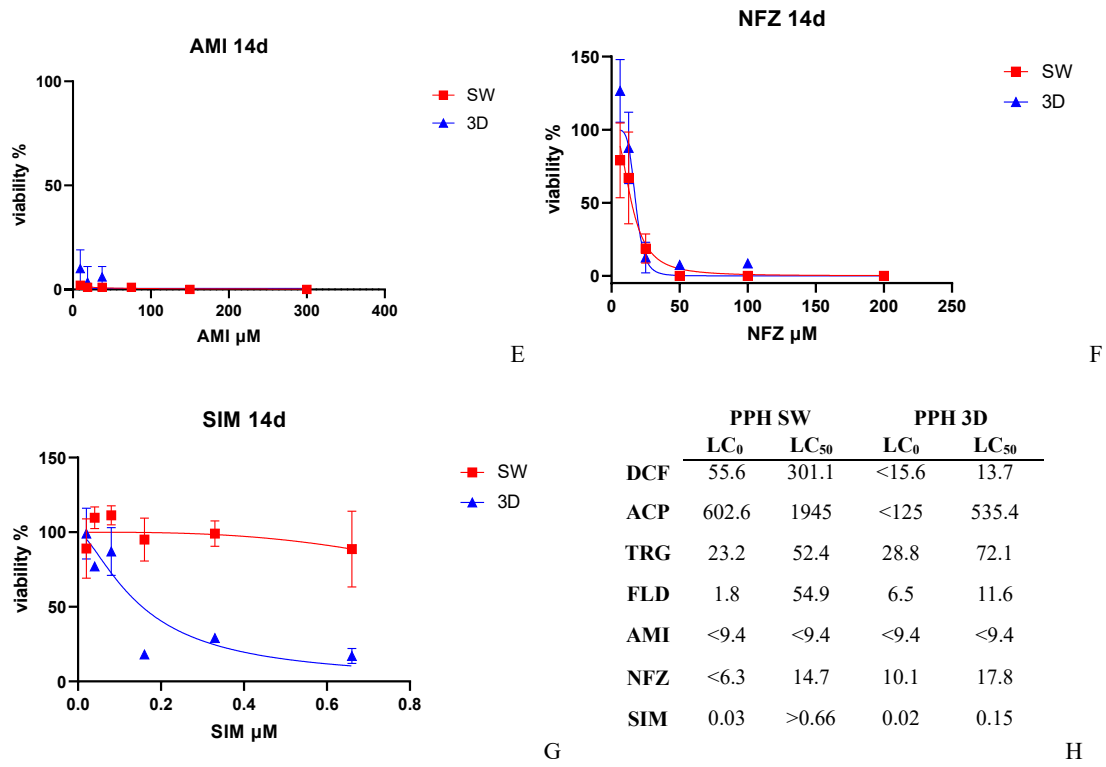

	PPH SW		PPH 3D	
	LC_0	LC_{50}	LC_0	LC_{50}
DCF	55.6	301.1	<15.6	13.7
ACP	602.6	1945	<125	535.4
TRG	23.2	52.4	28.8	72.1
FLD	1.8	54.9	6.5	11.6
AMI	<9.4	<9.4	<9.4	<9.4
NFZ	<6.3	14.7	10.1	17.8
SIM	0.03	>0.66	0.02	0.15

H

Figure 22. Viability percentage of PPH monolayer (2D), sandwich (SW), and spheroids (3D) cultures after 14 days of repeated doses of drugs. Drugs abbreviations: DCF= Diclofenac; ACP= Acetaminophen; TRG= Troglitazone; FLD= Fialuridine; AMI= Amiodarone; NFZ= Nefazodone; SIM= Simvastatin. X-axis: drug concentrations, µM. Y-axes: Cell viability is expressed as a percentage of control cells (cells treated with DMSO only). Data are presented as mean ± SEM of three independent experiments. Table (h) reports LC0 and LC50 values, extrapolated from the dose-viability curves of each compound relative to PPH 2D, SW, and 3D systems exposed to a single drug administration. LC50 values were calculated using non-linear regression analysis with a sigmoidal dose-response model (GraphPad Prism 8.3.0; GraphPad Software, San Diego, CA). Comparison between systems was made using two-way ANOVA followed by Tukey's multiple comparison test (GraphPad Prism 8.3.0; GraphPad Software, San Diego, CA). $p<0.05$ was considered statistically significant.

Remarkably, fialuridine and simvastatin, which did not affect cell viability at 48h, induced high cell death when applied repeatedly for 14 days (Fig. 22D, 22G). This effect was more evident in spheroids than in sandwich cultures (Fig 22D). A significant difference in mortality was induced between sandwich and spheroids cultures at fialuridine concentrations of 60, 30, and 15 µM and at simvastatin concentrations of 0.66 µM and 0.33 µM ($p<0.001$). Particularly, fialuridine`s lethality increased proportionally with the dose after two weeks of treatment and caused 100% and 50% of cell mortality, respectively, in PPH spheroid and sandwich cultures at 60 µM (Fig. 22D). This indicates the higher sensitivity of 3D systems to this compound. To the best of our knowledge, fialuridine's toxicity was never tested *in vitro* in pig hepatocytes. However, *in vivo* preclinical studies conducted on other animal species subjected to one hundred times the human dose of fialuridine did not reveal any sign of acute hepatotoxicity, whereas chronic administration of the drug caused mitochondria damage in liver cells after 12 weeks (Attarwala H, 2010; Lewis W, Dalakas MC, 1995). This result is compliant with the different lethality of fialuridine observed between our short- and long-term toxicity assessments. In fact, as mentioned, fialuridine 60 µM induced a drastic reduction of PPH spheroid viability after two weeks

of treatment (22D). Conversely, no cell mortality was detected when the drug was administered at a single dose (Fig 21D).

The impact of simvastatin on cell viability resulted in a consistent difference between sandwich and spheroids cultures of PPH after two weeks of treatment. In fact, while the drug did not affect the viability of the PPH sandwich, the cell death rate of PPH spheroids rapidly increased, starting from the dose of 0.16 µM onward (Fig. 22G). The toxicity of simvastatin in pig hepatocytes has not been extensively studied, but there is some evidence that it may be similar to that of human hepatocytes. Some molecular mechanisms of simvastatin's toxicity seem to be related to the compound *per se* and its principal metabolites, both interfering with the synthesis and function of molecules responsible for membrane integrity like CoQ10. Depletion of CoQ10 is responsible for mitochondria dysfunction that could lead to impairment of ATP production and cell apoptosis (Kaminsky YG and Kosenko EA, 2010).

Despite the administration of repeated doses of simvastatin causing high cell mortality in PPH spheroids, the single administration of the drug to the three systems did not provoke any cell death (Fig 21G and 22G). Our *in vitro* prediction of simvastatin's long-term toxicity performed in spheroids cultures confirmed the cytotoxicity found previously in other assessments. A recent *in vivo* study, where a group of female pigs were exposed to simvastatin for one month, showed a high propensity of hepatocytes to apoptosis and several histological signs of hepatocyte damage, indicating alterations of membrane permeability, alterations in glycogen and lipid metabolism as well as signs of fibrosis and hepatitis (Mikiewicz M et al., 2019).

The different response to simvastatin observed in the present study between sandwich and spheroids at 14 days of treatment highlights that spheroids were able to predict drug toxicity in pig hepatocytes analogously to *in vivo* systems, while sandwich cultures failed in this prediction. Thus, spheroids could represent an accurate *in vitro* model for hepatotoxicity prediction of simvastatin in pigs as their susceptibility to the drug reflects that of the *in vivo* environment.

Similarly to simvastatin, diclofenac and acetaminophen revealed very different cytotoxic effects between PPH sandwich and spheroids cultures after two weeks of treatment (Fig. 22A, 22B). Cells' viability resulted much higher in sandwich than spheroid cultures for every drug concentration tested, indicating the higher sensitivity of 3D systems in predicting drug adverse effects compared to 2D systems again. Particularly, a significant decrease in cells' viability was detected in spheroids exposed to diclofenac 62.5 µM and acetaminophen 1000 µM ($p<0.001$) compared to sandwich cultures. In line with these findings, LC_{50} of diclofenac diminished from 301.1 µM in sandwich to 13.7 µM in spheroids. Analogously, acetaminophen's LC_{50} dropped from 1945 µM in sandwich to 535.4 µM in spheroids (Fig 22H). A very high decrease was also seen for the LC_0 values for both compounds passing from sandwich to spheroids cultures (Fig. 22H).

On the other hand, the drugs amiodarone and nefazodone did not show significant discrepancies in cell viability between 2D and 3D systems in our 14-days cytotoxicity assessment (Fig. 22E, 22F). As it is shown in the dose-response graphs, red and blue curves, representing respectively sandwich and spheroids, show a very similar trend (Fig. 22E, 22F). The hepatotoxicity induced by these compounds is so marked that cell death is rapidly induced, independently from the cell system tested.

Toxicity exerted by troglitazone on 2D and 3D PPH cultures was similar, even though sandwich cultures showed higher sensitivity to the drug compared to spheroids at concentrations higher than 50 µM (Fig. 22C, p<0.001).

The comparison of lethal drug concentrations found in the short and long-term cytotoxicity evaluations clearly indicates that the lethality of drugs increases with the exposure time and the number of doses administered. LC_0 and LC_{50} values, both recorded for PPH spheroids exposed to drugs for 48h and 14 days, are shown in the following graph bars (Fig.23).

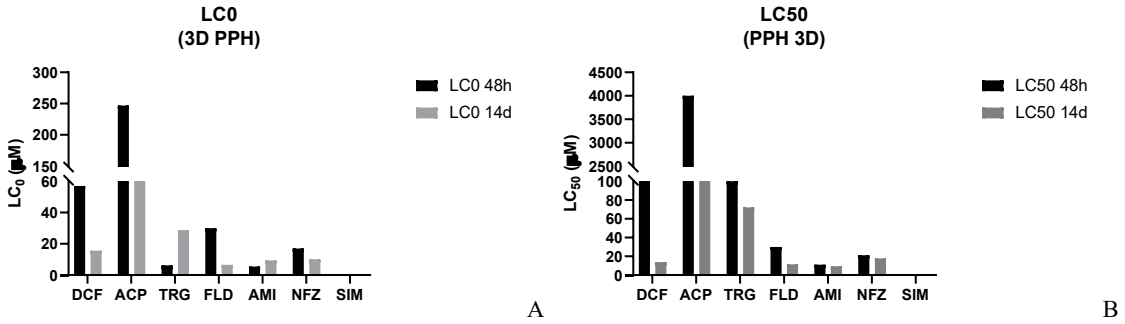

Figure 23. Comparison of LC_0 (A) and LC_{50} (B) values of tested drugs between short (48h) and long-term (14d) treatment of PPH spheroids.

For example, diclofenac's LC_{50} decreased from 208 µM to 16.7 µM; acetaminophen's LC_{50} decreased from >4000 µM to 535.4 µM; fialuridine's LC_{50} from >30 µM to 11.6 µM; troglitazone's LC_{50} from > 100 µM to 72.1 µM (Fig.23B). A similar decreasing trend is shown for the LC_0 values, except for troglitazone (Fig. 23A). Overall, this result shows the reliability of our *in vitro* toxicity prediction as it succeeded in reproducing the different lethality induced by toxic drugs during short- and long-term exposures.

In summary, during this section of the study, primary hepatocytes were successfully isolated from pig liver. After recovering, primary cells showed the typical cuboid shape of hepatocytes, and the immunofluorescence stain revealed albumin production as a specific hepatic biomarker. Monolayer and sandwich cultures of primary pig hepatocytes (PPH) were maintained for four weeks. During this time, cells showed a significant change in morphology, shifting from the polygonal to the spindle shape, reflecting a phenotype mutation, before reaching senescence.

Spheroids of PPH were generated as a valuable 3D model with the aim to resemble the *in vivo* liver environment more accurately than 2D *in vitro* systems. After the first week of culture, spheroids gradually reached a homogeneous round shape, increasing their compactness.

Monolayer, sandwich, and spheroids of isolated PPH were prepared to test drugs' cytotoxicity. At acute drug administration, among all the compounds, nefazodone and amiodarone showed the highest toxicity (lowest LD_{50}s) in all the systems tested. Acetaminophen and diclofenac showed medium-high toxicity, proportionally increasing with the concentration, while fialuridine and simvastatin did not induce cell death.

Conversely, the results showed that repeated exposure to the drugs increased their toxicity and caused cell death even for drugs that did not show any acute lethality, such as fialuridine and simvastatin, in concordance with previous studies demonstrating their toxicity only in chronic regimens.

In general, our toxicity evaluation performed on PPH showed that all drugs induced the same effects in the three experimental systems when added one time, while repeated applications of diclofenac, acetaminophen, fialuridine, and simvastatin over two weeks induced a higher cell mortality in 3D spheroids, indicating the higher sensitivity of 3D systems to these drugs. By contrast, amiodarone, nefazodone, and troglitazone exerted a very similar lethality on both sandwich and spheroids cultures of PPH in the long-term exposure.

Ultimately, our prediction model of toxicity in PPH has proved to be accurate, as it successfully replicated short- and long-term effects of different drugs similarly to outcomes found in preclinical trials.

5. *In vitro* hepatotoxicity comparison across human and animal species

In this section of the study, we present a comparative analysis of the drugs' cytotoxic effect observed across the three species tested: human, represented by the HepaRG cell line, and primary hepatocytes from pig and rat species. Our aim is to determine which cell line best represents the human liver environment *in vitro* and which culture system is the most reliable for predicting human hepatotoxicity.

Comparing how drugs affected the viability of hepatocytes of each species was crucial to remark on species-specific differences in toxicity outcomes.

5a. Comparison of drugs' hepatotoxicity across species at 48h of exposure

In this part of the study, we started by comparing the toxicity of the selected drugs at 48h after the single administration. The graphs in Fig. 24 report the drugs' effect on cell viability of human (HepaRG, green),

pig (PPH, red), and rat hepatocytes (RPH, blue) cultured both in 2D sandwich (bold lines) and 3D spheroids (dashed lines) after two days of treatment.

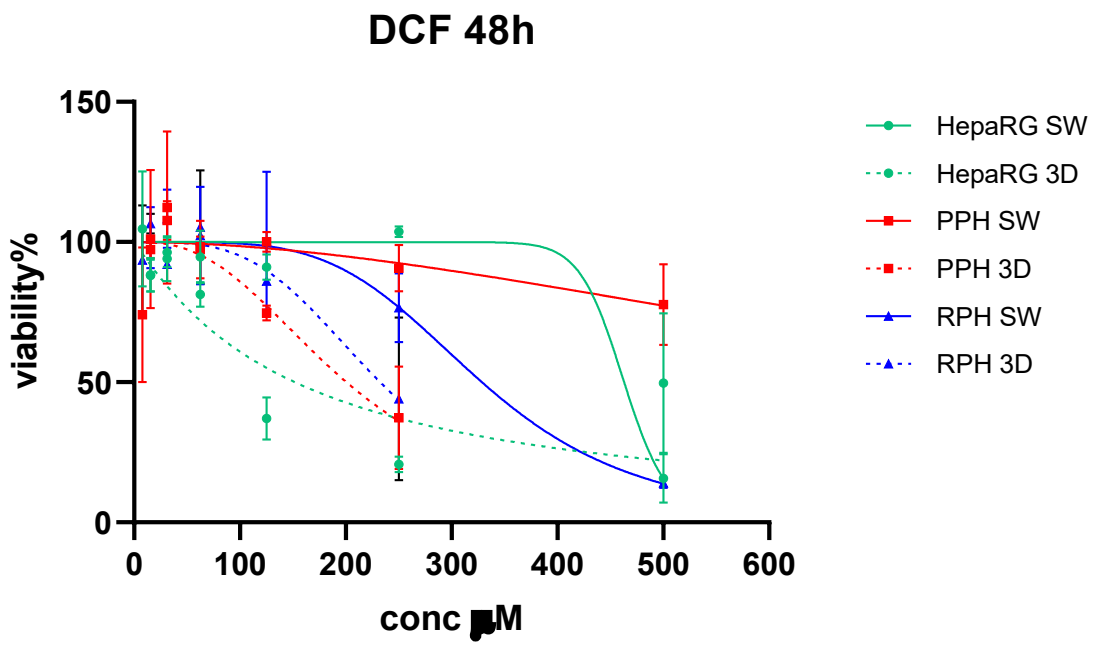

A

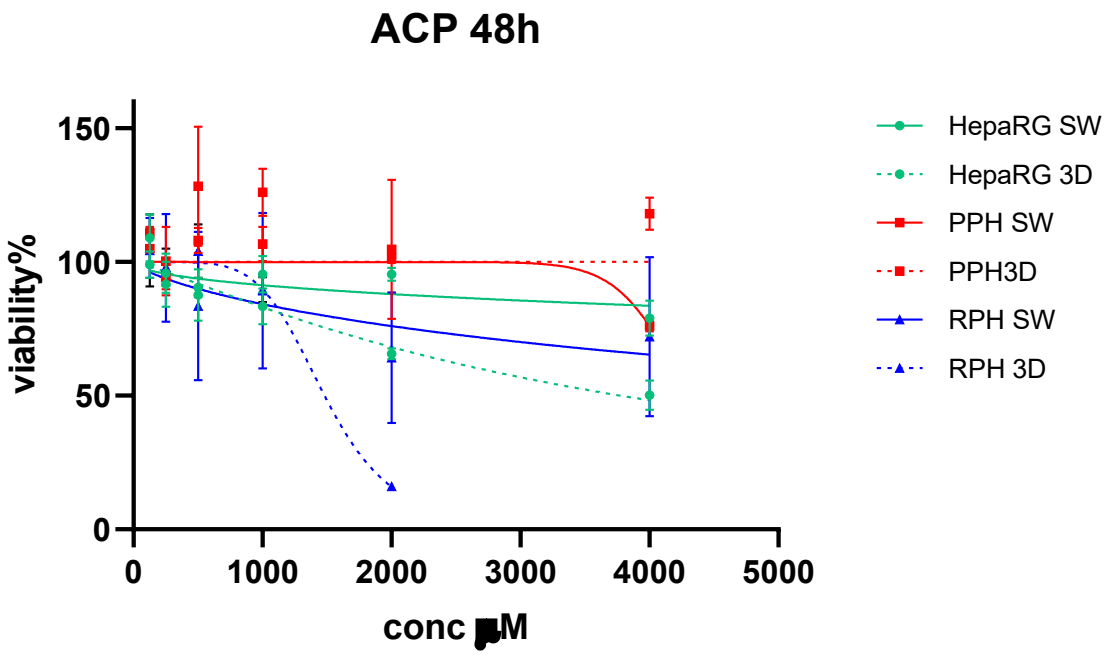

B

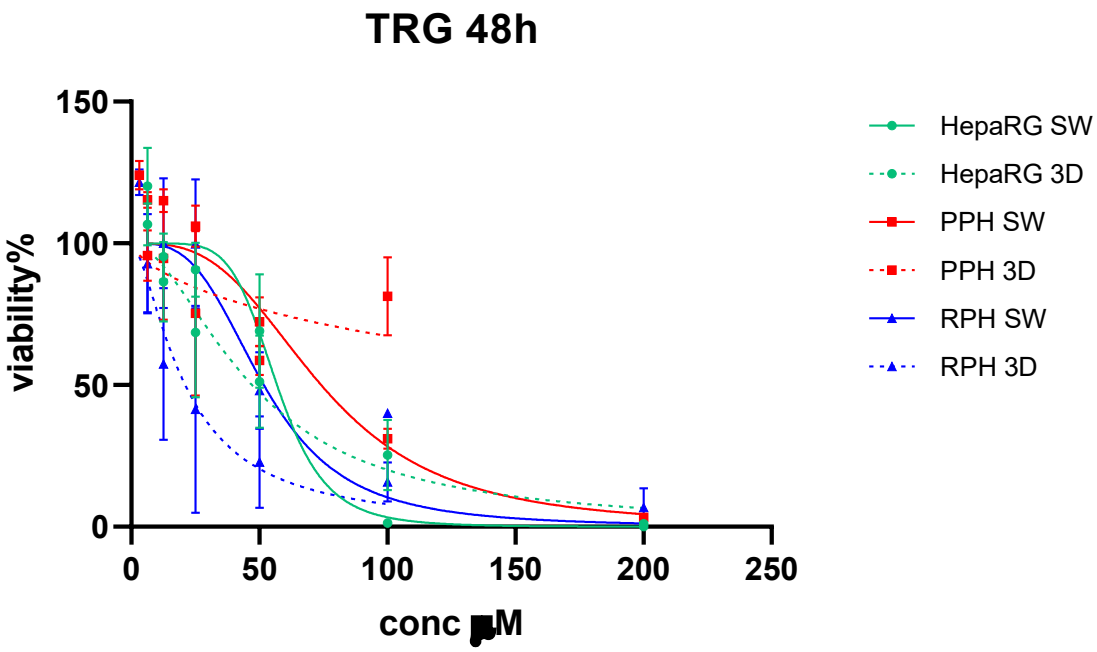
TRG 48h
viability%
150
100
50
0
0
50
100
150
200
250
conc µM
HepaRG SW
HepaRG 3D
PPH SW
PPH 3D
RPH SW
RPH 3D

C

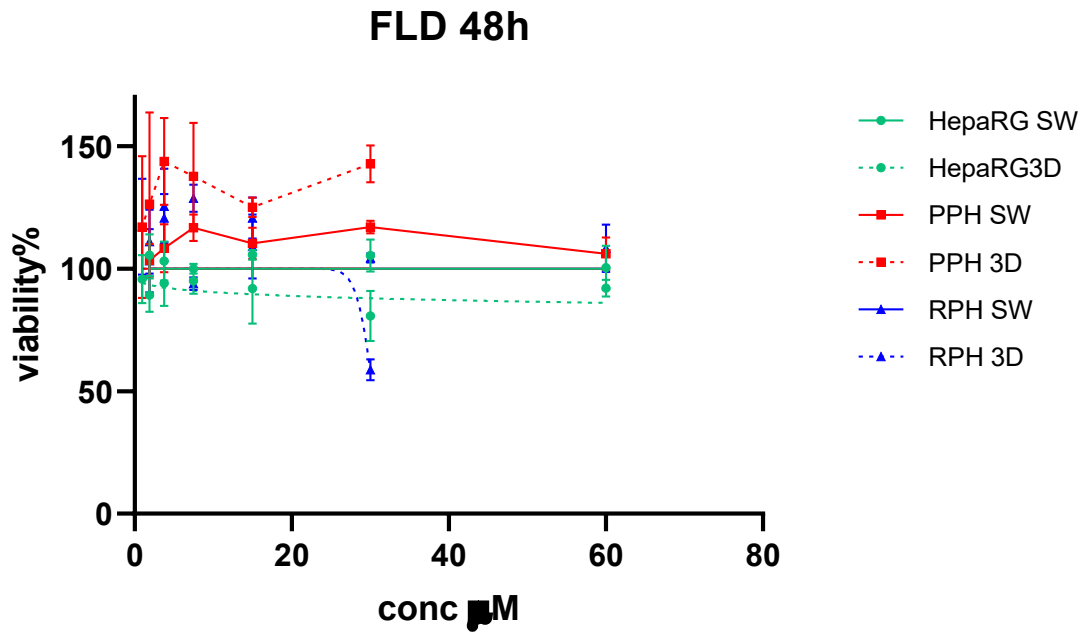
FLD 48h
viability%
150
100
50
0
0
20
40
60
80
conc µM
HepaRG SW
HepaRG3D
PPH SW
PPH 3D
RPH SW
RPH 3D

D

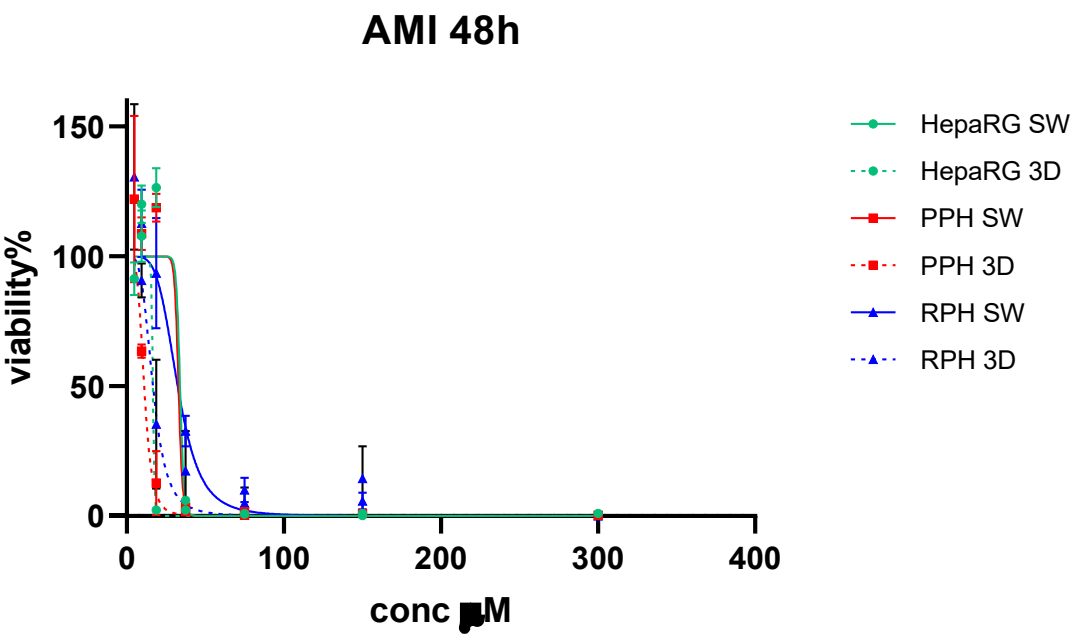
AMI 48h
viability%
150
100
50
0
0
100
200
300
400
conc µM
HepaRG SW
HepaRG 3D
PPH SW
PPH 3D
RPH SW
RPH 3D

E

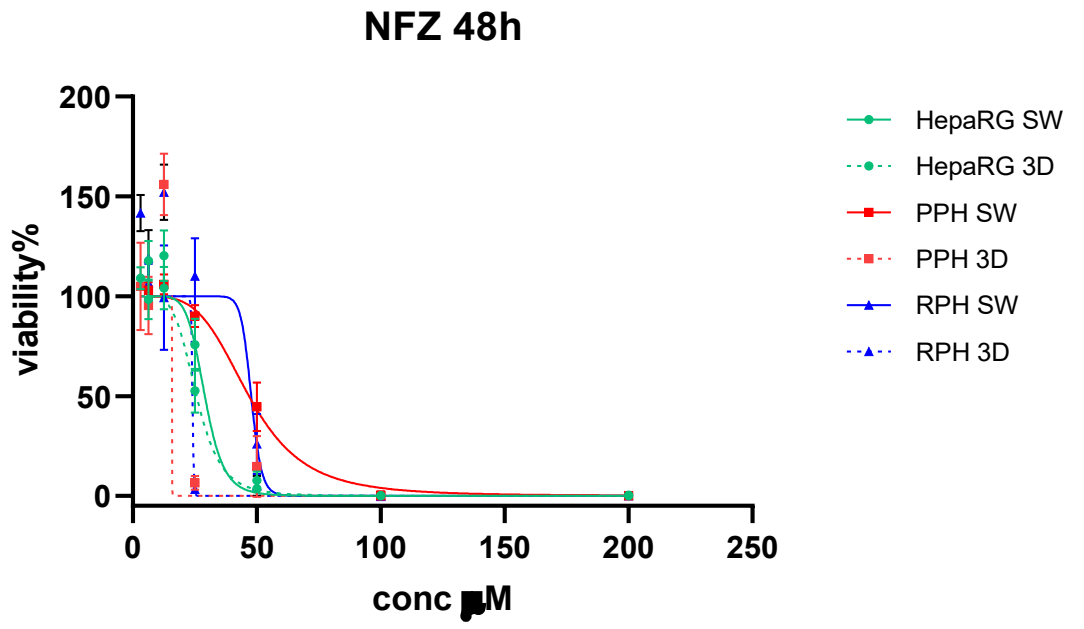
NFZ 48h
viability%
200
150
100
50
0
0
50
100
150
200
250
conc µM
HepaRG SW
HepaRG 3D
PPH SW
PPH 3D
RPH SW
RPH 3D

F

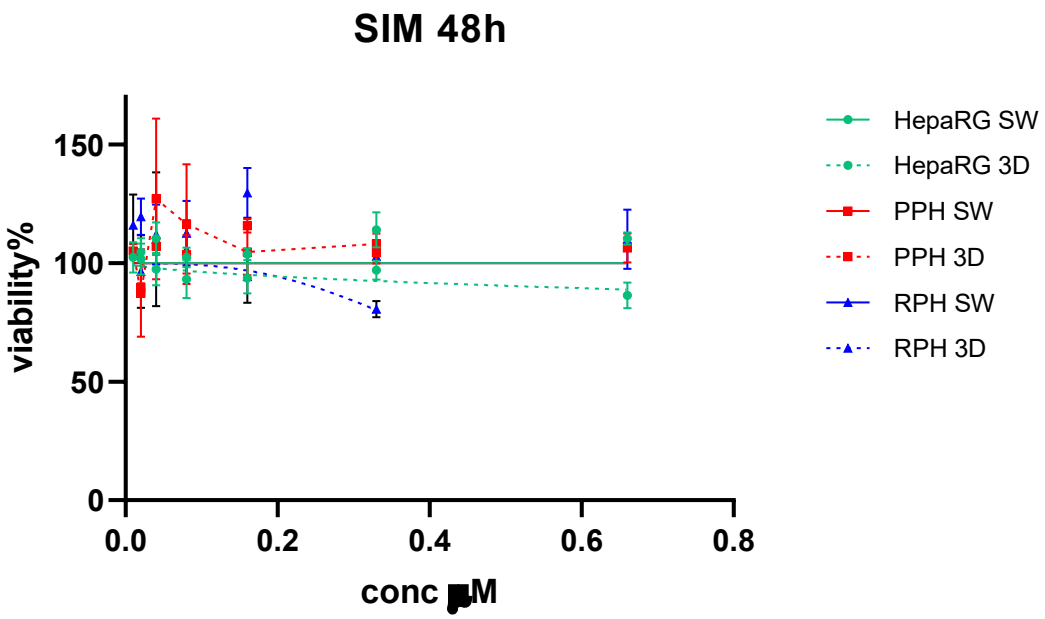

G

Figure 24. Drugs' effect on cell viability at 48h compared across species: HepaRG (human hepatocytes; green), PPH (pig primary hepatocytes; red), RPH (rat primary hepatocytes; blue). For each cell line, both sandwich cultures (SW, bold lines) and spheroids (3D, dashed lines) are shown. SW= sandwich cultures; 3D= spheroids. Drugs abbreviations: DCF= Diclofenac; ACP= Acetaminophen; TRG= Troglitazone; FLD= Fialuridine; AMI= Amiodarone; NFZ= Nefazodone; SIM= Simvastatin. X-axis: drug concentrations, µM. Y-axes: Cell viability is expressed as a percentage of control cells (cells treated with DMSO only). Data are presented as mean ± SEM of three independent experiments. Plots were generated using non-linear regression analysis with a sigmoidal dose-response model (GraphPad Prism 8.3.0; GraphPad Software, San Diego, CA). Comparison between systems was made using two-way ANOVA followed by Tukey's multiple comparison test (GraphPad Prism 8.3.0; GraphPad Software, San Diego, CA). $p<0.05$ was considered statistically significant.

	HepaRG SW		PPH SW		RPH SW	
	LC_0	LC_{50}	LC_0	LC_{50}	LC_0	LC_{50}
DCF	<15.7	**463.0**	59	**>500**	126	**328.7**
ACP	125	**>4000**	208	**>4000**	202.8	**>4000**
TRG	9.6	**56.9**	29	**74.1**	13.6	**51.8**
FLD	>60	**>60**	1.8	**>60**	>60	**>60**
AMI	20.7	**33.9**	20.4	**32.9**	14.9	**32.4**
NFZ	17.3	**29.1**	17	**46.9**	11.9	**47.8**
SIM	>0.66	**>0.66**	0.03	**>0.66**	>0.66	**>0.66**

A

	HepaRG 3D		PPH 3D		RPH 3D	
	LC_0	LC_{50}	LC_0	LC_{50}	LC_0	LC_{50}
DCF	8.3	**151.9**	57	**200.7**	20.7	**232.5**
ACP	191	**3779**	247	**>4000**	213	**1481**
TRG	6.9	**47.1**	6.2	**280.2**	6.6	**21.0**
FLD	<0.95	**>60**	>30	**>60**	6.7	**30.5**
AMI	9	**16.6**	5.5	**11.1**	8	**16.7**
NFZ	5.6	**25.7**	17	**13.9**	17	**22.4**
SIM	0.014	**>0.66**	0.01	**>0.33**	0.02	**>0.33**

B

Table 4. Drugs LC_0 and LC_{50} comparison between species after 48h of drug exposure. LC_0 and LC_{50} values found in sandwich cultures (SW) of HepaRG (green), PPH (red), and RPH (blue) are shown in Table A; LC_0 and LC_{50} found in 3D spheroids (3D) are shown in Table B. LC_{50} values were calculated using non-linear regression analysis of dose-response curves (Fig.24) with a sigmoidal dose-response model (GraphPad Prism 8.3.0; GraphPad Software, San Diego, CA).

As shown in Fig. 24A, the acute effect of diclofenac on cells' viability was different in our tested species. Rat hepatocytes were the most susceptible to diclofenac's toxicity among the three species cultured in sandwich configuration (Fig. 24A, bold lines), with the lowest LC_{50} of 328.7 μM (Table 4A). More precisely, although the drug seemed to not affect viability of any species at low concentrations (up to 125 μM), at concentrations of diclofenac higher than 250 μM the gap between RPH and the other two species is significant ($p<0.001$), while at the concentration of diclofenac equal to 500 μM the drug effect between RPH and HepaRG is similar, and yet still marked in comparison to PPH cultures ($p<0.01$).

By contrast, when diclofenac was administered to spheroids cultures, human HepaRG resulted in the most sensitive species, as clearly visible from the dose-response curve showing a decrease of viability significantly deeper than that of rat and pig hepatocytes (Fig. 24A, dashed lines). Both LC_0 and LC_{50} of 3D spheroids were lower in HepaRG than PPH and RPH. Particularly, LC_{50} of diclofenac reported for HepaRG was 151.9 μM (Table 4B), while that of PPH and RPH were 200.7 μM and 232.5 μM respectively (Table 4B).

Remarkably, for each species considered, spheroids were more sensitive to diclofenac than the respective sandwich cultures, as shown by the curves (Fig. 24A) and by the LC_{50} values. Overall, these results demonstrate the superior sensibility of 3D systems to toxicity compared to 2D systems and highlight how the choice of the culture system can influence the outcome and completely change the toxicity interpretation.

Besides idiosyncratic reactions due to diclofenac acyl glucuronide, the diclofenac's metabolites responsible for rare but fatal acute hepatitis are mainly recognized in reactive benzo-quinone imines, formed by diclofenac oxidation in the liver, able to generate proteins adducts (Tang W, 2003). Both in rats and humans, these reactive metabolites were identified by previous studies. In humans, this oxidation is performed by CYP3A4 and CYP2C9; in rats, by CYP2C, 3A, and 2B subfamilies (Ponsoda X et al., 1995; Tang W et al., 1999; Kumar S et al., 2002; Boelsterli UA, 2003). Differences in such CYP subfamily expression between human and rat species may explain the different toxicity shown by the drug in our *in vitro* models (Hammer H et al., 2021).

In pigs, diclofenac's metabolism has not been studied in detail, but it is believed to be similar to that of humans, as CYPs' expression in pigs is similar to humans. However, a study reported a lower CYP2C9 activity in pigs than in humans (Thorn HA et al., 2011). Another study conducted in parallel in liver human and pig microsomes showed the reduced diclofenac's metabolism by CYP2C9 in pigs (Thörn HA et al., 2011). This could account for the reduced formation of metabolites and, therefore, the lower toxicity observed in pigs compared to humans.

Acute toxicity of diclofenac is very rarely reported and appears to be idiosyncratic (Aithal GP, 2004); therefore, it is very challenging to compare our data on acute hepatotoxicity to clinical data, as idiosyncrasy is an unpredictable immune-mediated reaction, not related to the dose (Uetrecht J, 2019; Roth AD and Lee MY, 2017).

Comparing the acute effect of acetaminophen within the three species, rat hepatocytes were the most susceptible to the drug, followed by HepaRG and pig hepatocytes, in both sandwich and spheroids cultures (Fig. 24B). Also, the different sensitivity to acetaminophen between species was much more evident in spheroids (Fig. 24B, dashed lines). Indeed, the discrepancy between rat hepatocytes' viability and that of the other two species cultured in spheroids was significantly visible at acetaminophen's concentration of 2000 µM ($p<0.01$). Additionally, the LC_{50} found for HepaRG was 3779 µM, and that of PPH spheroids was >4000 µM, whereas that of RPH spheroids was 1481 µM (Table 4B). This result suggests that rat hepatocytes are more susceptible to acetaminophen's acute toxicity than pig and human species.

Although acetaminophen metabolism follows essentially the same pathways in humans, rats, and pigs, there are some differences in the proportions of the metabolites produced among these species. In humans, at high doses, approximately 60% of acetaminophen is metabolized by glucuronidation, about 35% by sulfation, and only 5% is oxidized by CYP2E1 into NAPQI, a toxic metabolite, which is further detoxified by GSH binding. At overdoses, GSH depletion leads to NAPQI accumulation, which triggers hepatic damage (Mazaleuskaya LL et al., 2015). Similarly to humans, when acetaminophen is overdosed, it causes hepatocyte necrosis in rat liver via the production of toxic metabolites (Kučera O et al., 2016). The principal metabolites identified in rats are the same as those found in humans (Nelson SD, 1990; Kučera O et al., 2016). Among all, NAPQI production, along with the depletion of GSH found in rat models, are responsible for the initiation of hepatocyte damage and suggest the same mechanism of toxicity as that observed in humans (Nelson SD, 1990; Kučera O et al., 2016).

According to our findings, rat hepatocytes were more sensitive to acetaminophen than human HepaRG in 3D systems. Similarly, several studies have demonstrated that human hepatocytes are more resistant to acetaminophen's toxicity than rat hepatocytes (Mitry RR et al., 2005; Jemnitz K et al., 2008). This may be related to the different expression of CYP2E1, the enzyme responsible for NAPQI formation. Previous studies reported that rat hepatocytes express higher levels of CYP2E1 and lower capacity for sulfation and glucuronidation than humans (Hammer H et al., 2021). Therefore, rats express a higher conversion rate of acetaminophen into the toxic metabolite NAPQI and a minor capacity of acetaminophen's detoxification.

In our study, pig primary hepatocytes were the least susceptible species to acetaminophen's acute toxicity. The viability of both sandwich and spheroids cultures of PPH was not affected by the drug, as shown by the dose-response curves (Fig. 24A, red). A recent study reported important differences in acetaminophen's metabolism between human and pig species that could explain our findings. The study showed that sulfation and oxidation are only minor routes of acetaminophen's biotransformation in pigs compared to humans, while glucuronidation represents the major route (Dargue R et al., 2020a; Capel I D et al., 1972). Consequently, NAPQI is only minimally produced in pigs. This could explain the low hepatotoxicity observed in this species. The study attributed these differences to different expressions

of key metabolic enzymes in the liver between pigs and humans. The study also identified another toxic metabolite, PAP-G, which is formed by deacetylation and glucuronidation of acetaminophen. This toxic product seems to be responsible for methemoglobinemia and nephrotoxicity in pigs exposed to acetaminophen. However, it seems not to be related to hepatotoxicity (Dargue R et al., 2020b). These findings are consistent with our results, which indicate no acute hepatotoxicity induced by acetaminophen in pigs' hepatocytes. This implies that pig hepatocyte cultures represent a poor translational model to evaluate acetaminophen's hepatotoxicity in humans.

Acute hepatotoxicity of acetaminophen is strictly dose-related. In humans, acetaminophen overdose with consequent liver injury occurs when doses over 7.5 g per day are administered in adults (Ye H et al., 2018). A blood concentration of acetaminophen superior to 150 µg/mL within four h after assumption is considered toxic (Agrawal S and Khazaeni B, 2024; McGill MR and Jaeschke H, 2018; Radke JB et al., 2018; Levine M et al., 2018). This blood concentration corresponds to the concentration of 1000 µM approximately. Remarkably, in our acetaminophen's dose-viability curves (Fig. 24B), cells' viability started to decrease at acetaminophen's concentration of 1000 µM in both HepaRG and rat cultures, showing that hepatotoxicity started to occur at the same toxic concentration found in humans *in vivo*.

The acute effect of the antidiabetic agent troglitazone on cell viability was consistent across HepaRG and RPH cultured in 2D sandwich mode (Fig. 24C, bold lines), as also indicated by the comparable values of LC_0 and LC_{50} found for the two species (Table 4A), while troglitazone's toxicity exerted on PPH sandwich cultures was lower (LC_{50}= 74.1 µM, Table 4A).

However, troglitazone caused different levels of cell death in the spheroids of the three species. Rat primary hepatocytes were the most sensitive to the drug, showing a sharp decline in cell viability even at low doses (Fig.24C, blue dashed line). Indeed, cell viability was already reduced by 50% at the concentration of 21 µM. On the other hand, when troglitazone was administered at 6.6 µM, viability was 100%. Such a narrow difference between LC_{50} and LC_0 indicates a low therapeutic index for this drug, which, therefore, creates a high risk of hepatotoxicity in rat hepatocytes. HepaRG cells showed a less marked reduction of viability, as shown in Fig. 24C (green dashed line), with an LC_{50} of 47.1 µM (Table 4B). By contrast, the viability of pig hepatocyte spheroids was only slightly affected by troglitazone (Fig. 24C, dashed lines). Viability of pig and rat spheroids decreased proportionally with increasing drug concentrations up to 50 µM. However, at the highest troglitazone dose (100 µM), viability seems to increase slightly in pig spheroid cultures (Fig. 24C, red dashed lines).

The molecular mechanism of troglitazone's hepatotoxicity has been extensively studied (Kassahun K et al., 2001; Smith MT, 2003; Masubuchi Y, 2006; Vaibhav A, 2011). Both metabolic and non-metabolic factors are responsible for troglitazone's toxicity (Masubuchi Y, 2006). In humans, troglitazone is detoxified into its sulfate conjugate and, in a minor percentage, by glucuronide conjugation. A third metabolic route, mediated by CYP3A4 and CYP2C8, oxidates troglitazone into a quinone-metabolite,

passing through the formation of a highly reactive intermediate, a quinone-methide, able to covalently bind cellular proteins and macromolecules, such as DNA, causing cellular damage (Vaibhav A, 2011). In addition, three other reactive intermediates were identified as a result of CYP3A4-mediated oxidation of the chroman ring of troglitazone (Smith MT, 2003).

Besides troglitazone's reactive metabolites, other mechanisms seem to be responsible for the drug toxicity in the liver. In fact, troglitazone as the parent compound was found to induce mitochondria impairment and apoptosis in several cell types, including human and rat hepatocytes (Yamamoto Y et al., 2001; Bae M et al., 2003).

Similarly to the human species, in rats, about 60% of troglitazone is metabolized by sulfation, whereas only a small percentage undergoes conjugation and oxidation (Kawai K. et al., 1997). Although rats and humans share the same metabolic pathways of troglitazone, some differences in the gene expression patterns of metabolic enzymes were identified. In a comparative study, it was reported that in human hepatocytes exposed for 24h to troglitazone, the drug significantly induced CYP3A4, CYP2C, and other CYP subfamilies, enhancing the production of troglitazone toxic metabolites deriving from the compound oxidation catalyzed by these enzymes. Conversely, the same upregulation did not occur in rats, suggesting that in this species, the drug has a reduced toxic metabolism (Lauer B et al., 2009). These findings confirm the higher sensitivity of human than rat hepatocytes to troglitazone-induced cytotoxicity that we observed in our 3D cultures.

Overall, PPH were the most resistant cells to troglitazone's toxic effects in both 2D and 3D cultures. Concordantly, in previous studies, PPH shows higher resistance than human primary hepatocytes to troglitazone. Some differences in the metabolic pathways of the drug were found between the two species. In fact, while in humans, the sulfate and quinone are the main metabolites produced and the glucuronide is the least, in pigs, the glucuronide form is the highest expressed (Kostrubsky V.E. et al., 2000). Troglitazone's glucuronidation is believed to be the main detoxification pathway of this drug (Hewitt NJ et al., 2002). Therefore, this would explain the lower susceptibility of pig hepatocytes to troglitazone's toxicity, which was found in our assessment.

In general, troglitazone's acute cases of liver injuries are idiosyncratic; therefore, they are not considered predictable as they are not related to the drug's dose, and they are very rare events (Jaeschke H, 2007). Therefore, predicting the acute drug's effects through *in vitro* models is very challenging.

The acute exposure to the drug fialuridine in sandwich cultures did not cause cell mortality in any of the three hepatocyte species. As it is visible from the graphs, cell viability remained around 100% for any fialuridine concentration added (Fig 24D, bold lines). However, in 3D spheroids, fialuridine significantly reduced the cell viability of RPH only at the highest concentration ($p<0.01$) while continuing to not affect the viability of PPH and HepaRG (Fig 14d, dashed lines). Overall, our results showed that the drug had a comparable impact on human and rat cells but no effect on pig cells, which

were completely resistant to the drug. In any case, however, 50% of cell mortality was never reached, even at fialuridine's highest doses. Concordantly with our acute hepatotoxicity results of fialuridine, it is amply described in literature that fialuridine does not exert any hepatotoxicity at acute administration, whereas its repeated application over time was demonstrated to induce accumulation of toxic metabolites which could interfere with mitochondrial DNA synthesis and function, leading to oxidative stress and apoptosis (Bell CC et al., 2016; Bell CC et al., 2018; McKenzie R et al., 1995; Hendriks DFG et al., 2019). Therefore, as expected, we did not observe an important toxic effect of the drug at 48h of treatment.

Analogously, simvastatin did not significantly affect the viability of any of the three species investigated in any system considered. As shown in Fig. 24G, viability stayed around 100% for every culture type and species. Only HepaRG and RPH spheroids cultures were slightly affected, but only at simvastatin 0.66 µM, the highest concentration tested, corresponding to 32 times Cmax. This result was expected, as simvastatin was never reported, to our knowledge, to cause acute hepatotoxicity after a single administration (Averbukh LD et al., 2022). Indeed, the present assessment showed no acute hepatotoxicity reported in our human and animal models.

Unlike fialuridine and simvastatin, which showed no acute hepatotoxic effects, amiodarone and nefazodone had a consistent and severe impact on liver cells across human, pig, and rat models. The hepatotoxic effects of these two drugs are well documented (Wu IJ and Tsai JH. & Ho, 2021; Ruch RJ et al., 1991; Spaniol M et al., 2001; Choi S, 2003; Dykens JA et al., 2008; Stratton A et al., 2015; Kostrubsky SE et al., 2006; Voican CS et al., 2014; Silva AM et al., 2016; Mueller SO et al., 2015). Our results corroborated the high toxicity reported in previous studies mentioned above. Both compounds significantly reduced cell viability after a single dose, regardless of the species, as indicated by the dose-viability curves (Fig 24E, F). LC_{50} and LC_0 values were very similar across human, pig, and rat hepatocytes in both sandwich and spheroids (Table 4).

Although amiodarone is mainly associated with chronic liver injuries, several cases of fatal acute liver failure developed after a single bolus or intravenous administration of the drug have been described (Jaiswal P et al., 2018; Lwakatare JM et al., 1990; Kalantzis N et al., 1991; Akbal E et al., 2013). When amiodarone was given intravenously, blood concentration reached 1.5 mg/L, corresponding to 2.2 µM (Gregory SA et al., 2002). This value is slightly lower compared to our amiodarone's LC_0 found for the acute treatment of our spheroids' cultures of human and animal species (9 µM in HepaRG; 5.5 µM in RPH; 8 µM in PPH, Tab. 4), indicating that in this case our model showed less accuracy in predicting amiodarone's acute hepatotoxicity.

Sandwich cultures of HepaRG showed higher sensitivity to nefazodone compared to the other species (LC_{50}HepaRG=29.1µM; LC_{50}PPH=46.9 µM LC_{50}RPH=47.8 µM, Table 4). However, no significant differences were observed between species within the 3D cultures subjected to nefazodone, as shown

by the similar LC_{50} values of such systems (Tab. 4). To our knowledge, hepatotoxicity after a single dose of nefazodone was never reported. However, cases of fatal liver failure occurred after only four weeks of therapy (Tzimas G et al., 2003). However, *in vitro* studies showed that nefazodone produced acute toxic effects in hepatocytes in a concentration between 8.98 μM and 38.4 μM (Dykens JA et al., 2008). Comparable nefazodone's LC_{50} values were found in this *in vitro* assessment (Tab. 4).

In general, 3D cultures were slightly more sensitive than 2D sandwich to the drugs' acute effects, as the LC_{50} values for spheroids were lower than those of sandwich (Table 4). Thus, the species' type did not affect the detection of amiodarone's and nefazodone's toxicity, whereas the choice of a three-dimensional system over a two-dimensional one was more important, as it showed more sensitivity to the drugs' insults.

In general, 3D spheroids demonstrated to be more sensitive to drugs' acute toxicity across the three species investigated, although in some cases, this difference was not as marked (e.g., simvastatin and amiodarone). Overall, the human cell line HepaRG resulted more susceptible to diclofenac, troglitazone, and fialuridine than PPH and RPH, as demonstrated by the dose-viability curves and their reduced LC_{50} values, compared to those of animal species. Conversely, rat hepatocytes were the most sensitive to the acute mortality induced by acetaminophen.

As expected, the compounds troglitazone, amiodarone, and nefazodone showed the highest lethality in the acute treatment, in concordance with what is reported in previous clinical cases, therefore demonstrating the overall reliability of our model in the acute toxicity prediction.

These assessments reveal how different species react differently to drugs, even in acute regimens. In fact, only a few drugs, such as amiodarone and nefazodone, showed similar toxic effects in our animal and human models, while the other drugs exerted species-specific effects. Thus, we can infer that human cells are more suitable for acute toxicity prediction than animal cells, which are only reliable in some cases.

5b. Comparison of drugs' hepatotoxicity across species at 14 days of exposure

To complete the analysis of hepatotoxicity evaluation in our *in vitro* systems, we compared the effects of repeated treatments of drugs over 14 days between species.

In each of the graphs below, it is reported the effect of increasing drug's concentration on the viability of human hepatocytes HepaRG, pig primary hepatocytes (PPH), and rat primary hepatocytes (RPH) in sandwich and 3D cultures (Fig.25).

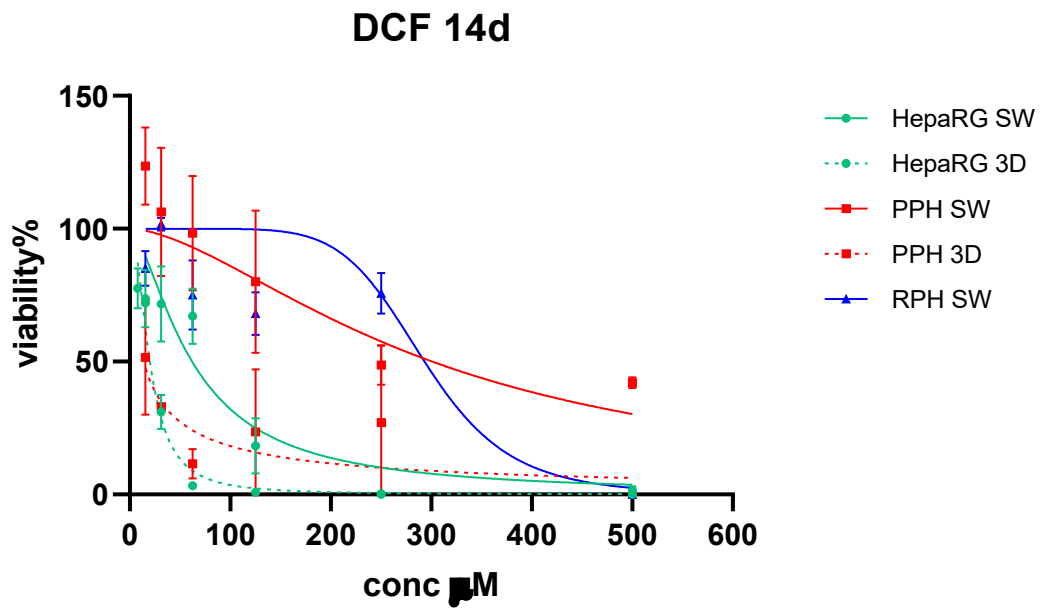
DCF 14d
viability%
150
100
50
0
0
100
200
300
400
500
600
conc µM
HepaRG SW
HepaRG 3D
PPH SW
PPH 3D
RPH SW

A

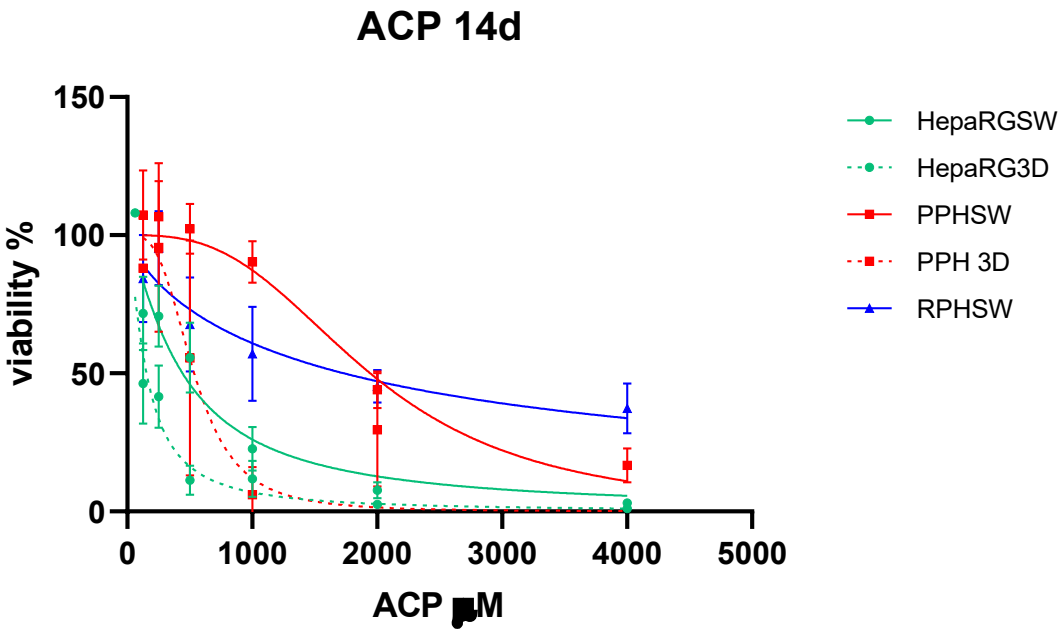
ACP 14d
viability %
150
100
50
0
0
1000
2000
3000
4000
5000
ACP µM
HepaRGSW
HepaRG3D
PPHSW
PPH 3D
RPHSW

B

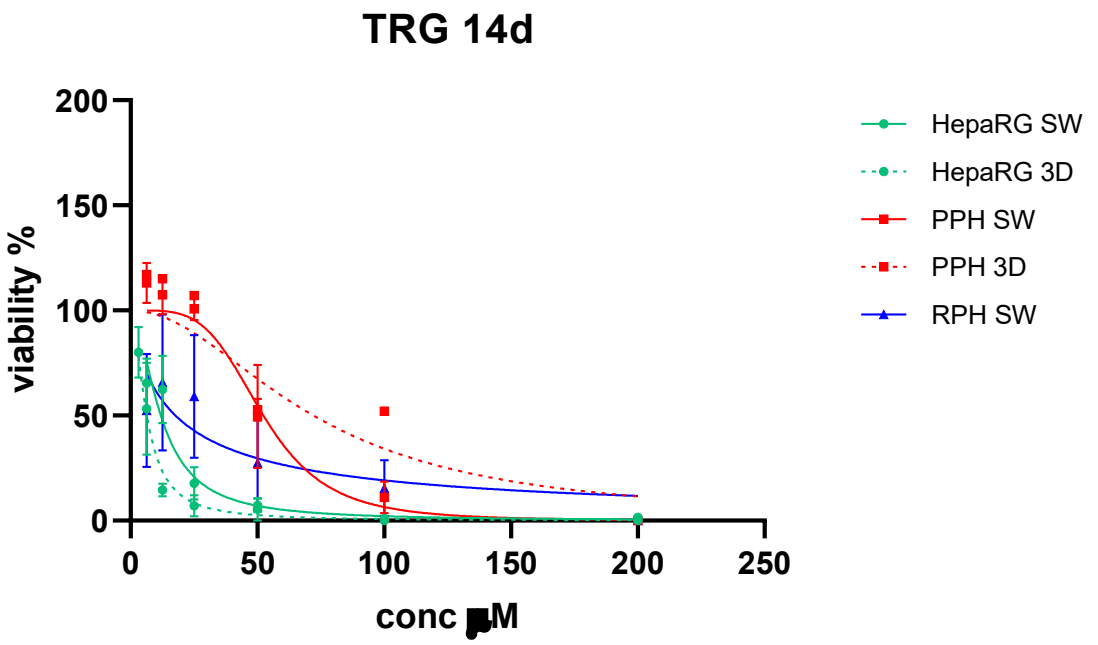
TRG 14d
viability %
200
150
100
50
0
0
50
100
150
200
250
conc µM
HepaRG SW
HepaRG 3D
PPH SW
PPH 3D
RPH SW

C

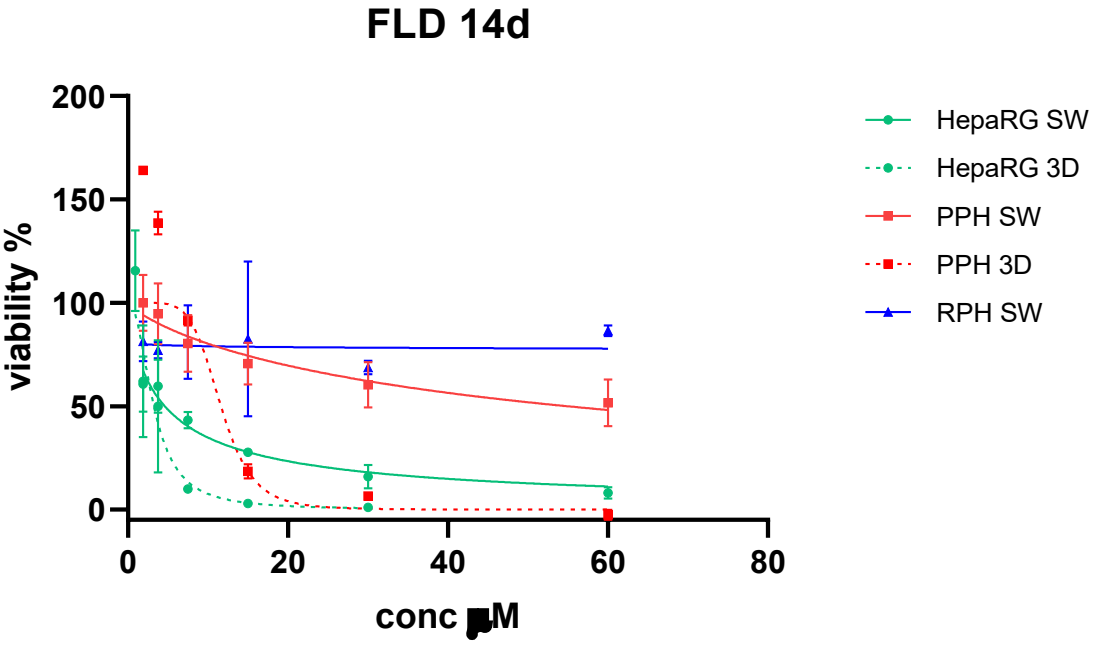
FLD 14d
viability %
200
150
100
50
0
0
20
40
60
80
conc µM
HepaRG SW
HepaRG 3D
PPH SW
PPH 3D
RPH SW

D

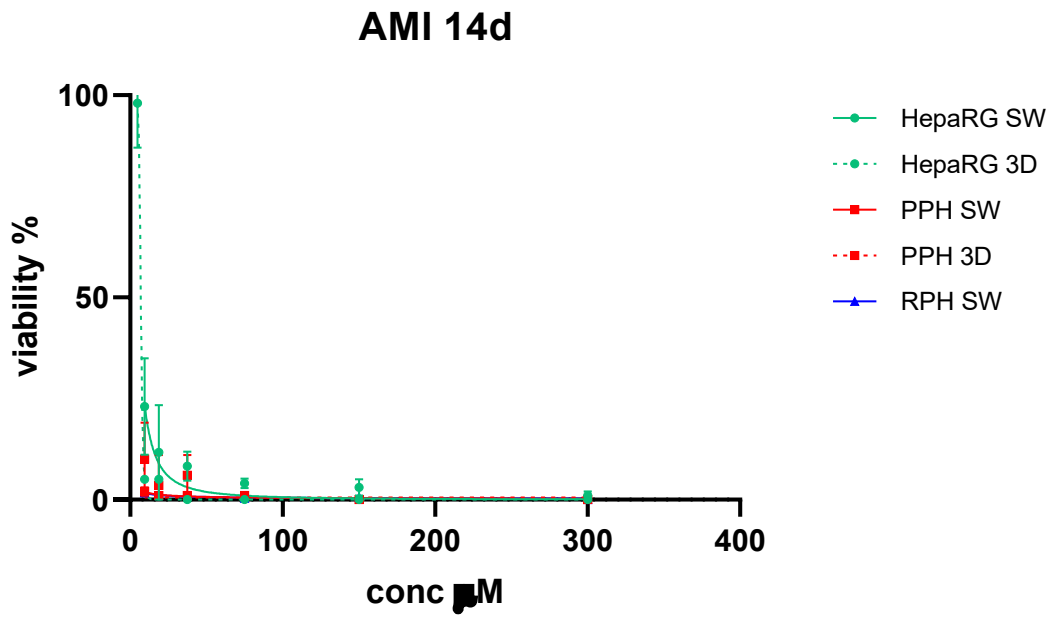
AMI 14d
viability %
100
50
0
0
100
200
300
400
conc µM
HepaRG SW
HepaRG 3D
PPH SW
PPH 3D
RPH SW

E

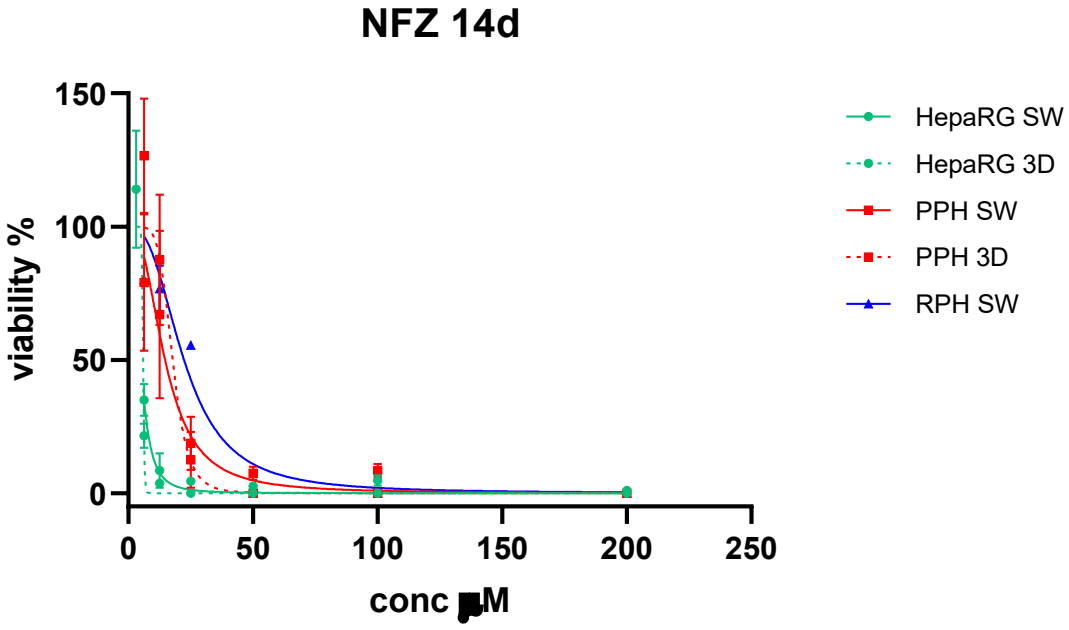
NFZ 14d
viability %
150
100
50
0
0
50
100
150
200
250
conc µM
HepaRG SW
HepaRG 3D
PPH SW
PPH 3D
RPH SW

F

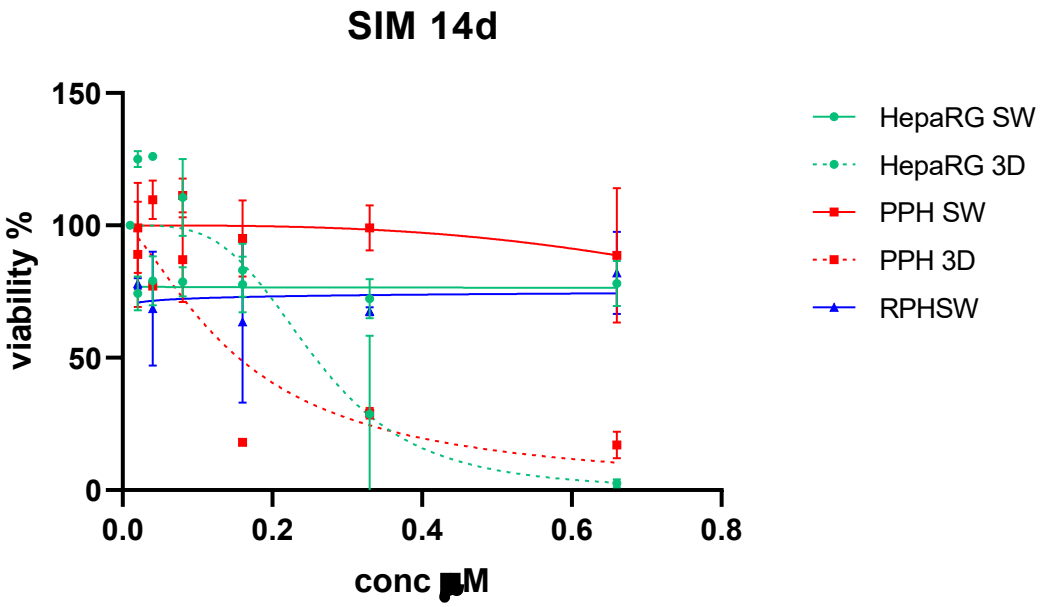

G

Figure 25. Drugs effect on cell viability at 14 days compared between species: HepaRG (human hepatocytes; green), PPH (pig primary hepatocytes; red), RPH (rat primary hepatocytes; blue). SW= sandwich cultures; 3D= spheroids. Drugs abbreviations: DCF= Diclofenac; ACP= Acetaminophen; TRG= Troglitazone; FLD= Fialuridine; AMI= Amiodarone; NFZ= Nefazodone; SIM= Simvastatin. X-axis: drug concentrations, µM. Y-axes: Cell viability is expressed as a percentage of control cells (cells treated with DMSO only). Data are presented as mean ± SEM of three independent experiments. Plots were generated using non-linear regression analysis with a sigmoidal dose-response model (GraphPad Prism 8.3.0; GraphPad Software, San Diego, CA). Comparison between systems was made using two-way ANOVA followed by Tukey's multiple comparison test (GraphPad Prism 8.3.0; GraphPad Software, San Diego, CA). $p<0.05$ was considered statistically significant.

	HepaRG SW		PPH SW		RPH SW	
	LC_0	LC_{50}	LC_0	LC_{50}	LC_0	LC_{50}
DCF	<15.7	**62.0**	55.6	**301.1**	31.3	**293.3**
ACP	<125	**442.1**	602.6	**1945**	<125	**1734**
TRG	<6.3	**11.9**	23.2	**52.4**	<6.2	**17.6**
FLD	<1.87	**4.6**	1.8	**54.9**	<1.9	**>60**
AMI	<9.37	**<9.37**	<9.4	**<9.4**	<9.4	**<9.4**
NFZ	<6.3	**<6.3**	<6.3	**14.7**	<6.2	**22.4**
SIM	<0.02	**>0.66**	0.03	**>0.66**	<0.02	**0.03**

A

	HepaRG 3D		PPH 3D	
	LC_0	LC_{50}	LC_0	LC_{50}
DCF	<7.8	**20.1**	<15.6	**13.7**
ACP	80.5	**153.8**	<125	**535.4**
TRG	<3.1	**6.4**	28.8	**72.1**
FLD	0.9	**3.2**	6.5	**11.6**
AMI	4.8	**6.9**	<9.4	**<9.4**
NFZ	3.1	**5.9**	10.1	**17.8**
SIM	0.08	**0.24**	0.02	**0.15**

B

Table 5. LC_{50} and LC_0 values comparison between species (HepaRG, PPH, and RPH) was obtained in the 14-days hepatotoxicity assessment. Table A refers to sandwich cultures, while Table B refers to 3D spheroids cultures. PPH= pig primary hepatocytes; RPH= rat primary hepatocytes; SW= sandwich cultures; 3D= three-dimensional cultures.

Analyzing the drugs' effects in sandwich cultures, overall, HepaRG showed higher susceptibility than rat and pig species. Specifically, the doses of 125 μM and 250 μM of diclofenac induced a significantly higher cytotoxicity in HepaRG compared to PPH (p<0.01) and RPH (p<0.001). Also, a significant difference in cells' viability was observed at the dose of 1000 μM of acetaminophen and 25 μM of troglitazone between HepaRG and PPH (p<0.001 and p<0.01, respectively), whereas in rat hepatocytes, the effect of these drugs was comparable to that of HepaRG. Importantly, the drug nefazodone induced significantly higher cell mortality in HepaRG than in both animal species, particularly visible at the drug concentration of 12.5 μM (p<0.01).

It is worth noting that in our 14 days' assessment, the drug fialuridine exerted a remarkably higher cytotoxicity in HepaRG than in pig and rat species. This high discrepancy between human and animal hepatocytes was particularly consistent at the drug's concentrations of 60 μM (p<0.1 for PPH and p<0.001 for RPH), 30 μM (p<0.1 for PPH and p< 0.01 for RPH) and 15 μM (p<0.1 for both PPH and RPH). This is a remarkable result highlighting that the drug exerts much stronger cytotoxic effects in human than animal hepatocytes. As mentioned previously in this study, fialuridine was discontinued due to fatal liver toxicity issues that occurred in clinical phase II after multiple doses of the drug were administered over about two months. Unfortunately, such severe adverse effects were not observed previously in animal models during preclinical trials, making the drug advance to clinical studies in humans. Our *in vitro* model for toxicity prediction, already at 14 days, was able to assess that fialuridine's hepatotoxic effect was remarkably higher in human HepaRG than in rat and pig hepatocytes, reproducing the real toxic effect of the drug faithfully. Additionally, this study showed that fialuridine's hepatotoxicity was not elicited after the single administration of the drug (see section 5a, "Results and Discussion") but only after repeated doses. This demonstrates the robustness of this *in vitro* model for toxicity prediction, which was able to discriminate between acute and chronic toxicity as well as different cytotoxic effects across species.

In general, within each species, 3D spheroids (Fig. 25, dashed and solid lines) showed higher vulnerability to drugs than sandwich cultures, confirming the superior accuracy of three-dimensional systems in hepatotoxicity detection over the bidimensional ones. This effect was particularly evident for simvastatin (Fig. 25G). Here, in fact, the two weeks' treatment of the drug did not affect sandwich cultures, which maintained cell viability at 100% (Fig. 25G, solid lines), whereas induced high mortality in HepaRG and PPH spheroids (Fig. 25G, dashed lines). The high disparity between the two systems could be explained by the different metabolizing capacities that they express. In fact, spheroids, expressing a metabolic activity more closely to that of *in vivo* hepatocytes, would produce toxic metabolites more efficiently than sandwich cultures. Although simvastatin-induced hepatotoxicity is rarely reported (Björnsson ES, 2016), it is believed that statins trigger hepatocytes' damage through ROS production. Within the entire class of statins, simvastatin is the one responsible for the higher production of these reactive species (Karahalil B et al., 2017; Abdoli N et al., 2014).

Among the three species tested, HepaRG spheroids exhibited the highest sensitivity to drug toxicity, as indicated by their highest cell mortality shown in Fig. 25 (green dashed lines). This effect was particularly marked for troglitazone, fialuridine, and nefazodone and less marked for diclofenac, acetaminophen, simvastatin, and amiodarone. Indeed, cell death was significantly higher in HepaRG than PPH at the doses of 25 μM and 12.5 μM of troglitazone (p<0.01), 3.75 μM of fialuridine (p<0.01), and at the doses of 12.5 μM (p<0.0001) and 6.3 μM of nefazodone (p<0.0001). The superior sensitivity of HepaRG spheroids is further supported by the lower LC_{50} values compared to those of animal hepatocytes (Table 5B).

These findings remark on the reliability of three-dimensional systems of HepaRG in our *in vitro* methodology for the detection of hepatotoxicity, particularly in long-term assessments. The higher sensitivity of HepaRG spheroids suggests that they represent a suitable model to accurately detect hepatotoxic effects over extended periods, similar to what was observed in the acute assessment.

As expected, comparing drugs' effects observed at 48h and 14 days, it is clearly visible that cell mortality was constantly higher in the long-term assessments than in the acute ones within each species considered (Fig. 24 and in Fig. 25). This result is further supported by the LC_{50} values (Fig. 26A and 26B).

Also, compounds characterized by proven high hepatotoxicity, like amiodarone and nefazodone, showed a more marked toxic effect in the long-term assessment compared to the short-term assessment, and no significant different outcomes were observed between species.

Conversely, compounds such as fialuridine and simvastatin exhibited markedly different outcomes when administered as single doses (48-hour assessment) compared to repeated doses (14 days assessment). It is worth noting that during the acute assessment, the single administration of fialuridine and simvastatin appeared to be completely harmless, as evidenced by the maintenance of cell viability around 100% in each cell line and system (Fig. 24D and 24G). However, upon multiple administrations of these drugs, a dose-dependent increase in cell mortality was observed, particularly pronounced in spheroid systems (Fig. 25D and 25G, dashed lines). This observation highlights the importance of considering prolonged exposure durations in toxicity assessments, as it more accurately reflects the potential effects of chronic drug exposure and assesses the reliability of the proposed *in vitro* procedure in the discrimination of short- and long-term drug hepatotoxicity evaluation.

To summarize and provide a clearer understanding of the toxicity exerted by the drugs in each species, we compared the LC_{50} values of the drugs under both acute (Fig. 26A) and long-term exposure (Fig. 26B), as illustrated in Figure 26.

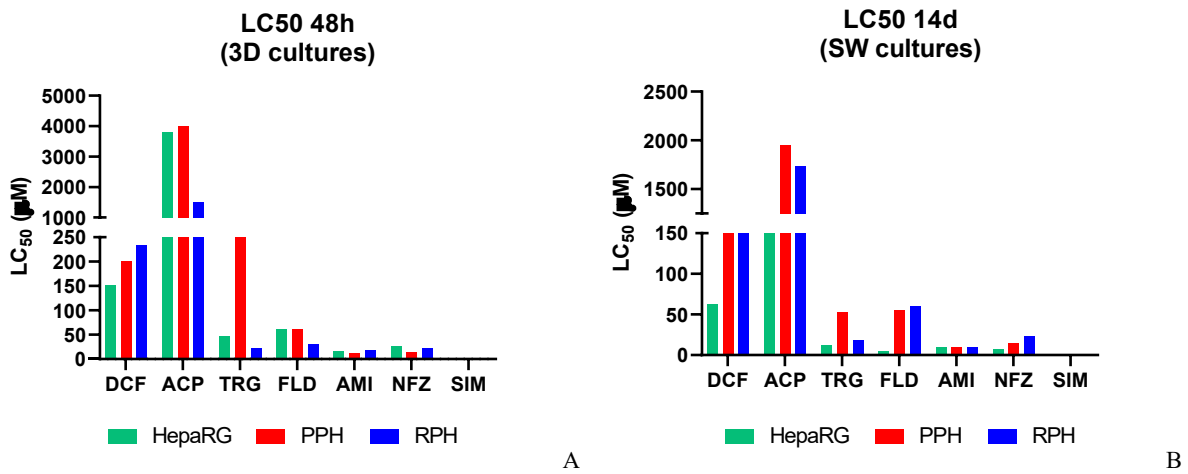

Figure 26. Comparison of drugs' LC_{50} values across human (green), pig (red) and rat (blue) species. The graphs refer to hepatocyte cultures treated for 48h (a) and 14 days (b) with the drugs diclofenac (DCF), acetaminophen (ACP), troglitazone (TRG), fialuridine (FLD), amiodarone (AMI), nefazodone (NFZ) and simvastatin (SIM).

Based on the LC_{50} values of the 48-hour assessment shown in Fig. 26A and Table 5, differences between species are primarily observed for acetaminophen, troglitazone, and fialuridine. RPH demonstrated higher sensitivity to these drugs in the acute hepatotoxicity assessment. Additionally, PPH appears to be more resistant to the acute effects of troglitazone compared to human and rat hepatocytes.

On the other hand, amiodarone and nefazodone demonstrated very low and similar LC_{50} values across all species, indicating very high cytotoxicity independent of the species considered. Furthermore, simvastatin exhibited similar LC_{50} values in short-term treatments (48 hours), comparable to their respective Cmax, suggesting no significant cytotoxicity for the compound.

Remarkably, analyzing the LC_{50} values of the 14-days test, HepaRG cells exhibited overall the highest sensitivity to repeated drug exposure across species in both sandwich and spheroids cultures (Table 5 and Fig. 26B).

This observation underscores the robustness of HepaRG cells as a sensible *in vitro* model for detecting hepatotoxicity in humans. Although HepaRG cells showed similar sensitivity to drugs as rat hepatocytes in some instances, it is important to note that animal models may not always efficiently substitute human models for determining acute hepatotoxicity.

Nonetheless, the higher sensitivity of HepaRG cells to repeated drug exposure highlights their utility in predicting the potential hepatotoxicity of drugs over extended periods.

These findings contribute to our understanding of the comparative performance of different cell models in hepatotoxicity detection, aiding in the selection of appropriate models for drug safety evaluation in early-stage drug development.

6. *In vitro* strategy for identification of toxic metabolites

As assessed in the previous sections of the present study, *in vitro* cell models demonstrated to be useful and accurate tools for determining compounds' hepatotoxicity. However, this is not enough to explain the mechanism of drugs' toxicity. In fact, in the hypothesis that hepatotoxicity is ascertained, it is important to assess if it is due to the parent drug or to its metabolites.

Upon administration, only a few drugs are eliminated in their unmodified form; the majority of them undergo biotransformation before excretion in the liver, the principal organ where metabolism occurs, mainly operated by microsomal enzymes of the CYP450 family.

Normally, this biotransformation is necessary to convert the parent drug into a (more) hydro-soluble form that can be easily eliminated. Sometimes, this conversion can activate the compound itself or generate toxic metabolites responsible for adverse effects. It turns out that, in many cases, the toxicological properties of drugs are due to hepatic metabolites. In general, there are three possible scenarios of toxicity occurring when a drug is administered:

1. Both the parent drug and its metabolites are toxic
2. The parent compound is toxic, but it is transformed into non-toxic metabolites (the desired outcome resulting from liver detoxification of xenobiotics)
3. The parent drug is not toxic, but it is converted into toxic substances by liver metabolism.

Therefore, to distinguish between the toxicity of parent drugs and that of their metabolites and fully elucidate the mechanism of DILI, an additional step is needed. Although this is not the main purpose of our study, we propose here an experimental approach that allows us to identify molecules responsible for hepatotoxicity. The strategy suggested here is based on the administration of drugs to two cell lines, HepaRG and HepG2, which express a different responsiveness to compounds.

Although both HepaRG and HepG2 are human hepatocytes, they differ in several features. HepG2 is a human liver cancer cell line derived from hepatocellular carcinoma. HepG2 are immortalized and very easy to grow, so they are widely used as a liver *in vitro* model to study liver physiology, cancer, and liver metabolism disorders. However, they exhibit only a few of the key metabolizing enzymes of the liver (e.g., CYP450 superfamily) at low levels (Guo L et al., 2011; Seo JE et al., 2019; Chen S et al., 2021; Westerink WN and Schoonen WG; 2007a; Westerink WN and Schoonen WG; 2007b; Wilkening S et al., 2003). This represents a limit when drugs' toxicity is studied, as many times, this toxicity is triggered by liver metabolites (Uetrecht J, 2008; Lammert C et al., 2010; Abboud G and Kaplowitz N, 2007).

By contrast, the HepaRG is an immortalized hepatic cell line that retains the key features of primary hepatocytes such as morphology, expression of specific nuclear receptors, and most importantly, metabolic hepatic enzymes of the CYP450 superfamily, as well as phase II metabolic enzymes (e.g., UGT and SULT), at levels comparable to those expressed in primary hepatocytes (Guillouzo A et al., 2007; Antherieu S et al., 2010; Yokoyama Y et al., 2018; Seo JE et al., 2019). Unlike primary

hepatocytes, which have a limited lifespan and variable characteristics depending on the donor, HepaRG is a stable hepatic cell line that retains the essential features of liver cells. Therefore, differentiated HepaRG cells are regarded as a valid alternative to primary hepatocytes, which have traditionally been the "gold standard" for *in vitro* liver models.

Each of the three possible scenarios of toxicity previously mentioned was experimentally reproduced in this section, taking three commercial drugs as an example: nefazodone, astemizole, and acetaminophen. These drugs were selected to test whether adverse effects are related to the compound *per se* or to its metabolites. For the great majority of approved drugs, the entire metabolism is well known and described, although the effects related to each metabolite more often remain unknown.

Nefazodone, a drug released in the market for depression treatment, was discontinued in 2003 due to fatal cases of DILI (Choi S, 2003; Edwards IR, 2003). Astemizole, a second-generation antihistaminic drug introduced in 1988 for allergy syndrome, was withdrawn in 1999 due to rare but potentially fatal cardiac effects (Gottlieb S, 1999; Charles O et al., 2019). To our knowledge, hepatotoxicity associated with astemizole has never been reported. Lastly, acetaminophen (also known as paracetamol), a widely used antipyretic drug, was chosen to validate its well-known hepatotoxicity induced at overdose, which results from its metabolism in the liver (Yan M et al., 2018).

The compounds were tested in parallel in the same conditions in both HepaRG and HepG2. Six different concentrations of each drug were added, ranging from the human plasma peak at therapeutic dose (Cmax) to 32 times Cmax. After 48h of drug treatment, the percentage of viable cells was measured within the two cells' populations to compare the cytotoxic effects. Dose-viability curves are reported in the figures below (Fig.1, 3, 4). As shown in Fig. 1, the effect of astemizole in HepG2 and HepaRG cells was markedly different.

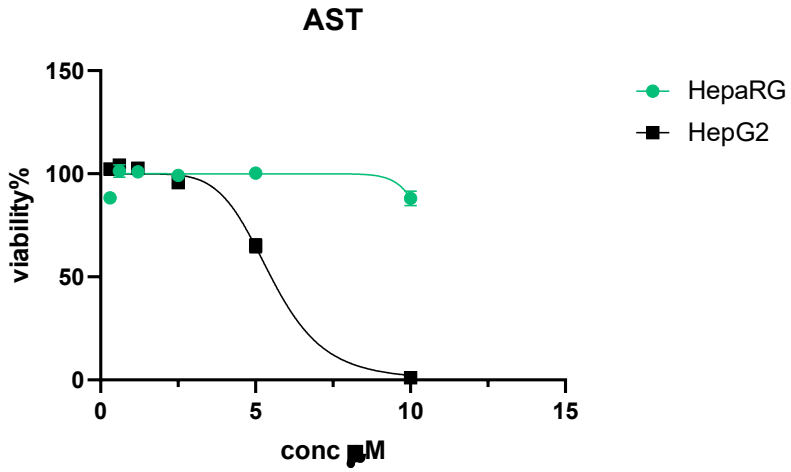

Figure 1. HepG2 and HepaRG viability % (y-axes) related to increasing concentrations of astemizole (x-axes), µM. Viability was expressed as a percentage of control (cells treated with 0.5% DMSO). Each value is reported in the plot as the average ± SEM of three or more values obtained in separate experiments. Plots were generated using non-linear regression analysis with a sigmoidal dose-response model (GraphPad Prism 8.3.0; GraphPad Software, San Diego, CA). Comparison between cell lines' viability was made using two-way ANOVA followed by Sidak's multiple comparison test (GraphPad Prism 8.3.0; GraphPad Software, San Diego, CA). $p<0.05$ was considered statistically significant.

HepG2 cells showed a dose-dependent increase in toxicity with astemizole exposure (Fig. 1, black line). At 5 μM (4 times Cmax), cell death began to occur, and at 10 μM (8 times Cmax), all HepG2 cells were killed. In contrast, HepaRG cells remained almost unaffected by any concentration of astemizole tested (Fig. 1, green line). At astemizole's concentrations of 5 μM and 10 μM the discrepancy in cells' viability between HepaRG and HepG2 is significantly visible (p<0.0001).

Astemizole undergoes extensive first-pass metabolism and represents an example of the typical detoxification operated by the liver. Astemizole's metabolites are formed by multiple CYP450 enzymes, including CYP2D6 and CYP3A4, the latter metabolizing a minor percentage of the drug. CYP2D6 catalyzes the formation of the main metabolite desmethylastemizole (DES-astemizole) and norastemizole (NOR-astemizole), while CYP3A4 catalyzes the formation of 6-hydroxyastemizole (6OH-astemizole) (Matsumoto S and Yamazoe Y, 2001; Matsumoto S et al., 2003).

The different effects observed between the two cell lines could be explained by considering their different metabolic capability.

While differentiated HepaRG expresses the high activity of both CYP3A4 and CYP2D6, the activity of these two enzymes was not, or barely detected in HepG2 (Seo J et al., 2019). Previous studies have demonstrated that HepaRG levels of the isoforms CYP3A4 and CYP2D6 are 19.1 and 1.82 times those of HepG2 cells, respectively (Gerets HH et al., 2012; Seo JE et al., 2019). Therefore, the results suggest that in HepaRG, astemizole was detoxified by its conversion into less toxic metabolites, while the same biotransformation could not occur in HepG2 due to a lack of CYP enzymes. Thus, the toxicological properties of the parent compound were exhibited. These findings indicate that astemizole is hepatotoxic as a compound *per se* while its metabolites are not and give a clear example of how potentially harmful xenobiotics are converted into safe products as a result of the liver's detoxifying activity.

However, in many cases, compound biotransformation in the liver generates metabolites characterized by high toxicity. This is the well-known case of paracetamol (also known as acetaminophen), the most used antipyretic drug in the world, whose metabolism is largely described and documented in scientific literature (Fig 2).

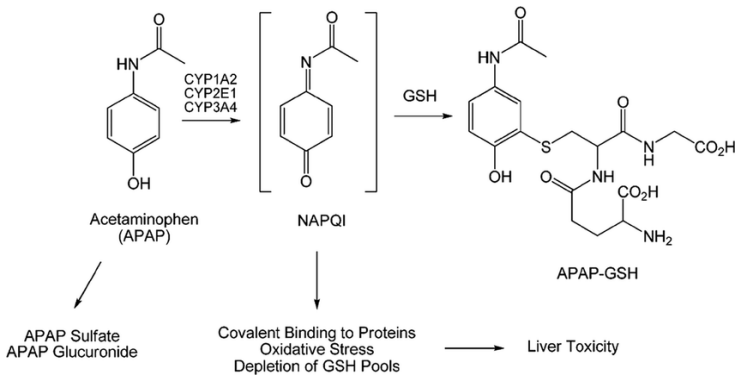

Fig 2. Liver metabolic pathway of acetaminophen (paracetamol). Source: Baillie TA, 2020.

When acetaminophen reaches the liver through portal circulation, glucuronide, and sulfate conjugates are produced as its principal metabolites. Only a minor percentage of the drug is transformed by Phase I enzymes into a highly reactive intermediate, *N*-acetyl-*p*-benzoquinone imine (NAPQI). NAPQI is further neutralized into mercapturic acid, a non-toxic metabolite, by a conjugation reaction via the GSH-S-transferase, a Phase II liver enzyme. However, when paracetamol is overdosed, the GSH-mediated detoxification pathway becomes saturated, and NAPQI accumulates inside the hepatocyte, causing cell damage, mostly related to the electrophilic nature of NAPQI that binds covalently proteins and causes suicide inhibition of enzymes. This process will lead to cell death and, in turn, to acute liver failure (Mingzhu Yan et al., 2018; Ramachandran A and Jaeschke H, 2017).

In light of the widely known paracetamol-related toxicity, this drug was used as an example to elucidate the case where non-toxic parent compound is converted into toxic products by liver metabolism.

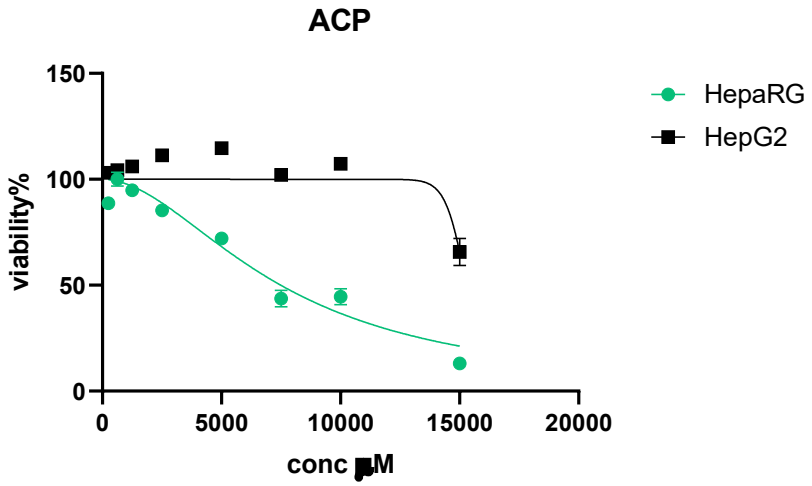

Fig. 3. HepG2 and HepaRG viability % (y-axes) related to increasing concentrations of paracetamol (acetaminophen) (x-axes), µM. Each value is reported in the plot as the average ± SEM of three or more values obtained in separate experiments. Plots were generated using non-linear regression analysis with a sigmoidal dose-response model (GraphPad Prism 8.3.0; GraphPad Software, San Diego, CA). Comparison between cell lines' viability was made using two-way ANOVA followed by Sidak's multiple comparison test (GraphPad Prism 8.3.0; GraphPad Software, San Diego, CA). $p<0.05$ was considered statistically significant.

When paracetamol (acetaminophen) was applied to HepG2, the effect on cell viability was only related to the compound *per se*, as this cell line does not express the needed enzyme for paracetamol's metabolism. In fact, no toxicity is shown in HepG2 (Fig. 3, black line). In contrast, the increasing drug concentration was found to decrease viability within the HepaRG population due to this cell line capability to metabolize the parent drug (Fig. 3, green line). Indeed, at paracetamol concentrations higher than 2500 µM, the drug-induced a significantly higher mortality in HepaRG compared to HepG2 ($p<0.0001$) (Fig. 3).

The enzyme responsible for paracetamol's oxidation into the toxic metabolite NAPQI is the isoform CYP2E1, poorly expressed by HepG2 and highly expressed by HepaRG (Chen S et al., 2021; Guo L et

al., 2010; Gullouzo A et al., 2007). Therefore, it can be easily deduced how toxicity induced by paracetamol is exhibited in HepaRG and not in HepG2 cells. These results are yet another confirmation of the effect linked to paracetamol's toxic metabolites.

Lastly, the effect induced by the drug nefazodone was examined as the third possible case of toxicity. When nefazodone was administered to HepaRG and HepG2, the cytotoxic effect was the same in both cell populations, meaning that the parent drug along with its metabolites (the latter produced in HepaRG) are toxic to the same extent (Fig. 4). In fact, cells' viability decreases in HepG2 and HepaRG in a very similar manner with increasing concentrations of nefazodone (Fig.4). It can be inferred that in this case, liver metabolism does not detoxify the parent compound.

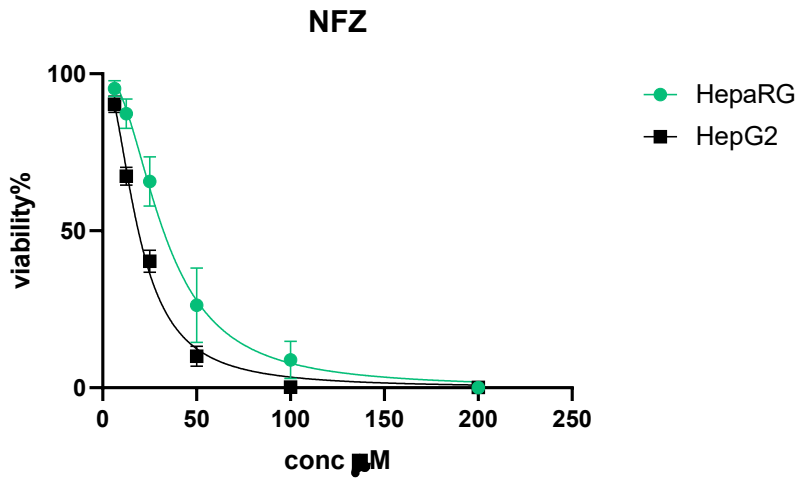

Fig 4. HepG2 (green line) and HepaRG (black line) viability % (y-axes) at 48h exposure to increasing concentrations of nefazodone (x-axes), µM. Each value is reported in the plot as the average ± SEM of three or more values obtained in separate experiments. Plots were generated using non-linear regression analysis with a sigmoidal dose-response model (GraphPad Prism 8.3.0; GraphPad Software, San Diego, CA). Comparison between cell lines' viability was made using two-way ANOVA followed by Sidak's multiple comparison test (GraphPad Prism 8.3.0; GraphPad Software, San Diego, CA). $p<0.05$ was considered statistically significant.

The approach described here provides a valuable method to distinguish whether a biological event, like drug toxicity, could be related to the drug *per se* or to its metabolites. Although this could seem like an endpoint, in reality, it should be considered a starting point to deepen the mechanism of toxicity. In the case of nefazodone, for example, we assume that both the parent compound and nefazodone's metabolites are toxic, but to understand which ones are responsible for toxicity, a further step is required to exhaustively elucidate the mechanism of toxicity. Thus, taking the drug nefazodone as a model, we decided to proceed by investigating the cytotoxicity of its principal metabolites.

Nefazodone's metabolism is very well documented. Previous studies reported that the drug is rapidly absorbed and metabolized. In total, at least nine metabolites were identified, and three of them represent the most abundant ones (Fig. 5, Rotzinger S and Baker GB, 2002). Nefazodone's main metabolites are produced in the liver and derive from an initial hydroxylation of the compound into hydroxy-nefazodone

(NFZ-OH) catalyzed by CYP3A4 and the oxidation into the triazole-dione metabolite (NFZ-TD). The third principal metabolite is metaclorophenylpiperazine (m-CPP), which is formed by N-dealkylation of the parent drug (Schatzberg AF and Nemeroff CB, 2017; Davis R et al., 1997; Rotzinger S and Baker GB, 2002). All three metabolites are active, but while hydroxy-nefazodone and m-CPP maintain the same potency as that of the parent compound, the potency of NFZ-TD is reduced by 1/7 (Davis R et al., 1997). A scheme of nefazodone's main metabolites is illustrated in Fig. 5.

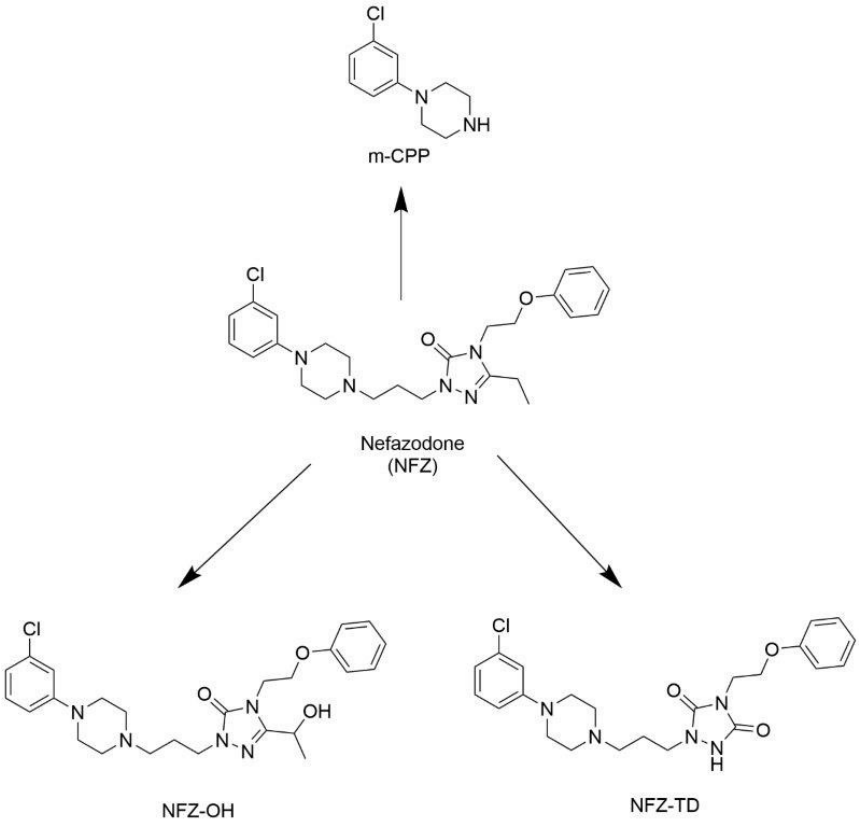

Fig.5. Principal metabolites of antidepressant nefazodone (NFZ). NFZ-OH: hydroxynefazodone; NFZ-TD: triazoledione-nefazodone; m-cPP: meta-clorophenylpiperazine (Source: Rotzinger S and Baker GB, 2002).

To the best of our knowledge, the toxicity of nefazodone's metabolites has never been investigated *in vitro*. Hence, we decided to explore the effect of NFZ-OH and NFZ-TD because they represent nefazodone's main metabolites with potential toxicity. We did not include m-CPP in our study as this molecule is considered a privileged scaffold largely employed in drug discovery, that is present in several drugs with different biological activities (Zhang RH et al., 2021).

Metabolites NFZ-OH and NFZ-TD were tested, as well as the parent compound nefazodone in HepG2 and HepaRG cells, to compare the effects on cells' viability (Fig. 6).

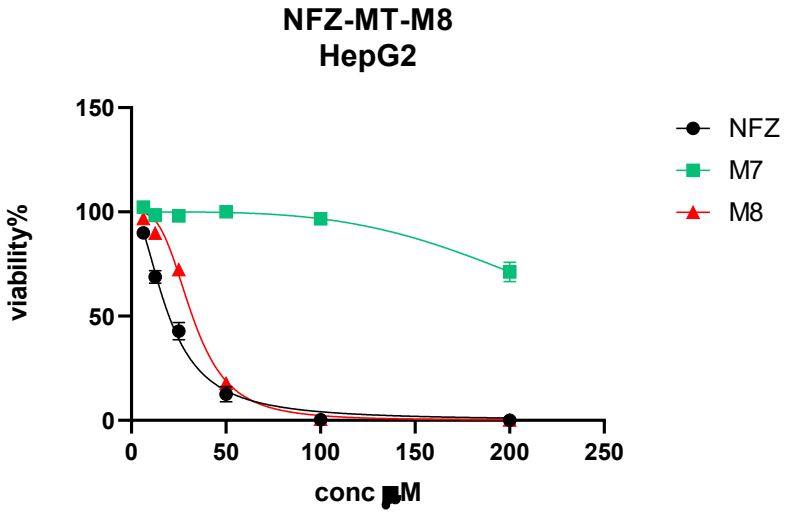

A

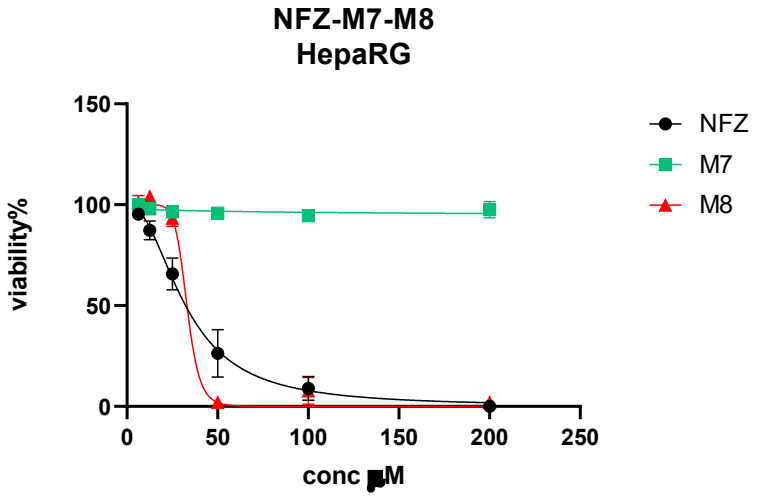

B

	LC_{50} in HepG2	LC_{50} in HepaRG
NFZ	19.9 µM	32.3 µM
NFZ-TD	257.7 µM	>200 µM
NFZ-OH	32.3 µM	33.1 µM

C

Figure 6. Dose-viability curves of HepG2 and HepaRG monolayer cultures treated 48h with the drug nefazodone (black line) and its metabolites NFZ-TD (triazoledione-nefazodone, green) and NFZ-OH (hydroxy-nefazodone, red). Cell viability is expressed as a percentage of control (cells treated with DMSO only). Data are presented as mean and 95% confidence interval. Data are presented as mean ± SEM of three or more independent experiments. LC_{50} values were calculated using non-linear regression analysis with a sigmoidal dose-response model (GraphPad Prism 8.3.0; GraphPad Software, San Diego, CA). Comparison between metabolites' toxicities was done using two-way ANOVA followed by Tukey's multiple comparison test (GraphPad Prism 8.3.0; GraphPad Software, San Diego, CA). $p<0.05$ was considered statistically significant.

Interestingly, NFZ-TD did not affect HepG2 viability, while NFZ-OH drastically induced high cell mortality in HepG2 population, very similarly to the nefazodone parent compound (Fig. 6A). The three compounds tested in HepaRG gave similar results to those observed in HepG2, with nefazodone and its metabolite NFZ-OH being highly toxic whereas NFZ-TD, being non-toxic to the HepaRG cells (Fig. 6B). Indeed, a significantly higher toxicity was observed between cells treated with NFZ or NFZ-OH,

and cells treated with NFZ-TD (p<0.0001). The LC_{50} values of the three compounds were comparable in both HepG2 and HepaRG (Fig 6C, table).

It is worth noting that the HepaRG cell line expresses high metabolizing properties, particularly high levels of CYP3A4, the isoform required for hydroxylation of nefazodone into hydroxynefazodone (Von Moltke L et al., 1999; Rotzinger S, Baker GB, 2002). Therefore, the toxicity observed in the dose-response curves (Fig. 6B) is caused by both compounds, nefazodone and NFZ-OH, the former being partly converted into the latter. On the other hand, NFZ-TD does not affect HepaRG's viability and has a slightly better safety profile than in HepG2 cells, as shown by the dose-response curves (Fig.6A, 6B, green lines).

We can conclude that nefazodone's hepatotoxicity is caused by both the parent compound and the toxic metabolite NFZ-OH, whereas the NFZ-TD is demonstrated to be a safe metabolite. For the first time, the toxicity of the metabolite NFZ-OH was reported *in vitro*. Therefore, this approach enabled us to finally identify metabolites responsible for cytotoxicity.

In summary, our findings show the reliability of this experimental method in discriminating toxicity induced by the parent drug from that induced by its metabolites. Although we used nefazodone as an example, this method could be useful for other drugs with similar challenges in metabolite analysis. In fact, for many compounds and approved drugs, toxicity of metabolites remains unknown. Our final goal will be to apply the approach described here to investigate compounds under development in order to prevent metabolic-related adverse events at later stages of drug discovery and optimize the go/no go decision, saving time and resources.

7. The use of a dynamic *in vitro* model based on the Hollow Fiber Bioreactor for an accurate prediction of chronic hepatotoxicity of drugs

In the previous part of the project, we evaluated short- and long-term effects of drugs in *in vitro* systems such as monolayer, sandwich, and 3D spheroids. We showed that 3D systems were more sensitive to drugs' toxic effects compared to bidimensional monolayer and sandwich cultures. However, all these systems, including spheroids, have two major limitations. The first is the fact that such systems cannot ensure stable cultures for more than 3-4 weeks. The second is that they are static systems, meaning that drug doses are added once at a time, and the concentration remains constant over the incubation time.
The inability to maintain these cultures for extended periods limits their use for chronic toxicity studies, which is crucial for understanding the effects of multiple drug doses over a long time, like one month or more. Moreover, the static nature of these systems fails to replicate the dynamic pharmacokinetic processes observed in living organisms, where drug concentrations changes over time.
Following administration, drug concentration increases in the blood, reaching a maximum defined as Cmax. The minimal time needed to reach Cmax is called Tmax. Then, the drug's concentration decreases in plasma to a minimum value (Cmin), and then a second dose is added. The cycle repeats every time a new dose is administered (Fig.1).

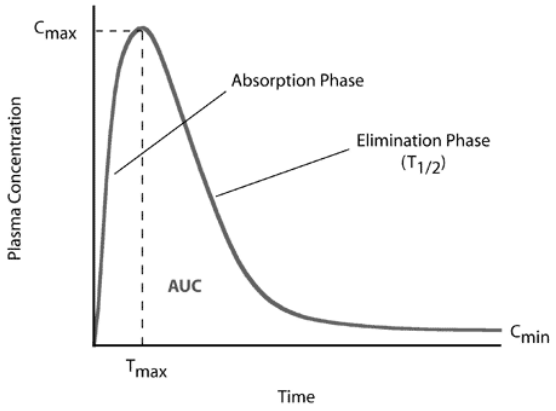

Figure 1. Typical pharmacokinetic profile of a drug administered orally. The main PK parameters are shown. C_{max}=maximum plasma concentration. T_{max}=minimum time to reach C_{max}. $T_{1/2}$= time required to reduce the plasma concentration of a drug by 50%. C_{min}=minimum plasma concentration at steady state. AUC=area under the curve after a single dose. Source: Cheung CY et al., 2008.

The pharmacokinetic parameters are specific for each drug and characterize the drug properties in the human body, affecting intensity, duration, onset of pharmacological effects, and, ultimately, toxicity.
A model that could efficiently predict the toxicity of drugs should mimic as much as possible the *in vivo* scenario following drug administration.
Static *in vitro* systems cannot reproduce the PK/PD profile of a drug, therefore, more sophisticated *in vitro* models are needed to better replicate the complex and dynamic nature of human biology, potentially incorporating elements such as continuous media flow to simulate blood circulation.

The Hollow Fiber Bioreactor is a perfusion-based culture system where mammalian cells, grown in 3D, are subjected to a dynamic media flow resembling the *in vivo*-like environment.
We hereby propose the use of the Hollow Fiber System (HFS) to accurately evaluate *in vitro* chronic hepatotoxicity of drugs. Its dynamic environment mimics the human body more closely than traditional static culture systems, potentially offering a more accurate assessment of chronic hepatotoxicity.
By utilizing HFS in the early stages of drug discovery, researchers can identify compounds with toxic profiles earlier, allowing the selection of safer compounds, which ultimately could significantly reduce the attrition rate of drug candidates in subsequent animal and human trials.

7a. The Hollow Fiber System technology

The hollow fiber bioreactor was developed in the early 1970s by Knazek, who described for the first time an innovative *in vitro* approach for cell culture based on artificial capillaries in a perfusion circuit (Knazek RA et al., 1972). Later, these systems found application in research and commercial settings, including scale-up of cell-derived products like monoclonal antibodies, recombinant proteins, and viruses for vaccine manufacturing (Jyothilekshmi I and Jayaprakash NS, 2021 Merten OW et al., 2016; Chu L and Robinson DK, 2001; Hou Y et al., 2022).
Recently, small-scale hollow fiber bioreactors have been used to create *in vitro* infection models, where antibiotic efficacy is tested against multi-drug resistant strains (Drusano GL, 2017). However, to the best of our knowledge, the HFS was never used to reproduce *in vitro* models for toxicity evaluation.
A schematic representation of the Hollow Fiber System (HFS) is illustrated in Fig. 2.

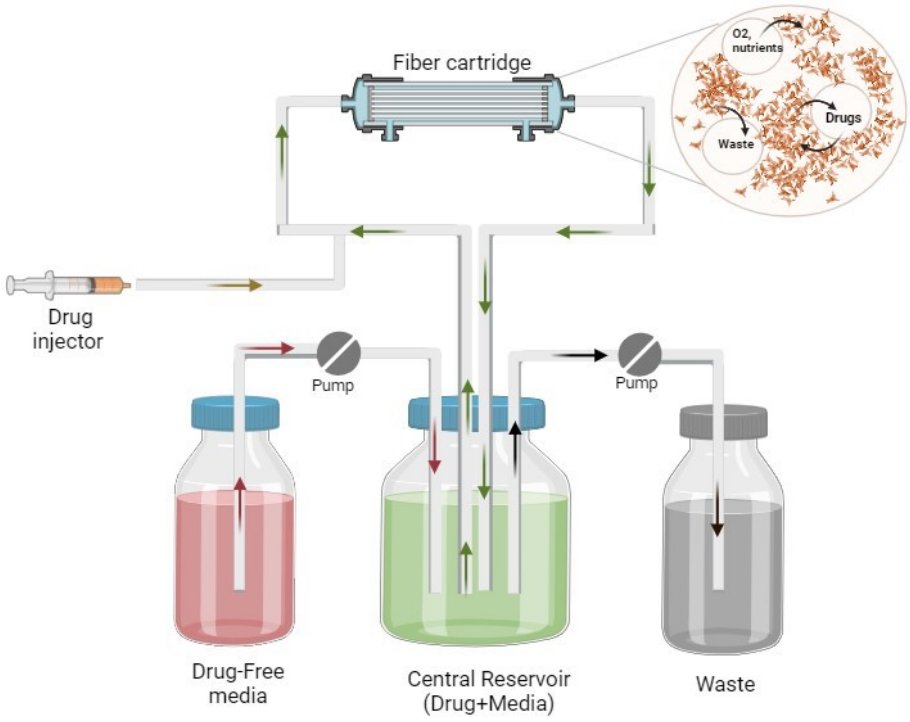

Figure 2. Schematic representation of a basic Hollow Fiber System unit (HFS). The upper part of the image shows the fiber cartridge with its enlarged section on the right showing the intra-capillary space (ICS) and the cells cultured in the extra-capillary space (ECS). Cells receive media pumped from the central reservoir (in green) into the cartridge. Media is also pumped into the central reservoir from the diluent reservoir (in pink) and out into the waste reservoir (in grey). The drug is injected into the central circulation by a pumped-controlled syringe.

A typical HFS is a dynamic multi-compartmental system used to grow cells in a controlled three-dimensional environment. The HFS consists of a cartridge containing thousands of hollow fibers with a diameter ranging from 0.03 µm to 0.1 µm. Cells are inoculated in the extra capillary space (ECS) and receive media delivered from the fibers, which is pumped from the central reservoir. The presence of pores, with a molecular cut-off of 10 to 30 kDa, in the surface of each fiber allows the exchange of nutrients, drugs, and gases, like oxygen and CO_2, between the media, flowing in the ICS and the cells, grown in the ECS. Media is continuously pumped through a system of tubes from the central reservoir into the cartridge and then back again into the central reservoir. This central circulation ensures the equality of composition between media in the central reservoir and media reaching the cells within the cartridge. Test compounds, like drugs, can be added through a direct injector connected to the central circulation at a selected and controlled rate. In order to reproduce a drug PK/PD profile, the drug concentration is finely set by regulating the volume in the central reservoir. Fresh media is pumped at a specific rate from the diluent reservoir into the central compartment, and media is also wasted from the central reservoir into the waste compartment. In this manner, by selecting the drug's injection rate and the volume of media pumped in and out of the central reservoir, it is possible to reproduce the typical pharmacokinetic profile of multiple doses of a drug.

In addition, fibers serve as support for adherent cells for establishing 3D cultures resembling an *in vivo*-like tissue. Here, the fibers act as blood capillaries, providing nutrients and oxygen. In this structure, cells maintain their natural morphology and cell-cell interactions, which are lost in conventional 2D cultures. These perfusion-based culture systems enable the continuous exchange of media, mimicking the dynamic nutrient and oxygen gradients found *in vivo*. As a result, the 3D culture generated in the HFS cells maintains their physiological functions closely to the *in vivo* environment and can be grown for a long time, allowing chronic toxicity testing.

By the accurate simulation of the PK/PD drug profile, along with the possibility of recreating an *in vivo*-like environment, the HFS represents an optimal tool to evaluate the toxic effects of drugs in human hepatocytes. The 3D architecture of hepatocytes cultured in the cartridge resembles the microenvironment of liver tissue and promotes the maintenance of liver-specific functions over extended culture periods, which is crucial for reliable drug safety evaluation.

7b. Preliminary studies of compatibility of HepaRG cells and diclofenac in the HFS

In order to proceed with the chronic hepatotoxicity evaluation of the selected drug using the HFS, it is necessary to perform preliminary studies to verify the compatibility between the fibers' material and both HepaRG cells and the selected drug. To validate the ability of the HFS to reproduce chronic hepatotoxicity, we chose the drug diclofenac, as its adverse effects in the liver are widely known and well-described (Ponsoda X et al., 1995; Jung SH et al., 2020; Aithal GP, 2004; O'Connor N et al., 2003; Lim MS et al., 2006).

The adequate compatibility between the fibers and the HepaRG cells is fundamental to allow cells' adherence, to achieve the needed growth and thereby the formation of 3D *in vivo*-like structures.

Preliminary studies involve the monitoring of cell proliferation rate, viability, and functionality, which must be maintained for the entire duration of the chronic tests.

The growth dynamics of the HepaRG cell line in the cartridge will be assessed by analyzing samples taken at different time points from the HFS ports to ensure their maintenance in the system up to 14 days of culture. HepaRG cells' viability will be tested using the resazurin assay.

The resazurin assay, also known as the trade name of Alamar blue™, is based on the reduction operated by living cells of the substrate resazurin into resofurin, a fluorescent and soluble product. Therefore, the evaluation of the amount of fluorescent and soluble resofurin gives an estimation of the number of living cells. The resazurin assay is not invasive as it does not require cell lysis. Previous studies showed the applicability of this assay for the real-time viability assessment of adherent mammalian cells cultured within the HFS. In this approach, samples of the culture medium are taken at multiple time points, and levels of resofurin in the medium are measured (Mueller D et al., 2012; Gloeckner H et al., 2001). In

the present project, resazurin will be used to evaluate the viability of HepaRG cultured in the HFS before and after exposure to the drug diclofenac for the evaluation of its chronic effects.

The compatibility of cartridge materials with a specific drug is a critical factor in pharmacokinetic (PK) studies. This validation process ensures that the material does not interact with the drug, which could alter its stability, efficacy, or delivery profile. The drug selected for our chronic hepatotoxicity assessment is diclofenac, an anti-inflammatory agent developed in 1973 to treat various types of pain and inflammations (Menassé R et al., 1979; Brogden RN et al., 1980; Small RE, 1989).

From the chemical point of view, diclofenac is a phenylacetic acid. Its constant acidity of 4 characterizes diclofenac as a weak acid. Its 13.4 partition coefficient indicates that the molecule is partially soluble in both aqueous and hydrophobic solvents. In addition, the possibility of generating the sodium salt from diclofenac's molecule makes the drug highly water-soluble (Sallmann AR, 1986; Altman R et al., 2015). Diclofenac sodium salt was therefore selected for this study because of its compatibility with hydrophilic cell media.

The compatibility of diclofenac with the cartridge will be tested by simulating the clinical PK profiles corresponding to the standard recommended dose of the drug (Table 1). The PK parameters of diclofenac mimicked in the HFS are available (Altman R et al., 2015) and indicated in Table 1.

PK parameter	Diclofenac
Dose	25-100 mg (oral)
C_{max}	1.4-2.0 µg/mL (single dose of 50 mg; max dose allowed per day: 150 mg)
T_{max}	2.0-2.75 h
$T_{1/2}$	1.8 h
Dosing frequency	50 mg 3 times per day
% exposure to 2xLC_{50} (14 days)	LC_{50}= 331 µM in primary human hepatocytes (Bort R et al., 1999)

Table 1. Pharmacokinetic parameters of the drug diclofenac (Altman R et al., 2015).

Samples for drug quantification will be taken at different time points from the HFS ports. Aliquots will be stored at -80˚C until quantification is performed at UNIZAR Mass Spectrometry Service Capabilities at CEQMA ("Centro de Química y Materiales de Aragón").

This compatibility test is necessary to determine firstly that diclofenac is compatible with the fibers' materials polyvinylidene fluoride (PVDF) and polysulfone (PS); second, that desired concentrations are achieved in the ECS (where cells actually reside) and third, to define the time needed for the drug to reach the equilibrium in ECS.

7c. PK/PD analysis of diclofenac for chronic toxicity evaluation in HepaRG cell line

To characterize the PK/PD relationship of diclofenac, HepaRG cells will be grown in the ECS of the cartridge for one week, and the selected compound will be dosed daily for seven days, simulating three dosing schedules (low, medium, and high doses of diclofenac) and mimicking the corresponding PK profile. A growth control without any treatment will be included for a total of 14 days.

For the PK analysis, samples will be taken from the HFS port for drug quantification. Specifically, five time-point samples will be taken during the first 24 hours. Additionally, time-point samples corresponding to diclofenac's Cmax and Cmin will be taken on days 2, 4, and 7.

A PD analysis will be performed to determine the toxic effect of the drug diclofenac in HepaRG cells. This will involve the measurement of cells' viability after exposure to multiple doses of diclofenac for two weeks. For the PD analysis, samples of cells' medium within the ECS will be taken on days 1, 7 (pre-dose), 8 (post-dose), 10 and 14. Resazurin assay will be performed on the media samples to determine cells' viability, which in turn will estimate the hepatotoxic effect of diclofenac on cells exposed to the drug in the long term.

This technology holds great promise for improving the predictive accuracy of chronic toxicity of compounds that could be applied to discard toxic compounds in early drug discovery, thereby reducing failure of candidates in animal and human clinical studies.

This part of the project has yet to be completed and constitutes the future work in continuation of the present research project.

8. *In silico* tools for drug toxicity prediction

Two main challenges arise when a reliable method for toxicity prediction is developed. The first is related to the translatability from *in vitro* to the *in vivo* toxicity evaluation. In fact, one of the limits of *in vitro* models, such as the widely used monolayer cultures, is that they are far different from the functionality and morphology of a real tissue. On the other hand, although studies carried out on animal models will perfectly mimic *in vivo* conditions, they will not lead to reliable results due to the interspecies differences between humans and animals.

Ideally, an *in vitro* model that could simulate the human *in vivo* environment would be the optimal solution. Many are the available 3D-like cell systems recently developed to simulate *in vivo* conditions used in drug discovery to investigate compounds' toxicity. Some of them were used in this study for *in vitro* toxicity assessments and are already described in the appropriate sections.

The second challenge in the development of a toxicity prediction model relies on the precise identification of the toxic molecule. In many cases, adverse effects are not related to the compound *per se* but to products of its metabolism (Baillie TA, 2007). This obviously represents a limit for the identification of metabolites responsible for toxicity because either metabolites are too many to be analyzed by *in vitro* tests or because, many times, they are unknown.

In recent years, machine learning tools have contributed to ameliorating drug discovery. Particularly, algorithms predicting bioactivity and physical properties of compounds represent the most promising tools for decision-making in early drug discovery, allowing successful candidates to be selected for animal experimentation.

8a. Metabolic modeling approach to predict compounds-proteins interactions within liver toxicity assessment.

In the present study, a method based on machine learning tools was created for the preliminary prediction of compounds' toxicity.

As previously mentioned, a great percentage of adverse effects is owed to products of drug metabolism. The liver is the principal body site where the metabolic transformation of xenobiotics occurs. Although biotransformation serves primarily to detoxify xenobiotics and convert them into their respective excretable forms, in some cases, this conversion results in noxious products. Indeed, liver tissue is normally the first site where drug-induced toxicity takes place.

For a rational prediction of drugs' toxic effects, we developed a method based on *in silico* tools to simulate the interaction between compounds and hepatic proteins with the aim of examining how compounds would affect liver pathways and eventually trigger any cell impairment.

Firstly, liver-specific Phase I and II metabolic reactions were created using the RDKit tool, a cheminformatics software for 2D and 3D molecule representations. This module also allows molecular modifications by introducing specific functions.

Secondly, the RDKit tool was again used to generate metabolites from Phase I and II reactions performed on a group of commercial drugs. Then, following criteria based on chemical rules, real compounds were selected among all the metabolites generated. The resulting "filtered" metabolites were used to simulate their interaction against a panel of 416 hepatic proteins comprised of both enzymes and transporters.

A simplified scheme of the project workflow is shown in Fig.1.

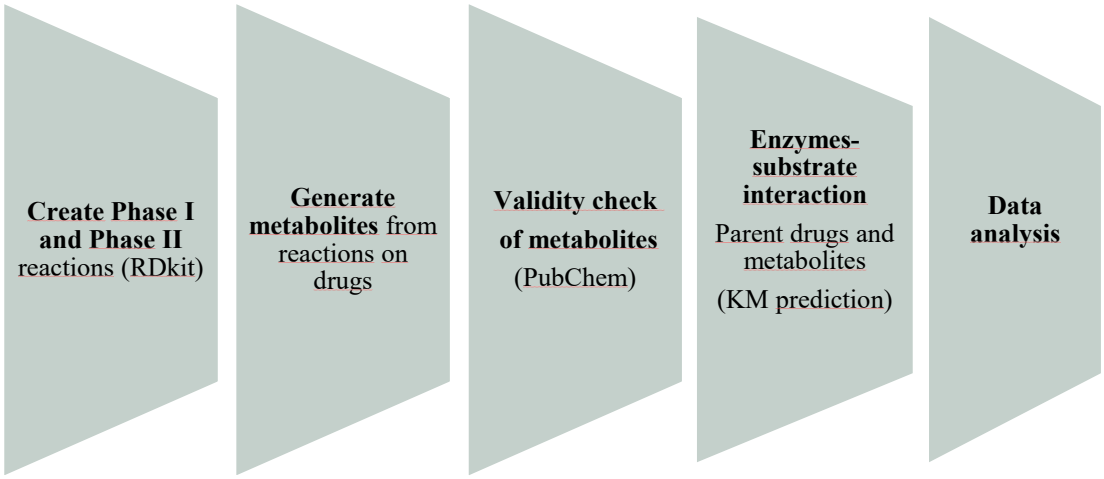

Figure 1. Development of the *in silico* method for compounds toxicity prediction: project workflow.

Overall, 22 Phase I reactions and 9 Phase II reactions were created in RDKit. Phase I reactions initially performed on 29 commercial drugs generated in total about 2000 metabolites. However, as the system creates metabolites based only on molecular pattern matches defined in each reaction, many metabolites produced were theoretically possible but not necessarily real. Therefore, to select only real compounds, each metabolite was compared to the PubChem database and analyzed here, considering chemical criteria, such as atom valence, number and type of bonds, charge, etc.

In this manner, all the invalid metabolites were discarded, and only metabolites that passed the "validity check" were kept to simulate the interaction against the hepatic proteins. All the simulations were

performed with KM Prediction, a software based on deep learning methods that accurately predicts the Michaelis-Menten constant values (Km) of enzyme-substrate couplings (Kroll A et al., 2020).

Although in minimal percentage, drug's adverse reactions can be triggered by parent drugs, so their effect cannot be neglected. Therefore, before simulating the interaction metabolites-proteins, we started by using parent drugs as substrates. The first simulation, executed with 29 parent drugs and 416 proteins (liver-specific enzymes and transporters), generated 13312 enzyme-substrate pairs, with Km ranging from 2 µM to 25 µM, that were listed from the lowest to the highest value of Km. The Michaelis-Menten constant, Km, is the parameter expressing the substrate affinity for an enzyme. The lower is the Km, the higher the affinity. To select overall the most representative interactions, we set 10 µM as the highest threshold for the Km, similar to the concentration's threshold adopted when assessing target-compound bindings in early drug discovery (Hughes JP et al., 2010).

At this stage of our study, filtering the interactions with a value of Km ≤ 10 µM allowed us to select a total of 1179 substrate-protein pairs, consistently reducing the amount of initial data. Within these interactions, 184 hepatic enzymes and transporters were involved, and they were all clustered according to their functional classes (Fig. 2).

PROTEIN CLASSES

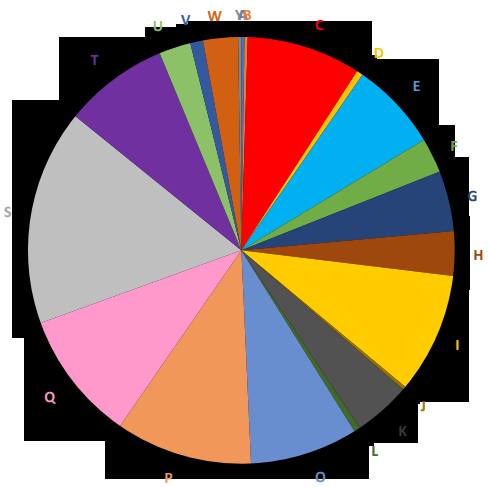

A

TYPE	FUNCTION
A	RNA processing and modification
B	Chromatin Structure and dynamics
C *	Energy production and conversion
D	Cell cycle control and mitosis
E *	Amino Acid metabolism
F	Nucleotide metabolism and transport
G	Carbohydrate metabolism and transport
H	Coenzyme metabolism
I *	Lipid metabolism
J	Translation
K	Transcription
L	Replication and repair
O *	PTMs, protein turnover, chaperones
P *	Inorganic ion transport and metabolism
Q *	Secondary metabolites synthesis, transport, catabolism
S	Unknown
T *	Signal transduction
U	Intracellular trafficing and secretion
V	Defense mechanism
W	Extracellular structures
Y	Nuclear structure
Z	Cytoskeleton

B

Figure 2. Hepatic enzymes and transporters involved in high-affinity interactions with the substrates (Km ≤ 10 µM) were classified by functionality according to the COG, *Clusters* of Orthologous Groups (A). COG functional classification: class type and related protein functions. Significantly high percentages (≥ 7%) of proteins are marked * (B).

Although the highest percentage of proteins (16%) that generated interactions resulted formed by unknown proteins (class "S"), other classes predominantly involved in the substrates binding were identified and characterized by function. Specifically, 10% of the total proteins belong to classes Q and

P, 9% to classes I and C, 8% to classes O and T, and 7% to class E. Therefore, relying on this prediction, the parent drugs tested here are more likely to affect lipid metabolism, ion transport, secondary metabolites biosynthesis and catabolism, signal transduction, amino acid, and energy metabolism.

The initial analysis of data showed that, among all interactions generated, a reduced set of enzymes established high-affinity bindings with multiple drugs, with a Km ranging between 2-4 μM. The drugs involved in such interactions more often included nefazodone (NFZ), its metabolites NFZ-TD (nefazodone-triazoledione) and NFZ-T3 (nefazodone-triazole-3-one), troglitazone (TRG), trazodone (TRZ), astemizole (AST), amiodarone (AMI) and imipramine (IMI), out of the 29 compounds tested.

According to our prediction results, this subset of compounds showed high affinity for GLYATL3 (Glycine N-acyltransferase-like protein), DHB13 (17-beta-hydroxysteroid dehydrogenase 13), and ATP11C (P-type ATPase encoded by ATP11C gene).

GLYATL3 is a mitochondrial enzyme catalyzing glycine-conjugation of xenobiotics before their excretion to bile and urine. Remarkably, a study showed that the expression of GLYATLs is suppressed in hepatocarcinoma cells but not in other liver disease models (Matsuo M et al., 2012).

The enzyme DHB13 (17-beta-hydroxysteroid dehydrogenase 13) plays a central role in hepatic lipid metabolism. It catalyzes the oxidation of a variety of lipid substrates, including 17-beta-estradiol, retinol, retinal, and leukotriene B4. A genomic study conducted in 2018 in the US, involving 46544 participants, related genetic variants of DHB13 to patients' serum levels of AST and ALT, two major biomarkers of liver injuries. They demonstrated that the loss-of-function of the gene encoding DHB13 enzyme reduced the risk of chronic hepatic diseases and the progression of steatosis to cirrhosis (Abul-Husn NS et al., 2018).

The ATP11C protein is a subunit of the ATP -dependent Flippase complex, a transporter essential to translocate phosphatidylserines and phosphatidylethanolamines across the plasma membrane. The mutated enzymes seem to be linked to impairment of bile flow in the familiar intrahepatic cholestatic disease (Segawa K et al., 2014) (Takatsu H et al., 2014).

The organic anion transporter 1B3 (OATP-1B3) was predicted to interact with nefazodone with a Km of 5 μM. The inhibitory effect of this drug on the OATP-1B3 was described in a previous study (Karlgren M et al., 2012). OATP transporters are a family of polypeptides expressed in the basolateral membrane of the hepatocytes, fundamental for xenobiotics' and bile acids' uptake in the liver. OATPs inhibition was demonstrated to be associated with hyperbilirubinemia and to affect xenobiotics' biodistribution through the portal system, thus causing specific drug-drug interactions (Smith NF et al., 2005; Kotsampasakou E et al., 2017).

As expected, many compounds investigated were found to interact with liver metabolizing enzymes of the CYP450 family (isoforms: 3A4, 2C8, 4F2, 2A6, 2D6, 4A22, and 4A11) and the Sulfotransferase

family (SULT isoforms 1A1, 1A2 and 1E1). For instance, according to our prediction, nefazodone, troglitazone, astemizole, and amiodarone are specific substrates for CYP3A4, confirming other studies regarding the CYP3A4 oxidation activity described in the literature (Rotzinger S et al., 2002; Zahno A, 2011; Dixit VA, Bharatam PV, 2011). The same drugs, along with trazodone, established high-affinity interaction with CYP2A6, while troglitazone seems to be the unique substrate for the CYP2C8. These results are consistent with previous investigations regarding CYP450 substrate specificity (Haduch A et al., 2005; Ramachandran V et al., 1999).

Some of the interactions with CYP450 enzymes found in our predictions were never described in literature before. Such results could represent new insights to elucidate unexplored pathways of drug metabolism. Moreover, identifying new compounds' targets within this class of enzymes is important not only to clarify the process of drug degradation but also to discover any other possible effect triggered by this enzyme-compounds binding. For instance, the discovery of CYP450 inhibitors or inducers can deeply impact other drugs` metabolism and lead to toxic products or generate drug-drug interactions.

An accurate protein-protein network analysis was carried out among the 38 proteins belonging to class I, which are involved in lipid metabolism. In this class, the highest number of connections were found, compared to the other protein classes. Here, three main clusters were identified (Fig. 3).

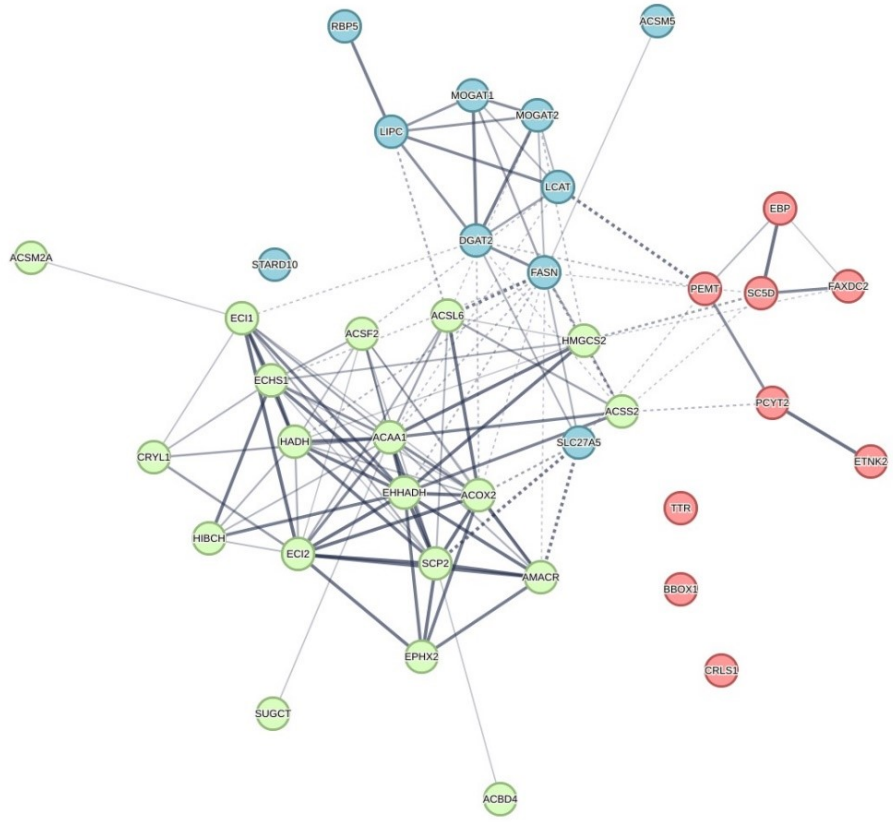

Fig. 3. Protein network analysis of the 38 proteins involved in hepatic lipid metabolism. Three main clusters were identified: the green cluster (19 proteins) shows protein connections identified within FA (fatty acid) and BA (Bile Acid) metabolism. The blue cluster (10 proteins) includes enzymes required for triglyceride biosynthesis. The red cluster (9 proteins) contains enzymes belonging to sterols and phospholipids metabolism.

Proteins forming the green cluster are enzymes implicated in two main metabolic pathways: fatty acid metabolism (synthesis, β-oxidation, and degradation) and primary bile acid biosynthesis. In particular, the enzymes of fatty acids metabolism include the Acyl CoA Synthetase (ACS isoforms M2A, M5, F2, L6); Enoil-CoA Delta-Isomerase 1 and 2, (ECI-1 and 2); the acetyl-CoA acyltransferase 1 (ACAA1) and the Hydroxymethylglutaryl-CoA-synthase-2 (HMGCS2). Interestingly, they all share the same substrates in our study: nefazodone (NFZ), nefazodone's metabolites (NFZ-TD and NFZ-T3), troglitazone (TRG), trazodone (TRZ), astemizole (AST) and amiodarone (AMI).

Three proteins were found in the primary bile acid biosynthesis cluster: AMACR (α-Methylacyl-CoA racemase), ACOX23 (acyl-CoA oxidase 23), and SCP2 (sterol carrier protein 2). While the first two are enzymes involved in bile acid intermediates' metabolism, the third is a non-specific lipid carrier protein. According to our prediction, AMACR and ACOX23 were able to establish high-affinity bindings with the drugs TRG, NFZ, NFZ-T3, AST, and TRZ.

The relationship between troglitazone, nefazodone, amiodarone, and drug-induced liver disease (DILI) is well documented. Several studies demonstrated disruption of lipid homeostasis and the consequent lipid accumulation leading to steatosis related to these drugs. Troglitazone was also associated with cholestasis, while amiodarone is responsible for phospholipidosis probably due to the inhibition of a specific phospholipase. Cirrhosis cases were reported as a severe adverse effect associated with amiodarone's chronic therapies (Masubuchi Y, 2006; Boelsterli UA et al., 2002; Anthérieu S et al., 2011). Mechanisms of nefazodone-induced hepatotoxicity have been described. Cases of acute liver failure associated with nefazodone's treatment led to drug withdrawal in 2003 (Babai S et al., 2021). Its toxicity seems to be mainly owed to mitochondria dysfunction, specifically caused by the impairment of the oxidative phosphorylation metabolizing enzymes (Silva AM et al., 2016).

In the blue cluster, three proteins form the principal network: the enzymes DGAT2 (Diacylglycerol O-acyltransferase 2), MOGAT-1 and 2 (respectively Mono-acylglycerol O-acyltransferase 1 and 2), all catalyzing essential steps in the triacylglycerol synthesis (Yen CL et al., 2008). DGAT2 is required in the liver for endogenous fatty acid incorporation into triacylglycerols and seems to have a pivotal role in lipid accumulation inside the cytosol (Brandt C et al., 2016). A recent study reported a clear connection between DGAT2 and severe diseases such as Non-alcoholic Fatty Liver Disease, hepatic inflammation, and fibrosis (Musso G et al., 2009). Remarkably, according to our results, DGAT2, MOGAT1, and MOGAT2 can establish high-affinity interactions with several drugs, including NFZ, NFZ-TD, TRG, TRZ, AMI, IMI, and SIM (Simvastatin). Interestingly, the same substrates were found to interact with SLC27A5 (solute carrier family 27 member 5), a long-chain fatty acid transporter that also expresses catalytic properties in bile acids metabolism. It has been proposed that it could mediate bile acid conjugation with glycine and taurine before their excretion in the bile (Mihalik SJ et al., 2002).

FASN (Fatty Acid Synthase) is the enzyme required for the last step of palmitate fatty acid synthesis in the *de novo* lipogenesis. An enhancement of this pathway has been reported in patients with Non-Alcoholic Fatty Liver Disease (NAFLD), which can progress into Non-Alcoholic Steatohepatitis (NASH) and cirrhosis. Also, FASN's inhibition was demonstrated to reduce triglycerides intrahepatic accumulation, the necessary step for steatosis initiation (O'Farrell M et al., 2022; Che L et al., 2019). In our study, nefazodone and its metabolite NFZ-T3 were the only two specific ligands of FASN.

The enzyme PCYT2 (ethanolamine-Phosphatase Cytidyl Transferase 2) is the rate-limiting enzyme in the synthesis of phosphatidylethanolamine, one of the principal phospholipids necessary for cell membrane homeostasis, also involved in several regulatory processes (Fig. 3, red cluster). It has been reported that the lack of PCYT2 is related to NASH (Grapentine S et al., 2022). In our prediction, the drugs TRG, NFZ-T3, NFZ, TRZ, AST, M7, and AMI showed high affinity for PCYT2. Therefore, it is plausible to assert that phosphatidylethanolamine's synthesis could be affected by these drugs, which hypothetically could have a role in the pathogenesis of steatohepatitis.

Results are summarized in Table 1. Here, a list of the enzymes involved in the highest number of interactions is presented with their respective substrates. The right column reports the function/activity or effects of each protein in the liver.

Protein	Function	Substrates	Related disease/effects
GLYATL3	Xenobiotic metabolism	NFZ, NFZ-T3, NFZ-TD, TRG, AMI, AST, TRZ, CIP, TMX, IMI, RAP, DCF, SIM, VAN, DOX	Hepatocarcinoma
DHB13	Lipid metabolism	NFZ, NFZ-T3, NFZ-TD, TRG, AMI, AST, IMI, CIP, TMX, SIM, RAP, DOX	Chronic hepatic diseases, steatohepatitis, cirrhosis
ATP11C	Phospholipid Transporter ATPase	NFZ, NFZ-T3, NFZ-TD, TRG, AST, TRZ, IMI, CIP, TMX, SIM, RAP, DOX, AMI	Cholestasis
OATP-1B3	Bile Acids Transporter	NFZ, NFZ-T3, NFZ-TD, TRG, AST, TRZ, CIP	Hyperbilirubinemia
CYP3A4	Xenobiotic metabolism	NFZ, NFZ-T3, NFZ-TD, TRG, AST, IMI, TRZ, TMX	Drugs interactions
ECI-1	Fatty acid ß-oxidation	NFZ-T3, NFZ-TD	Non-alcoholic Fatty Liver Disease
ECI-2	Fatty acid ß-oxidation	NFZ, NFZ-T3, NFZ-TD, TRG, AMI, AST, IMI, CIP, TMX, SIM	Non-alcoholic Fatty Liver Disease
ACAA1	Lipid metabolism, peroxisomal ß-oxidation	TRG, NFZ-T3, NFZ	Non-alcoholic Fatty Liver Disease
HMGCS2	Lipid metabolism	NFZ, NFZ-T3, NFZ-TD, TRG, TRZ	
AMACR	Bile acid biosynthesis	NFZ, NFZ-T3, NFZ-TD, TRG, AST, TRZ, AMI, CIP, SIM	Primary Bile Acid Disorder
ACOX23	Lipid metabolism, peroxisomal ß-oxidation	NFZ, NFZ-T3, NFZ-TD, TRG, AST, TRZ, CIP	Primary Bile Acid Disorder
MOGAT-1	Triacylglycerol biosynthesis	NFZ, NFZ-T3, NFZ-TD, TRG, AMI, AST, TRZ, CIP, TMX, IMI, RAP, DCF, SIM, VAN, DOX, BLE, DCF, NIT	Cytosolic lipid accumulation
MOGAT-2	Triacylglycerol biosynthesis	NFZ, NFZ-TD, TRG, TRZ, AMI, IMI, SIM	Cytosolic lipid accumulation

DGAT2	Triacylglycerol biosynthesis	NFZ, NFZ-T3, NFZ-TD, TRG, AST, TRZ, IMI, TMX, SIM, AMI, RAP, CIP	Hepatic inflammation and fibrosis
FASN	Fatty Acids biosynthesis	NFZ, NFZ-T3	NAFLD, NASH, hepatocarcinoma
PCYT2	Phospholipid metabolism	NFZ, NFZ-T3, NFZ-TD, TRG, AST, TRZ, CIP, TMX, AMI, IMI	Non-alcoholic steatohepatitis

Table 1. Summary table of results. Liver proteins and their respective substrates (drugs) are reported along with the proteins' function/activity and their hepatotoxic effects. NFZ (nefazodone), NFZ-T3 (nefazodone-triazole-3-one), NFZ-TD (nefazodone-triazoledione), TRG (troglitazone), AMI (amiodarone), AST (astemizole), TRZ (trazodone), CIP (ciprofloxacin), TMX (tamoxifen), IMI (imipramine), RAP (rapamycin), DCF (diclofenac), SIM (simvastatin), VAN (vancomycin), DOX (doxorubicin), BLE (bleomycin), NIT (nitrofurantoin).

It is worth noting that the great majority of the target proteins here reported can establish high-affinity interaction with the same subset of drugs (NFZ, NFZ-T3, NFZ-TD, TRG, TRZ, AMI, AST) and that these substrates are associated with severe adverse reaction in the liver such as steatosis, cholestasis, phospholipidosis, NASH and cirrhosis originating from impairment of lipid metabolism and bile acid cycle. These notions are consistent with the forecasts provided by this study. However, although the model enables to predict interactions between drugs and liver proteins, it does not provide information about the type of interactions that could either inhibit or enhance the functions of the proteins involved. Accordingly, further investigations are needed to reveal the effect of such interactions in order to provide a plausible toxicological or pharmacological mechanism for the drugs concerned.

The approach developed in this study, through the analysis of specific drug-target interactions, could allow the validation of toxic effects for a group of approved drugs already found experimentally in *in vitro* liver systems. Indeed, *in vitro* cytotoxicity tests were previously carried out under this project. In particular, the viability of HepaRG cells was measured after their exposure to several drugs, including nefazodone and its metabolites, troglitazone, and amiodarone. The results showed that the highest rate of cell mortality was precisely associated with the administration of these drugs. Therefore, it would be possible to make assumptions explaining the mechanism behind such toxic effects based on compounds-proteins interactions assessed by our prediction and their influence on cellular pathways where the targeted proteins are involved.

Moreover, by examining interactions not yet reported in the literature, it is possible to hypothesize further effects, which shall be experimentally demonstrated. In this manner, this approach can be very useful to understand, at molecular level, mechanisms of pathogenesis of a disease or to elucidate pharmacological processes.

The next steps will be the analysis of the predicted interactions between all the metabolites generated by Phase I and II reactions, and the panel of hepatic proteins previously used. The enormous number of interactions expected to be generated from this simulation perhaps represents the main limitation of this

type of approach. On the other hand, the use of analytical tools available nowadays for interpreting data will certainly facilitate the analysis.

The final aim of the developed tool will be its employment in drug discovery to predict the toxicity of compounds under investigation. This will constitute the complementary part of experimental studies before the compound´s entry into preclinical trials.

8b. *In silico* structure-based analysis for drugs' toxicity prediction (DEREK Nexus®6.1.0)

A complementary work to the experimental part regarding the *in vitro* assessment of hepatotoxicity was carried out *in silico* using Derek Nexus®6.1.0.

Derek Nexus®6.1.0 is a software platform used for computational toxicology that was used in this project to predict the toxicity of a set of compounds previously tested in liver cell lines to understand to what extent *in silico* predictions confirm experimental results. The software is designed to generate endpoint predictions for any chemical structure, and it is particularly useful in the field of safety assessment in drug discovery. The use of Derek Nexus aligns with ICH guidelines and supports the 3Rs principle, which is highly encouraged by EMA and FDA to reduce the need for animal testing in research.

DEREK Nexus is a knowledge-based toxicology software of chemicals that provides predictions of compounds' toxicity by examining chemical structures. By matching chemical features found in the investigated molecule to structurally-related compounds, the system looks for toxicophores, identifying which are the possible toxicological endpoints and how likely they will occur. The likelihood of toxicity is expressed as the assignment of various "alerts" that can range from "certain," "probable," "plausible," "equivocal," "improbable," or "impossible."

Several toxicological patterns can be identified by examining compounds by Derek Nexus, including hepatotoxicity, cardiotoxicity, nephrotoxicity, carcinogenicity, genotoxicity, neurotoxicity, respiratory sensitization, reproductive toxicity, skin sensitization, and thyroid impairment.

In the present study, we used this tool to process the following set of compounds: diclofenac, acetaminophen, troglitazone, fialuridine, amiodarone, nefazodone, nefazodone's metabolite NFZ-TD and simvastatin. Results are summarized in Table 2, which reports the predicted toxicity outcomes for each drug along with the probability of occurrence (alert type).

Compound	Function	Hepatotoxicity	Nephrotoxicity	Cardiotoxicity	Carcinogenicity	Others
Diclofenac	antiinflammatory	++	++	-	-	-
Acetaminophen	antipyretic	+++	++	-	-	+++
Troglitazone	antidiabetic	+++	-	-	++	-
Fialuridine	antiviral	-	-	-	-	-
Amiodarone	antiarrhythmic	+++	-	++	++	++
Nefazodone	antidepressant	-	-	++	-	++
NFZ-TD	antidepressant	-	-	++	-	++
Simvastatin	anticholesterol	+++	-	-	-	-

Table 2. Summary of toxic effects of the selected compounds in different body systems predicted by DEREK Nexus 6.1.0. Alert types of adverse effects are indicated by symbols (++++ certain; +++ probable; ++ plausible; + improbable or equivocal; - impossible). Column "others" could include genotoxicity, neurotoxicity, respiratory tract irritation, reproductive toxicity, skin irritation, thyroid toxicity, androgen receptor modulation.

For the drug diclofenac, the report generated by Derek revealed plausible hepatotoxicity and nephrotoxicity. The first alert found for diclofenac describes hepatotoxicity of 2-aryl acetic and 3-aryl propionic acids, chemical structures present in several NSAIDs, including diclofenac (Fig. 4 B, C).

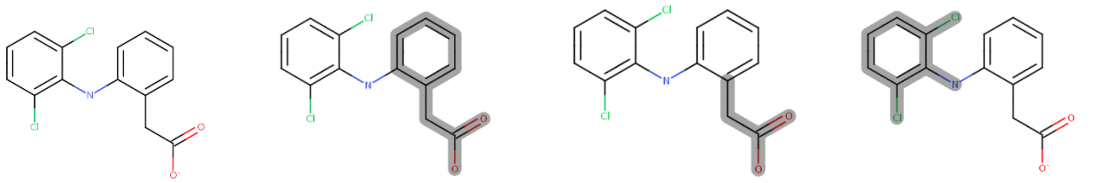

Figure 4. Diclofenac structure (A) and its alerts: 2-aryl acetic (B), 3-aryl propionic acid (C), halogenated benzene (D).

Such structures have been associated with acute or chronic hepatitis, in most cases deriving from idiosyncratic metabolic reactions, mainly dose-independent (Boelsterli UA, 2003; Zimmerman HJ, 1999). Most of the time, diclofenac's hepatotoxic reactions are rare but can range from a mild elevation of serum transaminases to severe cholestasis and hepatocellular injuries leading progressively to fulminant hepatitis (Laine L et al., 2009). Moreover, Derek's report indicates that acyl conjugates derived from diclofenac metabolism are another cause of hepatotoxicity resulting from protein adduct formation. Indeed, acyl glucuronides are very reactive species that can form covalent binding with plasma and tissue proteins (Li C et al., 2003; Bailey MJ and Dickinson RG, 2003).

The second alert found for diclofenac describes nephrotoxicity also associated with aryl acetic or 2-arylpropionic acid (4 B, C). These compounds have a carboxylic acid group that is transformed by UGT

enzymes into acyl glucuronides, which are the main way they are eliminated from the body (Regan SL et al., 2010; Ritter JK, 2000). These metabolites are reactive and can bind to proteins, such as in the kidneys, where they may cause damage (Regan SL et al., 2010; Ritter JK, 2000). Kidneys are more vulnerable because they filter out glucuronides (Regan SL et al., 2010) and also have specific UGT enzymes (Ritter JK, 2000) that may increase local toxicity.

Three alerts were identified for the drug acetaminophen: probable hepatotoxicity, chromosome damage, and plausible nephrotoxicity. In this case, hepatotoxicity alert was associated with the exact match in the query molecule of the para-aminophenol moiety (Fig.5 B, C).

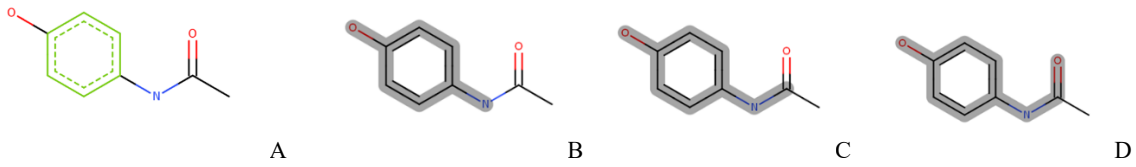

Figure 5. Acetaminophen structure (A) and its alerts: phenol (B), para-aminophenol (C), para-aminophenol or derivative (D).

The reactive metabolite is the N-acetylbenzoquinone imine (NAPQI), deriving from the metabolic transformation of the para-aminophenol moiety by the cytochrome P450 system. When glutathione is depleted after a toxic dose of the drug, NAPQI can bind to several target proteins inside the cell, leading to mitochondrial damage and ATP depletion. Acetaminophen can cause serious and sometimes fatal liver injuries if taken in doses higher than the maximum recommended daily dose of 4 g in humans (Zimmerman HJ, 1999; Larson AM et al., 2005).

The effects of acetaminophen in the liver of mice and rats have been reviewed (Zimmerman HJ, 1999; James LP et al., 2003). The common pattern of injury seen with these models is necrosis with increased aminotransferase levels (Kikkawa R et al., 2006; Gujral JS et al., 2002).

It is believed that nephrotoxicity of para-aminophenol derivatives, like acetaminophen, is likely to be mediated by the formation of a reactive para-benzoquinone imine metabolite (Hinson JA, 1983; Kalgutkar AS et al., 2005; Elseviers MM and De Broe ME, 2008). The p-benzoquinone imine metabolite can bind cellular macromolecules in the kidneys, causing nephrotoxicity.

Lastly, the genetic damage, classified as a probable warning by Derek Nexus, is based on evidence from Hoffmann-La Roche AG. They showed that phenols with nitrogen or oxygen in the para position cause positive results in the test for chromosome aberrations *in vitro* (Fig. 5D).

Derek's report for the antidiabetic drug troglitazone revealed probable hepatotoxicity alert and plausible carcinogenicity in mammals. The carcinogenicity warning is due to the 4-Alkylether phenol present in the troglitazone's structure (Fig. 6B).

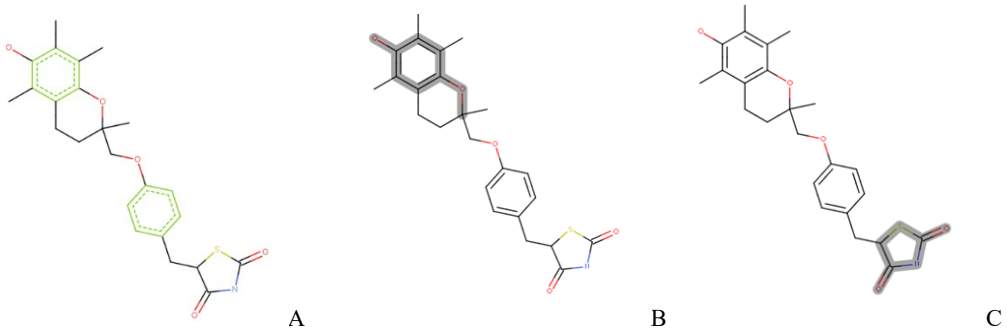

Figure 6. Troglitazone structure (A) and its chemical alerts: 4-Alkylether phenol (B), thiazolidinedione(C).

The assumption is funded by the analogy of this chemical feature with butyl-hydroxyanisole, found to cause squamous cell carcinomas and papillomas in rodents (IARC, 1986; Ito N et al., 1983).

The second alert is due to the thiazolidinedione structure (Fig. 6C). 2,4-thiazolidinediones, commonly referred as glitazones, are a class of pharmaceuticals developed for type-2 diabetes treatment, including troglitazone, rosiglitazone, and pioglitazone. Troglitazone has been associated with cases of liver failure leading to transplantation and death (Lee WM, 2003; Kohlroser J et al., 2000; Graham DJ et al., 2003a, b). Rosiglitazone and pioglitazone, two newer analogs, do not show toxicity to the same extent. Toxicity may be due to an intrinsic effect of the thiazolidinedione moiety, as shown in a study conducted in rats by Kennedy et al. (2003). The oxidative breakage of the thiazolidinedione ring, along with the oxidation of the chromane ring, leads to the formation of highly reactive metabolites, which account for troglitazone's toxicity as they are responsible for protein adduct formation. Moreover, a possible explanation for the increased liver toxicity of troglitazone compared to rosiglitazone is the difference in the dosages administered since troglitazone requires a much higher dose than the other drugs in the same class (Scheen AJ, 2001; Lebovitz HE et al., 2002).

For the antiviral drug fialuridine, Derek Nexus did not detect any toxicity warnings.

Several alerts are described in Derek Nexus' report for the compound amiodarone (Fig 7). Hepatotoxicity in mammals is predicted as "probable," and it is related, according to this prediction, to the part of amiodarone's molecule containing the halogenated aromatic ring bond to the benzofuran ring (Fig. 7B, C, D, G, H). In fact, as amply documented, amiodarone is a potent antiarrhythmic agent found to be responsible for many hepatic injuries, including cholestasis, phospholipidosis, steatosis, acute and chronic hepatitis, and cirrhosis (Zimmerman HJ, 1999; Chang CC et al., 1999; Lewis JH et al., 1989). It is worth noting that the role of the benzofuran ring in the impairment of mitochondrial function and beta-oxidation has been proved (Spaniol M et al., 2001).

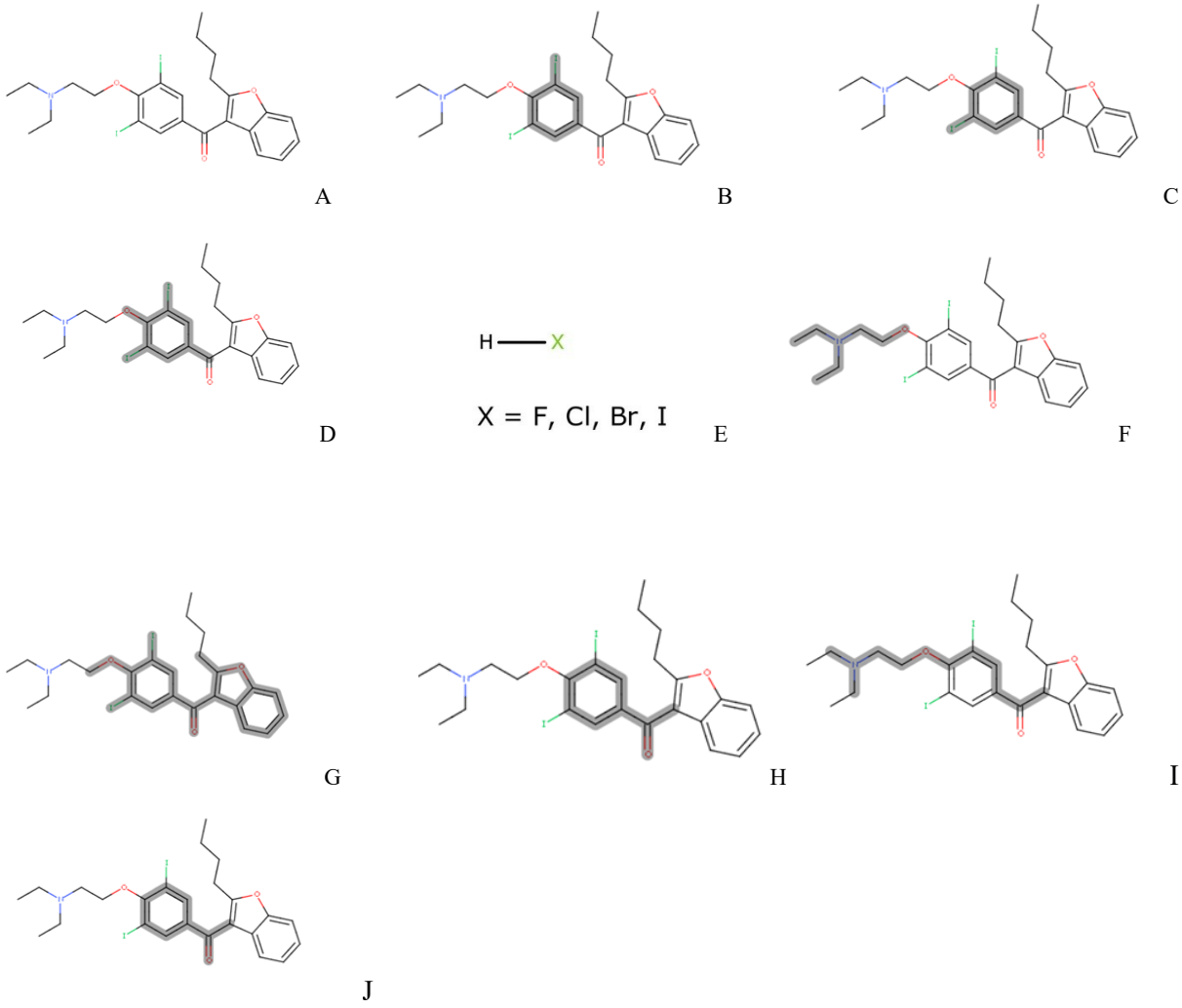

Figure 9. Amiodarone structure (A) and its alerts: aromatic iodo-compound (B), aromatic iodo-compound (C), Polyhalogenated aromatic (D), hydrogen halide(E), ethanamine or piperidine (F), amiodarone or analog (G) HERG pharmacophore III (I), diaryl ketone (J).

All the plausible alerts generated for amiodarone include HERG channel inhibition, thyroid toxicity, carcinogenicity, and irritation of the eye, skin, and respiratory tract.

Aromatic iodo-compounds, such as amiodarone, are able to inhibit the enzyme converting the hormone T3 to T4 at the peripheral level, causing low T3 serum levels (Fig. 7). For compensation, the thyroid gland is continuously stimulated by increased TSH secretion to raise T3 levels. This chronic stimulation can induce over time hyperplasia or neoplasms of the thyroid gland (Capen CC, 1997; McClain RM,1995; Hill RN et al., 1989; Burgi et al., 1976).

The carcinogenic properties of amiodarone are due to the presence in the molecule of a di-iodo aromatic ring group (Fig.7 B, C, D, G, H, I). All aromatic polyhalogenated compounds (e.g., hexachlorobenzene,

para-dichlorobenzene) are classified according to IARC as carcinogens of group 2B (IARC 2001; IARC 1999). For instance, para-dichlorobenzene may damage DNA in the liver and spleen of mice, so it is classified as possibly carcinogenic to humans (group 2B). Similarly, hexachlorobenzene caused tumors in the liver and kidney of mice, the liver and thyroid gland of hamsters, and in the liver, parathyroid glands, and adrenal glands of rats (IARC, 1999). The other feature responsible for the carcinogenicity of amiodarone is thought to be the diaryl-ketone moiety (Fig. 7J). Several compounds containing this feature were demonstrated to induce carcinogenesis in humans and animals with a non-genotoxic mechanism involving the activation of the PXR receptor (Mikamo E et al., 2002; NTP 2000; US EPA, 2009).

Amiodarone's cardiac adverse effects are associated with its capacity to block HERG potassium channels, leading to an elongation of the ventricular repolarization phase and the consequent extension of the QT interval (Crumb W and Cavero I, 1999). Amiodarone shares the same pharmacophore of other HERG channel inhibitors, indicated as Pharmacophore III (Fig.7I) (Pearlstein RA et al., 2003; Cavalli A et al., 2002; Ekins S et al., 2002).

Finally, potential irritation of eye, skin and respiratory tract induced by amiodarone is that of the hydrogen halides (Fig. 7E) (Holland G et al., 1996).

Derek Nexus' predicted three "probable" alerts for the antidepressant agent nefazodone: HERG channel inhibition, androgen receptor modulation and irritation of skin, eye and respiratory tract. Nefazodone contains a specific moiety shared with others HERG inhibitors, like astemizole and serindole, referred as Pharmacophore I (Fig. 8B, C) (Rampe D et al., 1998; Pearlstein RA et al., 2003; Zhou Z et al., 1999; Taglialatela Met al., 2000; Drolet Bet al., 2003).

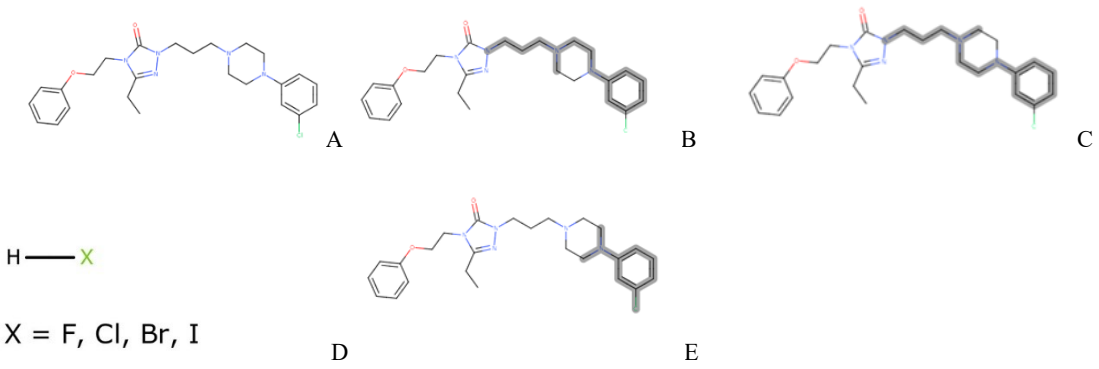

Figure 8. Nefazodone structure (A) and its alerts: HERG Pharmacophore I (B), HERG Pharmacophore I (C), hydrogen halide (D), 4-(2,5-Dioxopyrrolidin-1-yl)-benzonitrile (E).

A common feature of these compounds is a positively charged amine linked to an aromatic ring by 2-8 bonds (Fig. 8 B, C). They also have a tail opposite to the aromatic region, which can be different groups, such as an alkylbenzene in astemizole or an alkylimidazolidinone ring in sertindole. The blockage of the

HERG potassium channel, according to this prediction, could be responsible for the potentially severe cardiac side effects of nefazodone.

The possible modulation of the androgen receptor by nefazodone is predicted to be associated with a specific moiety discovered by previous studies that analyzed more than 400 chemicals' activity toward the androgen receptor. In nefazodone, this chemical alert is illustrated in Fig. 8E. This alert applies to compounds that display an aromatic ring with an electron-withdrawing group in para or meta position to a heteroatom (Guo C et al., 2011; Guo C et al., 2012; Hamann LG et al., 2007; Kinoyama I et al., 2006; Nique F et al., 2012; Sexton KE et al., 2011).

Nefazodone is a halogenated compound that can cause irritation of the skin, eye, and respiratory tract, according to Derek Nexus' prediction (Holland G et al., 1996). The chemical alert identified by Derek is shown in Fig. 8D.

Despite nefazodone's high hepatotoxicity being widely described and assessed *in vitro* and *in vivo*, unexpectedly, no hepatotoxicity was detected by Derek Nexus for this drug.

As expected, for nefazodone's metabolite NFZ-TD, the two alerts found, cardiotoxicity and androgen receptor modulation, were the same as those found for the parent compound. The plausible cardiotoxicity warning is due to the presence of Parmacophore I (Fig. 9 C, D) inhibiting cardiac HERG channels (Aronov AM, 2005; Mitcheson JS et al., 2000). The plausible androgen receptor modulation is associated with a specific feature shared by several compounds investigated by previous studies, able to strongly bind the androgen receptor, either as agonists or antagonists. The structure needed for the androgen receptor interaction is constituted by an aromatic ring containing a withdrawing atom in meta or para position (Chlorine in meta in the specific case of NFZ-TD) with respect to a heteroatom (Nitrogen, in the specific case of NFZ-TD), the latter being part of a separate ring or representing a linker for another ring system (Fig. 9B) (Guo C et al., 2011; Guo C et al., 2012; Hamann LG et al., 2007; Kinoyama I et al., 2006; Nique F et al., 2012; Sexton KE et al., 2011).

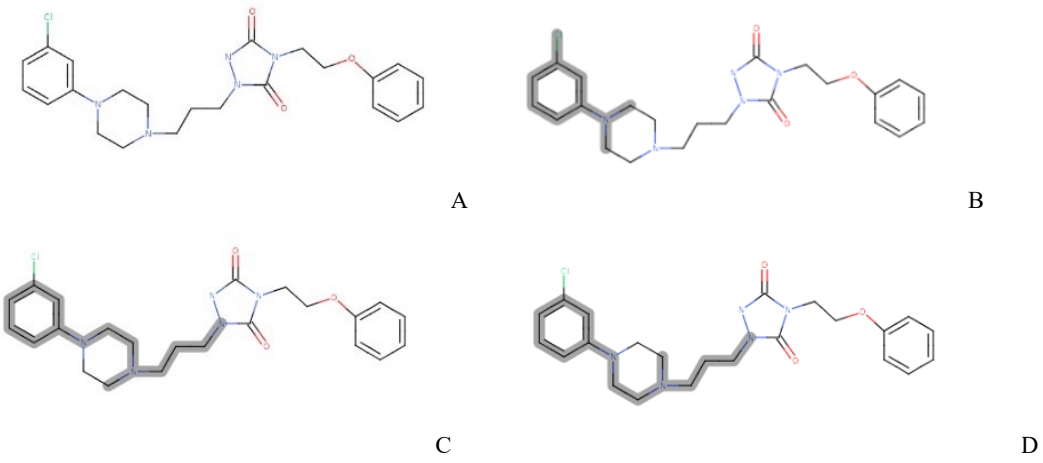

Figure 9. Nefazodone's metabolite NFZ-TD structure (A) and its alerts: 4-(2,5-Dioxopyrrolidin-1-yl)-benzonitrile (B); Pharmacophore I (C); Pharmacophore I (D).

Unexpectedly, for the anti-cholesterol drug simvastatin, which did not cause significant hepatotoxic effects in *in vitro* tests of the present work, Derek Nexus reported a probable alert of hepatotoxicity. Liver toxicity of statins, observed in rare cases, refers to ALT elevation. (Tolman KG, 2000). However, in 1-3% of cases, serious ALT elevation was associated with cholestatic liver injuries (Perger L et al., 2003; Pelli N et al., 2003; Grimbert S et al., 1994; Feydy P and Bogomoletz WV; 1991). In animal species like rabbits, rats, and guinea pigs, administered with statins, ALT elevation and hepatic degeneration and necrosis were also observed (Kornbrust DJ et al., 1989; Horsmans Y et al., 1990; Gerson RJ et al., 1989).

The putative mechanism of toxicity is not well known but it is thought to be the same as Statins' mechanism of action, the inhibition of HMG-Coa reductase in the cholesterol synthesis (Steiner S et al., 2001). Therefore, in this case pharmacophore and toxicophore coincide (Fig. 10B).

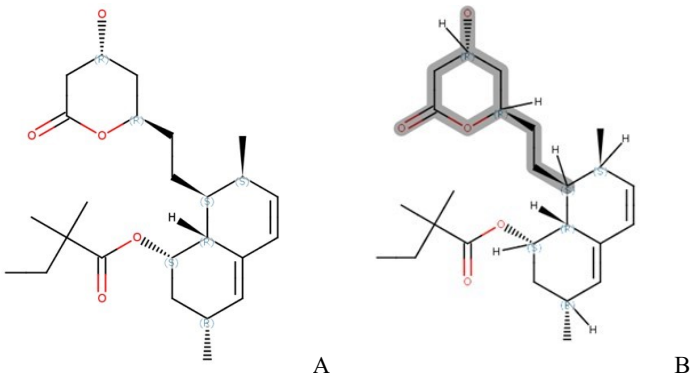

Figure 10. Simvastatin structure (A) and its alerts: Statin's moiety (B).

Indeed, as described in Derek Nexus' prediction for simvastatin, the feature of the molecule responsible for the hepatotoxic effect is the lactone moiety mimicking the HMG-CoA reductase's natural substrate (Fig. 10B).

The set of compounds analyzed through Derek Nexus was previously tested *in vitro* in this study in human and animal hepatocytes to assess liver toxicity. The prediction built by Derek was consistent in some cases with our experimental results. For instance, the high hepatotoxicity shown for amiodarone and troglitazone was confirmed by Derek Nexus, which predicted a "probable alert" for hepatotoxicity for these compounds.

For acetaminophen, whose hepatotoxicity *in vitro* was highly expressed only after multiple doses of administration, Derek predicted high liver damage, with a "probable alert" as well.

Derek assigned a plausible hepatotoxic effect to the drug diclofenac, which is consistent with our experimental observations, as the drug-induced high hepatocyte mortality only in long-term exposure. Finally, for nefazodone's metabolite NFZ-TD, the *in silico* prediction confirmed the compound's safety found experimentally.

However, discordant results were found for the drugs nefazodone, simvastatin, and fialuridine. For nefazodone, in fact, Derek Nexus predicted no liver toxicity, while the drug was demonstrated to be one of the most noxious compounds in our in vitro testing of both human and animal hepatocytes. Although fialuridine showed no toxicity at acute administration, it induced high cell mortality in hepatocytes exposed to the drug for two weeks. However, in this case, Derek Nexus was unable to reveal such toxicity. In contrast, simvastatin, which showed a safe profile in all human and animal hepatocyte cultures, turned out to be a severe hepatotoxicant, according to Derek Nexus' report (Table 2).

In summary, the *in silico* toxicity predictions by Derek Nexus aligned with the experimental findings for the drugs diclofenac, acetaminophen, troglitazone, amiodarone, and the nefazodone's metabolite NFZ-TD. However, Derek Nexus' predictions were inconsistent with the experimental data for nefazodone (parent compound), simvastatin, and fialuridine.

It is important to note that Derek Nexus is a powerful platform that can be used as a screening tool to predict the likely toxicity of any compound without the need for synthesis and testing. Derek Nexus integrates data from assays and structure-activity relationship predictions, linking chemical classes to the observation of key events, which are used to construct networks for toxicity predictions. This approach has been found useful for understanding sequences of events that lead to adverse outcomes such as toxicity. However, no predictive model is perfect, therefore, Derek should be used as part of a comprehensive assessment that includes other methods and expert judgment. In fact, the purpose of *in silico* tools like Derek Nexus is to generate predictions that could facilitate the Go/No-go decision in drug discovery phases, but, as with every prediction, it is not certain and, therefore, needs to be experimentally validated.

CONCLUSIONS AND FUTURE PERSPECTIVES

The objective of the present study was to develop and validate *in vitro* and *in silico* methods to predict the toxicity of compounds that could be harnessed in early drug discovery.

To this aim, *in vitro* toxicity was evaluated initially in monolayer culture of human cell lines representative of several organs in order to confirm the toxic effects of a set of commercial drugs. However, as the liver is the principal organ in the body affected by the toxicity of drugs due to its primary role in xenobiotics' biotransformation and detoxification, we focused our *in vitro* study on the development of a reliable procedure to predict hepatotoxicity.

Hepatotoxicity evaluation *in vitro* was carried out using three different cell culture formats. Bidimensional (2D) cell culture models included conventional monolayer and sandwich systems, whereas spheroids were used as models of 3D culture systems. Hepatotoxicity validation was assessed using approved drugs belonging to different medical classes, covering a broad range of known hepatotoxic effects, from low to high hepatotoxicity outcomes reported in clinics. Our set of drugs included simvastatin, an anti-cholesterol agent rarely associated with hepatotoxicity, as well as drugs withdrawn from the market following severe liver injuries, such as the antidiabetic troglitazone and the antidepressant nefazodone. The anti-inflammatory diclofenac and the widely used antipyretic acetaminophen were used as a model of liver toxicity occurring at high doses only. The drug fialuridine was used as a model to replicate long-term hepatotoxicity, as this compound, terminated in clinical trial II, induced five deaths and two liver transplantations due to severe liver injuries that occurred only at chronic administrations. Finally, the antiarrhythmic amiodarone was introduced in our set of drugs for its known severe and acute liver toxicity.

In this study, both acute and long-term hepatotoxicity were assessed. Acute drugs' effects, evaluated at 48h after the single drug administration, were compared to long-term effects observed at 14 days after repeated drug doses.

All *in vitro* hepatotoxicity tests were performed in human hepatocytes, using the HepaRG cell line as a model, as well as in pig primary hepatocytes (PPH) and rat primary hepatocytes (RPH) to compare species-specific hepatotoxic outcomes and to align with the authorities' guidelines in drug discovery, which require the use of a rodent and a non-rodent animal model in drug discovery testing. The same set of drugs was tested in the same conditions in all hepatocyte species to test both short-term and long-term toxicity. All tests were performed in monolayer, sandwich, and spheroids cultures within each species to compare cells' sensitivity to compounds within each format.

Our study showed that within each species, the acute effects of drugs did not show significant differences between monolayer, sandwich, and spheroids cultures of hepatocytes. However, at long-term exposure,

3D spheroids were more sensitive to drugs' toxicity, demonstrated by lower viability and lower LC_{50} values of drugs compared to those found in 2D systems (monolayer and sandwich cultures). This effect was particularly evident for the drugs simvastatin, fialuridine, and acetaminophen, which induced at 14 days of treatment significantly higher mortality in spheroids compared to sandwich cultures.

For the advantages provided, such as easy handling and maintenance, 2D formats remain valuable systems for acute hepatotoxicity prediction. However, our data indicate that they are not ideal for long-term assessments. Conversely, 3D spheroids, demonstrating higher sensitivity at multiple doses of exposure, constitute a more reliable *in vitro* model to assess long-term hepatotoxicity. Although more complex than 2D systems, 3D spheroids are still amenable to HTS, offering the advantage of being applicable for compounds' screening in early drug discovery.

Overall, these results emphasize the importance of utilizing a suitable *in vitro* system for cytotoxicity studies. Particularly, our study highlights the superior sensitivity of 3D spheroids compared to sandwich and monolayer formats. Indeed, in 3D culture systems, cells retain their natural three-dimensional shape and morphology, reflecting the natural organization and disposition of surface receptors, fundamental for cell signalling, inter-cell communication, interaction with ECM components, and response to drugs. All these features provide an *in vivo*-like environment that allows cells to maintain their physiological status, retaining their natural functions for a longer time compared to 2D systems, which lack all these properties.

In general, the viability of cells observed after two weeks of multiple treatments was lower than that observed after a single drug treatment for every drug tested. This indicates the importance of considering the duration and frequency of drugs' exposure when evaluating their potential adverse effects, emphasizing the need for comprehensive and long-term toxicity assessments in drug development studies. Although this result was expected, it confirms the reliability of this *in vitro* model for long-term hepatotoxicity evaluation.

Considering prolonged exposure durations enables us to capture the potential cumulative effects of drugs over time, which may not be evident during short-term assessments. This approach allows for a more accurate evaluation of the safety profile of drugs and provides valuable insights into their potential long-term risks. Moreover, assessing both short- and long-term toxicity helps in identifying drugs that may exhibit delayed or progressive toxic effects, which could have significant implications for their clinical use. By adopting this comprehensive approach, we can enhance the predictive value of *in vitro* toxicity testing and improve our ability to identify potential safety concerns early in the drug development process.

The comparison of drugs' effects between species indicated further insights. While acute outcomes of hepatotoxicity were similar between HepaRG, PPH, and RPH cultured in sandwich format, differences across species were observed within spheroids' cultures. Particularly, at 48h, spheroids of HepaRG were

more sensitive than other species to diclofenac, whereas toxicity of acetaminophen, troglitazone, and fialuridine was higher in RPH spheroids than in human and pig species.

Remarkably, the scenario changed significantly when repeated doses of drugs were administered for two weeks. In this case, HepaRG spheroids showed a significantly higher sensitivity to diclofenac, acetaminophen, troglitazone, and fialuridine compared to pig and rat spheroids cultures, indicating the HepaRG cells' high value in predicting long-term adverse effects in humans. However, no significant differences were observed between species exposed to amiodarone and nefazodone. Being these drugs high hepatotoxic compounds, they induced strong mortality in all cell types, already at low doses, without discrimination of species.

It is worth noting that our *in vitro* study successfully replicated the documented case of fialuridine-induced hepatotoxicity. During the preclinical phase, fialuridine did not exhibit hepatotoxicity in animal models, which allowed the drug to advance to clinical trials. In humans, no hepatotoxicity was initially observed at the acute administration; however, after a few months of exposure, severe liver injuries occurred, resulting in five deaths and leading to two liver transplantations. Our model effectively reproduced the marked differences in toxicity between human and animal species, as well as the different acute and chronic effects of the drug. Specifically, fialuridine showed a safe profile across all species after the single administration, with no mortality observed in HepaRG, PPH, or RPH at 48h. However, after two weeks of repeated treatments, the viability of the HepaRG population was dramatically affected, while RPH and PPH cultures were only slightly affected. These findings led to two key conclusions. First, our model successfully distinguished between the acute and long-term effects of fialuridine. Second, it revealed species-specific differences in the drug's toxicity. This is a crucial observation because preclinical animal models failed to detect the hepatotoxicity of fialuridine, allowing the drug to proceed to human clinical trials, where severe liver injuries led to the trial's termination. Collectively, these results highlight the reliability of our *in vitro* assessment, which accurately replicated the toxic profile of this drug in alignment with clinical results.

Overall, our findings suggest the reliability of the present *in vitro* model for the acute and long-term hepatotoxicity evaluation, remarking the relevance of choosing a reliable *in vitro* system, such as 3D spheroids, when assessing long-term toxicity testing, and the importance of accounting for inter-species differences in the metabolic activity of each species. Differences in metabolism among humans, pigs, and rats may have implications for the pharmacokinetics, pharmacodynamics, and toxicity of drugs in these species. Therefore, caution should be exercised when extrapolating data from animal studies to human investigations.

Despite the static systems described so far (2D and 3D) providing valuable models for drug toxicity screening, they have limitations. Static models do not rely on continuous medium flow, therefore nutrients, as well as the drug's concentration in contact with cells, remain constant. As a consequence,

the *in vivo* microenvironment is not accurately mimicked, and the typical PK/PD profile of drugs cannot be reproduced. A further step in this study was the introduction of the Hollow Fiber Bioreactor System (HFS), a dynamic *in vitro* system where cells, cultured in a 3D-like format, are continuously perfused by media and are therefore subjected to a controlled fluctuation of nutrients oxygen, and drug concentration over time as it happens *in vivo*. Such a system allows a precise reproduction of the PK/PD profile of drugs, permitting the study of pharmacological and toxicological effects of drugs, which closely reflect the *in vivo* condition. Furthermore, in the HFS, cells can be maintained viable and functioning for a longer time compared to 2D or spheroids systems, allowing accurate studies of chronic toxicity. In this study, we planned to start with preliminary tests concerning long-term HepaRG cells' viability within the HFS, compatibility tests between cells and scaffold materials of the HFS, as well as the PK/PD profile assessment of diclofenac, the selected compound for this part of the project. Once preliminary tests are done, we will proceed by testing the chronic toxicity of diclofenac in HepaRG cells to assess the potential of the HFS in predictive toxicology. Altogether, these studies will represent future steps in the progression of the present work.
To complete the *in vitro* section of the study, we finally proposed a procedure for toxic metabolites identification based on testing drugs in metabolizing and non-metabolizing conditions, using HepaRG and HepG2 cells. The HepaRG cell line, known for its high expression of the main liver metabolic enzymes, expresses a high metabolizing capacity. Therefore, when exposed to drugs, the effects will be mostly related to metabolites. On the other hand, HepG2 cells, exhibiting a very reduced metabolic activity, will show the effects of the parent compounds.

We used three different drugs to validate this method: astemizole, whose toxicity is known to be associated with the parent drug and not to its metabolites; acetaminophen, known to induce high hepatotoxicity through the production of its toxic metabolite NAPQI; nefazodone, which exerts liver toxicity through both the parent compound and its metabolites. This method successfully reproduced these different cases of toxicity, providing a useful tool to discriminate if toxicity is caused by parent compounds, liver metabolites, or both.

Using this approach, we further explored nefazodone's hepatotoxicity by testing nefazodone's main metabolites, NFZ-OH and NFZ-TD, singularly in HepaRG and HepG2. We showed, for the first time, that nefazodone-induced hepatoxicity is triggered not only by nefazodone parent drug but also by the metabolite NFZ-OH, whereas the other main metabolite, NFZ-TD, was not toxic. Therefore, we believe that the proposed *in vitro* procedure could be exploited to identify toxic metabolites, elucidating the mechanism of drugs' toxicity. Furthermore, this method could be used to guide leads' selection and analogs' design in drug discovery and to refine or enhance existing *in silico* models for toxicity prediction.

The other section of this project included the use of computational models for toxicity prediction of compounds. The first *in silico* tool that we used, DEREK Nexus, is a software for structural alerts (SAs)

identification. DEREK Nexus is a knowledge-based software that compares substructures of a given molecule to its database, containing chemical structures associated with any type of toxicity reported in previous studies, identifying in this way the SAs of the query molecule. By uploading a molecule, DEREK Nexus generates a report where, based on the SAs found, toxicity outcomes are listed as "certain," "probable," "plausible," "improbable or equivocal," and "not found," giving in this way a prediction of toxicity.

In this study, the toxicity prediction generated by DEREK Nexus for the drugs tested *in vitro* is not always aligned with the experimental findings. For instance, "probable" hepatotoxicity was correctly predicted for the drugs amiodarone, acetaminophen, and troglitazone, and "plausible" hepatotoxicity for diclofenac. Hepatotoxicity is well recognized in the literature and clinics of all these drugs, and it was additionally confirmed in the present study. However, DEREK Nexus erroneously did not predict hepatotoxicity for the drugs fialuridine and nefazodone, which were both withdrawn from the market following severe liver injuries. Finally, the software predicted "probable" hepatotoxicity for the drug simvastatin, which was rarely associated with liver adverse events.

Despite the rationale behind DEREK Nexus and its advantage in providing a rapid and cost-effective toxicity prediction of chemicals with no need to synthesize and test compounds experimentally, our results suggest that DEREK Nexus' prediction has sometimes proven inadequate. Therefore, these predictions should be validated through experimental findings.

As the final part of the *in silico* work of this project, a computational model for toxicity prediction of drugs was developed in collaboration with the Quantitative and Theoretical Biology (QTB) department of the Heinrich Heine University (HHU). The model, based on *in silico* tools, allows the simulation of interactions between drugs and human liver proteins, including enzymes and transporters, to explore which liver pathways are affected and eventually identify pathways involved in hepatotoxicity.

Within the model simulation, not only parent drugs are considered, but also metabolites generated by Phase I and Phase II liver reactions, as they are often implicated in hepatotoxic mechanisms. From the analysis of simulations generated with 28 parent drugs, we found that high-affinity interactions were established with 184 hepatic proteins, involving enzymes of lipid and energetic metabolism, organic anions transporters, and signal transduction proteins. Additionally, many interactions were found that involved several isoforms of CYP450 enzymes, confirming already known metabolic processes of the drugs investigated. Furthermore, some interactions involved isoforms never described before for these drugs, therefore providing insights of possible new metabolic pathways implicating these drugs.

Noteworthy, proteins of lipid metabolism involved in liver diseases such as steatosis, non-alcoholic fatty liver disease, non-alcoholic steatohepatitis, and bile acid disorders were found in this model to establish high-affinity interactions with nefazodone, amiodarone, and troglitazone confirming their well-known association with such liver pathologies, adding knowledge of possible mechanisms of toxicity.

Ultimately, by generating specific drug-protein interactions, the computational model developed here could be used to validate ascertained toxic effects of drugs, such as those found experimentally, providing putative mechanisms of toxicity. Additionally, by predicting interactions never reported before, it could aid the elucidation of new mechanisms of toxicity triggered by drugs and their metabolites.

In conclusion, we believe that the integration of the proposed *in vitro* and *in silico* methods marks a significant advancement in the early detection of compounds' toxicity. It represents a key approach allowing us to accurately identify harmful compounds at early stages, thereby preventing the risk of adverse effects at late clinical phases. This combined approach not only enhances the reliability of toxicity predictions but also complies with the 3Rs principles by reducing reliance on animal testing. These innovations are crucial in the field of toxicology, providing a more ethical and efficient pathway for risk assessment of new compounds.

REFERENCES

Abdoli N, Azarmi Y, Eghbal MA. Mitigation of statins-induced cytotoxicity and mitochondrial dysfunction by L-carnitine in freshly-isolated rat hepatocytes. Res Pharm Sci. 2015 Mar-Apr;10(2):143-51. PMID: 26487891; PMCID: PMC4584453.

Abdoli N, Azarmi Y, Eghbal MA. Protective effects of N-acetylcysteine against the statins cytotoxicity in freshly isolated rat hepatocytes. Adv Pharm Bull 2014; 4:249-54. doi: 10.5681/apb.2014.036

Abdullah, C.S., Alam, S., Aishwarya, R. et al. Doxorubicin-induced cardiomyopathy associated with inhibition of autophagic degradation process and defects in mitochondrial respiration. Sci Rep 9, 2002 (2019). https://doi.org/10.1038/s41598-018-37862-3

Abdullah-Al-Shoeb M, Sasaki K, Kikutani S, Namba N, Ueno K, Kondo Y, Maeda H, Maruyama T, Irie T, Ishitsuka Y. The Late-Stage Protective Effect of Mito-TEMPO against Acetaminophen-Induced Hepatotoxicity in Mouse and Three-Dimensional Cell Culture Models. *Antioxidants*. 2020; 9(10):965. https://doi.org/10.3390/antiox9100965

Afsar T, Razak S, Almajwal A, Al-Disi D. Doxorubicin-induced alterations in kidney functioning, oxidative stress, DNA damage, and renal tissue morphology; Improvement by Acacia hydaspica tannin-rich ethyl acetate fraction. Saudi J Biol Sci. 2020 Sep;27(9):2251-2260. doi: 10.1016/j.sjbs.2020.07.011. Epub 2020 Jul 10. PMID: 32884406; PMCID: PMC7451730.

Agarwal A, Hunt B, Stegemann M, Rochwerg B, Lamontagne F, Siemieniuk RA, Agoritsas T, Askie L, Lytvyn L, Leo YS, Macdonald H, Zeng L, Alhadyan A, Muna A, Amin W, da Silva ARA, Aryal D, Barragan FAJ, Bausch FJ, Burhan E, Calfee CS, Cecconi M, Chacko B, Chanda D, Dat VQ, De Sutter A, Du B, Freedman S, Geduld H, Gee P, Haider M, Gotte M, Harley N, Hashimi M, Hui D, Ismail M, Jehan F, Kabra SK, Kanda S, Kim YJ, Kissoon N, Krishna S, Kuppalli K, Kwizera A, Lado Castro-Rial M, Lisboa T, Lodha R, Mahaka I, Manai H, Mendelson M, Migliori GB, Mino G, Nsutebu E, Peter J, Preller J, Pshenichnaya N, Qadir N, Ranganathan SS, Relan P, Rylance J, Sabzwari S, Sarin R, Shankar-Hari M, Sharland M, Shen Y, Souza JP, Swanstrom R, Tshokey T, Ugarte S, Uyeki T, Evangelina VC, Venkatapuram S, Vuyiseka D, Wijewickrama A, Tran L, Zeraatkar D, Bartoszko JJ, Ge L, Brignardello-Petersen R, Owen A, Guyatt G, Diaz J, Kawano-Dourado L, Jacobs M, Vandvik PO. A living WHO guideline on drugs for covid-19. BMJ. 2020 Sep 4;370:m3379. doi: 10.1136/bmj.m3379. Update in: BMJ. 2020 Nov 19;371:m4475. Update in: BMJ. 2021 Mar 31;372:n860. Update in: BMJ. 2021 Jul 6;374:n1703. Update in: BMJ. 2021 Sep 23;374:n2219. Erratum in: BMJ. 2022 Apr 25;377:o1045. PMID: 32887691.

Agrawal S, Khazaeni B. Acetaminophen Toxicity. [Updated 2023 Jun 9]. In: StatPearls [Internet]. Treasure Island (FL): StatPearls Publishing; 2024 Jan-. Available from: https://www.ncbi.nlm.nih.gov/books/NBK441917/

Ahmed, A.Y., Aowda, S.A. & Hadwan, M.H. A validated method to assess glutathione peroxidase enzyme activity. Chem. Pap. 75, 6625–6637 (2021). https://doi.org/10.1007/s11696-021-01826-1

Aires C.C.P., Ijlst L., Stet F., Prip-Buus C., de Almeida I.T., Duran M., Wanders R.J.A., Silva M.F.B. Inhibition of Hepatic Carnitine Palmitoyl-Transferase I (CPT IA) by Valproyl-CoA as a Possible Mechanism of Valproate-Induced Steatosis. Biochem. Pharmacol. 2010; 79:792–799. doi: 10.1016/j.bcp.2009.10.011

Aithal GP. Diclofenac-induced liver injury: a paradigm of idiosyncratic drug toxicity. Expert Opin Drug Saf. 2004 Nov;3(6):519-23. doi: 10.1517/14740338.3.6.519. PMID: 15500411.

Akbal E, Batgi H, Koçak E, Canatan T, Köklü S. Low-dose amiodarone-induced fatal liver failure. Drug Chem Toxicol. 2013 Apr;36(2):261-2. doi: 10.3109/01480545.2011.653489. Epub 2012 Feb 23. PMID: 22356138.

Aliberti S, Grignani G, Allione P, Fizzotti M, Galatola G, Pisacane A, Aglietta M. An acute hepatitis resembling autoimmune hepatitis occurring during imatinib therapy in a gastrointestinal stromal tumor patient. Am J Clin Oncol. 2009 Dec;32(6):640-1. doi: 10.1097/COC.0b013e31802b4ef7. PMID: 19955903.

Almazroo OA, Miah MK, Venkataramanan R. Drug Metabolism in the Liver. Clin Liver Dis. 2017 Feb;21(1):1-20. doi: 10.1016/j.cld.2016.08.001. Epub 2016 Oct 15. PMID: 27842765.

Alonso R, Cuevas A, Mata P. Lomitapide: a review of its clinical use, efficacy, and tolerability. Core Evid. 2019 Jul 1;14:19-30. doi: 10.2147/CE.S174169. PMID: 31308834; PMCID: PMC6615460.

Altman R, Bosch B, Brune K, Patrignani P, Young C. Advances in NSAID development: evolution of diclofenac products using pharmaceutical technology. Drugs. 2015 May;75(8):859-77. doi: 10.1007/s40265-015-0392-z. PMID: 25963327; PMCID: PMC4445819.

Amacher DE, Chalasani N. Drug-induced hepatic steatosis. Semin Liver Dis. 2014 May;34(2):205-14. doi: 10.1055/s-0034-1375960. Epub 2014 May 31. PMID: 24879984.

Anderson, W.H. (2020). Antidepressants. In: Levine, B.S., KERRIGAN, S. (eds) Principles of Forensic Toxicology. Springer, Cham. https://doi.org/10.1007/978-3-030-42917-1_27

Aninat C, Piton A, Glaise D, Le Charpentier T, Langouët S, Morel F, Guguen-Guillouzo C, Guillouzo A. Expression of cytochromes P450, conjugating enzymes and nuclear receptors in human hepatoma HepaRG cells. Drug Metab Dispos. 2006 Jan;34(1):75-83. doi: 10.1124/dmd.105.006759. Epub 2005 Oct 4. PMID: 16204462.

Anthérieu S, Chesné C, Li R, Camus S, Lahoz A, Picazo L, Turpeinen M, Tolonen A, Uusitalo J, Guguen-Guillouzo C, Guillouzo A. Stable expression, activity, and inducibility of cytochromes P450 in differentiated HepaRG cells. Drug Metab Dispos. 2010 Mar;38(3):516-25. doi: 10.1124/dmd.109.030197. Epub 2009 Dec 17. PMID: 20019244.

Antoni D, Burckel H, Josset E, Noel G. Three-dimensional cell culture: a breakthrough in vivo. Int J Mol Sci. 2015 Mar 11;16(3):5517-27. doi: 10.3390/ijms16035517. PMID: 25768338; PMCID: PMC4394490.

Aranda-Michel J, Koehler A, Bejarano PA, Poulos JE, Luxon BA, Khan CM, Ee LC, Balistreri WF, Weber FL Jr. Nefazodone-induced liver failure: report of three cases. Ann Intern Med. 1999 Feb 16;130(4 Pt 1):285-8. doi: 10.7326/0003-4819-130-4-199902160-00013. PMID: 10068386.

Argyriou, A.A., Cavaletti, G., Bruna, J. et al. Bortezomib-induced peripheral neurotoxicity: an update. Arch Toxicol 88, 1669–1679 (2014). https://doi.org/10.1007/s00204-014-1316-5

Aronov AM. (2005) Predictive in silico modeling for hERG channel blockers., Drug Discovery Today, 10 , 149-155 DOI: 10.1016/S1359-6446(04)03278-7

Asadpour E, Sadeghnia H. Comparative bioavailability study of oral formulations of imipramine tablets in healthy volunteers. European Journal of Hospital Pharmacy 2012;19:188-189.

Asai T, Adachi N, Moriya T, Oki H, Maru T, Kawasaki M, Suzuki K, Chen S, Ishii R, Yonemori K, Igaki S, Yasuda S, Ogasawara S, Senda T, Murata T. Cryo-EM Structure of K^+-Bound hERG Channel Complexed with the Blocker Astemizole. Structure. 2021 Mar 4;29(3):203-212.e4. doi: 10.1016/j.str.2020.12.007. Epub 2021 Jan 14. PMID: 33450182.

Ascenzi P, Fasano M. Serum heme-albumin: an allosteric protein. IUBMB Life. 2009 Dec;61(12):1118-22. doi: 10.1002/iub.263. PMID: 19946891.

Ashby J, Tennant RW. Chemical structure, Salmonella mutagenicity and extent of carcinogenicity as indicators of genotoxic carcinogenesis among 222 chemicals tested in rodents by the U.S. NCI/NTP. Mutat Res. 1988 Jan;204(1):17-115. doi: 10.1016/0165-1218(88)90114-0. PMID: 3277047.

Ashworth L. Is my antihistamine safe? Home Care Provid. 1997 Jun;2(3):117-20. doi: 10.1016/s1084-628x(97)90134-9. PMID: 9274181.

Attarwala H. TGN1412: From Discovery to Disaster. J Young Pharm. 2010 Jul;2(3):332-6. doi: 10.4103/0975-1483.66810. PMID: 21042496; PMCID: PMC2964774.

Averbukh LD, Turshudzhyan A, Wu DC, Wu GY. Statin-induced Liver Injury Patterns: A Clinical Review. J Clin Transl Hepatol. 2022 Jun 28;10(3):543-552. doi: 10.14218/JCTH.2021.00271. Epub 2022 Jan 10. PMID: 35836753; PMCID: PMC9240239.

Ayla S, Seckin I, Tanriverdi G, Cengiz M, Eser M, Soner BC, Oktem G. Doxorubicin induced nephrotoxicity: protective effect of nicotinamide. Int J Cell Biol. 2011;2011:390238. doi: 10.1155/2011/390238. Epub 2011 Jun 16. PMID: 21789041; PMCID: PMC3140777.

Azizgolshani H, Coppeta JR, Vedula EM, Marr EE, Cain BP, Luu RJ, Lech MP, Kann SH, Mulhern TJ, Tandon V, Tan K, Haroutunian NJ, Keegan P, Rogers M, Gard AL, Baldwin KB, de Souza JC, Hoefler BC, Bale SS, Kratchman LB, Zorn A, Patterson A, Kim ES, Petrie TA, Wiellette EL, Williams C, Isenberg BC, Charest JL. High-throughput organ-on-chip platform with integrated programmable fluid flow and real-time sensing for complex tissue models in drug development workflows. Lab Chip. 2021 Apr 20;21(8):1454-1474. doi: 10.1039/d1lc00067e. PMID: 33881130.

Babai S, Auclert L, Le-Louët H. Safety data and withdrawal of hepatotoxic drugs. Therapie. 2021 Nov-Dec;76(6):715-723. doi: 10.1016/j.therap.2018.02.004. Epub 2018 Feb 21. PMID: 29609830.

Babatin M, Lee SS, Pollak PT. Amiodarone hepatotoxicity. Curr Vasc Pharmacol. 2008 Jul;6(3):228-36. doi: 10.2174/157016108784912019. PMID: 18673162.

Badrinath M, John S. Isoniazid Toxicity. [Updated 2022 Jun 27]. In: StatPearls [Internet]. Treasure Island (FL): StatPearls Publishing; 2024 Jan-.

Badrinath M, John S. Isoniazid Toxicity. [Updated 2022 Jun 27]. In: StatPearls [Internet]. Treasure Island (FL): StatPearls Publishing; 2024 Jan-. Available from: https://www.ncbi.nlm.nih.gov/books/NBK531488/

Bae, M. A., Rhee, H., and Song, B. J. (2003) Troglitazone but not rosiglitazone induces G1 cell cycle arrest and apoptosis in human and rat hepatoma cell lines. Toxicol. Lett. 139, 67-75.

Bailey MJ and Dickinson RG. (2003) Acyl glucuronide reactivity in perspective: biological consequences., Chemico-Biological Interactions, 145 , 117-137 DOI: 10.1016/S0009-2797(03)00020-6

Baillie, T. A. (2020). Drug–protein adducts: past, present, and future. Medicinal Chemistry Research, 29(7), 1093-1104.

Baillie TA. Metabolism and toxicity of drugs. Two decades of progress in industrial drug metabolism. Chem Res Toxicol. 2008 Jan;21(1):129-37. doi: 10.1021/tx7002273. Epub 2007 Dec 4. PMID: 18052111.

Bajusz D, Rácz A, Héberger K (2017) 3.14—chemical data formats, fingerprints, and other molecular descriptions for database analysis and searching. In: Chackalamannil S, Rotella D, Ward SE (eds) Comprehensive medicinal chemistry III. Elsevier, Oxford, pp 329–378

Bamgbola O. Review of vancomycin-induced renal toxicity: an update. Ther Adv Endocrinol Metab. 2016 Jun;7(3):136-47. doi: 10.1177/2042018816638223. Epub 2016 Mar 30. PMID: 27293542; PMCID: PMC4892398.

Bang S, Jeong S, Choi N, Kim HN. Brain-on-a-chip: A history of development and future perspective. Biomicrofluidics. 2019 Oct 8;13(5):051301. doi: 10.1063/1.5120555. PMID: 31616534; PMCID: PMC6783295.

Barbhaiya RH, Marathe PH, Greene DS, Mayol RF, Shukla UA, Gammans RR, Pittman KA, Robinson D. Safety, tolerance, and preliminary pharmacokinetics of nefazodone after administration of single and multiple oral doses to healthy adult male volunteers: a double-blind, phase I study. J Clin Pharmacol. 1995 Oct;35(10):974-84. doi: 10.1002/j.1552-4604.1995.tb04013.x. PMID: 8568015.

Barceló-Vidal J, Rodríguez-García E, Grau S. Extremely high levels of vancomycin can cause severe renal toxicity. Infect Drug Resist. 2018 Jul 30;11:1027-1030. doi: 10.2147/IDR.S171669. PMID: 30104890; PMCID: PMC6071627

Barlow AD, Nicholson ML, Herbert TP. Evidence for rapamycin toxicity in pancreatic β-cells and a review of the underlying molecular mechanisms. Diabetes. 2013 Aug;62(8):2674-82. doi: 10.2337/db13-0106. PMID: 23881200; PMCID: PMC3717855.

Barpe DR, Rosa DD, Froehlich PE. Pharmacokinetic evaluation of doxorubicin plasma levels in normal and overweight patients with breast cancer and simulation of dose adjustment by different indexes of body mass. Eur J Pharm Sci. 2010 Nov 20;41(3-4):458-63. doi: 10.1016/j.ejps.2010.07.015. Epub 2010 Aug 3. PMID: 20688160.

Barrett B, Bauer AJ. The effects of amiodarone on thyroid function in pediatric and adolescent patients. Curr Opin Pediatr. 2021 Aug 1;33(4):436-441. doi: 10.1097/MOP.0000000000001040. PMID: 34117173.

Bataller R, Brenner DA. Liver fibrosis. J Clin Invest. 2005 Feb;115(2):209-18. doi: 10.1172/JCI24282. Erratum in: J Clin Invest. 2005 Apr;115(4):1100. PMID: 15690074; PMCID: PMC546435.

Batzlaff C, Koroscil M. Nitrofurantoin-Induced Pulmonary Toxicity: Always Review the Medication List. Cureus. 2020 Aug 17;12(8):e9807. doi: 10.7759/cureus.9807. PMID: 32953319; PMCID: PMC7494418.

Baust JM, Campbell LH, Harbell JW. Best practices for cryopreserving, thawing, recovering, and assessing cells. In Vitro Cell Dev Biol Anim. 2017 Dec;53(10):855-871. doi: 10.1007/s11626-017-0201-y. Epub 2017 Nov 2. PMID: 29098516.

Beard J; Australian Rural Health Research Collaboration. DDT and human health. Sci Total Environ. 2006 Feb 15;355(1-3):78-89.

Beers RF Jr, Sizer IW. A spectrophotometric method for measuring the breakdown of hydrogen peroxide by catalase. J Biol Chem. 1952 Mar;195(1):133-40. PMID: 14938361.

Beilmann M, Boonen H, Czich A, Dear G, Hewitt P, Mow T, Newham P, Oinonen T, Pognan F, Roth A, Valentin JP, Van Goethem F, Weaver RJ, Birk B, Boyer S, Caloni F, Chen AE, Corvi R, Cronin MTD, Daneshian M, Ewart LC, Fitzgerald RE, Hamilton GA, Hartung T, Kangas JD, Kramer NI, Leist M, Marx U, Polak S, Rovida C, Testai E, Van der Water B, Vulto P, Steger-Hartmann T. Optimizing drug discovery by Investigative Toxicology: Current and future trends. ALTEX. 2019;36(2):289-313. doi: 10.14573/altex.1808181. Epub 2018 Dec 20. PMID: 30570669.

Bell CC, Dankers ACA, Lauschke VM, Sison-Young R, Jenkins R, Rowe C, Goldring CE, Park K, Regan SL, Walker T, Schofield C, Baze A, Foster AJ, Williams DP, van de Ven AWM, Jacobs F, Houdt JV, Lähteenmäki T, Snoeys J, Juhila S, Richert L, Ingelman-Sundberg M. Comparison of Hepatic 2D Sandwich Cultures and 3D Spheroids for Long-term Toxicity

Applications: A Multicenter Study. Toxicol Sci. 2018 Apr 1;162(2):655-666. doi: 10.1093/toxsci/kfx289. PMID: 29329425; PMCID: PMC5888952.

Bell, C. C., Hendriks, D. F., Moro, S. M., Ellis, E., Walsh, J., Renblom, A., Puigvert, L. F., Dankers, A. C., Jacobs, F., Jan Snoeys, J., et al. (2016). Characterization of primary human hepatocyte spheroids as a model system for drug-induced liver injury, liver function and disease. Sci. Rep. 6, 25187. https://doi.org/10.1038/srep25187

Beraldo DO, Melo JF, Bonfim AV, Teixeira AA, Teixeira RA, Duarte AL. Acute cholestatic hepatitis caused by amoxicillin/clavulanate. World J Gastroenterol. 2013 Dec 14;19(46):8789-92. doi: 10.3748/wjg.v19.i46.8789. PMID: 24379601; PMCID: PMC3870529.

Berson, A., De Beco, V., Lette´ron, P., Robin, M. A., Moreau, C., El Kahwaji, J., Verthier, N., Feldmann, G., Fromenty, B., and Pessayre, D. (1998). Steatohepatitis-inducing drugs cause mitochondrial dysfunction and lipid peroxidation in rat hepatocytes. Gastroenterology 114, 764–774

Bi YA, Kazolias D, Duignan DB (2006) Use of cryopreserved human hepatocytes in sandwich culture to measure hepatobiliary transport. Drug Metab Dispos 34:1658–1665

Białkowska K, Komorowski P, Bryszewska M, Miłowska K. Spheroids as a Type of Three-Dimensional Cell Cultures-Examples of Methods of Preparation and the Most Important Application. Int J Mol Sci. 2020 Aug 28;21(17):6225. doi: 10.3390/ijms21176225. PMID: 32872135; PMCID: PMC7503223.

Bielajew BJ, Hu JC, Athanasiou KA. Collagen: quantification, biomechanics, and role of minor subtypes in cartilage. Nat Rev Mater. 2020 Oct;5(10):730-747. doi: 10.1038/s41578-020-0213-1. Epub 2020 Jul 20. PMID: 33996147; PMCID: PMC8114887.

Bircsak KM, DeBiasio R, Miedel M, Alsebahi A, Reddinger R, Saleh A, Shun T, Vernetti LA, Gough A. A 3D microfluidic liver model for high throughput compound toxicity screening in the OrganoPlate®. Toxicology. 2021 Feb 28;450:152667. doi: 10.1016/j.tox.2020.152667. Epub 2021 Jan 6. PMID: 33359578.

Bishop RO, Gaudry PL. Prolonged Q-T interval following astemizole overdose. Arch Emerg Med. 1989 Mar;6(1):63-5. doi: 10.1136/emj.6.1.63. PMID: 2565725; PMCID: PMC1285561.

Björnsson ES, Bergmann OM, Björnsson HK, Kvaran RB, Olafsson S. Incidence, presentation, and outcomes in patients with drug-induced liver injury in the general population of Iceland. Gastroenterology. 2013 Jun;144(7):1419-25, 1425.e1-3; quiz e19-20. doi: 10.1053/j.gastro.2013.02.006. Epub 2013 Feb 16. PMID: 23419359.

Björnsson ES. Drug-induced liver injury: an overview over the most critical compounds. Arch Toxicol. 2015 Mar;89(3):327-34. doi: 10.1007/s00204-015-1456-2. Epub 2015 Jan 25. PMID: 25618544.

Björnsson ES. Hepatotoxicity of statins and other lipid-lowering agents. Liver Int. 2017 Feb;37(2):173-178. doi: 10.1111/liv.13308. Epub 2016 Nov 27. PMID: 27860156.

Blagosklonny MV. Cancer prevention with rapamycin. Oncotarget. 2023 Apr 14;14:342-350. doi: 10.18632/oncotarget.28410. PMID: 37057884; PMCID: PMC10103596.

Blunston MA, Yonovitz A, Woodahl EL, Smolensky MH. Gentamicin-induced ototoxicity and nephrotoxicity vary with circadian time of treatment and entail separate mechanisms. Chronobiol Int. 2015;32(9):1223-32. doi: 10.3109/07420528.2015.1082483. Epub 2015 Oct 27. PMID: 26506922; PMCID: PMC5013539.

Boelsterli UA, Lee KK. Mechanisms of isoniazid-induced idiosyncratic liver injury: emerging role of mitochondrial stress. J Gastroenterol Hepatol. 2014 Apr;29(4):678-87. doi: 10.1111/jgh.12516. PMID: 24783247.

Boelsterli UA. Diclofenac-induced liver injury: a paradigm of idiosyncratic drug toxicity. Toxicol Appl Pharmacol. 2003 Nov 1;192(3):307-22. doi: 10.1016/s0041-008x(03)00368-5. PMID: 14575648.

Bolleddula J, Gopalakrishnan S, Hu P, Dong J, Venkatakrishnan K. Alternatives to rifampicin: A review and perspectives on the choice of strong CYP3A inducers for clinical drug-drug interaction studies. Clin Transl Sci. 2022 Sep;15(9):2075-2095. doi: 10.1111/cts.13357. Epub 2022 Jul 25. PMID: 35722783; PMCID: PMC9468573.

Bondesson I, Ekwall B, Hellberg S, Romert L, Stenberg K, Walum E. MEIC--a new international multicenter project to evaluate the relevance to human toxicity of in vitro cytotoxicity tests. Cell Biol Toxicol. 1989 Nov;5(3):331-47. doi: 10.1007/BF01795360. PMID: 2688844.

Bort R, Ponsoda X, Jover R, Gómez-Lechón MJ, Castell JV. Diclofenac toxicity to hepatocytes: a role for drug metabolism in cell toxicity. J Pharmacol Exp Ther. 1999 Jan;288(1):65-72. PMID: 9862754.

Bouwmeester MC, Tao Y, Proença S, van Steenbeek FG, Samsom RA, Nijmeijer SM, Sinnige T, van der Laan LJW, Legler J, Schneeberger K, Kramer NI, Spee B. Drug Metabolism of Hepatocyte-like Organoids and Their Applicability in In Vitro Toxicity Testing. Molecules. 2023 Jan 7;28(2):621. doi: 10.3390/molecules28020621. PMID: 36677681; PMCID: PMC9867526.

Bowsher RR, Compton JA, Kirkwood JA, Place GD, Jones CD, Mabry TE, Hyslop DL, Hatcher BL, DeSante KA. Sensitive and specific radioimmunoassay for fialuridine: initial assessment of pharmacokinetics after single oral doses to healthy volunteers. Antimicrob Agents Chemother. 1994 Sep;38(9):2134-42. doi: 10.1128/AAC.38.9.2134. PMID: 7811032; PMCID: PMC284697.

Brandt C, McFie PJ, Stone SJ. Biochemical characterization of human acyl coenzyme A: 2-monoacylglycerol acyltransferase-3 (MGAT3). Biochem Biophys Res Commun. 2016 Jul 1;475(3):264-70. doi: 10.1016/j.bbrc.2016.05.071. Epub 2016 May 13. PMID: 27184406.

Brennan PN, Cartlidge P, Manship T, Dillon JF. Guideline review: EASL clinical practice guidelines: drug-induced liver injury (DILI). Frontline Gastroenterol. 2021 Jul 29;13(4):332-336. doi: 10.1136/flgastro-2021-101886. PMID: 35722609; PMCID: PMC9186030.

Brewer GJ, Cotman CW. Survival and growth of hippocampal neurons in defined medium at low density: advantages of a sandwich culture technique or low oxygen. Brain Res 494: 65–74, 1989. doi: 10.1016/0006-8993(89)90144-3.

Brogden RN, Heel RC, Pakes GE, Speight TM, Avery GS. Diclofenac sodium: a review of its pharmacological properties and therapeutic use in rheumatic diseases and pain of varying origin. Drugs. 1980 Jul;20(1):24-48. doi: 10.2165/00003495-198020010-00002. PMID: 6772422.

Brook CG, Jarvis SN, Newman CG. Linear growth of children with limb deformities following exposure to thalidomide in utero. Acta Paediatr Scand. 1977 Nov;66(6):673-5. doi: 10.1111/j.1651-2227.1977.tb07969.x. PMID: 920161.

Buggey J, Kappus M, Lagoo AS, Brady CW. Amiodarone-Induced Liver Injury and Cirrhosis. ACG Case Rep J. 2015 Jan 16;2(2):116-8. doi: 10.14309/crj.2015.23. PMID: 26157932; PMCID: PMC4435372.

Buhaescu I, Izzedine H, Covic A. Sirolimus--challenging current perspectives. Ther Drug Monit. 2006 Oct;28(5):577-84. doi: 10.1097/01.ftd.0000245377.93401.39. PMID: 17038868.

Bunchorntavakul C, Reddy KR. Acetaminophen-related hepatotoxicity. Clin Liver Dis. 2013 Nov;17(4):587-607, viii. doi: 10.1016/j.cld.2013.07.005. Epub 2013 Sep 4. PMID: 24099020.

Burgi H, Wimpfheimer C, Burger A, Zaunbauer W, Rosler H and Lemarchand-Beraud T. (1976) Changes of circulating thyroxine, triiodothyronine and reverse triiodothyronine after radiographic contrast agents., Journal of Clinical Endocrinology and Metabolism, 43 , 1203-1210

Calderon-Martinez E, Landazuri-Navas S, Kaya G, Cinicola J. Chronic Oral Amiodarone as a Cause of Acute Liver Failure. J Med Cases. 2023 Feb;14(2):59-63. doi: 10.14740/jmc4044. Epub 2023 Feb 25. PMID: 36896369; PMCID: PMC9990705.

Cali JJ, Niles A, Valley MP, O'Brien MA, Riss TL, Shultz J. Bioluminescent assays for ADMET. Expert Opin Drug Metab Toxicol. 2008 Jan;4(1):103-20. doi: 10.1517/17425255.4.1.103. PMID: 18370862.

Capel I. D., French M. R., Millburn P., Smith R. L., Williams R. T. (1972). The fate of (14C)phenol in various species. Xenobiotica 2, 25–35.

Capen CC. (1997) Mechanistic data and risk assessment of selected toxic end points of the thyroid gland., Toxicologic Pathology, 25, 39-48. DOI: 10.1177/019262339702500109

Cardoso BD, Castanheira EMS, Lanceros-Méndez S, Cardoso VF. Recent Advances on Cell Culture Platforms for In Vitro Drug Screening and Cell Therapies: From Conventional to Microfluidic Strategies. Adv Healthc Mater. 2023 Jul;12(18):e2202936. doi: 10.1002/adhm.202202936. Epub 2023 Mar 20. PMID: 36898671.

Carter BL, Woodhead JC, Cole KJ, Milavetz G. Gastrointestinal side effects with erythromycin preparations. Drug Intell Clin Pharm. 1987 Sep;21(9):734-8. doi: 10.1177/106002808702100914. PMID: 3498618.

Casale F, Canaparo R, Serpe L, Muntoni E, Pepa CD, Costa M, Mairone L, Zara GP, Fornari G, Eandi M. Plasma concentrations of 5-fluorouracil and its metabolites in colon cancer patients. Pharmacol Res. 2004 Aug;50(2):173-9. doi: 10.1016/j.phrs.2004.01.006. PMID: 15177306.

Cavalli A, Poluzzi E, De Ponti F and Recanatini M. (2002) Toward a pharmacophore for drugs inducing the long QT syndrome: insights from a CoMFA study of HERG K+ channel blockers., Journal of Medicinal Chemistry, 45 , 3844-3853 DOI: 10.1021/jm0208875

Center for Drug Evaluation and Research, application number: 022450orig1s000 Clinical Pharmacology and Biopharmaceutics review, 2009.

Chalasani N, Bonkovsky HL, Fontana R, Lee W, Stolz A, Talwalkar J, Reddy KR, Watkins PB, Navarro V, Barnhart H, Gu J, Serrano J; United States Drug Induced Liver Injury Network. Features and Outcomes of 899 Patients With Drug-Induced Liver Injury: The DILIN Prospective Study. Gastroenterology. 2015 Jun;148(7):1340-52.e7. doi: 10.1053/j.gastro.2015.03.006. Epub 2015 Mar 6. PMID: 25754159; PMCID: PMC4446235.

Chalasani N, Bonkovsky HL, Stine JG, Gu J, Barnhart H, Jacobsen E, Björnsson E, Fontana RJ, Kleiner DE, Hoofnagle JH; Drug-Induced Liver Injury Network (DILIN) Study Investigators. Clinical characteristics of antiepileptic-induced liver injury in patients from the DILIN prospective study. J Hepatol. 2022 Apr;76(4):832-840. doi: 10.1016/j.jhep.2021.12.013. Epub 2021 Dec 22. PMID: 34953957; PMCID: PMC8944173.

Chang CC, Petrelli M, Tomashefski JF Jr and McCullough AJ. (1999) Severe intrahepatic cholestasis caused by amiodarone toxicity after withdrawal of the drug: a case report and review of the literature., Archives of Pathology and Laboratory Medicine, 123, 251-256

Charles O, Onakpoya I, Benipal S, Woods H, Bali A, Aronson JK, Heneghan C, Persaud N. Withdrawn medicines included in the essential medicines lists of 136 countries. PLoS One. 2019 Dec 2;14(12):e0225429. doi: 10.1371/journal.pone.0225429. PMID: 31791048; PMCID: PMC6887519.

Charwat V, Egger D. (2018). The Third Dimension in Cell Culture: From 2D to 3D Culture Formats. In: Kasper, C., Charwat, V., Lavrentieva, A. (eds) Cell Culture Technology. Learning Materials in Biosciences. Springer, Cham. https://doi.org/10.1007/978-3-319-74854-2_5

Chatterjee K, Zhang J, Honbo N, Karliner JS. Doxorubicin cardiomyopathy. Cardiology. 2010;115(2):155-62. doi: 10.1159/000265166. Epub 2009 Dec 11. PMID: 20016174; PMCID: PMC2848530.

Chatterjee K, Zhang J, Honbo N, Karliner JS. Doxorubicin cardiomyopathy. Cardiology. 2010;115(2):155-62. doi: 10.1159/000265166. Epub 2009 Dec 11. PMID: 20016174; PMCID: PMC2848530.

Chen S, Wu Q, Li X, Li D, Mei N, Ning B, Puig M, Ren Z, Tolleson WH, Guo L. Characterization of cytochrome P450s (CYP)-overexpressing HepG2 cells for assessing drug and chemical-induced liver toxicity. J Environ Sci Health C Toxicol Carcinog. 2021;39(1):68-86. doi: 10.1080/26896583.2021.1880242. PMID: 33576714; PMCID: PMC7931144.

Chen SS, Fitzgerald W, Zimmerberg J, Kleinman HK, Margolis L. Cell-cell and cell-extracellular matrix interactions regulate embryonic stem cell differentiation. Stem Cells. 2007 Mar;25(3):553-61. doi: 10.1634/stemcells.2006-0419. PMID: 17332514.

Chen, X., Zhong, Z., Xu, Z., Chen, L., & Wang, Y. (2010). 2′,7′-Dichlorodihydrofluorescein as a fluorescent probe for reactive oxygen species measurement: Forty years of application and controversy. Free Radical Research, 44(6), 587–604. https://doi.org/10.3109/10715761003709802

Chesné C, Guyomard C, Fautrel A, Poullain MG, Frémond B, De Jong H, Guillouzo A. Viability and function in primary culture of adult hepatocytes from various animal species and human beings after cryopreservation. Hepatology. 1993 Aug;18(2):406-14. doi: 10.1002/hep.1840180227. PMID: 8340070.

Cheung CY, van der Heijden J, Hoogtanders K, Christiaans M, Liu YL, Chan YH, Choi KS, van de Plas A, Shek CC, Chau KF, Li CS, van Hooff J, Stolk L. Dried blood spot measurement: application in tacrolimus monitoring using limited sampling strategy and abbreviated AUC estimation. Transpl Int. 2008 Feb;21(2):140-5. doi: 10.1111/j.1432-2277.2007.00584.x. Epub 2007 Oct 17. PMID: 17944802.

Chiruvella V, Annamaraju P, Guddati AK. Management of nephrotoxicity of chemotherapy and targeted agents: 2020. Am J Cancer Res. 2020 Dec 1;10(12):4151-4164. PMID: 33414992; PMCID: PMC7783750.

Chistiakov DA, Orekhov AN, Bobryshev YV. Effects of shear stress on endothelial cells: go with the flow. Acta Physiol (Oxf). 2017 Feb;219(2):382-408. doi: 10.1111/apha.12725. Epub 2016 Jun 19. PMID: 27246807.

Choi S. Nefazodone (Serzone) withdrawn because of hepatotoxicity. CMAJ. 2003 Nov 25;169(11):1187

Chu L, Robinson DK. Industrial choices for protein production by large-scale cell culture. Curr Opin Biotechnol. 2001 Apr;12(2):180-7. doi: 10.1016/s0958-1669(00)00197-x. PMID: 11287235.

Clark M, Steger-Hartmann T. A big data approach to the concordance of the toxicity of pharmaceuticals in animals and humans. Regul Toxicol Pharmacol. 2018 Jul;96:94-105. doi: 10.1016/j.yrtph.2018.04.018. Epub 2018 May 3. PMID: 29730448.

Clarke L, Waxman DJ. Oxidative metabolism of cyclophosphamide: identification of the hepatic monooxygenase catalysts of drug activation. Cancer Res. 1989 May 1;49(9):2344-50. PMID: 2706622.

Clay KD, Hanson JS, Pope SD, Rissmiller RW, Purdum PP 3rd, Banks PM. Brief communication: severe hepatotoxicity of telithromycin: three case reports and literature review. Ann Intern Med. 2006 Mar 21;144(6):415-20. doi: 10.7326/0003-4819-144-6-200503210-00121. Epub 2006 Feb 15. PMID: 16481451.

Clemedson C, Andersson M, Aoki Y, et al. MEIC Evaluation of Acute Systemic Toxicity: Part IV In Vitro Results from 67 Toxicity Assays Used to Test Reference Chemicals 31–50 and a Comparative Cytotoxicity Analysis. Alternatives to Laboratory Animals. 1998;26(1_suppl):131-183. doi:10.1177/026119299802601s03

Cobbina E, Akhlaghi F. Non-alcoholic fatty liver disease (NAFLD) - pathogenesis, classification, and effect on drug metabolizing enzymes and transporters. Drug Metab Rev. 2017 May;49(2):197-211. doi: 10.1080/03602532.2017.1293683. Epub 2017 Mar 17. PMID: 28303724; PMCID: PMC5576152.

Code of Federal Regulations Title 21 (21CFR) 201.57 [https://www.accessdata.fda.gov/scripts/cdrh/cfdocs/cfCFR/CFRSearch.cfm?fr=201.57]

Collazos J, Martínez E, Mayo J, Ibarra S. Pulmonary reactions during treatment with amphotericin B: review of published cases and guidelines for management. Clin Infect Dis. 2001 Oct 1;33(7):E75-82. doi: 10.1086/322668. Epub 2001 Aug 22. PMID: 11528589.

Comis RL. Bleomycin pulmonary toxicity: current status and future directions. Semin Oncol 1992; 19 (Suppl 5): 64–70.

Cook, D., Brown, D., Alexander, R. et al. (2014). Lessons learned from the fate of AstraZeneca's drug pipeline: A five-dimensional framework. Nat Rev Drug Discov 13, 419-431. doi:10.1038/ nrd4309

Cowling T, Farrah K. Fluoroquinolones for the Treatment of Other Respiratory Tract Infections: A Review of Clinical Effectiveness, Cost-Effectiveness, and Guidelines [Internet]. Ottawa (ON): Canadian Agency for Drugs and Technologies in Health; 2019 May 31. PMID: 31433606.

Crumb W and Cavero I. (1999) QT interval prolongation by non-cardiovascular drugs: issues and solutions for novel drug development., Pharmaceutical Science and Technology Today, 2 , 270-280 DOI: 10.1016/S1461-5347(99)00172-8

Cukierman E, Pankov R, Stevens DR, Yamada KM. Taking cell-matrix adhesions to the third dimension. Science. 2001 Nov 23;294(5547):1708-12. doi: 10.1126/science.1064829. PMID: 11721053.

Currie PF, Boon NA. Immunopathogenesis of HIV-related heart muscle disease: current perspectives. AIDS. 2003 Apr;17 Suppl 1:S21-8. doi: 10.1097/00002030-200304001-00004. PMID: 12870527.

Cuthbert R, Speirs AL. Thalidomide induced malformations--a radiological survey. Clin Radiol. 1963 Apr;14:163-9. doi: 10.1016/s0009-9260(63)80077-x. PMID: 14024392.

Czaja AJ. Drug-induced autoimmune-like hepatitis. Dig Dis Sci. 2011 Apr;56(4):958-76. doi: 10.1007/s10620-011-1611-4. Epub 2011 Feb 16. PMID: 21327704.

Daly AK, Day CP. Genetic association studies in drug-induced liver injury. Drug Metab Rev. 2012 Feb;44(1):116-26. doi: 10.3109/03602532.2011.605790. Epub 2011 Sep 14. PMID: 21913872.

Danan G, Benichou C. Causality assessment of adverse reactions to drugs—I. A novel method based on the conclusions of international consensus meetings: application to drug-induced liver injuries. J Clin Epidemiol 1993; 46: 1323–1330

Dargue R, Grant I, Nye LC, Nicholls A, Dare T, Stahl SH, Plumb RS, Lee K, Jalan R, Coen M, Wilson ID. (a). The analysis of acetaminophen (paracetamol) and seven metabolites in rat, pig and human plasma by U(H)PLC-MS. Bioanalysis. 2020 Apr;12(7):485-500. doi: 10.4155/bio-2020-0015. Epub 2020 Apr 28. PMID: 32343149.

Dargue R, Zia R, Lau C, Nicholls AW, Dare TO, Lee K, Jalan R, Coen M, Wilson ID. (b). Metabolism and Effects on Endogenous Metabolism of Paracetamol (Acetaminophen) in a Porcine Model of Liver Failure. Toxicol Sci. 2020 May 1;175(1):87-97. doi: 10.1093/toxsci/kfaa023. PMID: 32061126; PMCID: PMC7197950.

Davis R, Whittington R, Bryson HM (1997). "Nefazodone. A review of its pharmacology and clinical efficacy in the management of major depression". Drugs. 53 (4): 608–36. doi:10.2165/00003495-199753040-00006. PMID 9098663. S2CID 239077479.

Dawson, S., Stahl, S., Paul, N., Barber, J., and Kenna, J. G. (2012). In vitro inhibition of the bile salt export pump correlates with risk of cholestatic drug-induced liver injury in humans. Drug Metab. Dispos. 40, 130–138

De Hoyos-Vega JM, Hong HJ, Stybayeva G, Revzin A. Hepatocyte cultures: From collagen gel sandwiches to microfluidic devices with integrated biosensors. APL Bioeng. 2021 Oct 14;5(4):041504. doi: 10.1063/5.0058798. PMID: 34703968; PMCID: PMC8519630.

Deloitte Report 2023 the Unbearable cost of drug development: Deloitte repost shows 15% jump in R&D to $2.3 billions.

Deodhar M, Al Rihani SB, Arwood MJ, Darakjian L, Dow P, Turgeon J, Michaud V. Mechanisms of CYP450 Inhibition: Understanding Drug-Drug Interactions Due to Mechanism-Based Inhibition in Clinical Practice. Pharmaceutics. 2020 Sep 4;12(9):846. doi: 10.3390/pharmaceutics12090846. PMID: 32899642; PMCID: PMC7557591.

Deray G. Amphotericin B nephrotoxicity. J Antimicrob Chemother. 2002 Feb;49 Suppl 1:37-41. doi: 10.1093/jac/49.suppl_1.37. PMID: 11801579.

Deryke CA, Crawford AJ, Uddin N, Wallace MR. Colistin dosing and nephrotoxicity in a large community teaching hospital. Antimicrob Agents Chemother. 2010 Oct;54(10):4503-5. doi: 10.1128/AAC.01707-09. Epub 2010 Jul 26. PMID: 20660694; PMCID: PMC2944569.

Di Stasi SL, MacLeod TD, Winters JD, Binder-Macleod SA. Effects of statins on skeletal muscle: a perspective for physical therapists. Phys Ther. 2010 Oct;90(10):1530-42. doi: 10.2522/ptj.20090251. Epub 2010 Aug 5. PMID: 20688875; PMCID: PMC2949584.

Di Zeo-Sánchez DE, Segovia-Zafra A, Matilla-Cabello G, Pinazo-Bandera JM, Andrade RJ, Lucena MI, Villanueva-Paz M. Modeling drug-induced liver injury: current status and future prospects. Expert Opin Drug Metab Toxicol. 2022 Sep;18(9):555-573. doi: 10.1080/17425255.2022.2122810. Epub 2022 Sep 16. PMID: 36107152.

DiMasi JA, Grabowski HG, Hansen RW. Innovation in the pharmaceutical industry: New estimates of R&D costs. J Health Econ. 2016 May;47:20-33. doi: 10.1016/j.jhealeco.2016.01.012. Epub 2016 Feb 12. PMID: 26928437.

Dirven H, Vist GE, Bandhakavi S, Mehta J, Fitch SE, Pound P, Ram R, Kincaid B, Leenaars CHC, Chen M, Wright RA, Tsaioun K. Performance of preclinical models in predicting drug-induced liver injury in humans: a systematic review. Sci Rep. 2021 Mar 18;11(1):6403. doi: 10.1038/s41598-021-85708-2. PMID: 33737635; PMCID: PMC7973584.

Dobbin SJH, Petrie MC, Myles RC, Touyz RM, Lang NN. Cardiotoxic effects of angiogenesis inhibitors. Clin Sci (Lond). 2021 Jan 15;135(1):71-100. doi: 10.1042/CS20200305. PMID: 33404052; PMCID: PMC7812690.

Dockens RC, Greene DS, Barbhaiya RH. Assessment of pharmacokinetic and pharmacodynamic drug interactions between nefazodone and digoxin in healthy male volunteers. J Clin Pharmacol. 1996 Feb;36(2):160-7. doi: 10.1002/j.1552-4604.1996.tb04181.x. PMID: 8852392.

Donato MT, Gallego-Ferrer G, Tolosa L. In Vitro Models for Studying Chronic Drug-Induced Liver Injury. Int J Mol Sci. 2022 Sep 28;23(19):11428. doi: 10.3390/ijms231911428. PMID: 36232728; PMCID: PMC9569683.

Donato MT, Tolosa L, Gómez-Lechón MJ. Culture and Functional Characterization of Human Hepatoma HepG2 Cells. Methods Mol Biol. 2015; 1250:77-93. doi: 10.1007/978-1-4939-2074-7_5. PMID: 26272135.

Dowden H, Munro J. Trends in clinical success rates and therapeutic focus. Nat Rev Drug ‘Discov 2019;18:495e6

Drolet B, Yang T, Daleau P, Roden DM and Turgeon J. (2003) Risperidone prolongs cardiac repolarization by blocking the rapid component of the delayed rectifier potassium current., Journal of Cardiovascular Pharmacology, 41 , 934-937

Drusano GL. Pre-clinical in vitro infection models. Curr Opin Pharmacol. 2017 Oct;36:100-106. doi: 10.1016/j.coph.2017.09.011. Epub 2017 Oct 14. PMID: 29035729.

Dunn JC, Yarmush ML, Koebe HG, Tompkins RG. Hepatocyte function and extracellular matrix geometry: long-term culture in a sandwich configuration. FASEB J. 1989 Feb;3(2):174-7. doi: 10.1096/fasebj.3.2.2914628. Erratum in: FASEB J 1989 May;3(7):1873. PMID: 2914628.

Duval K, Grover H, Han LH, Mou Y, Pegoraro AF, Fredberg J, Chen Z. Modeling Physiological Events in 2D vs. 3D Cell Culture. Physiology (Bethesda). 2017 Jul;32(4):266-277. doi: 10.1152/physiol.00036.2016. PMID: 28615311; PMCID: PMC5545611.

Dykens JA, Jamieson JD, Marroquin LD, Nadanaciva S, Xu JJ, Dunn MC, Smith AR, Will Y. In vitro assessment of mitochondrial dysfunction and cytotoxicity of nefazodone, trazodone, and buspirone. Toxicol Sci. 2008 Jun;103(2):335-45. doi: 10.1093/toxsci/kfn056. Epub 2008 Mar 15. PMID: 18344530.

Edwards IR. Withdrawing drugs: nefazodone, the start of the latest saga. Lancet. 2003 Apr 12;361(9365):1240. doi: 10.1016/S0140-6736(03)13030-9. PMID: 12699949.

Efremov, Y.M., Zurina, I.M., Presniakova, V.S. et al. Mechanical properties of cell sheets and spheroids: the link between single cells and complex tissues. Biophys Rev 13, 541–561 (2021). https://doi.org/10.1007/s12551-021-00821-w

Eglen R, Reisine T. Primary cells and stem cells in drug discovery: emerging tools for high-throughput screening. Assay Drug Dev Technol. 2011 Apr;9(2):108-24. doi: 10.1089/adt.2010.0305. Epub 2010 Dec 27. PMID: 21186936.

Ehrentraut S, Rothenhäusler HB, Gerbes AL, Rau HG, Thiel M, Schirren CA, Kapfhammer HP. Akutes Leberversagen unter Nefazodon-Therapie? Ein Fallbericht [Acute liver failure in nefazodone therapy? A case report]. Nervenarzt. 2002 Jul;73(7):686-9. German. doi: 10.1007/s00115-002-1350-z. PMID: 12212533.

Einhorn LH, Williams SD, Loehrer PJ et al. Evaluation of optimal duration of chemotherapy in favorable-prognosis disseminated germ cell tumors: a Southeastern Cancer Study Group protocol. J Clin Oncol 1989; 7: 387–391.

Eisenbeis CF, Winn D, Poelman S, Polsky CV, Rubenstein JH, Olopade OI. A case of pulmonary toxicity associated with G-CSF and doxorubicin administration. Ann Hematol. 2001 Feb;80(2):121-3. doi: 10.1007/s002770000232. PMID: 11261324; PMCID: PMC7101872.

Ekins S, Crumb WJ, Sarazan RD, Wikel JH and Wrighton SA. (2002) Three-dimensional quantitative structure-activity relationship for inhibition of human ether-a-go-gorelated gene potassium channel., Journal of Pharmacology and Experimental Therapeutics, 301 , 427-434 DOI: 10.1124/jpet.301.2.427

Ekwall B, Gómez-Lechón MJ, Hellberg S, Bondesson I, Castell JV, Jover R, Högberg J, Ponsoda X, Romert L, Stenberg K, Walum E. Preliminary results from the Scandinavian multicentre evaluation of in vitro cytotoxicity (MEIC). Toxicol In Vitro. 1990;4(4-5):688-91. doi: 10.1016/0887-2333(90)90143-h. PMID: 20702257.

Ekwall B. Screening of toxic compounds in mammalian cell cultures. Ann N Y Acad Sci. 1983; 407:64-77. doi: 10.1111/j.1749-6632.1983.tb47814.x. PMID: 6349488.

Elaut G, Henkens T, Papeleu P, Snykers S, Vinken M, Vanhaecke T, Rogiers V. Molecular mechanisms underlying the dedifferentiation process of isolated hepatocytes and their cultures. Curr Drug Metab. 2006 Aug;7(6):629-60. doi: 10.2174/138920006778017759. PMID: 16918317.

Ellis D. Amphotericin B: spectrum and resistance. J Antimicrob Chemother. 2002 Feb;49 Suppl 1:7-10. doi: 10.1093/jac/49.suppl_1.7. PMID: 11801575.

Ellison C, Hewitt M, Przybylak K. In Silico Models for Hepatotoxicity. Methods Mol Biol. 2022;2425:355-392. doi: 10.1007/978-1-0716-1960-5_14. PMID: 35188639.

Elseviers MM and De Broe ME. (2008) Analgesics and 5-aminosalicylic acid., Clinical Nephrotoxins: Renal Injury from Drugs and Chemicals, 399-417

Elsherbiny NM, El-Sherbiny M. Thymoquinone attenuates Doxorubicin-induced nephrotoxicity in rats: Role of Nrf2 and NOX4. Chem Biol Interact. 2014 Nov 5;223:102-8. doi: 10.1016/j.cbi.2014.09.015. Epub 2014 Sep 28. PMID: 25268985.

Emoto C, Fukuda T, Cox S, Christians U, Vinks AA. Development of a Physiologically-Based Pharmacokinetic Model for Sirolimus: Predicting Bioavailability Based on Intestinal CYP3A Content. CPT Pharmacometrics Syst Pharmacol. 2013 Jul 24;2(7):e59. doi: 10.1038/psp.2013.33. PMID: 23884207; PMCID: PMC3731827.

Eriksson U, Seifert B, Schaffner A. Comparison of effects of amphotericin B deoxycholate infused over 4 or 24 hours: randomised controlled trial. BMJ. 2001 Mar 10;322(7286):579-82. doi: 10.1136/bmj.322.7286.579. PMID: 11238151; PMCID: PMC26549.

Esch MB, Mahler GJ, Stokol T, Shuler ML. Body-on-a-chip simulation with gastrointestinal tract and liver tissues suggests that ingested nanoparticles have the potential to cause liver injury. Lab Chip. 2014 Aug 21;14(16):3081-92. doi: 10.1039/c4lc00371c. PMID: 24970651; PMCID: PMC4144667.

Espina JA, Cordeiro MH, Milivojevic M, Pajić-Lijaković I, Barriga EH. Response of cells and tissues to shear stress. J Cell Sci. 2023 Sep 15;136(18):jcs260985. doi: 10.1242/jcs.260985. Epub 2023 Sep 25. PMID: 37747423; PMCID: PMC10560560.

Essrani R, Mehershahi S, Essrani RK, Ravi SJK, Bhura S, Sudhakaran A, Hossain M, Mehmood A. Amiodarone-Induced Acute Liver Injury. Case Rep Gastroenterol. 2020 Feb 20;14(1):87-90. doi: 10.1159/000506184. PMID: 32231507; PMCID: PMC7098330.

Eto K. Minamata disease. Neuropathology. 2000 Sep;20 Suppl:S14-9.

Ewart L, Apostolou A, Briggs SA, Carman CV, Chaff JT, Heng AR, Jadalannagari S, Janardhanan J, Jang KJ, Joshipura SR, Kadam MM, Kanellias M, Kujala VJ, Kulkarni G, Le CY, Lucchesi C, Manatakis DV, Maniar KK, Quinn ME, Ravan JS, Rizos AC, Sauld JFK, Sliz JD, Tien-Street W, Trinidad DR, Velez J, Wendell M, Irrechukwu O, Mahalingaiah PK, Ingber DE, Scannell JW, Levner D. Performance assessment and economic analysis of a human Liver-Chip for predictive toxicology. Commun Med (Lond). 2022 Dec 6;2(1):154. doi: 10.1038/s43856-022-00209-1. Erratum in: Commun Med (Lond). 2023 Jan 12;3(1):7. Erratum in: Commun Med (Lond). 2023 Feb 2;3(1):16. PMID: 36473994; PMCID: PMC9727064.

Fanali G, di Masi A, Trezza V, Marino M, Fasano M, Ascenzi P. Human serum albumin: from bench to bedside. Mol Aspects Med. 2012 Jun;33(3):209-90. doi: 10.1016/j.mam.2011.12.002. Epub 2011 Dec 30. PMID: 22230555.

Fang Y, Eglen RM. Three-Dimensional Cell Cultures in Drug Discovery and Development. SLAS Discov. 2017 Jun;22(5):456-472. doi: 10.1177/1087057117696795. Erratum in: SLAS Discov. 2021 Oct;26(9):NP1. PMID: 28520521; PMCID: PMC5448717.

Fayez R, Gupta V. Imipramine. [Updated 2023 May 22]. In: StatPearls [Internet]. Treasure Island (FL): StatPearls Publishing; 2024 Jan-. Available from: https://www.ncbi.nlm.nih.gov/books/NBK557656/

Fellström B. Cyclosporine nephrotoxicity. Transplant Proc. 2004 Mar;36(2 Suppl):220S-223S. doi: 10.1016/j.transproceed.2004.01.028. PMID: 15041341.

Feng S, Coward J, McCaffrey E, Coucher J, Kalokerinos P, O'Byrne K. Pembrolizumab-Induced Encephalopathy: A Review of Neurological Toxicities with Immune Checkpoint Inhibitors. J Thorac Oncol. 2017 Nov;12(11):1626-1635. doi: 10.1016/j.jtho.2017.08.007. Epub 2017 Aug 24. PMID: 28843363.

Feydy P and Bogomoletz WV. (1991) A case of hepatitis caused by simvastatin (French)., Gastroenterologie Clinique et Biologique, 15 , 94-95

Filippone EJ, Kraft WK, Farber JL. The Nephrotoxicity of Vancomycin. Clin Pharmacol Ther. 2017 Sep;102(3):459-469. doi: 10.1002/cpt.726. Epub 2017 Jun 5. PMID: 28474732; PMCID: PMC5579760.

Fisher K, Vuppalanchi R, Saxena R. Drug-Induced Liver Injury. Arch Pathol Lab Med. 2015 Jul;139(7):876-87. doi: 10.5858/arpa.2014-0214-RA. PMID: 26125428.

Fitzgerald KA, Malhotra M, Curtin CM, O' Brien FJ, O' Driscoll CM. Life in 3D is never flat: 3D models to optimise drug delivery. J Control Release. 2015 Oct 10;215:39-54. doi: 10.1016/j.jconrel.2015.07.020. Epub 2015 Jul 26. PMID: 26220617.

Fogel DB. Factors associated with clinical trials that fail and opportunities for improving the likelihood of success: A review. Contemp Clin Trials Commun. 2018 Aug 7;11:156-164. doi: 10.1016/j.conctc.2018.08.001. PMID: 30112460; PMCID: PMC6092479.

Foglietta F, Canaparo R, Muccioli G, Terreno E, Serpe L. Methodological aspects and pharmacological applications of three-dimensional cancer cell cultures and organoids. Life Sci. 2020 Aug 1;254:117784. doi: 10.1016/j.lfs.2020.117784. Epub 2020 May 19. PMID: 32416169.

Fois CAM, Schindeler A, Valtchev P, Dehghani F. Dynamic flow and shear stress as key parameters for intestinal cells morphology and polarization in an organ-on-a-chip model. Biomed Microdevices. 2021 Oct 16;23(4):55. doi: 10.1007/s10544-021-00591-y. PMID: 34655329; PMCID: PMC8520520.

Fontana RJ. Pathogenesis of idiosyncratic drug-induced liver injury and clinical perspectives. Gastroenterology. 2014 Apr;146(4):914-28. doi: 10.1053/j.gastro.2013.12.032. Epub 2013 Dec 31. PMID: 24389305; PMCID: PMC4031195.

Forsgren A, Bredberg A, Riesbeck K. Effect of ciprofloxacin on human lymphocytes--laboratory studies. Scand J Infect Dis Suppl. 1989;60:39-45. PMID: 2667107.

Fowler, S., and Schnall, J. G. (2014). TOXNET: information on toxicology and environmental health. Am. J. Nurs. 114, 61–63. doi: 10.1097/01.NAJ.0000443783.75162.79

Fraczek J, Bolleyn J, Vanhaecke T, Rogiers V, Vinken M (2013) Primary hepatocyte cultures for pharmaco-toxicological studies: at the busy crossroad of various anti-dedifferentiation strategies

Frank E, Hall, M., Trigg, L., Holmes, G., and Witten, I. H. (2004). Data mining in bioinformatics using Weka. Bioinformatics 20, 2479–2481. doi: 10.1093/bioinformatics/bth261

Frantz C, Stewart KM, Weaver VM. The extracellular matrix at a glance. J Cell Sci. 2010 Dec 15;123(Pt 24):4195-200. doi: 10.1242/jcs.023820. PMID: 21123617; PMCID: PMC2995612.

Froehlich K, Haeger JD, Heger J, Pastuschek J, Photini SM, Yan Y, Lupp A, Pfarrer C, Mrowka R, Schleußner E, Markert UR, Schmidt A. Generation of Multicellular Breast Cancer Tumor Spheroids: Comparison of Different Protocols. J Mammary Gland Biol Neoplasia. 2016 Dec;21(3-4):89-98. doi: 10.1007/s10911-016-9359-2. Epub 2016 Aug 12. PMID: 27518775.

Fromenty B. Inhibition of Mitochondrial Fatty Acid Oxidation in Drug-Induced Hepatic Steatosis. Liver Res. 2019;3:157–169. doi: 10.1016/j.livres.2019.06.001.

Fromenty B., Fisch C., Labbe G., Degott C., Deschamps D., Berson A., Letteron P., Pessayre D. Amiodarone Inhibits the Mitochondrial Beta-Oxidation of Fatty Acids and Produces Microvesicular Steatosis of the Liver in Mice. J. Pharmacol. Exp. Ther. 1990;255:1371–1376.

Fromenty B., Pessayre D. Inhibition of Mitochondrial Beta-Oxidation as a Mechanism of Hepatotoxicity. Pharmacol. Ther. 1995;67:101–154. doi: 10.1016/0163-7258(95)00012-6.

Fuchs WS, Leary WP, van der Meer MJ, Gay S, Witschital K, von Nieciecki A. Pharmacokinetics and bioavailability of tamoxifen in postmenopausal healthy women. Arzneimittelforschung. 1996 Apr;46(4):418-22. PMID: 8740091.

Fuhr LM, Marok FZ, Hanke N, Selzer D, Lehr T. Pharmacokinetics of the CYP3A4 and CYP2B6 Inducer Carbamazepine and Its Drug-Drug Interaction Potential: A Physiologically Based Pharmacokinetic Modeling Approach. Pharmaceutics. 2021 Feb 17;13(2):270. doi: 10.3390/pharmaceutics13020270. PMID: 33671323; PMCID: PMC7922031.

Fulgencio J.P., Kohl C., Girard J., Pégorier J.P. Troglitazone Inhibits Fatty Acid Oxidation and Esterification, and Gluconeogenesis in Isolated Hepatocytes from Starved Rats. Diabetes. 1996;45:1556–1562. doi: 10.2337/diab.45.11.1556.

Fung M, Thornton A, Mybeck K, Wu J, Hornbuckle K, Muniz E. Evaluation of the characteristics of safety withdrawal of prescription drugs from worldwide pharmaceutical markets −1960 to 1999. Drug Inf J. 2001; 35:293–317.

Funk, C., Pantze, M., Jehle, L., Ponelle, C., Scheuermann, G., Lazendic, M., and Gasser, R. (2001a). Troglitazone-induced intrahepatic cholestasis by an interference with the hepatobiliary export of bile acids in male and female rats. Correlation with the gender difference in troglitazone sulfate formation and the inhibition of the canalicular bile salt export pump (Bsep) by troglitazone and troglitazone sulfate. Toxicology 167, 83–98

Gai Z, Samodelov SL, Kullak-Ublick GA, Visentin M. Molecular Mechanisms of Colistin-Induced Nephrotoxicity. Molecules. 2019 Feb 12;24(3):653. doi: 10.3390/molecules24030653. PMID: 30759858; PMCID: PMC6384669.

Galati S, Di Stefano M, Martinelli E, Macchia M, Martinelli A, Poli G, Tuccinardi T. VenomPred: A Machine Learning Based Platform for Molecular Toxicity Predictions. Int J Mol Sci. 2022 Feb 14;23(4):2105. doi: 10.3390/ijms23042105. PMID: 35216217; PMCID: PMC8877213.

Gale EA. Lessons from the glitazones: a story of drug development. Lancet. 2001 Jun 9;357(9271):1870-5. doi: 10.1016/S0140-6736(00)04960-6. PMID: 11410214.

Gao RY, Mukhopadhyay P, Mohanraj R, Wang H, Horváth B, Yin S, Pacher P. Resveratrol attenuates azidothymidine-induced cardiotoxicity by decreasing mitochondrial reactive oxygen species generation in human cardiomyocytes. Mol Med Rep. 2011 Jan-Feb;4(1):151-5. doi: 10.3892/mmr.2010.390. Epub 2010 Oct 27. PMID: 21461578; PMCID: PMC3075855.

Garbuzenko DV. Pathophysiological mechanisms of hepatic stellate cells activation in liver fibrosis. World J Clin Cases. 2022 Apr 26;10(12):3662-3676. doi: 10.12998/wjcc.v10.i12.3662. PMID: 35647163; PMCID: PMC9100727.

Garcia-Cortes, M., Robles-Diaz, M., Stephens, C. et al. Drug induced liver injury: an update. Arch Toxicol 94, 3381–3407 (2020). https://doi.org/10.1007/s00204-020-02885-1

Garside H, Marcoe KF, Chesnut-Speelman J, Foster AJ, Muthas D, Kenna JG, Warrior U, Bowes J, Baumgartner J. Evaluation of the use of imaging parameters for the detection of compound-induced hepatotoxicity in 384-well cultures of HepG2 cells and cryopreserved primary human hepatocytes. Toxicol In Vitro. 2014 Mar;28(2):171-81. doi: 10.1016/j.tiv.2013.10.015. Epub 2013 Nov 1. PMID: 24189122.

Ge V, Banakh I, Tiruvoipati R, Haji K. Bleomycin-induced pulmonary toxicity and treatment with infliximab: A case report. Clin Case Rep. 2018 Sep 4;6(10):2011-2014. doi: 10.1002/ccr3.1790. PMID: 30349718; PMCID: PMC6186889.

Gerson RJ, MacDonald JS, AlbertsAW, Kornbrust DJ, Majka JA, Stubbs RJ and Bokelman DL. (1989) Animal safety and toxicology of simvastatin and related hydroxy-methylglutaryl-coenzyme A reductase inhibitors., American Journal of Medicine, 87 (supplement 4A) , 28S-38S DOI: 10.1016/S0002-9343(89)80596-0

Ghabril M, Bonkovsky HL, Kum C, Davern T, Hayashi PH, Kleiner DE, Serrano J, Rochon J, Fontana RJ, Bonacini M; US Drug-Induced Liver Injury Network. Liver injury from tumor necrosis factor-α antagonists: analysis of thirty-four cases. Clin Gastroenterol Hepatol. 2013 May;11(5):558-564.e3. doi: 10.1016/j.cgh.2012.12.025. Epub 2013 Jan 17. PMID: 23333219; PMCID: PMC3865702.

Ghalamkari M, Khatuni M, Toogeh G, Haghighi S, Taherkhani M. Reversible Acute Lung Injury due to Bleomycin. Tanaffos. 2022 Feb;21(2):253-256. PMID: 36879731; PMCID: PMC9985134.

Gillett RC Jr, Norrell A. Considerations for safe use of statins: liver enzyme abnormalities and muscle toxicity. Am Fam Physician. 2011 Mar 15;83(6):711-6. PMID: 21404982.

Gillooly JF, Hayward A, Hou C, Burleigh JG. Explaining differences in the lifespan and replicative capacity of cells: a general model and comparative analysis of vertebrates. Proc Biol Sci. 2012 Oct 7;279(1744):3976-80. doi: 10.1098/rspb.2012.1129. Epub 2012 Jul 18. PMID: 22810428; PMCID: PMC3427577.

Ginès P, Krag A, Abraldes JG, Solà E, Fabrellas N, Kamath PS. Liver cirrhosis. Lancet. 2021 Oct 9;398(10308):1359-1376. doi: 10.1016/S0140-6736(21)01374-X. Epub 2021 Sep 17. PMID: 34543610.

Gloeckner H, Jonuleit T, Lemke HD. Monitoring of cell viability and cell growth in a hollow-fiber bioreactor by use of the dye Alamar Blue. J Immunol Methods. 2001 Jun 1;252(1-2):131-8. doi: 10.1016/s0022-1759(01)00347-7. PMID: 11334972.

Gnann JW Jr, Barton NH, Whitley RJ. Acyclovir: mechanism of action, pharmacokinetics, safety and clinical applications. Pharmacotherapy. 1983 Sep-Oct;3(5):275-83. doi: 10.1002/j.1875-9114.1983.tb03274.x. PMID: 6359082.

Gold JR, Grubb T, Court MH, Villarino NF. Pharmacokinetics of acetaminophen after a single Oral administration of 20 or 40 mg/kg to 7-9 Day-old foals. Front Vet Sci. 2023 Jul 6;10:1198940. doi: 10.3389/fvets.2023.1198940. PMID: 37483288; PMCID: PMC10359069.

Goldberg RJ. Nefazodone: a novel antidepressant. Psychiatr Serv. 1995 Nov;46(11):1113-4. doi: 10.1176/ps.46.11.1113. PMID: 8564497.

Goldiner PL, Carlon GC, Cvitkovic E et al. Factors influencing post operative morbidity and mortality in patients treated with bleomycin. BrMed J 1978; 1: 1664–1667.

Gómez-Lechón MJ, Ponsoda X, O'Connor E, Donato T, Jover R, Castell JV. Diclofenac induces apoptosis in hepatocytes. Toxicol In Vitro. 2003 Oct-Dec;17(5-6):675-80. doi: 10.1016/s0887-2333(03)00105-x. PMID: 14599462.

Gómez-Lechón MJ, Tolosa L, Donato MT. Metabolic activation and drug-induced liver injury: in vitro approaches for the safety risk assessment of new drugs. J Appl Toxicol. 2016 Jun;36(6):752-68. doi: 10.1002/jat.3277. Epub 2015 Dec 22. PMID: 26691983.

Gottlieb S. Antihistamine drug withdrawn by manufacturer. BMJ. 1999 Jul 3;319(7201):7. doi: 10.1136/bmj.319.7201.7a. PMID: 10390435; PMCID: PMC1116178.

Graham DJ, Drinkard CR and Shatin D. (2003a) Incidence of idiopathic acute liver failure and hospitalized liver injury in patients treated with troglitazone., American Journal of Gastroenterology, 98 , 175-179 DOI: 10.1111/j.1572-0241.2003.07175.x

Graham DJ, Green L, Senior JR, Nourjah P. Troglitazone-induced liver failure: a case study. Am. J. Med. 2003b; 114:299–306

Grapentine, S., Singh, R.K., Basu, P. *et al.* Pcyt2 deficiency causes age-dependant development of nonalcoholic steatohepatitis and insulin resistance that could be attenuated with phosphonoethylamine. *Sci Rep* **12**, 1048 (2022). https://doi.org/10.1038/s41598-022-05140-y

Gregory SA, Webster JB, Chapman GD. Acute hepatitis induced by parenteral amiodarone. Am J Med. 2002 Aug 15;113(3):254-5. doi: 10.1016/s0002-9343(02)01149-x. PMID: 12208392.

Grem JL. 5-Fluorouracil: forty-plus and still ticking. A review of its preclinical and clinical development. Invest New Drugs. 2000 Nov;18(4):299-313. doi: 10.1023/a:1006416410198. PMID: 11081567.

Griffin JP. Famous names in toxicology. Claude Bernard 1813-1878. Adverse Drug React Toxicol Rev. 1993 Winter;12(4):213-4.

Griffith LG, Swartz MA. Capturing complex 3D tissue physiology in vitro. Nat Rev Mol Cell Biol. 2006 Mar;7(3):211-24. doi: 10.1038/nrm1858. PMID: 16496023.

Grill MF, Maganti RK. Neurotoxic effects associated with antibiotic use: management considerations. Br J Clin Pharmacol. 2011 Sep;72(3):381-93. doi: 10.1111/j.1365-2125.2011.03991.x. PMID: 21501212; PMCID: PMC3175508.

Grimbert S, Pessayre D, Degott C and Benhamou JP. (1994) Acute hepatitis induced by HMG-CoA reductase inhibitor, lovastatin., Digestive Diseases and Sciences, 39 , 2032-2033 DOI: 10.1007/BF02088142

Guengerich FP. Cytochrome P450s and other enzymes in drug metabolism and toxicity. AAPS J. 2006 Mar 10;8(1):E101-11. doi: 10.1208/aapsj080112. PMID: 16584116; PMCID: PMC2751428.

Guengerich FP. Mechanisms of Cytochrome P450-Catalyzed Oxidations. ACS Catal. 2018 Dec 7;8(12):10964-10976. doi: 10.1021/acscatal.8b03401. Epub 2018 Oct 18. PMID: 31105987; PMCID: PMC6519473.

Guillouzo A, Corlu A, Aninat C, Glaise D, Morel F, Guguen-Guillouzo C. The human hepatoma HepaRG cells: a highly differentiated model for studies of liver metabolism and toxicity of xenobiotics. Chem Biol Interact. 2007 May 20;168(1):66-73. doi: 10.1016/j.cbi.2006.12.003. Epub 2006 Dec 16. PMID: 17241619.

Gujral JS, Knight TR, Farhood A, Bajt ML and Jaeschke H. (2002). Mode of cell death after acetaminophen overdose in mice: apoptosis or oncotic necrosis?,Toxicological Sciences, 67 , 322-328 DOI: 10.1093/toxsci/67.2.322

Gunness P, Mueller D, Shevchenko V, Heinzle E, Ingelman-Sundberg M, Noor F. 3D organotypic cultures of human HepaRG cells: a tool for in vitro toxicity studies. Toxicol Sci. 2013 May;133(1):67-78. doi: 10.1093/toxsci/kft021. Epub 2013 Feb 1. PMID: 23377618.

Guo C, Kephart S, Ornelas M, Gonzalez J, Linton A, Pairish M, Nagata A, Greasley S, Elleraas J, Hosea N, Engebretsen J and Fanjul AN. (2012) Discovery of 3-aryloxy-lactam analogs as potent androgen receptor full antagonists for treating castration resistant prostate cancer., Bioorganic and Medicinal Chemistry Letters, 22 , 1230-1236 DOI: 10.1016/j.bmcl.2011.11.068

Guo C, Linton A, Kephart S, Ornelas M, Pairish M, Gonzalez J, Greasley S, Nagata A, Burke BJ, Edwards M, Hosea N, Kang P, Hu W, Engebretsen J, Briere D, Shi M, Gukasyan H, Richardson P, Dack K, Underwood T, Johnson P, Morell A, Felstead R, Kuruma H, Matsimoto H, Zoubeidi A, Gleave M, Los G and Fanjul AN. (2011) Discovery of aryloxy tetramethylcyclobutanes as novel androgen receptor antagonists., Journal of Medicinal Chemistry, 54 , 7693-7704 DOI: 10.1021/jm201059s Derek Nexus Prediction Report Page 15 of 20

Guo L, Dial S, Shi L, Branham W, Liu J, Fang JL, Green B, Deng H, Kaput J, Ning B. Similarities and differences in the expression of drug-metabolizing enzymes between human hepatic cell lines and primary human hepatocytes. Drug Metab Dispos. 2011 Mar;39(3):528-38. doi: 10.1124/dmd.110.035873. Epub 2010 Dec 13. PMID: 21149542; PMCID: PMC3061558.

Guo L, Zhang L, Sun Y, Muskhelishvili L, Blann E, Dial S, Shi L, Schroth G, Dragan YP. Differences in hepatotoxicity and gene expression profiles by anti-diabetic PPAR gamma agonists on rat primary hepatocytes and human HepG2 cells. Mol Divers. 2006 Aug;10(3):349-60. doi: 10.1007/s11030-006-9038-0. Epub 2006 Sep 21. PMID: 17031537.

Gupta S, Portales-Castillo I, Daher A, Kitchlu A. Conventional Chemotherapy Nephrotoxicity. Adv Chronic Kidney Dis. 2021 Sep;28(5):402-414.e1. doi: 10.1053/j.ackd.2021.08.001. PMID: 35190107.

Habanjar O, Diab-Assaf M, Caldefie-Chezet F, Delort L. 3D Cell Culture Systems: Tumor Application, Advantages, and Disadvantages. Int J Mol Sci. 2021 Nov 11;22(22):12200. doi: 10.3390/ijms222212200. PMID: 34830082; PMCID: PMC8618305.

Haddad PM, Anderson IM. Antipsychotic-related QTc prolongation, torsade de pointes and sudden death. Drugs. 2002;62(11):1649-71. doi: 10.2165/00003495-200262110-00006. PMID: 12109926.

Hadwan MH. Simple spectrophotometric assay for measuring catalase activity in biological tissues. BMC Biochem. 2018 Aug 3;19(1):7. doi: 10.1186/s12858-018-0097-5. PMID: 30075706; PMCID: PMC6091033.

Hajji M, Jebali H, Mrad A, Blel Y, Brahmi N, Kheder R, Beji S, Fatma LB, Smaoui W, Krid M, Hmida FB, Rais L, Zouaghi MK. Nephrotoxicity of Ciprofloxacin: Five Cases and a Review of the Literature. Drug Saf Case Rep. 2018 Apr 18;5(1):17. doi: 10.1007/s40800-018-0073-4. PMID: 29671145; PMCID: PMC5906393.

Hall MP, Gruber MG, Hannah RR, Jennens-Clough ML, Wood KV. Stabilization of fi refl y luciferase using directed evolution. In: Bioluminescence and Chemiluminescence: Perspectives for the 21st Century. Rode A, Pazzagli M, Kricka LJ, Stanley PE (Eds), John Wiley & Sons, Chichester; 1998 . p. 392- 5.

Hamann LG, Manfredi MC, Sun C, Krystek SR Jr, Huang Y, Bi Y, Augeri DJ, Wang T, Zou Y, Betebenner DA, Fura A, Seethala R, Golla R, Kuhns JE, Lupisella JA, Darienzo CJ, Custer LL, Price JL, Johnson JM, Biller SA, Zahler R and Ostrowski J. (2007) Tandem optimization of target activity and elimination of mutagenic potential in a potent series of N-aryl bicyclic hydantoin-based selective androgen receptor modulators., Bioorganic and Medicinal Chemistry Letters, 17 , 1860-1864 DOI: 10.1016/j.bmcl.2007.01.076

Hamill, R.J. Amphotericin B Formulations: A Comparative Review of Efficacy and Toxicity. Drugs 73, 919–934 (2013). https://doi.org/10.1007/s40265-013-0069-4

Hammer H, Schmidt F, Marx-Stoelting P, Pötz O, Braeuning A. Cross-species analysis of hepatic cytochrome P450 and transport protein expression. Arch Toxicol. 2021 Jan;95(1):117-133. doi: 10.1007/s00204-020-02939-4. Epub 2020 Nov 4. PMID: 33150952; PMCID: PMC7811513.

Hancox JC, Hasnain M, Vieweg WV, Gysel M, Methot M, Baranchuk A. Erythromycin, QTc interval prolongation, and torsade de pointes: Case reports, major risk factors and illness severity. Ther Adv Infect Dis. 2014 Apr;2(2):47-59. doi: 10.1177/2049936114527744. PMID: 25165555; PMCID: PMC4072045.

Harada M. Minamata disease: methylmercury poisoning in Japan caused by environmental pollution. Crit Rev Toxicol. 1995;25(1):1-24.

Harahap Y, Sasongko L, Prasaja B, Indriati E, Lusthom W, Lipin. Comparative bioavailability of two dexamethasone tablet formulations in Indonesian healthy volunteers. Arzneimittelforschung. 2009;59(4):191-4. doi: 10.1055/s-0031-1296384. PMID: 19517895.

Harmon EG, McConnie R, Kesavan A. Minocycline-Induced Autoimmune Hepatitis: A Rare But Important Cause of Drug-Induced Autoimmune Hepatitis. Pediatr Gastroenterol Hepatol Nutr. 2018 Oct;21(4):347-350. doi: 10.5223/pghn.2018.21.4.347. Epub 2018 Oct 10. PMID: 30345250; PMCID: PMC6182477.

Harrison RK. Phase II and phase III failures: 2013-2015. Nat Rev Drug Discov. 2016 Dec;15(12):817-818. doi: 10.1038/nrd.2016.184. Epub 2016 Nov 4. PMID: 27811931.

Hartmut Jaeschke, Troglitazone Hepatotoxicity: Are We Getting Closer to Understanding Idiosyncratic Liver Injury?, Toxicological Sciences, Volume 97, Issue 1, May 2007, Pages 1–3, https://doi.org/10.1093/toxsci/kfm021

Hawkes SP, Li H, Taniguchi GT. Zymography and reverse zymography for detecting MMPs and TIMPs. Methods Mol Biol. 2010; 622:257-69. doi: 10.1007/978-1-60327-299-5_16. PMID: 20135288.

Hay J, Shahzeidi S, Laurent G. Mechanisms of bleomycin-induced lung damage. Arch Toxicol. 1991;65(2):81-94. doi: 10.1007/BF02034932. PMID: 1711838.

Hay M, Thomas, D. W., Craighead, J. L., Economides, C. & Rosenthal, J. Clinical development success rates for investigational drugs. Nat. Biotechnol. 32, 40–51 (2014).

Hayes AN, Gilbert SG. Historical milestones and discoveries that shaped the toxicology sciences. EXS. 2009; 99:1-35.

Helfgott SM, Sandberg-Cook J, Zakim D, Nestler J. Diclofenac-associated hepatotoxicity. JAMA. 1990 Nov 28;264(20):2660-2. PMID: 2232043.

Hendriks DFG, Hurrell T, Riede J, van der Horst M, Tuovinen S, Ingelman-Sundberg M. Mechanisms of Chronic Fialuridine Hepatotoxicity as Revealed in Primary Human Hepatocyte Spheroids. Toxicol Sci. 2019 Oct 1;171(2):385-395. doi: 10.1093/toxsci/kfz195. PMID: 31505000.

Henney JE. Withdrawal of Troglitazone and Cisapride. JAMA. 2000;283(17):2228. doi:10.1001/jama.283.17.2228

Herrmann, J. Adverse cardiac effects of cancer therapies: cardiotoxicity and arrhythmia. Nat Rev Cardiol 17, 474–502 (2020). https://doi.org/10.1038/s41569-020-0348-1

Heslop, J.A., Rowe, C., Walsh, J. et al. Mechanistic evaluation of primary human hepatocyte culture using global proteomic analysis reveals a selective dedifferentiation profile. Arch Toxicol 91, 439–452 (2017). https://doi.org/10.1007/s00204-016-1694-y

Hewitt M, Przybylak K. In Silico Models for Hepatotoxicity. Methods Mol Biol. 2016;1425:201-36. doi: 10.1007/978-1-4939-3609-0_11. PMID: 27311469.

Hewitt NJ, Lloyd S, Hayden M, Butler R, Sakai Y, Springer R, Fackett A, Li AP. Correlation between troglitazone cytotoxicity and drug metabolic enzyme activities in cryopreserved human hepatocytes. Chem Biol Interact. 2002 Nov 10;142(1-2):73-82. doi: 10.1016/s0009-2797(02)00055-8. PMID: 12399156.

Hill RN, Erdreich LS, Paynter OE, Roberts PA, Rosenthal SL and Wilkinson CF. (1989) Thyroid follicular cell carcinogenesis., Fundamental and Applied Toxicology, 12 , 629-697 DOI: 10.1016/0272-0590(89)90001-8

Hingorani AD, Kuan V, Finan C, Kruger FA, Gaulton A, Chopade S, Sofat R, MacAllister RJ, Overington JP, Hemingway H, Denaxas S, Prieto D, Casas JP. Improving the odds of drug development success through human genomics: modelling study. Sci Rep. 2019 Dec 11;9(1):18911. doi: 10.1038/s41598-019-54849-w. PMID: 31827124; PMCID: PMC6906499.

Hinson JA. (1983) Reactive metabolites of phenacetin and acetaminophen: a review., Environmental Health Perspectives, 49 , 71-79

Ho C., Lin R., Chen R., Chin C., Gong S., Chang H., Peng H., Hsu L., Yew T., Chang S., et al. Liver-cell patterning Lab Chip: mimicking the morphology of liver lobule tissue. Lab Chip. 2013;13:3578. doi: 10.1039/c3lc50402f.

Hodiamont CJ, van den Broek AK, de Vroom SL, Prins JM, Mathôt RAA, van Hest RM. Clinical Pharmacokinetics of Gentamicin in Various Patient Populations and Consequences for Optimal Dosing for Gram-Negative Infections: An Updated Review. Clin Pharmacokinet. 2022 Aug;61(8):1075-1094. doi: 10.1007/s40262-022-01143-0. Epub 2022 Jun 27. PMID: 35754071; PMCID: PMC9349143.

Hofmann R, Steinwender C, Kammler J, Kypta A, Leisch F. Effects of a high dose intravenous bolus amiodarone in patients with atrial fibrillation and a rapid ventricular rate. Int J Cardiol. 2006 Jun 7;110(1):27-32. doi: 10.1016/j.ijcard.2005.06.048. Epub 2005 Jul 19. PMID: 16046015.

Holland G, York M and Basketter DA. (1996) Irritants: corrosive materials, oxidising/reducing agents, acids, and alkalis, concentrated salt solutions etc., The Irritant Contact Dermatitis Syndrome, , 55-64

Holmberg L, Boman G. Pulmonary reactions to nitrofurantoin. 447 cases reported to the Swedish Adverse Drug Reaction Committee 1966-1976. Eur J Respir Dis. 1981 Jun;62(3):180-9. PMID: 7308333.

Hoofnagle JH, Björnsson ES. Drug-Induced Liver Injury - Types and Phenotypes. N Engl J Med. 2019 Jul 18;381(3):264-273. doi: 10.1056/NEJMra1816149. PMID: 31314970.

Horsmans Y, Desager JP and Harvengt C. (1990) Biochemical changes and morphological alterations of the liver in guinea-pigs after administration of simvastatin (HMG CoA reductase-inhibitor)., Pharmacology and Toxicology, 67 , 336-339

Hou Y, Mi K, Sun L, Zhou K, Wang L, Zhang L, Liu Z, Huang L. The Application of Hollow Fiber Cartridge in Biomedicine. Pharmaceutics. 2022 Jul 18;14(7):1485. doi: 10.3390/pharmaceutics14071485. PMID: 35890380; PMCID: PMC9316653.

Hu, C., Li, L. In vitro culture of isolated primary hepatocytes and stem cell-derived hepatocyte-like cells for liver regeneration. Protein Cell 6, 562–574 (2015). https://doi.org/10.1007/s13238-015-0180-2

Hua Y, Cui X, Liu B, Shi Y, Guo H, Zhang R, Li X. SApredictor: An Expert System for Screening Chemicals Against Structural Alerts. Front Chem. 2022 Jul 13;10:916614. doi: 10.3389/fchem.2022.916614. PMID: 35910729; PMCID: PMC9326022.

Huang Y, Qian JY, Cheng H, Li XM. Effects of shear stress on differentiation of stem cells into endothelial cells. World J Stem Cells. 2021 Jul 26;13(7):894-913. doi: 10.4252/wjsc.v13.i7.894. PMID: 34367483; PMCID: PMC8316872.

Hughes, James P., et al. "Principles of early drug discovery." *British journal of pharmacology* 162.6 (2011): 1239-1249.

Huh D, Matthews BD, Mammoto A, Montoya-Zavala M, Hsin HY, Ingber DE. Reconstituting organ-level lung functions on a chip. Science. 2010 Jun 25;328(5986):1662-8. doi: 10.1126/science.1188302. PMID: 20576885; PMCID: PMC8335790.

Hussain N, Bhattacharyya A, Prueksaritanond S. Amiodarone-induced cirrhosis of liver: what predicts mortality? ISRN Cardiol. 2013;2013:617943. doi: 10.1155/2013/617943. Epub 2013 Mar 14. PMID: 23577267; PMCID: PMC3612472.

Huttner A, Verhaegh EM, Harbarth S, Muller AE, Theuretzbacher U, Mouton JW. Nitrofurantoin revisited: a systematic review and meta-analysis of controlled trials. J Antimicrob Chemother. 2015 Sep;70(9):2456-64. doi: 10.1093/jac/dkv147. Epub 2015 Jun 11. PMID: 26066581.

Hwang TJ, Carpenter D, Lauffenburger JC, Wang B, Franklin JM, Kesselheim AS. Failure of Investigational Drugs in Late-Stage Clinical Development and Publication of Trial Results. JAMA Intern Med. 2016 Dec 1;176(12):1826-1833. doi: 10.1001/jamainternmed.2016.6008. PMID: 27723879.

IARC (International Agency for Research on Cancer). (1999) Some chemicals that cause tumours of the kidney or urinary bladder in rodents and some other substances., IARC Monographs on the Evaluation of Carcinogenic Risks to Humans, 73 , 223-276

IARC (International Agency for Research on Cancer). (2001) Some thyrotropic agents., IARC Monographs on the Evaluation of Carcinogenic Risks to Humans, 79 , 493-568

IARC. International Agency for Research on Cancer (IARC). (1987) Overall evaluations of carcinogenicity: an updating of IARC Monographs volumes 1 to 42., IARC Monographs on the Evaluation of Carcinogenic Risks to Humans, supplement 7, 56-74

Ingber DE. Human organs-on-chips for disease modelling, drug development and personalized medicine. Nat Rev Genet. 2022 Aug;23(8):467-491. doi: 10.1038/s41576-022-00466-9. Epub 2022 Mar 25. PMID: 35338360; PMCID: PMC8951665.

Institute of Medicine (US) Committee to Review the Fialuridine (FIAU/FIAC) Clinical Trials. Review of the Fialuridine (FIAU) Clinical Trials. Manning FJ, Swartz M, editors. Washington (DC): National Academies Press (US); 1995. PMID: 25121268.

Isaacson SH, Carr J, Rowan AJ. Ciprofloxacin-induced complex partial status epilepticus manifesting as an acute confusional state. Neurology. 1993 Aug;43(8):1619-21. doi: 10.1212/wnl.43.8.1619-a. PMID: 8351027.

Ito N, Fukushima S, Hagiwara A, Shibata M and Ogiso T. (1983) Carcinogenicity of butylated hydroxyanisole in F344 rats., Journal of the National Cancer Institute, 70 , 343-352

Jackson JP, Brouwer KR. The C-DILI™ Assay: An Integrated In Vitro Approach to Predict Cholestatic Hepatotoxicity. Methods Mol Biol. 2019;1981:75-85. doi: 10.1007/978-1-4939-9420-5_5. PMID: 31016648.

Jain R, Gupta K, Bhatia A, Bansal A, Bansal D. Hepatic Sinusoidal-obstruction Syndrome and Busulfan-induced Lung Injury in a Post-autologous Stem Cell Transplant Recipient. Indian Pediatr. 2017 Sep 15;54(9):765-770. doi: 10.1007/s13312-017-1172-5. PMID: 28984258; PMCID: PMC7097441.

Jaiswal P, Attar BM, Yap JE, Devani K, Jaiswal R, Wang Y, Szynkarek R, Patel D, Demetria M. Acute liver failure with amiodarone infusion: A case report and systematic review. J Clin Pharm Ther. 2018 Feb;43(1):129-133. doi: 10.1111/jcpt.12594. Epub 2017 Jul 16. PMID: 28714083.

James LP, Mayeux PR and Hinson JA. (2003) Acetaminophen-induced hepatotoxicity., Drug Metabolism and Disposition, 31 , 1499-1506

Jang KJ, Mehr AP, Hamilton GA, McPartlin LA, Chung S, Suh KY, Ingber DE. Human kidney proximal tubule-on-a-chip for drug transport and nephrotoxicity assessment. Integr Biol (Camb). 2013 Sep;5(9):1119-29. doi: 10.1039/c3ib40049b. PMID: 23644926.

Jang KJ, Otieno MA, Ronxhi J, Lim HK, Ewart L, Kodella KR, Petropolis DB, Kulkarni G, Rubins JE, Conegliano D, Nawroth J, Simic D, Lam W, Singer M, Barale E, Singh B, Sonee M, Streeter AJ, Manthey C, Jones B, Srivastava A, Andersson LC, Williams D, Park H, Barrile R, Sliz J, Herland A, Haney S, Karalis K, Ingber DE, Hamilton GA. Reproducing human and cross-species drug toxicities using a Liver-Chip. Sci Transl Med. 2019 Nov 6;11(517):eaax5516. doi: 10.1126/scitranslmed.aax5516. PMID: 31694927.

Jazaeri F, Sheibani M, Nezamoleslami S, Moezi L, Dehpour AR. Current Models for Predicting Drug-induced Cholestasis: The Role of Hepatobiliary Transport System. Iran J Pharm Res. 2021 Spring;20(2):1-21. doi: 10.22037/ijpr.2020.113362.14254. PMID: 34567142; PMCID: PMC8457732.

Jeeyavudeen MS, Pappachan JM, Arunagirinathan G. Statin-related Muscle Toxicity: An Evidence-based Review. touchREV Endocrinol. 2022 Nov;18(2):89-95. doi: 10.17925/EE.2022.18.2.89. Epub 2022 Nov 21. PMID: 36694885; PMCID: PMC9835810.

Jemnitz K, Veres Z, Monostory K, Kóbori L, Vereczkey L. Interspecies differences in acetaminophen sensitivity of human, rat, and mouse primary hepatocytes. Toxicol In Vitro. 2008 Jun;22(4):961-7. doi: 10.1016/j.tiv.2008.02.001. Epub 2008 Feb 13. PMID: 18346862.

Jenkins A, Austin A, Hughes K, Sadowski B, Torres D. Infliximab-induced autoimmune hepatitis. BMJ Case Rep. 2021 May 24;14(5):e239944. doi: 10.1136/bcr-2020-239944. PMID: 34031069; PMCID: PMC8149306.

Jinpeng Li, Raja S. Settivari, Matthew J. LeBaron, and Mary Sue Marty. Functional Comparison of HepaRG Cells and Primary Human Hepatocytes in Sandwich and Spheroid Culture as Repeated-Exposure Models for Hepatotoxicity.Applied In Vitro Toxicology.Dec 2019.187-195.http://doi.org/10.1089/aivt.2019.0008

Jones DP, Lemasters JJ, Han D, Boelsterli UA, Kaplowitz N. Mechanisms of pathogenesis in drug hepatotoxicity putting the stress on mitochondria. Mol Interv. 2010 Apr;10(2):98-111. doi: 10.1124/mi.10.2.7. PMID: 20368370; PMCID: PMC2895369.

Jorro G, Morales C, Brasó JV, Peláez A. Anaphylaxis to erythromycin. Ann Allergy Asthma Immunol. 1996 Dec;77(6):456-8. doi: 10.1016/S1081-1206(10)63349-2. PMID: 8970433.

Judson, R., Richard, A., Dix, D., Houck, K., Elloumi, F., Martin, M., et al. (2008). ACToR–Aggregated computational toxicology resource. Toxicol. Appl. Pharmacol. 233, 7–13. doi: 10.1016/j.taap.2007.12.03

Jung SH, Lee W, Park SH, Lee KY, Choi YJ, Choi S, Kang D, Kim S, Chang TS, Hong SS, Lee BH. Diclofenac impairs autophagic flux via oxidative stress and lysosomal dysfunction: Implications for hepatotoxicity. Redox Biol. 2020 Oct;37:101751. doi: 10.1016/j.redox.2020.101751. Epub 2020 Oct 12. PMID: 33080439; PMCID: PMC7575798.

Jurima-Romet M, Crawford K, Huang HS. Comparative cytotoxicity of non-steroidal anti-inflammatory drugs in primary cultures of rat hepatocytes. Toxicol In Vitro. 1994 Feb;8(1):55-66. doi: 10.1016/0887-2333(94)90208-9. PMID: 20692889.

Jyothilekshmi I, Jayaprakash NS. Trends in Monoclonal Antibody Production Using Various Bioreactor Syst. J Microbiol Biotechnol. 2021 Mar 28;31(3):349-357. doi: 10.4014/jmb.1911.11066. PMID: 32238761; PMCID: PMC9705917.

Kabbara WK, Kordahi MC. Nitrofurantoin-induced pulmonary toxicity: A case report and review of the literature. J Infect Public Health. 2015 Jul-Aug;8(4):309-13. doi: 10.1016/j.jiph.2015.01.007. Epub 2015 Mar 5. PMID: 25747822.

Kachel DL, Martin WJ 2nd. Cyclophosphamide-induced lung toxicity: mechanism of endothelial cell injury. J Pharmacol Exp Ther. 1994 Jan;268(1):42-6. PMID: 8301583.

Kaden T, Graf K, Rennert K, Li R, Mosig AS, Raasch M. Evaluation of drug-induced liver toxicity of trovafloxacin and levofloxacin in a human microphysiological liver model. Sci Rep. 2023 Aug 16;13(1):13338. doi: 10.1038/s41598-023-40004-z. PMID: 37587168; PMCID: PMC10432496.

Kalantzis N, Gabriel P, Mouzas J, et al. Acute amiodarone- induced hepatitis. Hepatogastroenterology. 1991;38:71-74

Kale P, Agrawal YK. Pharmacokinetics of single oral dose trazodone: a randomized, two-period, cross-over trial in healthy, adult, human volunteers under fed condition. Front Pharmacol. 2015 Oct 2;6:224. doi: 10.3389/fphar.2015.00224. PMID: 26483693; PMCID: PMC4591485.

Kalgutkar AS, Gardner I, Obach RS, Shaffer CL, Callegari E, Henne KR, Mutlib AE, Dalvie DK, Lee JS,Nakai Y, O'Donnell JP, Boer J and Harriman SP. (2005)A comprehensive listing of bioactivation pathways of organic functional groups., Current DrugMetabolism, 6 , 161-225 DOI: 10.2174/1389200054021799

Kalivendi SV, Konorev EA, Cunningham S, Vanamala SK, Kaji EH, Joseph J, Kalyanaraman B. Doxorubicin activates nuclear factor of activated T-lymphocytes and Fas ligand transcription: role of mitochondrial reactive oxygen species and calcium. Biochem J. 2005 Jul 15;389(Pt 2):527-39. doi: 10.1042/BJ20050285. PMID: 15799720; PMCID: PMC1175131.

Kalyanaraman B, Darley-Usmar V, Davies KJ, Dennery PA, Forman HJ, Grisham MB, Mann GE, Moore K, Roberts LJ 2nd, Ischiropoulos H. Measuring reactive oxygen and nitrogen species with fluorescent probes: challenges and limitations. Free Radic Biol Med. 2012 Jan 1;52(1):1-6. doi: 10.1016/j.freeradbiomed.2011.09.030. Epub 2011 Oct 2. PMID: 22027063; PMCID: PMC3911769.

Kaminsky, Y.G., Kosenko, E.A. Molecular mechanisms of toxicity of simvastatin, widely used cholesterol-lowering drug. A review. cent.eur.j.med 5, 269–279 (2010). https://doi.org/10.2478/s11536-009-0123-5

Kamm DR, McCommis KS. Hepatic stellate cells in physiology and pathology. J Physiol. 2022 Apr;600(8):1825-1837. doi: 10.1113/JP281061. Epub 2022 Mar 30. PMID: 35307840; PMCID: PMC9012702.

Kan WC, Chen YC, Wu VC, Shiao CC. Vancomycin-Associated Acute Kidney Injury: A Narrative Review from Pathophysiology to Clinical Application. Int J Mol Sci. 2022 Feb 12;23(4):2052. doi: 10.3390/ijms23042052. PMID: 35216167; PMCID: PMC8877514.

Kanehisa M, Goto S. KEGG: kyoto encyclopedia of genes and genomes. Nucleic Acids Res. 2000 Jan 1;28(1):27-30. doi: 10.1093/nar/28.1.27. PMID: 10592173; PMCID: PMC102409.

Kapałczyńska M, Kolenda T, Przybyła W, Zajączkowska M, Teresiak A, Filas V, Ibbs M, Bliźniak R, Łuczewski Ł, Lamperska K. 2D and 3D cell cultures - a comparison of different types of cancer cell cultures. Arch Med Sci. 2018 Jun;14(4):910-919. doi: 10.5114/aoms.2016.63743. Epub 2016 Nov 18. PMID: 30002710; PMCID: PMC6040128.

Kaplowitz N. Idiosyncratic drug hepatotoxicity. Nat Rev Drug Discov 2005;4:489-499

Karahalil B, Hare E, Koç G, Uslu İ, Şentürk K, Özkan Y. Hepatotoxicity associated with statins. Arh Hig Rada Toksikol. 2017 Dec 20;68(4):254-260. doi: 10.1515/aiht-2017-68-2994. PMID: 29337684.

Kassahun K, Pearson PG, Tang W, McIntosh I, Leung K, Elmore C, Dean D, Wang R, Doss G, Baillie TA. Studies on the metabolism of troglitazone to reactive intermediates in vitro and in vivo. Evidence for novel biotransformation pathways involving quinone methide formation and thiazolidinedione ring scission. Chem Res Toxicol. 2001 Jan;14(1):62-70. doi: 10.1021/tx000180q. PMID: 11170509.

Kaur G, Dufour JM. Cell lines: Valuable tools or useless artifacts. Spermatogenesis. 2012 Jan 1;2(1):1-5. doi: 10.4161/spmg.19885. PMID: 22553484; PMCID: PMC3341241.

Kaur I, Vasudevan A, Rawal P, Tripathi DM, Ramakrishna S, Kaur S, Sarin SK. Primary Hepatocyte Isolation and Cultures: Technical Aspects, Challenges and Advancements. Bioengineering (Basel). 2023 Jan 18;10(2):131. doi: 10.3390/bioengineering10020131. PMID: 36829625; PMCID: PMC9952008.

Kaur R, Sidhu P, Singh S. What failed BIA 10-2474 Phase I clinical trial? Global speculations and recommendations for future Phase I trials. J Pharmacol Pharmacother. 2016 Jul-Sep;7(3):120-6. doi: 10.4103/0976-500X.189661. PMID: 27651707; PMCID: PMC5020770.

Kaviyarasi Renu, Lakshmi Prasanna Pureti, Balachandar Vellingiri & Abilash Valsala Gopalakrishnan (2022) Toxic effects and molecular mechanism of doxorubicin on different organs – an update, Toxin Reviews, 41:2, 650-674, DOI: 10.1080/15569543.2021.1912099

Kawai K., Kawasaki-Tokui Y., Odaka T., Tsuruta F., Kazui M., Iwabuchi H., Nakamura T., Kinoshita T., Ikeda T., Yoshioka T., Komai T., Nakamura K., Disposition and metabolism of the new oral antidiabetic drug troglitazone in rats, mice and dogs, Arzeim Forsch Drug Res. 47 (1997) 356- 368

Kennedy EL, Tchao R and Harvison PJ. (2003) Nephrotoxic and hepatotoxic potential of imidazolidinedione-, oxazolidinedione- and thiazolidinedione-containing analogues of N-(3,5-dichlorophenyl)succinimide (NDPS) in Fischer 344 rats., Toxicology, 186 , 79-91 DOI: 10.1016/S0300-483X(02)00692-3

Keseru GM, Makara GM. Hit discovery and hit-to-lead approaches. Drug Discov Today. 2006 Aug;11(15-16):741-8. doi: 10.1016/j.drudis.2006.06.016. PMID: 16846802.

Kesterson JW, Granneman GR, Machinist JM. The hepatotoxicity of valproic acid and its metabolites in rats. I. Toxicologic, biochemical and histopathologic studies. Hepatology. 1984 Nov-Dec;4(6):1143-52. doi: 10.1002/hep.1840040609. PMID: 6437960.

Khafaga AF, Mousa SA, Aleya L, Abdel-Daim MM. Three-dimensional (3D) cell culture: a valuable step in advancing treatments for human hepatocellular carcinoma. Cancer Cell Int. 2022 Jul 30;22(1):243. doi: 10.1186/s12935-022-02662-3. PMID: 35908054; PMCID: PMC9339175.

Khalid MM, Waseem M. Tricyclic Antidepressant Toxicity. 2023 Jul 17. In: StatPearls [Internet]. Treasure Island (FL): StatPearls Publishing; 2024 Jan–. PMID: 28613681.

Kijanska M, Kelm J. In vitro 3D Spheroids and Microtissues: ATP-based Cell Viability and Toxicity Assays. 2016 Jan 21. In: Markossian S, Grossman A, Arkin M, Auld D, Austin C, Baell J, Brimacombe K, Chung TDY, Coussens NP, Dahlin JL, Devanarayan V, Foley TL, Glicksman M, Gorshkov K, Haas JV, Hall MD, Hoare S, Inglese J, Iversen PW, Lal-Nag M, Li Z, Manro JR, McGee J, McManus O, Pearson M, Riss T, Saradjian P, Sittampalam GS, Tarselli M, Trask OJ Jr, Weidner JR, Wildey MJ, Wilson K, Xia M, Xu X, editors. Assay Guidance Manual [Internet]. Bethesda (MD): Eli Lilly & Company and the National Center for Advancing Translational Sciences; 2004–. PMID: 26844332.

Kikkawa R, Fujikawa M, Yamamoto T, Hamada Y, Yamada H and Horii I. (2006). In vivo hepatotoxicity study of rats in comparison with in vitro hepatotoxicity screening system., Journal of Toxicological Sciences, 31 , 23-34

Kim SH, Turnbull J, Guimond S. Extracellular matrix and cell signalling: the dynamic cooperation of integrin, proteoglycan and growth factor receptor. J Endocrinol. 2011 May;209(2):139-51. doi: 10.1530/JOE-10-0377. Epub 2011 Feb 9. PMID: 21307119.

Kim Y, Lasher CD, Milford LM, Murali TM, Rajagopalan P. A comparative study of genome-wide transcriptional profiles of primary hepatocytes in collagen sandwich and monolayer cultures. Tissue Eng Part C Methods. 2010 Dec;16(6):1449-60. doi: 10.1089/ten.tec.2010.0012. Epub 2010 Jun 7. PMID: 20412007; PMCID: PMC2988646.

Kimes BW, Brandt BL. Properties of a clonal muscle cell line from rat heart. Exp Cell Res. 1976 Mar 15;98(2):367-81. doi: 10.1016/0014-4827(76)90447-x. PMID: 943302.

Kinoyama I, Taniguchi N, Toyoshima A, Nozawa E, Kamikubo T, Imamura M, Matsuhisa A, Samizu K, Kawanimani E, Niimi T, Hamada N, Koutoku H, Furutani T, Kudoh M, Okada M, Ohta M and Tsukamoto S. (2006) (+)-(2R,5S)-4-[4-Cyano-3-(trifluoromethyl)phenyl]-2,5-dimethyl-N-[6-(trifluoromethyl)pyridin-3- yl]piperazine-1-carboxamide (YM580) as an orally potent and peripherally selective nonsteroidal androgen receptor antagonist., Journal of Medicinal Chemistry, 49 , 716-726 DOI: 10.1021/jm050293c

Kiriiri, G.K., Njogu, P.M. & Mwangi, A.N. Exploring different approaches to improve the success of drug discovery and development projects: a review. Futur J Pharm Sci 6, 27 (2020). https://doi.org/10.1186/s43094-020-00047-9

Kishor K, Dhasmana N, Kamble SS, Sahu RK. Linezolid Induced Adverse Drug Reactions - An Update. Curr Drug Metab. 2015;16(7):553-9. doi: 10.2174/1389200216666151001121004. PMID: 26424176.

Kitayama A, Yoshizaki H, Ohmiya Y, Ueda H, Nagamune T. Creation of a thermostable firefly luciferase with pH-insensitive luminescent color. Photochem Photobiol. 2003 Mar;77(3):333-8. doi: 10.1562/0031-8655(2003)077<0333:coatfl>2.0.co;2. PMID: 12685663.

Kleiner DE, Berman D. Pathologic changes in ipilimumab-related hepatitis in patients with metastatic melanoma. Dig Dis Sci. 2012 Aug;57(8):2233-40. doi: 10.1007/s10620-012-2140-5. Epub 2012 Mar 21. PMID: 22434096; PMCID: PMC3792485.

Knazek RA, Gullino PM, Kohler PO, Dedrick RL. Cell culture on artificial capillaries: an approach to tissue growth in vitro. Science. 1972 Oct 6;178(4056):65-6. doi: 10.1126/science.178.4056.65. PMID: 4560879.

Kobuchi S, Ito Y, Sakaeda T. Population Pharmacokinetic-Pharmacodynamic Modeling of 5-Fluorouracil for Toxicities in Rats. Eur J Drug Metab Pharmacokinet. 2017 Aug;42(4):707-718. doi: 10.1007/s13318-016-0389-3. PMID: 27889876.

Kohlroser J, Mathai J, Reichheld J, Banner BF and Bonkovsky HL. (2000) Hepatotoxicity due to troglitazone: report of two cases and review of adverse events reported to the United States Food and Drug Administration., American Journal of Gastroenterology, 95 , 272-276 DOI: 10.1111/j.1572-0241.2000.01707.x

Kohonen P, Benfenati E, Bower D, Ceder R, Crump M, Cross K, Grafström RC, Healy L, Helma C, Jeliazkova N, Jeliazkov V, Maggioni S, Miller S, Myatt G, Rautenberg M, Stacey G, Willighagen E, Wiseman J, Hardy B. The ToxBank Data Warehouse: Supporting the Replacement of In Vivo Repeated Dose Systemic Toxicity Testing. Mol Inform. 2013 Jan;32(1):47-63. doi: 10.1002/minf.201200114. Epub 2013 Jan 17. PMID: 27481023.

Koksharov MI, Ugarova NN. Approaches to engineer stability of beetle luciferases. Comput Struct Biotechnol J. 2012 Oct 9;2:e201209004. doi: 10.5936/csbj.201209004. PMID: 24688645; PMCID: PMC3962189.

Kolaric TO, Nincevic V, Kuna L, Duspara K, Bojanic K, Vukadin S, Raguz-Lucic N, Wu GY, Smolic M. Drug-induced Fatty Liver Disease: Pathogenesis and Treatment. J Clin Transl Hepatol. 2021 Oct 28;9(5):731-737. doi: 10.14218/JCTH.2020.00091. Epub 2021 Sep 14. PMID: 34722188; PMCID: PMC8516847.

Kornbrust DJ, MacDonald JS, Peter CP, Duchai DM, Stubbs RJ, Germershausen JI and Alberts AW. (1989) Toxicity of the HMG-coenzyme A reductase inhibitor, lovastatin, to rabbits., Journal of Pharmacology and Experimental Therapeutics, 248 , 498-505

Korzeniewski C, Callewaert DM. An enzyme-release assay for natural cytotoxicity. J Immunol Methods. 1983 Nov 25;64(3):313-20. doi: 10.1016/0022-1759(83)90438-6. PMID: 6199426.

Kostrubsky SE, Strom SC, Kalgutkar AS, Kulkarni S, Atherton J, Mireles R, Feng B, Kubik R, Hanson J, Urda E, Mutlib AE. Inhibition of hepatobiliary transport as a predictive method for clinical hepatotoxicity of nefazodone. Toxicol Sci. 2006 Apr;90(2):451-9. doi: 10.1093/toxsci/kfj095. Epub 2006 Jan 12. PMID: 16410371.

Kostrubsky V.E., Sinclair J.F., Ramachandran V., Venkataramanan R., Wen Y.H., Kindt E., Galchev V., Rose K., Sinz M., Strom S.C., The role of conjugation in hepatotoxicity of troglitazone in human and porcine hepatocyte cultures, Drug Metab. Disp. 28 (2000) 1192-1197.

Kroll A, Engqvist MKM, Heckmann D, Lercher MJ. Deep learning allows genome-scale prediction of Michaelis constants from structural features. PLoS Biol. 2021 Oct 19;19(10):e3001402.

Kučera O, Endlicher R, Rychtrmoc D, Lotková H, Sobotka O, Červinková Z. Acetaminophen toxicity in rat and mouse hepatocytes in vitro. Drug Chem Toxicol. 2017 Oct;40(4):448-456. doi: 10.1080/01480545.2016.1255953. Epub 2016 Dec 14. PMID: 27960556.

Kumar S, Samuel K, Subramanian R, Braun MP, Stearns RA, Chiu SH, Evans DC, Baillie TA. Extrapolation of diclofenac clearance from in vitro microsomal metabolism data: role of acyl glucuronidation and sequential oxidative metabolism of the acyl glucuronide. J Pharmacol Exp Ther. 2002 Dec;303(3):969-78. doi: 10.1124/jpet.102.038992. PMID: 12438516.

Kyrylkova K, Kyryachenko S, Leid M, Kioussi C. Detection of apoptosis by TUNEL assay. Methods Mol Biol. 2012;887:41-7. doi: 10.1007/978-1-61779-860-3_5. PMID: 22566045.

Laine L, Goldkind L, Curtis SP, Connors LG, Yanqiong Z, Cannon CP. How common is diclofenac-associated liver injury? Analysis of 17,289 arthritis patients in a long-term prospective clinical trial. Am J Gastroenterol. 2009 Feb;104(2):356-62. doi: 10.1038/ajg.2008.149. Epub 2009 Jan 27. PMID: 19174782.

Lamberti M, Porto S, Zappavigna S, Addeo E, Marra M, Miraglia N, Sannolo N, Vanacore D, Stiuso P, Caraglia M. A mechanistic study on the cardiotoxicity of 5-fluorouracil in vitro and clinical and occupational perspectives. Toxicol Lett. 2014 Jun 16;227(3):151-6. doi: 10.1016/j.toxlet.2014.03.018. Epub 2014 Apr 1. PMID: 24704391.

Lammert C, Bjornsson E, Niklasson A, Chalasani N. Oral medications with significant hepatic metabolism at higher risk for hepatic adverse events. Hepatology. 2010 Feb;51(2):615-20. doi: 10.1002/hep.23317. PMID: 19839004.

Langhans SA. Three-Dimensional in Vitro Cell Culture Models in Drug Discovery and Drug Repositioning. Front Pharmacol. 2018 Jan 23;9:6. doi: 10.3389/fphar.2018.00006. PMID: 29410625; PMCID: PMC5787088.

Langrock T, Hoffmann R. Analysis of Hydroxyproline in Collagen Hydrolysates. Methods Mol Biol. 2019;2030:47-56. doi: 10.1007/978-1-4939-9639-1_5. PMID: 31347109.

Lanza IR, Nair KS. Mitochondrial metabolic function assessed in vivo and in vitro. Curr Opin Clin Nutr Metab Care. 2010 Sep;13(5):511-7. doi: 10.1097/MCO.0b013e32833cc93d. PMID: 20616711; PMCID: PMC3070485.

Larrey D. Hépatites médicamenteuses: aspects épidémiologiques, cliniques, diagnostiques et physiopathologiques en 1995 [Drug-induced hepatitis: epidemiologic, clinical, diagnostic and physiopathologic aspects in 1995]. Rev Med Interne. 1995;16(10):752-8. French. doi: 10.1016/0248-8663(96)80784-3. PMID: 8525155.

Larson AM, Polson J, Fontana RJ, Davern TJ, Lalani E, Hynan LS, Reisch JS, Schiødt FV, Ostapowicz G, Shakil AO, Lee WM; Acute Liver Failure Study Group. Acetaminophen-induced acute liver failure: results of a United States multicenter, prospective study. Hepatology. 2005 Dec;42(6):1364-72. doi: 10.1002/hep.20948. PMID: 16317692.

Lasser KE, Allen PD, Woolhandler SJ, Himmelstein DU, Wolfe SM, Bor DH. Timing of new black box warnings and withdrawals for prescription medications. JAMA. 2002 May 1;287(17):2215-20. doi: 10.1001/jama.287.17.2215. PMID: 11980521.

Laster J, Satoskar R. Aspirin-Induced Acute Liver Injury. ACG Case Rep J. 2014 Oct 10;2(1):48-9. doi: 10.14309/crj.2014.81. PMID: 26157904; PMCID: PMC4435341.

Lauer B, Tuschl G, Kling M, Mueller SO. Species-specific toxicity of diclofenac and troglitazone in primary human and rat hepatocytes. Chem Biol Interact. 2009 Apr 15;179(1):17-24. doi: 10.1016/j.cbi.2008.10.031. Epub 2008 Oct 31. PMID: 19022234.

Lawsin L, Light JA. Severe acute renal failure after exposure to sirolimus–tacrolimus in two living donor kidney recipients. Transplantation 2003; 75: 157–160

Lebovitz HE, Kreider M and Freed MI. (2002) Evaluation of liver function in type 2 diabetic patients during clinical trials: evidence that rosiglitazone does not cause hepatic dysfunction., Diabetes Care, 25 , 815-821

Lee EW, Lai Y, Zhang H, Unadkat JD. Identification of the mitochondrial targeting signal of the human equilibrative nucleoside transporter 1 (hENT1): implications for interspecies differences in mitochondrial toxicity of fialuridine. J Biol Chem. 2006 Jun 16;281(24):16700-6. doi: 10.1074/jbc.M513825200. Epub 2006 Apr 4. PMID: 16595656.

Lee PJ, Hung PJ, Lee LP. An artificial liver sinusoid with a microfluidic endothelial-like barrier for primary hepatocyte culture. Biotechnol Bioeng. 2007 Aug 1;97(5):1340-6. doi: 10.1002/bit.21360. PMID: 17286266.

Lee S, Lee HA, Kim SJ, Kim KS. Cellular mechanisms for trazodone-induced cardiotoxicity. Hum Exp Toxicol. 2016 May;35(5):501-10. doi: 10.1177/0960327115595683. Epub 2015 Jul 17. PMID: 26187900.

Lee WM. (2003) Drug-induced hepatotoxicity., New England Journal of Medicine, 349 , 474-485

Lehmann DF, Eggleston WD, Wang D. Validation and Clinical Utility of the hERG IC50:Cmax Ratio to Determine the Risk of Drug-Induced Torsades de Pointes: A Meta-Analysis. Pharmacotherapy. 2018 Mar;38(3):341-348. doi: 10.1002/phar.2087. Epub 2018 Feb 19. PMID: 29380488.

Lenz W. A short history of thalidomide embryopathy. Teratology. 1988 Sep;38(3):203-15.

LePage KT, Dickey RW, Gerwick WH, Jester EL, Murray TF. On the use of neuro-2a neuroblastoma cells versus intact neurons in primary culture for neurotoxicity studies. Crit Rev Neurobiol. 2005;17(1):27-50. doi: 10.1615/critrevneurobiol.v17.i1.20. PMID: 16307526.

Leuratti C, Loprete L, Rossini M, Frangione V, Rovati S, Radicioni M. Pharmacokinetics and Safety of a Diclofenac Sodium 75 mg/1 mL Solution (Akis®/Dicloin®) Administered as a Single Intravenous Bolus Injection in Healthy Men and Women. Eur J Drug Metab Pharmacokinet. 2019 Oct;44(5):681-689. doi: 10.1007/s13318-019-00558-8. PMID: 31077065; PMCID: PMC6746683.

Levine M, Stellpflug SJ, Pizon AF, Peak DA, Villano J, Wiegand T, Dib C, Thomas SH. Hypoglycemia and lactic acidosis outperform King's College criteria for predicting death or transplant in acetaminophen toxic patients. Clin Toxicol (Phila). 2018 Jul;56(7):622-625.

Lewis A, Keshara R, Kim YH, Grapin-Botton A. Self-organization of organoids from endoderm-derived cells. J Mol Med (Berl). 2021 Apr;99(4):449-462. doi: 10.1007/s00109-020-02010-w. Epub 2020 Nov 22. PMID: 33221939; PMCID: PMC8026476.

Lewis JH, Ranard RC, Caruso A, Jackson LK, Mullick F, Ishak KG, Seeff LB and Zimmerman HJ. (1989) Amiodarone hepatotoxicity: prevalence and clinicopathologic correlations among 104 patients., Hepatology, 9 , 679-685 DOI: 10.1002/hep.1840090504

Lewis W, Dalakas MC. Mitochondrial toxicity of antiviral drugs. Nat Med. 1995 May;1(5):417-22. doi: 10.1038/nm0595-417. PMID: 7585087.

Lewis, D.F.; Ioannides, C.; Parke, D.V. Cytochromes P450 and species differences in xenobiotic metabolism and activation of carcinogen. Environ. Health Perspect. 1998, 106, 633–641.

Li C, Grillo MP and Benet LZ. (2003). In vivo mechanistic studies on the metabolic activation of 2-phenylpropionic acid in rat., Journal of Pharmacology and Experimental Therapeutics, 305 , 250-256

Li Y, Yan XP, Chen C, Xia YL, Jiang Y. Human serum albumin-mercurial species interactions. J Proteome Res. 2007 Jun;6(6):2277-86. doi: 10.1021/pr0700403. Epub 2007 May 10. PMID: 17489621.

Li, Jinpeng; Settivari, Raja S.; LeBaron, Matthew J.; Marty, Mary Sue (2019). Functional Comparison of HepaRG Cells and Primary Human Hepatocytes in Sandwich and Spheroid Culture as Repeated-Exposure Models for Hepatotoxicity. Applied In Vitro Toxicology, 5(4), 187–195. doi:10.1089/aivt.2019.0008

Liang Y, Yan C, Schor NF. Apoptosis in the absence of caspase 3. Oncogene. 2001 Oct 4;20(45):6570-8. doi: 10.1038/sj.onc.1204815. PMID: 11641782.

Lim MS, Lim PL, Gupta R, Boelsterli UA. Critical role of free cytosolic calcium, but not uncoupling, in mitochondrial permeability transition and cell death induced by diclofenac oxidative metabolites in immortalized human hepatocytes. Toxicol Appl Pharmacol. 2006 Dec 15;217(3):322-31. doi: 10.1016/j.taap.2006.09.012. Epub 2006 Oct 5. PMID: 17097122.

Lin RZ, Chou LF, Chien CC, Chang HY. Dynamic analysis of hepatoma spheroid formation: roles of E-cadherin and beta1-integrin. Cell Tissue Res. 2006 Jun;324(3):411-22. doi: 10.1007/s00441-005-0148-2. Epub 2006 Feb 18. PMID: 16489443.

Liston DR, Davis M. Clinically Relevant Concentrations of Anticancer Drugs: A Guide for Nonclinical Studies. Clin Cancer Res. 2017 Jul 15;23(14):3489-3498. doi: 10.1158/1078-0432.CCR-16-3083. Epub 2017 Mar 31. PMID: 28364015; PMCID: PMC5511563.

Liu W, Zeng X, Liu Y, Liu J, Li C, Chen L, Chen H, Ouyang D. The Immunological Mechanisms and Immune-Based Biomarkers of Drug-Induced Liver Injury. Front Pharmacol. 2021 Oct 15;12:723940. doi: 10.3389/fphar.2021.723940. PMID: 34721020; PMCID: PMC8554067.

LiverTox: Clinical and Research Information on Drug-Induced Liver Injury [Internet]. Bethesda (MD): National Institute of Diabetes and Digestive and Kidney Diseases; 2012-. Acetaminophen. [Updated 2016 Jan 28]. Available from: https://www.ncbi.nlm.nih.gov/books/NBK548162/

LiverTox: Clinical and Research Information on Drug-Induced Liver Injury .Bethesda (MD): National Institute of Diabetes and Digestive and Kidney Diseases; 2012-. Simvastatin. [Updated 2021 Dec 1]. Available from: https://www.ncbi.nlm.nih.gov/books/NBK548720/

LiverTox: Clinical and Research Information on Drug-Induced Liver Injury [Internet]. Bethesda (MD): National Institute of Diabetes and Digestive and Kidney Diseases; 2012-. Nefazodone. [Updated 2020 Mar 6]. Available from: https://www.ncbi.nlm.nih.gov/books/NBK548179/

LiverTox: Clinical and Research Information on Drug-Induced Liver Injury [Internet]. Bethesda (MD): National Institute of Diabetes and Digestive and Kidney Diseases; 2012-. Acute Fatty Liver with Lactic Acidosis and Hepatic Dysfunction. [Updated 2019 May 4]. Available from: https://www.ncbi.nlm.nih.gov/books/NBK547917/

LiverTox: Clinical and Research Information on Drug-Induced Liver Injury [Internet]. Bethesda (MD): National Institute of Diabetes and Digestive and Kidney Diseases; 2012-. Amiodarone. [Updated 2016 Mar 1]. Available from: https://www.ncbi.nlm.nih.gov/books/NBK548109/

Lomakina GY, Modestova YA, Ugarova NN. Bioluminescence assay for cell viability. Biochemistry (Mosc). 2015 Jun;80(6):701-13. doi: 10.1134/S0006297915060061. PMID: 26531016.

Long TJ, Cosgrove PA, Dunn RT 2nd, Stolz DB, Hamadeh H, Afshari C, McBride H, Griffith LG. Modeling Therapeutic Antibody-Small Molecule Drug-Drug Interactions Using a Three-Dimensional Perfusable Human Liver Coculture Platform. Drug Metab Dispos. 2016 Dec;44(12):1940-1948. doi: 10.1124/dmd.116.071456. Epub 2016 Sep 12. PMID: 27621203; PMCID: PMC5118635.

Lorente S, Hautefeuille M, Sanchez-Cedillo A. The liver, a functionalized vascular structure. Sci Rep. 2020 Oct 1;10(1):16194. doi: 10.1038/s41598-020-73208-8. PMID: 33004881; PMCID: PMC7531010.

Louch WE, Sheehan KA, Wolska BM. Methods in cardiomyocyte isolation, culture, and gene transfer. J Mol Cell Cardiol. 2011 Sep;51(3):288-98. doi: 10.1016/j.yjmcc.2011.06.012. Epub 2011 Jun 24. PMID: 21723873; PMCID: PMC3164875.

Louisse J, Wüst RCI, Pistollato F, Palosaari T, Barilari M, Macko P, Bremer S, Prieto P. Assessment of acute and chronic toxicity of doxorubicin in human induced pluripotent stem cell-derived cardiomyocytes. Toxicol In Vitro. 2017 Aug;42:182-190. doi: 10.1016/j.tiv.2017.04.023. Epub 2017 Apr 26. PMID: 28456566.

Lucena MI, Andrade RJ, Gomez-Outes A, Rubio M, Cabello MR. Acute liver failure after treatment with nefazodone. Dig Dis Sci. 1999 Dec;44(12):2577-9. doi: 10.1023/a:1026620029470. PMID: 10630516.

Luttringer O, Theil FP, Lavé T, Wernli-Kuratli K, Guentert TW, de Saizieu A. Influence of isolation procedure, extracellular matrix and dexamethasone on the regulation of membrane transporters gene expression in rat hepatocytes. Biochem Pharmacol. 2002 Dec 1;64(11):1637-50. doi: 10.1016/s0006-2952(02)01382-5. PMID: 12429353.

Lv HJ, Zhao HW. Amiodarone-induced hepatotoxicity - quantitative measurement of iodine density in the liver using dual-energy computed tomography: Three case reports. World J Clin Cases. 2020 Oct 26;8(20):4958-4965. doi: 10.12998/wjcc.v8.i20.4958. PMID: 33195667; PMCID: PMC7642530.

Lwakatare JM, Morris-Jones S, Knight EJ. Fatal fulminating liver failure possibly related to amiodarone treatment. Br J Hosp Med. 1990; 44:60-61.

Macdonald JS. Toxicity of 5-fluorouracil. Oncology (Williston Park). 1999 Jul;13(7 Suppl 3):33-4. PMID: 10442356.

MacFadyen RJ, Palmer TJ, Hisamuddin K. Rapidly fatal acute amiodarone hepatitis occurring in the context of multiple organ failure. Int J Cardiol. 2003;91:245-247.

Mak IT, Chmielinska JJ, Kramer JH, Weglicki WB. AZT-induced oxidative cardiovascular toxicity: attenuation by Mg-supplementation. Cardiovasc Toxicol. 2009 Jun;9(2):78-85. doi: 10.1007/s12012-009-9040-8. Epub 2009 May 12. PMID: 19484392; PMCID: PMC3734550.

Mak IW, Evaniew N, Ghert M. Lost in translation: animal models and clinical trials in cancer treatment. Am J Transl Res. 2014 Jan 15;6(2):114-8. PMID: 24489990; PMCID: PMC3902221.

Malik SW, Myers JL, DeRemee RA, Specks U. Lung toxicity associated with cyclophosphamide use. Two distinct patterns. Am J Respir Crit Care Med. 1996 Dec;154(6 Pt 1):1851-6. doi: 10.1164/ajrccm.154.6.8970380. PMID: 8970380.

Manning FJ, Swartz M, editors. Institute of Medicine (US) Committee to Review the Fialuridine (FIAU/FIAC) Clinical Trials; Review of the Fialuridine (FIAU) Clinical Trials. Washington (DC): National Academies Press (US); 1995. Executive Summary. Available from: https://www.ncbi.nlm.nih.gov/books/NBK232082/

Manoguerra AS, Erdman AR, Woolf AD, Chyka PA, Caravati EM, Scharman EJ, Booze LL, Christianson G, Nelson LS, Cobaugh DJ, Troutman WG; American Association of Poison Control Centers. Valproic acid poisoning: an evidence-based consensus guideline for out-of-hospital management. Clin Toxicol (Phila). 2008 Aug;46(7):661-76. doi: 10.1080/15563650802178136. PMID: 18608263.

Mansoorifar A, Gordon R, Bergan R, Bertassoni LE. Bone-on-a-chip: microfluidic technologies and microphysiologic models of bone tissue. Adv Funct Mater. 2021 Feb 3;31(6):2006796. doi: 10.1002/adfm.202006796. Epub 2020 Oct 25. PMID: 35422682; PMCID: PMC9007546.

Mariño G, Kroemer G. Mechanisms of apoptotic phosphatidylserine exposure. Cell Res. 2013 Nov;23(11):1247-8. doi: 10.1038/cr.2013.115. Epub 2013 Aug 27. PMID: 23979019; PMCID: PMC3817543.

Marion MJ, Hantz O, Durantel D. The HepaRG cell line: biological properties and relevance as a tool for cell biology, drug metabolism, and virology studies. Methods Mol Biol. 2010;640:261-72. doi: 10.1007/978-1-60761-688-7_13. PMID: 20645056.

Marti HP, Frey FJ. Nephrotoxicity of rapamycin: an emerging problem in clinical medicine. Nephrol Dial Transplant. 2005 Jan;20(1):13-5. doi: 10.1093/ndt/gfh639. PMID: 15632347.

Martignoni M, Groothuis GM, de Kanter R. Species differences between mouse, rat, dog, monkey and human CYP-mediated drug metabolism, inhibition and induction. Expert Opin Drug Metab Toxicol. 2006 Dec;2(6):875-94. doi: 10.1517/17425255.2.6.875. PMID: 17125407.

Martinez MA, Vuppalanchi R, Fontana RJ, Stolz A, Kleiner DE, Hayashi PH, Gu J, Hoofnagle JH, Chalasani N. Clinical and histologic features of azithromycin-induced liver injury. Clin Gastroenterol Hepatol. 2015 Feb;13(2):369-376.e3. doi: 10.1016/j.cgh.2014.07.054. Epub 2014 Aug 9. PMID: 25111234; PMCID: PMC4321982.

Martinez V, Henary M. Nile Red and Nile Blue: Applications and Syntheses of Structural Analogues. Chemistry. 2016 Sep 19;22(39):13764-13782. doi: 10.1002/chem.201601570. Epub 2016 Jul 13. PMID: 27406265.https://doi.org/10.1186/s12944-018-0663-2

Marumoto A, Roytman MM, Tsai NC. Trial and error: investigational drug induced liver injury, a case series report. Hawaii J Med Public Health. 2013 Sep;72(9 Suppl 4):30-3. PMID: 24052916; PMCID: PMC3764585.

Massart, J., Borgne-Sanchez, A., Fromenty, B. (2018). Drug-Induced Mitochondrial Toxicity. In: Oliveira, P. (eds) Mitochondrial Biology and Experimental Therapeutics. Springer, Cham. https://doi.org/10.1007/978-3-319-73344-9_13

Masubuchi Y. Metabolic and non-metabolic factors determining troglitazone hepatotoxicity: a review. Drug Metab Pharmacokinet. 2006 Oct;21(5):347-56. doi: 10.2133/dmpk.21.347. PMID: 17072088.

Matsui T, Shinozawa T. Human Organoids for Predictive Toxicology Research and Drug Development. Front Genet. 2021 Nov 1;12:767621. doi: 10.3389/fgene.2021.767621. PMID: 34790228; PMCID: PMC8591288.

Matsumoto S, Hirama T, Kim HJ, Nagata K, Yamazoe Y. In vitro inhibition of human small intestinal and liver microsomal astemizole O-demethylation: different contribution of CYP2J2 in the small intestine and liver. Xenobiotica. 2003 Jun;33(6):615-23. doi: 10.1080/0049825031000105778. PMID: 12851038.

Matsumoto S, Yamazoe Y. Involvement of multiple human cytochromes P450 in the liver microsomal metabolism of astemizole and a comparison with terfenadine. Br J Clin Pharmacol. 2001 Feb;51(2):133-42. doi: 10.1111/j.1365-2125.2001.01292.x. PMID: 11259984; PMCID: PMC2014443.

Matsuo M, Terai K, Kameda N, Matsumoto A, Kurokawa Y, Funase Y, Nishikawa K, Sugaya N, Hiruta N, Kishimoto T. Designation of enzyme activity of glycine-N-acyltransferase family genes and depression of glycine-N-acyltransferase in human hepatocellular carcinoma. Biochem Biophys Res Commun. 2012 Apr 20;420(4):901-6. doi: 10.1016/j.bbrc.2012.03.099. Epub 2012 Mar 27. PMID: 22475485.

Mazaleuskaya LL, Sangkuhl K, Thorn CF, FitzGerald GA, Altman RB, Klein TE. PharmGKB summary: pathways of acetaminophen metabolism at the therapeutic versus toxic doses. Pharmacogenet Genomics. 2015 Aug;25(8):416-26. doi: 10.1097/FPC.0000000000000150. PMID: 26049587; PMCID: PMC4498995.

McCauley HA, Wells JM. Pluripotent stem cell-derived organoids: using principles of developmental biology to grow human tissues in a dish. Development. 2017 Mar 15;144(6):958-962. doi: 10.1242/dev.140731. PMID: 28292841; PMCID: PMC5358106.

McClain RM. (1995). Mechanistic considerations for the relevance of animal data on thyroid neoplasia to human risk assessment., Mutation Research, 333 , 131-142. DOI: 10.1016/0027-5107(95)00139-5

McGill MR, Jaeschke H. Biomarkers of drug-induced liver injury: progress and utility in research, medicine, and regulation. Expert Rev Mol Diagn. 2018 Sep;18(9):797-807.

McGill MR, Jaeschke H. Metabolism and disposition of acetaminophen: recent advances in relation to hepatotoxicity and diagnosis. Pharm Res. 2013 Sep;30(9):2174-87. doi: 10.1007/s11095-013-1007-6. Epub 2013 Mar 6. PMID: 23462933; PMCID: PMC3709007.

McKenzie R, Fried MW, Sallie R, Conjeevaram H, Di Bisceglie AM, Park Y, Savarese B, Kleiner D, Tsokos M, Luciano C, et al. Hepatic failure and lactic acidosis due to fialuridine (FIAU), an investigational nucleoside analogue for chronic hepatitis B. N Engl J Med. 1995 Oct 26;333(17):1099-105. doi: 10.1056/NEJM199510263331702. PMID: 7565947.

McKoy JM, Angelotta C, Bennett CL, Tallman MS, Wadleigh M, Evens AM, Kuzel TM, Trifilio SM, Raisch DW, Kell J, DeAngelo DJ, Giles FJ. Gemtuzumab ozogamicin-associated sinusoidal obstructive syndrome (SOS): an overview from the research on adverse drug events and reports (RADAR) project. Leuk Res. 2007 May;31(5):599-604. doi: 10.1016/j.leukres.2006.07.005. Epub 2006 Sep 7. PMID: 16959316.

Mehlem A, Hagberg CE, Muhl L, Eriksson U, Falkevall A. Imaging of neutral lipids by oil red O for analyzing the metabolic status in health and disease. Nat Protoc. 2013 Jun;8(6):1149-54. doi: 10.1038/nprot.2013.055. Epub 2013 May 23. PMID: 23702831.

Menassé R, Hedwall PR, Kraetz J, Pericin C, Riesterer L, Sallmann A, Ziel R, Jaques R. Pharmacological properties of diclofenac sodium and its metabolites. Scand J Rheumatol Suppl. 1978;(22):5-16. doi: 10.3109/03009747809097211. PMID: 98835.

Meng X, Mojaverian P, Doedée M, Lin E, Weinryb I, Chiang ST, Kowey PR. Bioavailability of amiodarone tablets administered with and without food in healthy subjects. Am J Cardiol. 2001 Feb 15;87(4):432-5. doi: 10.1016/s0002-9149(00)01396-5. PMID: 11179527.

Meregalli C. An Overview of Bortezomib-Induced Neurotoxicity. Toxics. 2015 Jul 27;3(3):294-303. doi: 10.3390/toxics3030294. PMID: 29051465; PMCID: PMC5606681.

Merten OW, Hebben M, Bovolenta C. Production of lentiviral vectors. Mol Ther Methods Clin Dev. 2016 Apr 13;3:16017. doi: 10.1038/mtm.2016.17. PMID: 27110581; PMCID: PMC4830361.

Mertz DR, Ahmed T, Takayama S. Engineering cell heterogeneity into organs-on-a-chip. Lab Chip. 2018 Aug 7;18(16):2378-2395. doi: 10.1039/c8lc00413g. PMID: 30040104; PMCID: PMC6081245.

Metushi I, Uetrecht J, Phillips E. Mechanism of isoniazid-induced hepatotoxicity: then and now. Br J Clin Pharmacol. 2016 Jun;81(6):1030-6. doi: 10.1111/bcp.12885. Epub 2016 Feb 25. PMID: 26773235; PMCID: PMC4876174.

Meunier L, Larrey D. Drug-Induced Liver Injury: Biomarkers, Requirements, Candidates, and Validation. Front Pharmacol. 2019 Dec 11;10:1482. doi: 10.3389/fphar.2019.01482. PMID: 31920666; PMCID: PMC6917655.

Mia Baxter-Holland, Crispin R Dass, Doxorubicin, mesenchymal stem cell toxicity and antitumour activity: implications for clinical use, Journal of Pharmacy and Pharmacology, Volume 70, Issue 3, March 2018, Pages 320–327, https://doi.org/10.1111/jphp.12869

Michaleas SN, Veskoukis AS, Samonis G, Pantos C, Androutsos G, Karamanou M. Mathieu Joseph Bonaventure Orfila (1787-1853): The Founder of Modern Toxicology. Maedica (Bucur). 2022 Jun;17(2):532-537.

Mihajlovic M, Vinken M. Mitochondria as the Target of Hepatotoxicity and Drug-Induced Liver Injury: Molecular Mechanisms and Detection Methods. Int J Mol Sci. 2022 Mar 18;23(6):3315. doi: 10.3390/ijms23063315. PMID: 35328737; PMCID: PMC8951158.

Mihalik SJ, Steinberg SJ, Pei Z, Park J, Kim DG, Heinzer AK, Dacremont G, Wanders RJ, Cuebas DA, Smith KD, Watkins PA. Participation of two members of the very long-chain acyl-CoA synthetase family in bile acid synthesis and recycling. J Biol Chem. 2002 Jul 5;277(27):24771-9. doi: 10.1074/jbc.M203295200. Epub 2002 Apr 29. PMID: 11980911.

Mikamo E, Harada S, Nishikawa J and Nishihara T. (2003) Endocrine disruptors induce cytochrome P450 by affecting transcriptional regulation via pregnane X receptor., Toxicology and Applied Pharmacology, 193 , 66-72 DOI: 10.1016/j.taap.2003.08.001

Mikiewicz M, Otrocka-Domagała I, Paździor-Czapula K. Influence of simvastatin on hepatocytes - histopathological and immunohistochemical study. Pol J Vet Sci. 2019 Jun;22(2):263-270. doi: 10.24425/pjvs.2019.127095. PMID: 31269349.

Milazzo E, Orellana G, Briceño-Bierwirth A, Korrapati VK. Acute lung toxicity by nitrofurantoin. BMJ Case Rep. 2021 Apr 14;14(4):e237571. doi: 10.1136/bcr-2020-237571. PMID: 33853812; PMCID: PMC8054053.

Miller, J.J. Targeting IDH-Mutant Glioma. Neurotherapeutics 19, 1724–1732 (2022). https://doi.org/10.1007/s13311-022-01238-3

Minderman H, Linssen PC, Wessels JM, Haanen C. Doxorubicin toxicity in relation to the proliferative state of human hematopoietic cells. Exp Hematol. 1991 Feb;19(2):110-4. PMID: 1991492.

Mingzhu Yan, Yazhen Huo, Shutao Yin, Hongbo Hu, Mechanisms of acetaminophen-induced liver injury and its implications for therapeutic interventions,Redox Biology, Volume 17, 2018, Pages 274-283, ISSN 2213-2317, https://doi.org/10.1016/j.redox.2018.04.019.

Mirabelli P, Coppola L, Salvatore M. Cancer Cell Lines Are Useful Model Systems for Medical Research. Cancers (Basel). 2019 Aug 1;11(8):1098. doi: 10.3390/cancers11081098. PMID: 31374935; PMCID: PMC6721418.

Mitcheson JS, Chen J, Lin M, Culberson C and Sanguinetti MC. (2000) A structural basis for drug-induced long QT syndrome., Proceedings of the National Academy of Sciences of the United States of America, 97 , 12329-12333 DOI: 10.1073/pnas.210244497

Mitry, R.R., Hughes, R.D., Bansal, S., Lehec, S.C., Wendon, J.A., Dhawan, A., 2005. Effects of serum from patients with acute liver failure due to paracetamol overdose on human hepatocytes in vitro. Transplantation Proceedings 37, 2391–2394.

Mohan G, Ajitkumar A, Bhide P, Ravilla J, Kramer V. Trazodone Overdose Manifesting as Hypotension and QT Prolongation. Cureus. 2023 Mar 29;15(3):e36871. doi: 10.7759/cureus.36871. PMID: 37123743; PMCID: PMC10147490.

Moman RN, Gupta N, Varacallo M. Physiology, Albumin. [Updated 2022 Dec 26]. In: StatPearls [Internet]. Treasure Island (FL): StatPearls Publishing; 2024 Jan-. Available from: https://www.ncbi.nlm.nih.gov/books/NBK459198/

Moon SJ, Lee S, Jang K, Yu KS, Yim SV, Kim BH. Comparative pharmacokinetic and tolerability evaluation of two simvastatin 20 mg formulations in healthy Korean male volunteers. Transl Clin Pharmacol. 2017 Mar;25(1):10-14. doi: 10.12793/tcp.2017.25.1.10. Epub 2017 Mar 15. PMID: 32095453; PMCID: PMC7033535.

Moore N. Coronary Risks Associated with Diclofenac and Other NSAIDs: An Update. Drug Saf. 2020 Apr;43(4):301-318. doi: 10.1007/s40264-019-00900-8. PMID: 31916080.

Morciano G, Sarti AC, Marchi S, Missiroli S, Falzoni S, Raffaghello L, Pistoia V, Giorgi C, Di Virgilio F, Pinton P. Use of luciferase probes to measure ATP in living cells and animals. Nat Protoc. 2017 Aug;12(8):1542-1562. doi: 10.1038/nprot.2017.052. Epub 2017 Jul 6. PMID: 28683062.

Moreau P, Karamanesht II, Domnikova N, Kyselyova MY, Vilchevska KV, Doronin VA, Schmidt A, Hulin C, Leleu X, Esseltine DL, Venkatakrishnan K, Skee D, Feng H, Girgis S, Cakana A, van de Velde H, Deraedt W, Facon T. Pharmacokinetic, pharmacodynamic and covariate analysis of subcutaneous versus intravenous administration of bortezomib in patients with relapsed multiple myeloma. Clin Pharmacokinet. 2012 Dec;51(12):823-9. doi: 10.1007/s40262-012-0010-0. PMID: 23018466.

Morgan K, Martucci N, Kozlowska A, Gamal W, Brzeszczyński F, Treskes P, Samuel K, Hayes P, Nelson L, Bagnaninchi P, Brzeszczynska J, Plevris J. Chlorpromazine toxicity is associated with disruption of cell membrane integrity and initiation of a pro-inflammatory response in the HepaRG hepatic cell line. Biomed Pharmacother. 2019 Mar;111:1408-1416. doi: 10.1016/j.biopha.2019.01.020. Epub 2019 Jan 19. PMID: 30841456.

Mormone E, George J, Nieto N. Molecular pathogenesis of hepatic fibrosis and current therapeutic approaches. Chem Biol Interact. 2011 Sep 30;193(3):225-31. doi: 10.1016/j.cbi.2011.07.001. Epub 2011 Jul 22. PMID: 21803030; PMCID: PMC3171510.

Morris DJ. Adverse effects and drug interactions of clinical importance with antiviral drugs. Drug Saf. 1994 Apr;10(4):281-91. doi: 10.2165/00002018-199410040-00002. PMID: 8018300.

Mosedale M, Watkins PB. Drug-induced liver injury: Advances in mechanistic understanding that will inform risk management. Clin Pharmacol Ther. 2017 Apr;101(4):469-480. doi: 10.1002/cpt.564. Epub 2017 Jan 11. PMID: 27861792; PMCID: PMC5359062.

Mosmann T. Rapid colorimetric assay for cellular growth and survival: application to proliferation and cytotoxicity assays. J Immunol Methods. 1983 Dec 16;65(1-2):55-63. doi: 10.1016/0022-1759(83)90303-4. PMID: 6606682.

Mudd TW, Guddati AK. Management of hepatotoxicity of chemotherapy and targeted agents. Am J Cancer Res. 2021 Jul 15;11(7):3461-3474. PMID: 34354855; PMCID: PMC8332851.

Mueller D, Tascher G, Damm G, Nüssler AK, Heinzle E, Noor F. Real-time in situ viability assessment in a 3D bioreactor with liver cells using resazurin assay. Cytotechnology. 2013 Mar;65(2):297-305. doi: 10.1007/s10616-012-9486-6. Epub 2012 Jul 25. PMID: 22828753; PMCID: PMC3560875.

Mueller SO, Guillouzo A, Hewitt PG, Richert L. Drug biokinetic and toxicity assessments in rat and human primary hepatocytes and HepaRG cells within the EU-funded Predict-IV project. Toxicol In Vitro. 2015 Dec 25;30(1 Pt A):19-26. doi: 10.1016/j.tiv.2015.04.014. Epub 2015 May 4. PMID: 25952325.

Murphy EJ, Davern TJ, Shakil AO, Shick L, Masharani U, Chow H, Freise C, Lee WM, Bass NM. Troglitazone-induced fulminant hepatic failure. Acute Liver Failure Study Group. Dig Dis Sci. 2000 Mar;45(3):549-53. doi: 10.1023/a:1005405526283. PMID: 10749332.

Murphy B, Coldeway J, Raeside D. Fatal acute fulminant hepatic failure caused by parenteral amiodarone: a case report and review of the literature. Scott Med J. 2009;54:58-58

Müsch A. The unique polarity phenotype of hepatocytes. Exp Cell Res. 2014 Nov 1;328(2):276-83. doi: 10.1016/j.yexcr.2014.06.006. Epub 2014 Jun 20. PMID: 24956563; PMCID: PMC4254207.

Nag S, Baidya ATK, Mandal A, Mathew AT, Das B, Devi B, Kumar R. Deep learning tools for advancing drug discovery and development. 3 Biotech. 2022 May;12(5):110. doi: 10.1007/s13205-022-03165-8. Epub 2022 Apr 9. PMID: 35433167; PMCID: PMC8994527.

Nagata T, Takata K, Shakado S, Hirai F. Amiodarone-induced hepatotoxicity. BMJ Case Rep. 2023 Nov 1;16(11):e256679. doi: 10.1136/bcr-2023-256679. PMID: 37914162; PMCID: PMC10626883.

Naruse K, Tang W, Makuuch M. Artificial and bioartificial liver support: a review of perfusion treatment for hepatic failure patients. World J Gastroenterol. 2007 Mar 14;13(10):1516-21. doi: 10.3748/wjg.v13.i10.1516. PMID: 17461442; PMCID: PMC4146892.

National Center for Biotechnology Information (2024). PubChem Compound Summary for CID 12560, Erythromycin. Retrieved March 29, 2024 from https://pubchem.ncbi.nlm.nih.gov/compound/Erythromycin.

Nebot C, Moutet M, Huet P, Xu JZ, Yadan JC, Chaudiere J. Spectrophotometric assay of superoxide dismutase activity based on the activated autoxidation of a tetracyclic catechol. Anal Biochem. 1993 Nov 1;214(2):442-51. doi: 10.1006/abio.1993.1521. PMID: 8109732.

Nelson SD. Molecular mechanisms of the hepatotoxicity caused by acetaminophen. Semin Liver Dis. 1990 Nov;10(4):267-78. doi: 10.1055/s-2008-1040482. PMID: 2281334.

Nichols WG, Steel HM, Bonny T, Adkison K, Curtis L, Millard J, Kabeya K, Clumeck N. Hepatotoxicity observed in clinical trials of aplaviroc (GW873140). Antimicrob Agents Chemother. 2008 Mar;52(3):858-65. doi: 10.1128/AAC.00821-07. Epub 2007 Dec 10. PMID: 18070967; PMCID: PMC2258506.

NIH. LiverTox: Clinical and Research Information on Drug-Induced Liver Injury. Bethesda: National Institutes of Health, U.S. Department of Health & Human Services; 2018. https://livertox. nih.gov/.

Niles AL, Moravec RA, Eric Hesselberth P, Scurria MA, Daily WJ, Riss TL. A homogeneous assay to measure live and dead cells in the same sample by detecting different protease markers. Anal Biochem. 2007 Jul 15;366(2):197-206. doi: 10.1016/j.ab.2007.04.007. Epub 2007 Apr 12. PMID: 17512890.

Niles AL, Moravec RA, Riss TL. Update on in vitro cytotoxicity assays for drug development. Expert Opin Drug Discov. 2008 Jun;3(6):655-69. doi: 10.1517/17460441.3.6.655. PMID: 23506147.

Nique F, Hebbe S, Peixoto C, Annoot D, Lefrancois JM, Duval E, Michoux L, Triballeau N, Lemoullec JM, Mollat P, Thauvin M, Prange T, Minet D, Clement-Lacroix P, Robin-Jagerschmidt C, Fleury D, Guedin D and Deprez P. (2012) Discovery of diarylhydantoins as new selective androgen receptor modulators., Journal of Medicinal Chemistry, 55 , 8225-8235 DOI: 10.1021/jm300249m

Nissen SE, Wolski K, Topol EJ. Effect of muraglitazar on death and major adverse cardiovascular events in patients with type 2 diabetes mellitus. JAMA. 2005 Nov 23;294(20):2581-6. doi: 10.1001/jama.294.20.joc50147. Epub 2005 Oct 20. PMID: 16239637.

Nochi Z, Olsen RKJ, Gregersen N. Short-chain acyl-CoA dehydrogenase deficiency: from gene to cell pathology and possible disease mechanisms. J Inherit Metab Dis. 2017 Sep;40(5):641-655. doi: 10.1007/s10545-017-0047-1. Epub 2017 May 17. PMID: 28516284.

Noor A, Preuss CV. Amphotericin B. [Updated 2023 Mar 24]. In: StatPearls [Internet]. Treasure Island (FL): StatPearls Publishing; 2023 Jan-. Available from: https://www.ncbi.nlm.nih.gov/books/NBK482327/

Noor F, Niklas J, Müller-Vieira U, Heinzle E. An integrated approach to improved toxicity prediction for the safety assessment during preclinical drug development using Hep G2 cells. Toxicol Appl Pharmacol. 2009 Jun 1;237(2):221-31. doi: 10.1016/j.taap.2009.03.011. Epub 2009 Mar 28. PMID: 19332084.

NTP, National Toxicology Program. (2000) Toxicity studies of benzophenone (CAS RN 119-61-19) administered in feed to F344/N rats and B6C3F1 mice., National Toxicology Program Report,

Nunes AS, Barros AS, Costa EC, Moreira AF, Correia IJ. 3D tumor spheroids as in vitro models to mimic in vivo human solid tumors resistance to therapeutic drugs. Biotechnol Bioeng. 2019 Jan;116(1):206-226. doi: 10.1002/bit.26845. Epub 2018 Oct 27. PMID: 30367820.

O'Brien, P.J.; Chan, K.; Silber, P.M. Human and animal hepatocytes in vitro with extrapolation in vivo. Chem. Biol. Interact. 2004, 150, 97–114.

O'Connor N, Dargan PI, Jones AL. Hepatocellular damage from non-steroidal anti-inflammatory drugs. QJM. 2003 Nov;96(11):787-91. doi: 10.1093/qjmed/hcg138. PMID: 14566034.

Octavia Y, Tocchetti CG, Gabrielson KL, Janssens S, Crijns HJ, Moens AL. Doxorubicin-induced cardiomyopathy: from molecular mechanisms to therapeutic strategies. J Mol Cell Cardiol. 2012 Jun;52(6):1213-25. doi: 10.1016/j.yjmcc.2012.03.006. Epub 2012 Mar 21. PMID: 22465037.

Oken MM, Crooke ST, Elson MK, Strong JE, Shafer RB. Pharmacokinetics of bleomycin after im administration in man. Cancer Treat Rep. 1981 May-Jun;65(5-6):485-9. PMID: 6165473.

Oktay Tacar, Pornsak Sriamornsak, Crispin R Dass, Doxorubicin: an update on anticancer molecular action, toxicity and novel drug delivery systems, Journal of Pharmacy and Pharmacology, Volume 65, Issue 2, February 2013, Pages 157–170, https://doi.org/10.1111/j.2042-7158.2012.01567.x

Ölander M, Wiśniewski JR, Flörkemeier I, Handin N, Urdzik J, Artursson P. A simple approach for restoration of differentiation and function in cryopreserved human hepatocytes. Arch Toxicol. 2019 Mar;93(3):819-829. doi: 10.1007/s00204-018-2375-9. Epub 2018 Dec 17. PMID: 30560367.

Olson H, Betton G, Robinson D, Thomas K, Monro A, Kolaja G, Lilly P, Sanders J, Sipes G, Bracken W, Dorato M, Van Deun K, Smith P, Berger B, Heller A. Concordance of the toxicity of pharmaceuticals in humans and in animals. Regul Toxicol Pharmacol. 2000 Aug;32(1):56-67. doi: 10.1006/rtph.2000.1399. PMID: 11029269.

Onakpoya IJ, Heneghan CJ, Aronson JK. Post-marketing withdrawal of 462 medicinal products because of adverse drug reactions: a systematic review of the world literature. BMC Med. 2016 Feb 4;14:10. doi: 10.1186/s12916-016-0553-2. Erratum in: BMC Med. 2019 Mar 2;17(1):56. PMID: 26843061; PMCID: PMC4740994.

Ordooei Javan A, Shokouhi S, Sahraei Z. A review on colistin nephrotoxicity. Eur J Clin Pharmacol. 2015 Jul;71(7):801-10. doi: 10.1007/s00228-015-1865-4. Epub 2015 May 27. PMID: 26008213.

Orman ES, Conjeevaram HS, Vuppalanchi R, Freston JW, Rochon J, Kleiner DE, Hayashi PH; DILIN Research Group. Clinical and histopathologic features of fluoroquinolone-induced liver injury. Clin Gastroenterol Hepatol. 2011 Jun;9(6):517-523.e3. doi: 10.1016/j.cgh.2011.02.019. Epub 2011 Feb 26. PMID: 21356330; PMCID: PMC3718017.

O'Sullivan JM, Huddart RA, Norman AR, Nicholls J, Dearnaley DP, Horwich A. Predicting the risk of bleomycin lung toxicity in patients with germ-cell tumours. Ann Oncol. 2003 Jan;14(1):91-6. doi: 10.1093/annonc/mdg020. PMID: 12488299.

Ott LM, Ramachandran K, Stehno-Bittel L. An Automated Multiplexed Hepatotoxicity and CYP Induction Assay Using HepaRG Cells in 2D and 3D. SLAS Discov. 2017 Jun;22(5):614-625. doi: 10.1177/2472555217701058. Epub 2017 Mar 27. PMID: 28346810.

Özkarakaş H, Köse I, Zincircioğlu Ç, Ersan S, Ersan G, Şenoğlu N, Köse Ş, Erbay RH. Risk factors for colistin-associated nephrotoxicity and mortality in critically ill patients. Turk J Med Sci. 2017 Aug 23;47(4):1165-1172. doi: 10.3906/sag-1604-60. PMID: 29156858.

Padda MS, Sanchez M, Akhtar AJ, Boyer JL. Drug-induced cholestasis. Hepatology. 2011 Apr;53(4):1377-87. doi: 10.1002/hep.24229. PMID: 21480339; PMCID: PMC3089004.

Page B, Page M, Noel C. A new fluorometric assay for cytotoxicity measurements in-vitro. Int J Oncol. 1993 Sep;3(3):473-6. PMID: 21573387.

Pajaree Sriuttha, Buntitabhon Sirichanchuen, Unchalee Permsuwan, "Hepatotoxicity of Nonsteroidal Anti-Inflammatory Drugs: A Systematic Review of Randomized Controlled Trials", International Journal of Hepatology, vol. 2018, Article ID 5253623, 13 pages, 2018. https://doi.org/10.1155/2018/5253623 Peloquin CA. Therapeutic drug monitoring in the treatment of tuberculosis. Drugs. 2002;62(15):2169-83. doi: 10.2165/00003495-200262150-00001. PMID: 12381217.

Palanca A, Casafont I, Berciano MT, Lafarga M. Proteasome inhibition induces DNA damage and reorganizes nuclear architecture and protein synthesis machinery in sensory ganglion neurons. Cell Mol Life Sci. 2014 May;71(10):1961-75. doi: 10.1007/s00018-013-1474-2. Epub 2013 Sep 24. PMID: 24061536.

Papiris SA, Triantafillidou C, Kolilekas L, Markoulaki D, Manali ED. Amiodarone: review of pulmonary effects and toxicity. Drug Saf. 2010 Jul 1;33(7):539-58. doi: 10.2165/11532320-000000000-00000. PMID: 20553056.

Park SE, Georgescu A, Huh D. Organoids-on-a-chip. Science. 2019 Jun 7;364(6444):960-965. doi: 10.1126/science.aaw7894. PMID: 31171693; PMCID: PMC7764943.

Pasqualotto A. C., Amphotericin B: The Higher the Dose, the Higher the Toxicity, Clinical Infectious Diseases, Volume 47, Issue 8, 15 October 2008, Page 1110, https://doi.org/10.1086/592117

Patel AR, Nagalli S. Valproate Toxicity. [Updated 2024 May 6]. In: StatPearls [Internet]. Treasure Island (FL): StatPearls Publishing; 2024 Jan-. Available from: https://www.ncbi.nlm.nih.gov/books/NBK560898/

Patel JM. Metabolism and pulmonary toxicity of cyclophosphamide. Pharmacol Ther. 1990;47(1):137-46. doi: 10.1016/0163-7258(90)90049-8. PMID: 2195554.

Patel V, Sanyal AJ. Drug-induced steatohepatitis. Clin Liver Dis. 2013 Nov;17(4):533-46, vii. doi: 10.1016/j.cld.2013.07.012. Epub 2013 Sep 4. PMID: 24099016; PMCID: PMC4888072.

Pauli-Magnus C, Meier PJ. Hepatocellular transporters and cholestasis. J Clin Gastroenterol. 2005 Apr;39(4 Suppl 2):S103-10. doi: 10.1097/01.mcg.0000155550.29643.7b. PMID: 15758645.

Pearlstein RA, Vaz RJ, Kang J, Chen XL, Preobrazhenskaya M, Shchekotikhin AE, Korolev AM, Lysenkova LN, Miroshnikova OV, Hendrix J and Rampe D. (2003) Characterization of HERG potassium channel inhibition using CoMSiA 3D QSAR and homology modeling approaches., Bioorganic and Medicinal Chemistry Letters, 13 , 1829-1835 DOI: 10.1016/S0960-894X(03)00196-3

Pedregosa, F., Varoquaux, G., Gramfort, A., Michel, V., Weiss, R., Dubourg, V., et al. (2011). Scikit-learn: machine learning in python. J. Mach. Learn. Res.12, 2825–2830. Available online at: http://scikitlearn.org/stable/about.html#citing-scikit-learn

Pelli N, Setti M, Ceppa P, Toncini C and Indiveri F. (2003) Autoimmune hepatitis revealed by atorvastatin., European Journal of Gastroenterology and Hepatology, 15 , 921-924

Penner, N.; Woodward, C.; Prakash, C. Drug Metabolizing Enzymes and Biotransformation Reactions. In ADME-Enabling Technologies in Drug Design and Development; Surapaneni, D.Z.a.S., Ed.; John Wiley & Sons, Inc.: New York, NY, USA, 2012; pp. 545–565

Pérez-López AM, Soria-Gila ML, Marsden ER, Lilienkampf A, Bradley M. Fluorogenic Substrates for In Situ Monitoring of Caspase-3 Activity in Live Cells. PLoS One. 2016 May 11;11(5):e0153209. doi: 10.1371/journal.pone.0153209. PMID: 27168077; PMCID: PMC4864350.

Perger L, Kohler M, Fattinger K, Flury R, Meier PJ and Pauli-Magnus C. (2003) Fatal liver failure with atorvastatin., Journal of Hepatology, 39 , 1096-1097 DOI: 10.1016/S0168-8278(03)00464-1

Perry SW, Norman JP, Barbieri J, Brown EB, Gelbard HA. Mitochondrial membrane potential probes and the proton gradient: a practical usage guide. Biotechniques. 2011 Feb;50(2):98-115. doi: 10.2144/000113610. PMID: 21486251; PMCID: PMC3115691.

Pessayre D, Mansouri A, Berson A, Fromenty B. Mitochondrial involvement in drug-induced liver injury. Handb Exp Pharmacol. 2010;(196):311-65. doi: 10.1007/978-3-642-00663-0_11. PMID: 20020267.

Peterman SM, Duczak N Jr, Kalgutkar AS, Lame ME, Soglia JR. Application of a linear ion trap/orbitrap mass spectrometer in metabolite characterization studies: examination of the human liver microsomal metabolism of the non-tricyclic anti-depressant nefazodone using data-dependent accurate mass measurements. J Am Soc Mass Spectrom. 2006 Mar;17(3):363-75. doi: 10.1016/j.jasms.2005.11.014. Epub 2006 Jan 25. PMID: 16442304.

Petinari L, Kohn LK, de Carvalho JE, Genari SC. Cytotoxicity of tamoxifen in normal and tumoral cell lines and its ability to induce cellular transformation in vitro. Cell Biol Int. 2004;28(7):531-9. doi: 10.1016/j.cellbi.2004.04.008. PMID: 15261161.

Piccinini, F., Tesei, A., Arienti, C. et al. Cell Counting and Viability Assessment of 2D and 3D Cell Cultures: Expected Reliability of the Trypan Blue Assay. Biol Proced Online 19, 8 (2017). https://doi.org/10.1186/s12575-017-0056-3

Pike M, Saltiel E. Colistin- and polymyxin-induced nephrotoxicity: focus on literature utilizing the RIFLE classification scheme of acute kidney injury. J Pharm Pract. 2014 Dec;27(6):554-61. doi: 10.1177/0897190014546116. Epub 2014 Sep 18. PMID: 25237156.

Pinerua RF, Hartnett BJ. Acute pulmonary reaction to nitrofurantoin. Thorax. 1974 Sep;29(5):599-602. doi: 10.1136/thx.29.5.599. PMID: 4428461; PMCID: PMC470207.

Pinevich, A.A., Bode, I.I., Vartanyan, N.L. et al. Temozolomide-Resistant Human T2 and T98G Glioblastoma Cells. Cell Tiss. Biol. 16, 339–351 (2022). https://doi.org/10.1134/S1990519X22040058

Pinto B, Henriques AC, Silva PMA, Bousbaa H. Three-Dimensional Spheroids as In Vitro Preclinical Models for Cancer Research. Pharmaceutics. 2020 Dec 6;12(12):1186. doi: 10.3390/pharmaceutics12121186. PMID: 33291351; PMCID: PMC7762220.

Pognan F, Beilmann M, Boonen HCM, Czich A, Dear G, Hewitt P, Mow T, Oinonen T, Roth A, Steger-Hartmann T, Valentin JP, Van Goethem F, Weaver RJ, Newham P. The evolving role of investigative toxicology in the pharmaceutical industry. Nat Rev Drug Discov. 2023 Apr;22(4):317-335. doi: 10.1038/s41573-022-00633-x. Epub 2023 Feb 13. PMID: 36781957; PMCID: PMC9924869.

Polderman JAW, Farhang-Razi V, van Dieren S, Kranke P, DeVries JH, Hollmann MW, Preckel B, Hermanides J. Adverse side-effects of dexamethasone in surgical patients - an abridged Cochrane systematic review. Anaesthesia. 2019 Jul;74(7):929-939. doi: 10.1111/anae.14610. Epub 2019 Mar 1. PMID: 30821852.

Poluektova L, Krzystyniak K, Desjardins R, Flipo D, Fournier M. In vitro lymphotoxicity and selective T cell immunotoxicity of high doses of acyclovir and its derivatives in mice. Int J Immunopharmacol. 1996 Jun-Jul;18(6-7):429-38. doi: 10.1016/s0192-0561(96)00017-3. PMID: 9024946.

Ponsoda X, Bort R, Jover R, Gómez-Lechón MJ, Castell JV. Molecular mechanism of diclofenac hepatotoxicity: Association of cell injury with oxidative metabolism and decrease in ATP levels. Toxicol In Vitro. 1995 Aug;9(4):439-44. doi: 10.1016/0887-2333(95)00035-7. PMID: 20650110.

Pramod Gaudel, Jordan Snyder, Abdulraheem Yacoub; Unusual Case of Hepatic Sinusoidal Obstruction Syndrome Induced By Low Dose Oral Cyclophosphamide. Blood 2020; 136 (Supplement 1): 37. doi: https://doi.org/10.1182/blood-2020-141516

Pugazhendhi A, Edison TNJI, Velmurugan BK, Jacob JA, Karuppusamy I. Toxicity of Doxorubicin (Dox) to different experimental organ systems. Life Sci. 2018 May 1;200:26-30. doi: 10.1016/j.lfs.2018.03.023. Epub 2018 Mar 10. PMID: 29534993.

Pye M, Northcote RJ, Cobbe SM. Acute hepatitis after parenteral amiodarone administration. Br Heart J. 1988 Jun;59(6):690-1. doi: 10.1136/hrt.59.6.690. PMID: 3395527; PMCID: PMC1276877.

Quigley EM. Cisapride: what can we learn from the rise and fall of a prokinetic? J Dig Dis. 2011 Jun;12(3):147-56. doi: 10.1111/j.1751-2980.2011.00491.x. PMID: 21615867.

Radke JB, Algren DA, Chenoweth JA, Owen KP, Ford JB, Albertson TE, Sutter ME. Transaminase and Creatine Kinase Ratios for Differentiating Delayed Acetaminophen Overdose from Rhabdomyolysis. West J Emerg Med. 2018 Jul;19(4):731-736.

Rahimi L, Rajpal A, Ismail-Beigi F. Glucocorticoid-Induced Fatty Liver Disease. Diabetes Metab Syndr Obes. 2020 Apr 16;13:1133-1145. doi: 10.2147/DMSO.S247379. PMID: 32368109; PMCID: PMC7171875.

Rahman M, Awosika AO, Nguyen H. Valproic Acid. [Updated 2023 Aug 17]. In: StatPearls [Internet]. Treasure Island (FL): StatPearls Publishing; 2024 Jan-. Available from: https://www.ncbi.nlm.nih.gov/books/NBK559112/

Ramachandran A, Jaeschke H. Acetaminophen Hepatotoxicity. Semin Liver Dis. 2019 May;39(2):221-234. doi: 10.1055/s-0039-1679919. Epub 2019 Mar 8. PMID: 30849782; PMCID: PMC6800176.

Ramachandran A, Jaeschke H. Mechanisms of acetaminophen hepatotoxicity and their translation to the human pathophysiology. J Clin Transl Res. 2017 Feb;3(Suppl 1):157-169. doi: 10.18053/jctres.03.2017S1.002. Epub 2017 Feb 12. PMID: 28670625; PMCID: PMC5489132.

Ramachandran A, Visschers RGJ, Duan L, Akakpo JY, Jaeschke H. Mitochondrial dysfunction as a mechanism of drug-induced hepatotoxicity: current understanding and future perspectives. J Clin Transl Res. 2018 May 28;4(1):75-100. doi: 10.18053/jctres.04.201801.005. PMID: 30873497; PMCID: PMC6261533.

Rampe D, Murawsky MK, Grau J and Lewis EW. (1998) The antipsychotic agent sertindole is a high affinity antagonist of the human cardiac potassium channel HERG., Journal of Pharmacology and Experimental Therapeutics, 286 , 788-793

Refaeian A, Vest EL, Schmidt M, Guerra JD, Refaei MN, Refaeian M, Floresca RA, Refaeian M. Ciprofloxacin-Induced Peripheral Neuropathy: A Case Report. HCA Healthc J Med. 2023 Oct 30;4(5):383-387. doi: 10.36518/2689-0216.1400. PMID: 37969850; PMCID: PMC10635701.

Regan SL, Maggs JL, Hammond TG, Lambert C, Williams DP, Park BK. Acyl glucuronides: the good, the bad and the ugly. Biopharm Drug Dispos. 2010 Oct;31(7):367-95. doi: 10.1002/bdd.720. PMID: 20830700.

Reinert, T., Baldotto, C. S. da R., Nunes, F. A. P., & Scheliga, A. A. de S. (2013). Bleomycin-Induced Lung Injury. Journal of Cancer Research, 2013, 1–9. doi:10.1155/2013/480608

Reuben A, Koch DG, Lee WM; Acute Liver Failure Study Group. Drug-induced acute liver failure: results of a U.S. multicenter, prospective study. Hepatology. 2010 Dec;52(6):2065-76. doi: 10.1002/hep.23937. Epub 2010 Oct 14. PMID: 20949552; PMCID: PMC3992250.

Richard AM, Gold LS, Nicklaus MC. Chemical structure indexing of toxicity data on the internet: moving toward a flat world. Curr Opin Drug Discov Devel. 2006 May;9(3):314-25. PMID: 16729727.

Richardson PG, Hideshima T, Anderson KC. Bortezomib (PS-341): a novel, first-in-class proteasome inhibitor for the treatment of multiple myeloma and other cancers. Cancer Control. 2003 Sep-Oct;10(5):361-9. doi: 10.1177/107327480301000502. PMID: 14581890.

Richter M, Piwocka O, Musielak M, Piotrowski I, Suchorska WM, Trzeciak T. From Donor to the Lab: A Fascinating Journey of Primary Cell Lines. Front Cell Dev Biol. 2021 Jul 22;9:711381. doi: 10.3389/fcell.2021.711381. PMID: 34395440; PMCID: PMC8356673.

Riesbeck K, Forsgren A, Henriksson A, Bredberg A. Ciprofloxacin induces an immunomodulatory stress response in human T lymphocytes. Antimicrob Agents Chemother. 1998 Aug;42(8):1923-30. doi: 10.1128/AAC.42.8.1923. PMID: 9687385; PMCID: PMC105711.

Riss TL, Moravec RA, Niles AL, et al. Cell Viability Assays. 2013 May 1 [Updated 2016 Jul 1]. In: Markossian S, Grossman A, Arkin M, et al., editors. Assay Guidance Manual [Internet]. Bethesda (MD): Eli Lilly & Company and the National Center for Advancing Translational Sciences; 2004-. Available from: https://www.ncbi.nlm.nih.gov/books/NBK144065/

Ritter JK. (2000) Roles of glucuronidation and UDP-glucuronosyltransferases in xenobiotic bioactivation reactions., Chemico-Biological Interactions, 129 , 171-193 DOI: 10.1016/S0009-2797(00)00198-8

Rittié, L. (2017). Method for Picrosirius Red-Polarization Detection of Collagen Fibers in Tissue Sections. In: Rittié, L. (eds) Fibrosis. Methods in Molecular Biology, vol 1627. Humana Press, New York, NY. https://doi.org/10.1007/978-1-4939-7113-8_26

Roda A, Cappelleri G, Aldini R, Roda E, Barbara L. Quantitative aspects of the interaction of bile acids with human serum albumin. J Lipid Res. 1982 Mar;23(3):490-5. PMID: 7077161.

Rodriguez-Antona C, Donato MT, Boobis A et al (2002) Cytochrome P450 expression in human hepatocytes and hepatoma cell lines: molecular mechanisms that determine lower expression in cultured cells. Xenobiotica 32:505–520

Roehlen N, Crouchet E, Baumert TF. Liver Fibrosis: Mechanistic Concepts and Therapeutic Perspectives. Cells. 2020 Apr 3;9(4):875. doi: 10.3390/cells9040875. PMID: 32260126; PMCID: PMC7226751.

Rohner TJ Jr, Sanford EJ. Imipramine toxicity. J Urol. 1975 Sep;114(3):402-3. doi: 10.1016/s0022-5347(17)67040-x. PMID: 1142523.

Roth A D, and Lee, MY (2017). Idiosyncratic Drug-Induced Liver Injury (IDILI): Potential Mechanisms and Predictive Assays. Biomed. Res. Int. 2017, 9176937. doi:10.1155/2017/9176937

Rotzinger S, Baker GB. Human CYP3A4 and the metabolism of nefazodone and hydroxynefazodone by human liver microsomes and heterologously expressed enzymes. Eur Neuropsychopharmacol. 2002 Apr;12(2):91-100. doi: 10.1016/s0924-977x(02)00005-6. PMID: 11872324.

Ruch RJ, Bandyopadhyay S, Somani P, Klaunig JE. Evaluation of amiodarone free radical toxicity in rat hepatocytes. Toxicol Lett. 1991 Apr;56(1-2):117-26. doi: 10.1016/0378-4274(91)90097-p. PMID: 2017769.

Rupasinghe J, Jasinarachchi M. Progressive encephalopathy with cerebral oedema and infarctions associated with valproate and diazepam overdose. J Clin Neurosci. 2011 May;18(5):710-1. doi: 10.1016/j.jocn.2010.08.022. Epub 2011 Feb 23. PMID: 21349718.

Ryan MJ, Johnson G, Kirk J, Fuerstenberg SM, Zager RA, Torok-Storb B. HK-2: an immortalized proximal tubule epithelial cell line from normal adult human kidney. Kidney Int. 1994 Jan;45(1):48-57. doi: 10.1038/ki.1994.6. PMID: 8127021.

Rybak MJ. The pharmacokinetic and pharmacodynamic properties of vancomycin. Clin Infect Dis. 2006 Jan 1;42 Suppl 1:S35-9. doi: 10.1086/491712. PMID: 16323118.

Sacks, L. V., Shamsuddin, H. H., Yasinskaya, Y. I. et al. (2014). Scientific and regulatory reasons for delay and denial of FDA approval of initial applications for new drugs, 2000-2012. JAMA 311, 378-384. doi:10.1001/jama.2013.282542

Sakamuru S, Attene-Ramos MS, Xia M. Mitochondrial Membrane Potential Assay. Methods Mol Biol. 2016;1473:17-22. doi: 10.1007/978-1-4939-6346-1_2. PMID: 27518619; PMCID: PMC5375165.

Sallmann AR. The history of diclofenac. Am J Med. 1986 Apr 28;80(4B):29-33. doi: 10.1016/0002-9343(86)90076-8. PMID: 3085489.

Sangweni NF, Dludla PV, Chellan N, Mabasa L, Sharma JR, Johnson R. The Implication of Low Dose Dimethyl Sulfoxide on Mitochondrial Function and Oxidative Damage in Cultured Cardiac and Cancer Cells. Molecules. 2021 Dec 1;26(23):7305. doi: 10.3390/molecules26237305. PMID: 34885888; PMCID: PMC8658933.

Santos MLC, de Brito BB, da Silva FAF, Botelho ACDS, de Melo FF. Nephrotoxicity in cancer treatment: An overview. World J Clin Oncol. 2020 Apr 24;11(4):190-204. doi: 10.5306/wjco.v11.i4.190. PMID: 32355641; PMCID: PMC7186234.

Sara JD, Kaur J, Khodadadi R, Rehman M, Lobo R, Chakrabarti S, Herrmann J, Lerman A, Grothey A. 5-fluorouracil and cardiotoxicity: a review. Ther Adv Med Oncol. 2018 Jun 18;10:1758835918780140. doi: 10.1177/1758835918780140. PMID: 29977352; PMCID: PMC6024329.

Saraswathibhatla A, Indana D, Chaudhuri O. Cell-extracellular matrix mechanotransduction in 3D. Nat Rev Mol Cell Biol. 2023 Jul;24(7):495-516. doi: 10.1038/s41580-023-00583-1. Epub 2023 Feb 27. PMID: 36849594; PMCID: PMC10656994.

Sarkar U, Rivera-Burgos D, Large EM, Hughes DJ, Ravindra KC, Dyer RL, Ebrahimkhani MR, Wishnok JS, Griffith LG, Tannenbaum SR. Metabolite profiling and pharmacokinetic evaluation of hydrocortisone in a perfused three-dimensional human liver bioreactor. Drug Metab Dispos. 2015 Jul;43(7):1091-9. doi: 10.1124/dmd.115.063495. Epub 2015 Apr 29. PMID: 25926431; PMCID: PMC4468434.

Savitsky AP, Rusanov AL, Zherdeva VV, Gorodnicheva TV, Khrenova MG, Nemukhin AV. FLIM-FRET Imaging of Caspase-3 Activity in Live Cells Using Pair of Red Fluorescent Proteins. Theranostics. 2012;2(2):215-26. doi: 10.7150/thno.3885. Epub 2012 Feb 15. PMID: 22375160; PMCID: PMC3287422.

Schatzberg AF, Nemeroff CB (2017). The American Psychiatric Association Publishing Textbook of Psychopharmacology, Fifth Edition. American Psychiatric Pub. pp. 460–. ISBN 978-1-58562-523-9.

Scheen AJ. (2001) Hepatotoxicity with thiazolidinediones: is it a class effect?, Drug Safety, 24 , 873-888

Schirren CA, Baretton G. Nefazodone-induced acute liver failure. Am J Gastroenterol. 2000 Jun;95(6):1596-7. doi: 10.1111/j.1572-0241.2000.02110.x. PMID: 10894614.

Schmeltzer PA, Kosinski AS, Kleiner DE, Hoofnagle JH, Stolz A, Fontana RJ, Russo MW; Drug-Induced Liver Injury Network (DILIN). Liver injury from nonsteroidal anti-inflammatory drugs in the United States. Liver Int. 2016 Apr;36(4):603-9. doi: 10.1111/liv.13032. Epub 2015 Dec 15. PMID: 26601797; PMCID: PMC5035108.

Schmidt M, Sørensen HT, Pedersen L. Diclofenac use and cardiovascular risks: series of nationwide cohort studies. BMJ. 2018 Sep 4;362:k3426. doi: 10.1136/bmj.k3426. PMID: 30181258; PMCID: PMC6122252.

Schwartz MT, Calvert JF. Potential neurologic toxicity related to ciprofloxacin. DICP. 1990 Feb;24(2):138-40. doi: 10.1177/106002809002400204. PMID: 2309508.

Scully LJ, Clarke D, Barr RJ. Diclofenac induced hepatitis. 3 cases with features of autoimmune chronic active hepatitis. Dig Dis Sci. 1993 Apr;38(4):744-51. doi: 10.1007/BF01316809. PMID: 8462374.

Seirup M, Sengupta S, Swanson S, McIntosh BE, Collins M, Chu LF, Cheng Z, Gorkin DU, Duffin B, Bolin JM, Argus C, Stewart R, Thomson JA. Rapid changes in chromatin structure during dedifferentiation of primary hepatocytes in vitro. Genomics. 2022 May;114(3):110330. doi: 10.1016/j.ygeno.2022.110330. Epub 2022 Mar 9. PMID: 35278615.

Selvarani R, Mohammed S, Richardson A. Effect of rapamycin on aging and age-related diseases-past and future. Geroscience. 2021 Jun;43(3):1135-1158. doi: 10.1007/s11357-020-00274-1. Epub 2020 Oct 10. PMID: 33037985; PMCID: PMC8190242.

Seo JE, Tryndyak V, Wu Q, Dreval K, Pogribny I, Bryant M, Zhou T, Robison TW, Mei N, Guo X. Quantitative comparison of in vitro genotoxicity between metabolically competent HepaRG cells and HepG2 cells using the high-throughput highcontent CometChip assay. Arch Toxicol. 2019 May;93(5):1433-1448. doi: 10.1007/s00204-019-02406-9. Epub 2019 Feb 21. PMID: 30788552.

Service JA, Waring WS. QT Prolongation and delayed atrioventricular conduction caused by acute ingestion of trazodone. Clin Toxicol (Phila). 2008 Jan;46(1):71-3. doi: 10.1080/15563650701275322. PMID: 18167038.

Serviddio G, Bellanti F, Giudetti AM, Gnoni GV, Capitanio N, Tamborra R, Romano AD, Quinto M, Blonda M, Vendemiale G, Altomare E. Mitochondrial oxidative stress and respiratory chain dysfunction account for liver toxicity during amiodarone but not dronedarone administration. Free Radic Biol Med. 2011 Dec 15;51(12):2234-42. doi: 10.1016/j.freeradbiomed.2011.09.004. Epub 2011 Sep 17. PMID: 21971348.

Sexton KE, Barrett S, Bridgwood K, Carroll M, Dettling D, Du D, Fakhoury S, Fedij V, Hu LY, Kostlan C, Pocalyko D, Raheja N, Smith Y, Shanmugasundaram V and Wade K. (2011) Pantolactams as androgen receptor antagonists for the topical suppression of sebum production., Bioorganic and Medicinal Chemistry Letters, 21 , 5230-5233 DOI: 10.1016/j.bmcl.2011.07.048

Sgro C, Clinard F, Ouazir K, Chanay H, Allard C, Guilleminet C, Lenoir C, Lemoine A, Hillon P. Incidence of drug-induced hepatic injuries: a French population-based study. Hepatology. 2002 Aug;36(2):451-5. doi: 10.1053/jhep.2002.34857. PMID: 12143055.

Shaffer EA. Cholestasis: the ABCs of cellular mechanisms for impaired bile secretion--transporters and genes. Can J Gastroenterol. 2002 Jun;16(6):380-9. doi: 10.1155/2002/842151. PMID: 12096302.

Shi S, Klotz U. Clinical use and pharmacological properties of selective COX-2 inhibitors. Eur J Clin Pharmacol. 2008 Mar;64(3):233-52. doi: 10.1007/s00228-007-0400-7. Epub 2007 Nov 13. PMID: 17999057.

Shiga T, Hiraide M. Cardiotoxicities of 5-Fluorouracil and Other Fluoropyrimidines. Curr Treat Options Oncol. 2020 Mar 19;21(4):27. doi: 10.1007/s11864-020-0719-1. PMID: 32266582; PMCID: PMC7138764.

Shirasaka Y, Sager JE, Lutz JD, Davis C, Isoherranen N. Inhibition of CYP2C19 and CYP3A4 by omeprazole metabolites and their contribution to drug-drug interactions. Drug Metab Dispos. 2013 Jul;41(7):1414-24. doi: 10.1124/dmd.113.051722. Epub 2013 Apr 25. PMID: 23620487; PMCID: PMC3684819.

Shulman M, Nahmias Y. Long-term culture and coculture of primary rat and human hepatocytes. Methods Mol Biol. 2013; 945:287-302. doi: 10.1007/978-1-62703-125-7_17. PMID: 23097113; PMCID: PMC3781339.

Silva AM, Barbosa IA, Seabra C, Beltrão N, Santos R, Vega-Naredo I, Oliveira PJ, Cunha-Oliveira T. Involvement of mitochondrial dysfunction in nefazodone-induced hepatotoxicity. Food Chem Toxicol. 2016 Aug;94:148-58. doi: 10.1016/j.fct.2016.06.001. Epub 2016 Jun 8. PMID: 27288927.

Simon TG, Wilechansky RM, Stoyanova S, Grossman A, Dichtel LE, Lauer GM, Miller KK, Hoshida Y, Corey KE, Loomba R, Chung RT, Chan AT. Aspirin for Metabolic Dysfunction-Associated Steatotic Liver Disease Without Cirrhosis: A Randomized Clinical Trial. JAMA. 2024 Mar 19;331(11):920-929. doi: 10.1001/jama.2024.1215. PMID: 38502074; PMCID: PMC10951738.

Sin A, Chin KC, Jamil MF, Kostov Y, Rao G, Shuler ML. The design and fabrication of three-chamber microscale cell culture analog devices with integrated dissolved oxygen sensors. Biotechnol Prog. 2004 Jan-Feb;20(1):338-45. doi: 10.1021/bp034077d. PMID: 14763861.

Singal PK, Iliskovic N. Doxorubicin-induced cardiomyopathy. N Engl J Med. 1998 Sep 24;339(13):900-5. doi: 10.1056/NEJM199809243391307. PMID: 9744975.

Siramshetty VB, Nickel J, Omieczynski C, Gohlke BO, Drwal MN, Preissner R. WITHDRAWN--a resource for withdrawn and discontinued drugs. Nucleic Acids Res. 2016 Jan 4;44(D1):D1080-6. doi: 10.1093/nar/gkv1192. Epub 2015 Nov 8. PMID: 26553801; PMCID: PMC4702851.

Sison-Young RL, Lauschke VM, Johann E, Alexandre E, Antherieu S, Aerts H, Gerets HHJ, Labbe G, Hoët D, Dorau M, Schofield CA, Lovatt CA, Holder JC, Stahl SH, Richert L, Kitteringham NR, Jones RP, Elmasry M, Weaver RJ, Hewitt PG, Ingelman-Sundberg M, Goldring CE, Park BK. A multicenter assessment of single-cell models aligned to standard measures of cell health for prediction of acute hepatotoxicity. Arch Toxicol. 2017 Mar;91(3):1385-1400. doi: 10.1007/s00204-016-1745-4. Epub 2016 Jun 25. PMID: 27344343; PMCID: PMC5316403.

Śliwa-Tytko P, Kaczmarska A, Lejman M, Zawitkowska J. Neurotoxicity Associated with Treatment of Acute Lymphoblastic Leukemia Chemotherapy and Immunotherapy. Int J Mol Sci. 2022 May 15;23(10):5515. doi: 10.3390/ijms23105515. PMID: 35628334; PMCID: PMC9146746.

Small RE. Diclofenac sodium. Clin Pharm. 1989 Aug;8(8):545-58. PMID: 2670397.

Smith MT. Mechanisms of troglitazone hepatotoxicity. Chem Res Toxicol. 2003 Jun;16(6):679-87. doi: 10.1021/tx034033e. PMID: 12807350.

Smith SJ. Cardiovascular toxicity of antihistamines. Otolaryngol Head Neck Surg. 1994 Sep;111(3 Pt 2):348-54. doi: 10.1177/01945998941113p203. PMID: 7916150.

Snider KL, Maitland ML. Cardiovascular toxicities: clues to optimal administration of vascular endothelial growth factor signaling pathway inhibitors. Target Oncol. 2009 Apr;4(2):67-76. doi: 10.1007/s11523-009-0106-0. Epub 2009 Apr 17. PMID: 19373440; PMCID: PMC3193279.

Soe KK, Lee MY. Arrhythmias in Severe Trazodone Overdose. Am J Case Rep. 2019 Dec 27;20:1949-1955. doi: 10.12659/AJCR.919833. PMID: 31879415; PMCID: PMC6956837.

Sorrentino, M.F., Kim, J., Foderaro, A.E., Truesdell, A.G., 2012. 5-Fluorouracil induced cardiotoxicity: review of the literature. Cardiol. J. 19, 453–458

Spaniol M, Bracher R, Ha HR, Follath F and Krahenbuhl S. (2001) Toxicity of amiodarone and amiodarone analogues on isolated rat liver mitochondria., Journal of Hepatology, 35 , 628-636 DOI: 10.1016/S0168-8278(01)00189-1

Spence JR, Mayhew CN, Rankin SA, Kuhar MF, Vallance JE, Tolle K, Hoskins EE, Kalinichenko VV, Wells SI, Zorn AM, Shroyer NF, Wells JM. Directed differentiation of human pluripotent stem cells into intestinal tissue in vitro. Nature. 2011 Feb 3;470(7332):105-9. doi: 10.1038/nature09691. Epub 2010 Dec 12. PMID: 21151107; PMCID: PMC3033971.

Spigset O, Hägg S, Bate A. Hepatic injury and pancreatitis during treatment with serotonin reuptake inhibitors: data from the World Health Organization (WHO) database of adverse drug reactions. Int Clin Psychopharmacol. 2003 May;18(3):157-61. doi: 10.1097/01.yic.0000066455.73432.d2. PMID: 12702895.

Sriuttha P, Sirichanchuen B, Permsuwan U. Hepatotoxicity of Nonsteroidal Anti-Inflammatory Drugs: A Systematic Review of Randomized Controlled Trials. Int J Hepatol. 2018 Jan 15;2018:5253623. doi: 10.1155/2018/5253623. PMID: 29568654; PMCID: PMC5820561.

Stein GH. T98G: an anchorage-independent human tumor cell line that exhibits stationary phase G1 arrest in vitro. J Cell Physiol. 1979 Apr;99(1):43-54. doi: 10.1002/jcp.1040990107. PMID: 222778.

Steiner S, Gatlin CL, Lennon JJ, McGrath AM, Seonarain MD, Makusky Aponte AM, Esquer-Blasco R and Anderson NL. (2001) Cholesterol biosynthesis regulation and protein changes in rat liver following treatment with fluvastatin., Toxicology Letters, 120 , 369-377 DOI: 10.1016/S0378-4274(01)00268-5

Stellavato, A., Pirozzi, A.V.A., de Novellis, F. et al. In vitro assessment of nutraceutical compounds and novel nutraceutical formulations in a liver-steatosis-based model. Lipids Health Dis 17, 24 (2018).

Stéphenne X, Sokal E, Najimi M (2010) Hepatocyte cryopreservation: is it time to change the strategy? World J Gastroenterol 16(1):1–14

Štěrbová K, Rychlá N, Matoušková P, Skálová L, Raisová Stuchlíková L. Short-chain dehydrogenases in Haemonchus contortus: changes during life cycle and in relation to drug-resistance. Vet Res. 2023 Mar 7;54(1):19. doi: 10.1186/s13567-023-01148-y. PMID: 36882840; PMCID: PMC9993613.

Stevens JL, Baker TK. The future of drug safety testing: expanding the view and narrowing the focus. Drug Discov Today. 2009 Feb;14(3-4):162-7. doi: 10.1016/j.drudis.2008.11.009. Epub 2009 Jan 3. PMID: 19100337.

Stewart DE. Hepatic adverse reactions associated with nefazodone. Can J Psychiatry. 2002 May;47(4):375-7. doi: 10.1177/070674370204700409. PMID: 12025437.

Stone, J., DeAngelis, L. Cancer-treatment-induced neurotoxicity—focus on newer treatments. Nat Rev Clin Oncol 13, 92–105 (2016). https://doi.org/10.1038/nrclinonc.2015.152

Stratton A, Fenderson J, Kenny P, Helman DL. Severe acute hepatitis following intravenous amiodarone : a case report and review of the literature. Acta Gastroenterol Belg. 2015 Jun;78(2):233-9. PMID: 26151694.

Stravitz RT, Lee WM. Acute liver failure. Lancet. 2019 Sep 7;394(10201):869-881. doi: 10.1016/S0140-6736(19)31894-X. PMID: 31498101; PMCID: PMC10836844.

Sudo RT, Melo PA, Suarez-Kurtz G. Pharmacokinetics of oral ciprofloxacin in healthy, young Brazilian subjects. Braz J Med Biol Res. 1990;23(12):1315-21. PMID: 2136565.

Sugahara G, Ishida Y, Lee JJ, Li M, Tanaka Y, Eoh H, Higuchi Y, Saito T. Long-term cell fate and functional maintenance of human hepatocyte through stepwise culture configuration. FASEB J. 2023 Feb;37(2):e22750. doi: 10.1096/fj.202201292RR. PMID: 36607308; PMCID: PMC9830592.

Suh JI. Drug-induced liver injury. Yeungnam Univ J Med. 2020 Jan;37(1):2-12. doi: 10.12701/yujm.2019.00297. Epub 2019 Aug 27. PMID: 31661757; PMCID: PMC6986960.

Suliman AM, Alamin MA, Ul Haq I. Nitrofurantoin-Induced Lung Injury: A Reminder of an Overlooked Threat. Cureus. 2023 Sep 5;15(9):e44730. doi: 10.7759/cureus.44730. PMID: 37809109; PMCID: PMC10553377.

Sun D, Gao W, Hu H, Zhou S. Why 90% of clinical drug development fails and how to improve it? Acta Pharm Sin B. 2022 Jul;12(7):3049-3062. doi: 10.1016/j.apsb.2022.02.002. Epub 2022 Feb 11. PMID: 35865092; PMCID: PMC9293739.

Sundaram V, Björnsson ES. Drug-induced cholestasis. Hepatol Commun. 2017 Sep 11;1(8):726-735. doi: 10.1002/hep4.1088. PMID: 29404489; PMCID: PMC5678916.

Sung JH, Wang YI, Narasimhan Sriram N, Jackson M, Long C, Hickman JJ, Shuler ML. Recent Advances in Body-on-a-Chip Systems. Anal Chem. 2019 Jan 2;91(1):330-351. doi: 10.1021/acs.analchem.8b05293. Epub 2018 Dec 11. PMID: 30472828; PMCID: PMC6687466.

Suntharalingam G, Perry MR, Ward S, Brett SJ, Castello-Cortes A, Brunner MD, Panoskaltsis N. Cytokine storm in a phase 1 trial of the anti-CD28 monoclonal antibody TGN1412. N Engl J Med. 2006 Sep 7;355(10):1018-28. doi: 10.1056/NEJMoa063842. Epub 2006 Aug 14. PMID: 16908486.

Sutherland RM, Inch WR, McCredie JA, Kruuv J. A multi-component radiation survival curve using an in vitro tumour model. Int J Radiat Biol Relat Stud Phys Chem Med. 1970;18(5):491-5. doi: 10.1080/09553007014551401. PMID: 5316564.

Syed M, Skonberg C, Hansen SH. Mitochondrial toxicity of diclofenac and its metabolites via inhibition of oxidative phosphorylation (ATP synthesis) in rat liver mitochondria: Possible role in drug induced liver injury (DILI). Toxicol In Vitro. 2016 Mar;31:93-102. doi: 10.1016/j.tiv.2015.11.020. Epub 2015 Nov 25. PMID: 26627130.

Szalowska E., van der Burg B., Man H.-Y., Hendriksen P.J.M., Peijnenburg A.A.C.M. Model Steatogenic Compounds (Amiodarone, Valproic Acid, and Tetracycline) Alter Lipid Metabolism by Different Mechanisms in Mouse Liver Slices. PLoS ONE. 2014;9:e86795. doi: 10.1371/journal.pone.0086795

Tabernilla, A.; dos SantosRodrigues, B.; Pieters, A.; Caufriez, A.; Leroy, K.; Van Campenhout, R.; Cooreman, A.; Gomes, A.R.; Arnesdotter, E.; Gijbels, E.; et al. In Vitro Liver Toxicity Testing of Chemicals: A Pragmatic Approach. Int. J. Mol. Sci. 2021, 22, 5038. https://doi.org/10.3390/ijms22095038

Tacar O, Sriamornsak P, Dass CR. Doxorubicin: an update on anticancer molecular action, toxicity and novel drug delivery systems. J Pharm Pharmacol. 2013 Feb;65(2):157-70. doi: 10.1111/j.2042-7158.2012.01567.x. Epub 2012 Aug 2. PMID: 23278683.

Taglialatela M, Pannaccione A, Castaldo P, Giorgio G and Annunziato L. (2000) Inhibition of HERG1 K+ channels by the novel second-generation antihistamine mizolastine., British Journal of Pharmacology, 131 , 1081-1088 DOI: 10.1038/sj.bjp.0703654

Takasato M, Er PX, Chiu HS, Maier B, Baillie GJ, Ferguson C, Parton RG, Wolvetang EJ, Roost MS, Chuva de Sousa Lopes SM, Little MH. Kidney organoids from human iPS cells contain multiple lineages and model human nephrogenesis. Nature. 2015 Oct 22;526(7574):564-8. doi: 10.1038/nature15695. Epub 2015 Oct 7. Erratum in: Nature. 2016 Aug 11;536(7615):238. PMID: 26444236.

Takatsu H, Tanaka G, Segawa K, Suzuki J, Nagata S, Nakayama K, Shin HW. Phospholipid flippase activities and substrate specificities of human type IV P-type ATPases localized to the plasma membrane. J Biol Chem. 2014 Nov 28;289(48):33543-56. doi: 10.1074/jbc.M114.593012. Epub 2014 Oct 14. Erratum in: J Biol Chem. 2016 Oct 7;291(41):21421. PMID: 25315773; PMCID: PMC4246107.

Takebe T, Imai R, Ono S. The Current Status of Drug Discovery and Development as Originated in United States Academia: The Influence of Industrial and Academic Collaboration on Drug Discovery and Development. Clin Transl Sci. 2018 Nov;11(6):597-606. doi: 10.1111/cts.12577. Epub 2018 Jul 30. PMID: 29940695; PMCID: PMC6226120.

Tamasi, V., Hazai, E., Porsmyr-Palmertz, M., Ingelman-Sundberg, M., Vereczkey, L., Monostory, K., 2003. GYKI-47261, a new AMPA [2- amino-3-(3-hydroxymethylisoxazole-4-yl)propionic acid] antagonist, is a CYP2E1 inducer. Drug Metabolism and Disposition 31, 1310–1314.

Tan, C.R.C., Abdul-Majeed, S., Cael, B. et al. Clinical Pharmacokinetics and Pharmacodynamics of Bortezomib. Clin Pharmacokinet 58, 157–168 (2019). https://doi.org/10.1007/s40262-018-0679-9

Tang W, Stearns RA, Bandiera SM, Zhang Y, Raab C, Braun MP, Dean DC, Pang J, Leung KH, Doss GA, Strauss JR, Kwei GY, Rushmore TH, Chiu SH, Baillie TA. Studies on cytochrome P-450-mediated bioactivation of diclofenac in rats and in human hepatocytes: identification of glutathione conjugated metabolites. Drug Metab Dispos. 1999 Mar;27(3):365-72. PMID: 10064567.

Tang W. The metabolism of diclofenac--enzymology and toxicology perspectives. Curr Drug Metab. 2003 Aug;4(4):319-29. doi: 10.2174/1389200033489398. PMID: 12871048.

Taparra K, Liu H, Polley MY, Ristow K, Habermann TM, Ansell SM. Bleomycin use in the treatment of Hodgkin lymphoma (HL): toxicity and outcomes in the modern era. Leuk Lymphoma. 2020 Feb;61(2):298-308. doi: 10.1080/10428194.2019.1663419. Epub 2019 Sep 13. PMID: 31517559.

Taylor M, Gerriets V. Acyclovir. [Updated 2023 May 7]. In: StatPearls [Internet]. Treasure Island (FL): StatPearls Publishing; 2024 Jan-. Available from: https://www.ncbi.nlm.nih.gov/books/NBK542180/

Ten Doesschate T, Hendriks K, van Werkhoven CH, van der Hout EC, Platteel TN, Groenewegen IAM, Muller AE, Hoepelman AIM, Bonten MJM, Geerlings SE. Nitrofurantoin 100 mg versus 50 mg prophylaxis for urinary tract infections, a cohort study. Clin Microbiol Infect. 2022 Feb;28(2):248-254. doi: 10.1016/j.cmi.2021.05.048. Epub 2021 Jun 8. PMID: 34111584.

Terada H. Uncouplers of Oxidative Phosphorylation. Environ. Health Perspect. 1990;87:213–218. doi: 10.1289/ehp.9087213

Terp, D. K., & Rybak, M. J. (1987). Ciprofloxacin. Drug Intelligence & Clinical Pharmacy, 21(7-8), 568–574. doi:10.1177/1060028087021007-801

Thörn HA, Lundahl A, Schrickx JA, Dickinson PA, Lennernäs H. Drug metabolism of CYP3A4, CYP2C9 and CYP2D6 substrates in pigs and humans. Eur J Pharm Sci. 2011 Jun 14;43(3):89-98. doi: 10.1016/j.ejps.2011.03.008. Epub 2011 Apr 5. PMID: 21447389.

Toepke MW, Beebe DJ. PDMS absorption of small molecules and consequences in microfluidic applications. Lab Chip. 2006 Dec;6(12):1484-6. doi: 10.1039/b612140c. Epub 2006 Oct 4. PMID: 17203151.

Tolman KG. (2000) Defining patient risks from expanded preventive therapies., American Journal of Cardiology, 85 , 15E-19E DOI: 10.1016/S0002-9149(00)00946-2

Tragiannidis A, Gkampeta A, Vousvouki M, Vasileiou E, Groll AH. Antifungal agents and the kidney: pharmacokinetics, clinical nephrotoxicity, and interactions. Expert Opin Drug Saf. 2021 Sep;20(9):1061-1074. doi: 10.1080/14740338.2021.1922667. Epub 2021 Jun 1. PMID: 33896310.

Treyer A, Müsch A. Hepatocyte polarity. Compr Physiol. 2013 Jan;3(1):243-87. doi: 10.1002/cphy.c120009. PMID: 23720287; PMCID: PMC3697931.

Tsaryk R, Yucel N, Leonard EV, Diaz N, Bondareva O, Odenthal-Schnittler M, Arany Z, Vaquerizas JM, Schnittler H, Siekmann AF. Shear stress switches the association of endothelial enhancers from ETV/ETS to KLF transcription factor binding sites. Sci Rep. 2022 Mar 21;12(1):4795. doi: 10.1038/s41598-022-08645-8. PMID: 35314737; PMCID: PMC8938417.

Tseng YJ, Huang SY, Kuo CH, Wang CY, Wang KC, Wu CC. Safety range of free valproic acid serum concentration in adult patients. PLoS One. 2020 Sep 2;15(9):e0238201. doi: 10.1371/journal.pone.0238201. PMID: 32877431; PMCID: PMC7467252.

Tsuda, T., Tada, H., Tanaka, Y. et al. Amiodarone-induced reversible and irreversible hepatotoxicity: two case reports. J Med Case Reports 12, 95 (2018). https://doi.org/10.1186/s13256-018-1629-8

Tzimas, G. N., Dion, B., & Deschenes, M. (2003). Early onset, nefazodone-induced fulminant hepatic failure. The American Journal of Gastroenterology, 98(7), 1663–1664. doi:10.1111/j.1572-0241.2003.07562.x

Uetrecht J, Naisbitt DJ. Idiosyncratic adverse drug reactions: current concepts. Pharmacol Rev. 2013 Mar 8;65(2):779-808. doi: 10.1124/pr.113.007450. PMID: 23476052; PMCID: PMC3639727.

Uetrecht J. Idiosyncratic drug reactions: past, present, and future. Chem Res Toxicol. 2008 Jan;21(1):84-92. doi: 10.1021/tx700186p. Epub 2007 Dec 4. PMID: 18052104.

Uetrecht J. Mechanistic Studies of Idiosyncratic DILI: Clinical Implications. Front Pharmacol. 2019 Jul 26;10:837. doi: 10.3389/fphar.2019.00837. PMID: 31402866; PMCID: PMC6676790.

Unadkat JD, Collier AC, Crosby SS, Cummings D, Opheim KE, Corey L. Pharmacokinetics of oral zidovudine (azidothymidine) in patients with AIDS when administered with and without a high-fat meal. AIDS. 1990 Mar;4(3):229-32. doi: 10.1097/00002030-199003000-00008. PMID: 2350441.

Urzì O, Gasparro R, Costanzo E, De Luca A, Giavaresi G, Fontana S, Alessandro R. Three-Dimensional Cell Cultures: The Bridge between In Vitro and In Vivo Models. Int J Mol Sci. 2023 Jul 27;24(15):12046. doi: 10.3390/ijms241512046. PMID: 37569426; PMCID: PMC10419178.

US EPA, United States Environmental Protection Agency (US EPA). (2009) Chronic and cancer endpoints., United States Environmental Protection Agency Web Server

US Food and Drug Administration, Application number 020720, S12, S14. (1999)

Vale, J. A., and Proudfoot, A. T. (1995). Paracetamol (acetaminophen) poisoning. Lancet 346, 547–552. doi: 10.1016/S0140-6736(95)91385-8

Van Heeckeren WJ, Bhakta S, Ortiz J, Duerk J, Cooney MM, Dowlati A, McCrae K, Remick SC. Promise of new vascular-disrupting agents balanced with cardiac toxicity: is it time for oncologists to get to know their cardiologists? J Clin Oncol. 2006 Apr 1;24(10):1485-8. doi: 10.1200/JCO.2005.04.8801. PMID: 16574996.

van Meer PJ, Kooijman M, Gispen-de Wied CC, Moors EH, Schellekens H. The ability of animal studies to detect serious post marketing adverse events is limited. Regul Toxicol Pharmacol. 2012 Dec;64(3):345-9. doi: 10.1016/j.yrtph.2012.09.002. Epub 2012 Sep 12. PMID: 22982732.

Van Norman GA. Limitations of Animal Studies for Predicting Toxicity in Clinical Trials: Is it Time to Rethink Our Current Approach? JACC Basic Transl Sci. 2019 Nov 25;4(7):845-854. doi: 10.1016/j.jacbts.2019.10.008. PMID: 31998852; PMCID: PMC6978558.

Varbiro G, Toth A, Tapodi A, Veres B, Sumegi B, Gallyas F Jr. Concentration dependent mitochondrial effect of amiodarone. Biochem Pharmacol. 2003 Apr 1;65(7):1115-28. doi: 10.1016/s0006-2952(02)01660-x. PMID: 12663047.

Varga ZV, Ferdinandy P, Liaudet L, Pacher P. Drug-induced mitochondrial dysfunction and cardiotoxicity. Am J Physiol Heart Circ Physiol. 2015 Nov;309(9):H1453-67. doi: 10.1152/ajpheart.00554.2015. Epub 2015 Sep 18. PMID: 26386112; PMCID: PMC4666974.

Velayudham LS, Farrell GC. Drug-induced cholestasis. Expert Opin Drug Saf. 2003 May;2(3):287-304. doi: 10.1517/14740338.2.3.287. PMID: 12904107.

Vermes I, Haanen C, Steffens-Nakken H, Reutelingsperger C. A novel assay for apoptosis. Flow cytometric detection of phosphatidylserine expression on early apoptotic cells using fluorescein labelled Annexin V. J Immunol Methods. 1995 Jul 17;184(1):39-51. doi: 10.1016/0022-1759(95)00072-i. PMID: 7622868.

Vinken M, Blaauboer BJ. In vitro testing of basal cytotoxicity: Establishment of an adverse outcome pathway from chemical insult to cell death. Toxicol In Vitro. 2017 Mar;39:104-110. doi: 10.1016/j.tiv.2016.12.004. Epub 2016 Dec 7. PMID: 27939612; PMCID: PMC5608076.

Vinken M, Maes M, Oliveira AG, Vanhaecke T, Rogiers V (2014) Primary hepatocytes and their cultures in liver apoptosis research. Arch Toxicol 88:199–212

Vinken, M., Hengstler, J.G. Characterization of hepatocyte-based in vitro systems for reliable toxicity testing. Arch Toxicol 92, 2981–2986 (2018). https://doi.org/10.1007/s00204-018-2297-6. Epub 2018 Aug 23. PMID: 30141065

Viravaidya K, Sin A, Shuler ML. Development of a microscale cell culture analog to probe naphthalene toxicity. Biotechnol Prog. 2004 Jan-Feb;20(1):316-23. doi: 10.1021/bp0341996. PMID: 14763858.

Voican CS, Corruble E, Naveau S, Perlemuter G. Antidepressant-induced liver injury: a review for clinicians. Am J Psychiatry. 2014 Apr;171(4):404-15. doi: 10.1176/appi.ajp.2013.13050709. PMID: 24362450.

Von Moltke, L., Greenblatt, D., Granda, B. et al. Nefazodone, meta-chlorophenylpiperazine, and their metabolites in vitro: cytochromes mediating transformation, and P450-3A4 inhibitory actions. Psychopharmacology 145, 113–122 (1999). https://doi.org/10.1007/s002130051039

Vora S. Acute renal failure due to vancomycin toxicity in the setting of unmonitored vancomycin infusion. Proc (Bayl Univ Med Cent). 2016 Oct;29(4):412-413. doi: 10.1080/08998280.2016.11929491. PMID: 27695180; PMCID: PMC5023302.

Vorrink SU, Ullah S, Schmidt S, Nandania J, Velagapudi V, Beck O, Ingelman-Sundberg M, Lauschke VM. Endogenous and xenobiotic metabolic stability of primary human hepatocytes in long-term 3D spheroid cultures revealed by a combination of targeted and untargeted metabolomics. FASEB J. 2017 Jun;31(6):2696-2708. doi: 10.1096/fj.201601375R. Epub 2017 Mar 6. PMID: 28264975; PMCID: PMC5434660.

Vorrink SU, Zhou Y, Ingelman-Sundberg M, Lauschke VM. Prediction of Drug-Induced Hepatotoxicity Using Long-Term Stable Primary Hepatic 3D Spheroid Cultures in Chemically Defined Conditions. Toxicol Sci. 2018 Jun 1;163(2):655-665. doi: 10.1093/toxsci/kfy058. PMID: 29590495; PMCID: PMC5974779.

Vuda M, Kamath A. Drug induced mitochondrial dysfunction: Mechanisms and adverse clinical consequences. Mitochondrion. 2016 Nov;31:63-74. doi: 10.1016/j.mito.2016.10.005. Epub 2016 Oct 19. PMID: 27771494.

Walker PA, Ryder S, Lavado A, Dilworth C, Riley RJ. The evolution of strategies to minimise the risk of human drug-induced liver injury (DILI) in drug discovery and development. Arch Toxicol. 2020 Aug;94(8):2559-2585. doi: 10.1007/s00204-020-02763-w. Epub 2020 May 6. PMID: 32372214; PMCID: PMC7395068. https://doi.org/10.1007/s00204-020-02763-w

Wallace KB, Sardão VA, Oliveira PJ. Mitochondrial Determinants of Doxorubicin-Induced Cardiomyopathy. Circ Res. 2020 Mar 27;126(7):926-941. doi: 10.1161/CIRCRESAHA.119.314681. Epub 2020 Mar 26. PMID: 32213135; PMCID: PMC7121924.

Wang K, Shindoh H, Inoue T, Horii I. Advantages of in vitro cytotoxicity testing by using primary rat hepatocytes in comparison with established cell lines. J Toxicol Sci. 2002 Aug;27(3):229-37. doi: 10.2131/jts.27.229. PMID: 12238146.

Wang MWH, Goodman JM, Allen TEH. Machine Learning in Predictive Toxicology: Recent Applications and Future Directions for Classification Models. Chem Res Toxicol. 2021 Feb 15;34(2):217-239. doi: 10.1021/acs.chemrestox.0c00316. Epub 2020 Dec 23. PMID: 33356168.

Wang P, Pradhan K, Zhong XB, Ma X. Isoniazid metabolism and hepatotoxicity. Acta Pharm Sin B. 2016 Sep;6(5):384-392. doi: 10.1016/j.apsb.2016.07.014. Epub 2016 Aug 3. PMID: 27709007; PMCID: PMC5045547.

Wang, W. W., Khetani, S. R., Krzyzewski, S., Duignan, D. B., and Obach, R. S. (2010). Assessment of a micropatterned hepatocyte coculture system to generate major human excretory and circulating drug metabolites. Drug Metab. Disposition 38, 1900–1905. doi: 10.1124/dmd.110.034876

Wang, Y., Gray, J. P., Mishin, V., Heck, D. E., Laskin, D. L., & Laskin, J. D. (2008). Role of cytochrome P450 reductase in nitrofurantoin-induced redox cycling and cytotoxicity. Free Radical Biology & Medicine, 44(6), 1169–1179. https://doi.org/10.1016/j.freeradbiomed.2007. 12.013

Wanigasekara J, Carroll LJ, Cullen PJ, Tiwari B, Curtin JF. Three-Dimensional (3D) in vitro cell culture protocols to enhance glioblastoma research. PLoS One. 2023 Feb 8;18(2):e0276248. doi: 10.1371/journal.pone.0276248. PMID: 36753513; PMCID: PMC9907841.

Waring MJ, Arrowsmith J, Leach AR, Leeson PD, Mandrell S, Owen RM, Pairaudeau G, Pennie WD, Pickett SD, Wang J, Wallace O, Weir A. An analysis of the attrition of drug candidates from four major pharmaceutical companies. Nat Rev Drug Discov. 2015 Jul;14(7):475-86.

Watkins PB. Drug safety sciences and the bottleneck in drug development. Clin Pharmacol Ther. 2011 Jun;89(6):788-90. doi: 10.1038/clpt.2011.63. PMID: 21593756.

Watkins PB. Idiosyncratic liver injury: challenges and approaches. Toxicol Pathol. 2005;33(1):1-5. doi: 10.1080/01926230590888306. PMID: 15805049.

Watkins SJ, Borthwick GM, Arthur HM. The H9C2 cell line and primary neonatal cardiomyocyte cells show similar hypertrophic responses in vitro. In Vitro Cell Dev Biol Anim. 2011 Feb;47(2):125-31. doi: 10.1007/s11626-010-9368-1. Epub 2010 Nov 17. PMID: 21082279.

Wei G, Bergquist A, Broomé U, Lindgren S, Wallerstedt S, Almer S, Sangfelt P, Danielsson A, Sandberg-Gertzén H, Lööf L, Prytz H, Björnsson E. Acute liver failure in Sweden: etiology and outcome. J Intern Med. 2007 Sep;262(3):393-401. doi: 10.1111/j.1365-2796.2007.01818.x. PMID: 17697161.

Weir M, Daly GJ, Lung toxicity and Nitrofurantoin: the tip of the iceberg?, QJM: An International Journal of Medicine, Volume 106, Issue 3, March 2013, Pages 271–272, https://doi.org/10.1093/qjmed/hcs129

Wen H, Yang HJ, An YJ, Kim JM, Lee DH, Jin X, Park SW, Min KJ, Park S. Enhanced phase II detoxification contributes to beneficial effects of dietary restriction as revealed by multi-platform metabolomics studies. Mol Cell Proteomics. 2013 Mar;12(3):575-86

Westerink WM, Schoonen WG. (a) Phase II enzyme levels in HepG2 cells and cryopreserved primary human hepatocytes and their induction in HepG2 cells. Toxicol In Vitro. 2007 Dec;21(8):1592-602. doi: 10.1016/j.tiv.2007.06.017. Epub 2007 Jul 18. PMID: 17716855.

Westerink WM, Schoonen WG. (b) Cytochrome P450 enzyme levels in HepG2 cells and cryopreserved primary human hepatocytes and their induction in HepG2 cells. Toxicol In Vitro. 2007 Dec;21(8):1581-91. doi: 10.1016/j.tiv.2007.05.014. Epub 2007 Jun 8. PMID: 17637504.

Wijma RA, Huttner A, Koch BCP, Mouton JW, Muller AE. Review of the pharmacokinetic properties of nitrofurantoin and nitroxoline. J Antimicrob Chemother. 2018 Nov 1;73(11):2916-2926. doi: 10.1093/jac/dky255. PMID: 30184207.

Wilding JL, Bodmer WF. Cancer cell lines for drug discovery and development. Cancer Res. 2014 May 1;74(9):2377-84. doi: 10.1158/0008-5472.CAN-13-2971. Epub 2014 Apr 9. PMID: 24717177.

Wilkening S, Stahl F, Bader A. Comparison of primary human hepatocytes and hepatoma cell line Hepg2 with regard to their biotransformation properties. Drug Metab Dispos. 2003 Aug;31(8):1035-42. doi: 10.1124/dmd.31.8.1035. PMID: 12867492.

Williams DP, Park BK. Idiosyncratic toxicity: the role of toxicophores and bioactivation. Drug Discov Today. 2003 Nov 15;8(22):1044-50. doi: 10.1016/s1359-6446(03)02888-5. PMID: 14690635.

Williams-DeVane, C. R., Wolf, M. A., and Richard, A. M. (2009). DSSTox chemical-index files for exposure-related experiments in Array Express and Gene Expression Omnibus: enabling toxico-chemogenomics data linkages. Bioinformatics 25, 692–694. doi: 10.1093/bioinformatics/btp042

Wingard JR, Hess AD, Stuart RK, Saral R, Burns WH. Effect of several antiviral agents on human lymphocyte functions and marrow progenitor cell proliferation. Antimicrob Agents Chemother. 1983 Apr;23(4):593-7. doi: 10.1128/AAC.23.4.593. PMID: 6305264; PMCID: PMC184707.

Winter R, Montanari F, Noé F, Clevert DA. Learning continuous and data-driven molecular descriptors by translating equivalent chemical representations. Chem Sci. 2018 Nov 19;10(6):1692-1701. doi: 10.1039/c8sc04175j. PMID: 30842833; PMCID: PMC6368215.

Wolkove N, Baltzan M. Amiodarone pulmonary toxicity. Can Respir J. 2009 Mar-Apr;16(2):43-8. doi: 10.1155/2009/282540. PMID: 19399307; PMCID: PMC2687560.

Wu J, Li J, Jing W, Tian X, Wang X. Valproic acid-induced encephalopathy: A review of clinical features, risk factors, diagnosis, and treatment. Epilepsy Behav. 2021 Jul; 120:107967. doi: 10.1016/j.yebeh.2021.107967. Epub 2021 May 15. PMID: 34004407.

Wu L, Zhang W, Tian L, Bao K, Li P, Lin J. Immunomodulatory effects of erythromycin and its derivatives on human T-lymphocyte in vitro. Immunopharmacol Immunotoxicol. 2007;29(3-4):587-96. doi: 10.1080/08923970701692841. PMID: 18075867.

Wu, IJ., Tsai, JH. & Ho, CM. Fatal acute-on-chronic liver failure in amiodarone-related steatohepatitis: a case report. BMC Gastroenterol 21, 50 (2021). https://doi.org/10.1186/s12876-021-01632-9

Xiang Y, Wen H, Yu Y, Li M, Fu X, Huang S. Gut-on-chip: Recreating human intestine in vitro. J Tissue Eng. 2020 Nov 18;11:2041731420965318. doi: 10.1177/2041731420965318. PMID: 33282173; PMCID: PMC7682210.

Xu JJ, Henstock PV, Dunn MC, Smith AR, Chabot JR, de Graaf D. Cellular imaging predictions of clinical drug-induced liver injury. Toxicol Sci. 2008 Sep;105(1):97-105. doi: 10.1093/toxsci/kfn109. Epub 2008 Jun 3. PMID: 18524759.

Xue J, Wu T, Dai Y, Xia Y. Electrospinning and Electrospun Nanofibers: Methods, Materials, and Applications. Chem Rev. 2019 Apr 24;119(8):5298-5415. doi: 10.1021/acs.chemrev.8b00593. Epub 2019 Mar 27. PMID: 30916938; PMCID: PMC6589095.

Yamada, N., Komada, T., Ohno, N. *et al.* Acetaminophen-induced hepatotoxicity: different mechanisms of acetaminophen-induced ferroptosis and mitochondrial damage. *Arch Toxicol* **94**, 2255–2257 (2020). https://doi.org/10.1007/s00204-020-02722-5

Yamamoto, Y., Nakajima, M., Yamazaki, H., and Yokoi, T. (2001) Cytotoxicity and apoptosis produced by troglitazone in human hepatoma cells. Life Sci. 70, 471-482.

Yan M, Huo Y, Yin S, Hu H. Mechanisms of acetaminophen-induced liver injury and its implications for therapeutic interventions. Redox Biol. 2018 Jul;17:274-283. doi: 10.1016/j.redox.2018.04.019. Epub 2018 Apr 22. PMID: 29753208; PMCID: PMC6006912.

Yang F, Li H, Li Y, Hao Y, Wang C, Jia P, Chen X, Ma S, Xiao Z. Crosstalk between hepatic stellate cells and surrounding cells in hepatic fibrosis. Int Immunopharmacol. 2021 Oct;99:108051. doi: 10.1016/j.intimp.2021.108051. Epub 2021 Aug 18. PMID: 34426110.

Yang G, Nowsheen S, Aziz K, Georgakilas AG. Toxicity and adverse effects of Tamoxifen and other anti-estrogen drugs. Pharmacol Ther. 2013 Sep;139(3):392-404. doi: 10.1016/j.pharmthera.2013.05.005. Epub 2013 May 24. PMID: 23711794.

Yang H, Li J, Wu Z, Li W, Liu G, Tang Y. Evaluation of Different Methods for Identification of Structural Alerts Using Chemical Ames Mutagenicity Data Set as a Benchmark. Chem Res Toxicol. 2017 Jun 19;30(6):1355-1364. doi: 10.1021/acs.chemrestox.7b00083. Epub 2017 May 23. PMID: 28485959.

Yang H, Sun L, Li W, Liu G, Tang Y. In Silico Prediction of Chemical Toxicity for Drug Design Using Machine Learning Methods and Structural Alerts. Front Chem. 2018 Feb 20;6:30. doi: 10.3389/fchem.2018.00030. Erratum in: Front Chem. 2018 Apr 13;6:129. PMID: 29515993; PMCID: PMC5826228.

Yang K, Guo C, Woodhead JL, St Claire RL 3rd, Watkins PB, Siler SQ, Howell BA, Brouwer KLR. Sandwich-Cultured Hepatocytes as a Tool to Study Drug Disposition and Drug-Induced Liver Injury. J Pharm Sci. 2016 Feb;105(2):443-459. doi: 10.1016/j.xphs.2015.11.008. PMID: 26869411; PMCID: PMC4894499.

Yang K, Köck K, Sedykh A, Tropsha A, Brouwer KL. An updated review on drug-induced cholestasis: mechanisms and investigation of physicochemical properties and pharmacokinetic parameters. J Pharm Sci. 2013 Sep;102(9):3037-57. doi: 10.1002/jps.23584. Epub 2013 May 7. PMID: 23653385; PMCID: PMC4369767.

Yang K, Köck K, Sedykh A, Tropsha A, Brouwer KL. An updated review on drug-induced cholestasis: mechanisms and investigation of physicochemical properties and pharmacokinetic parameters. J Pharm Sci. 2013 Sep;102(9):3037-57. doi: 10.1002/jps.23584. Epub 2013 May 7. PMID: 23653385; PMCID: PMC4369767.

Yang L, Zhang XC, Yu SF, Zhu HQ, Hu AP, Chen J, Shen P. Pharmacokinetics and safety of cyclophosphamide and docetaxel in a hemodialysis patient with early stage breast cancer: a case report. BMC Cancer. 2015 Nov 18;15:917. doi: 10.1186/s12885-015-1932-3. PMID: 26582454; PMCID: PMC4652348.

Ye H, Nelson LJ, Gómez Del Moral M, Martínez-Naves E, Cubero FJ. Dissecting the molecular pathophysiology of drug-induced liver injury. World J Gastroenterol. 2018 Apr 7;24(13):1373-1385. doi: 10.3748/wjg.v24.i13.1373. PMID: 29632419; PMCID: PMC5889818.

Yen CL, Stone SJ, Koliwad S, Harris C, Farese RV Jr. Thematic review series: glycerolipids. DGAT enzymes and triacylglycerol biosynthesis. J Lipid Res. 2008 Nov;49(11):2283-301.

Yokoi, T. (2010). Troglitazone. In: Uetrecht, J. (eds) Adverse Drug Reactions. Handbook of Experimental Pharmacology, vol 196. Springer, Berlin, Heidelberg. https://doi.org/10.1007/978-3-642-00663-0_14

Yokoyama Y, Sasaki Y, Terasaki N, Kawataki T, Takekawa K, Iwase Y, Shimizu T, Sanoh S, Ohta S. Comparison of Drug Metabolism and Its Related Hepatotoxic Effects in HepaRG, Cryopreserved Human Hepatocytes, and HepG2 Cell Cultures. Biol Pharm Bull. 2018 May 1;41(5):722-732. doi: 10.1248/bpb.b17-00913. Epub 2018 Feb 14. PMID: 29445054.

Yokoyama Y, Sasaki Y, Terasaki N, Kawataki T, Takekawa K, Iwase Y, Shimizu T, Sanoh S, Ohta S. Comparison of Drug Metabolism and Its Related Hepatotoxic Effects in HepaRG, Cryopreserved Human Hepatocytes, and HepG2 Cell Cultures. Biol Pharm Bull. 2018 May 1;41(5):722-732. doi: 10.1248/bpb.b17-00913. Epub 2018 Feb 14. PMID: 29445054.

Yoon E, Babar A, Choudhary M, Kutner M, Pyrsopoulos N. Acetaminophen-Induced Hepatotoxicity: a Comprehensive Update. J Clin Transl Hepatol. 2016 Jun 28;4(2):131-42. doi: 10.14218/JCTH.2015.00052. Epub 2016 Jun 15. PMID: 27350943; PMCID: PMC4913076.

Yorulmaz A, Sahin EB, Sener M, Kulcu Cakmak S. Acyclovir-induced bullous reaction in a patient with metastatic breast cancer. Cutan Ocul Toxicol. 2017 Mar;36(1):85-87. doi: 10.3109/15569527.2016.1140180. Epub 2016 Feb 24. PMID: 26911608.

Yun JS, Kim SY. Antihistamines modulate the integrin signaling pathway in h9c2 rat cardiomyocytes: Possible association with cardiotoxicity. Hum Exp Toxicol. 2015 Aug;34(8):796-807. doi: 10.1177/0960327114559988. Epub 2014 Nov 25. PMID: 25425550.

Zabidi MS, Abu Bakar R, Musa N, Mustafa S, Wan Yusuf WN. Population Pharmacokinetics of Colistin Methanesulfonate Sodium and Colistin in Critically Ill Patients: A Systematic Review. Pharmaceuticals (Basel). 2021 Sep 6;14(9):903. doi: 10.3390/ph14090903. PMID: 34577603; PMCID: PMC8472798.

Zhang Q, Fan X, Ye R, Hu Y, Zheng T, Shi R, Cheng W, Lv X, Chen L, Liang P. The Effect of Simvastatin on Gut Microbiota and Lipid Metabolism in Hyperlipidemic Rats Induced by a High-Fat Diet. Front Pharmacol. 2020 Apr 29;11:522. doi: 10.3389/fphar.2020.00522. PMID: 32410994; PMCID: PMC7201051.

Zhang RH, Guo HY, Deng H, Li J, Quan ZS. Piperazine skeleton in the structural modification of natural products: a review. J Enzyme Inhib Med Chem. 2021 Dec;36(1):1165-1197. doi: 10.1080/14756366.2021.1931861. PMID: 34080510; PMCID: PMC8183565.

Zhang YS, Arneri A, Bersini S, Shin SR, Zhu K, Goli-Malekabadi Z, Aleman J, Colosi C, Busignani F, Dell'Erba V, Bishop C, Shupe T, Demarchi D, Moretti M, Rasponi M, Dokmeci MR, Atala A, Khademhosseini A. Bioprinting 3D microfibrous scaffolds for engineering endothelialized myocardium and heart-on-a-chip. Biomaterials. 2016 Dec;110:45-59. doi: 10.1016/j.biomaterials.2016.09.003. Epub 2016 Sep 5. PMID: 27710832; PMCID: PMC5198581.

Zheng, J., Yuan, Q., Zhou, C. *et al.* Mitochondrial stress response in drug-induced liver injury. *Mol Biol Rep* **48**, 6949–6958 (2021). https://doi.org/10.1007/s11033-021-06674-6

Zhou Z, Vorperian VR, Gong Q, Zhang S and January CT. (1999) Block of HERG potassium channels by the antihistamine astemizole and its metabolites desmethylastemizole and norastemizole., Journal of Cardiovascular Electrophysiology, 10 , 836-843 DOI: 10.1111/j.1540-8167.1999.tb00264.x

Ziegerer C, Wuttke A, Marsico G, Seifert S, Kalaidzidis Y, Zerial M (2016) Functional properties of hepatocytes in vitro are correlated with cell polarity maintenance. Exp Cell Res 350:242–252

Zimmerman HJ. (1999) Hepatotoxicity: The Adverse Effects of Drugs and other Chemicals on the Liver., Hepatotoxicity: The Adverse Effects of Drugs and other Chemicals on the Liver

Zoio P, Oliva A. Skin-on-a-Chip Technology: Microengineering Physiologically Relevant In Vitro Skin Models. Pharmaceutics. 2022 Mar 21;14(3):682. doi: 10.3390/pharmaceutics14030682. PMID: 35336056; PMCID: PMC8955316.

Zollner G, Trauner M. Mechanisms of cholestasis. Clin Liver Dis. 2008 Feb;12(1):1-26, vii. doi: 10.1016/j.cld.2007.11.010 PMID: 18242495.

AKNOWLEDGEMENTS

I would like to acknowledge INNOTARGETS project for the financial support and extend my gratitude to all the members of this Consortium, including the supervisors for the scientific guidance as well Peter and Karin for taking care of the administrative and organizational efforts. Their collective support has contributed significantly to my growth, not only as a future scientist but also as a person, thanks to the constructive relationships established during our meetings. It has been an honour to be part of a such prestigious and outstanding scientific programme.

I express my heartfelt gratitude to my supervisor, Dr. Domingo Gargallo, for giving me the opportunity to be part of this project at ABAC Therapeutics and for his invaluable guidance throughout this journey.

An immense thank goes to Dr. Toni Torrens, for supervising a particular section of this work, providing outstanding feedbacks, sharing knowledge and offering precious advises, not only related to our work but also about enjoying the beautiful city of Barcelona.

Working at ABAC Therapeutics has been an amazing experience, thanks to my colleagues Paco, Catalina, Soraya, Monica, and Sonia, with whom I shared my everyday life at work, making these three years a pleasant journey.

I also extend my gratitude to Prof. Oliver Ebenhöh for supervising me during my secondment at the QTB of the Heinrich Heine University of Dusseldörf. Thank you for all your teachings; it was a highly instructive period where I acquired knowledge in a scientific field that was entirely new to me.

Thanks to IRTA CReSA for hosting me during my other secondment, particularly to my supervisor there, Virginia Aragon.

A heartfelt thank you to my fantastic colleagues, the Early Stage Researchers of INNOTARGETS—Jennifer, Nader, Sally, Gaia, Lawrence, Hettie, Dina, Pareena, Sandra, Maria, Ayelen, and Christelle—for their support, help, chats, and for sharing dreams, laughter, pressure, and challenges. They made these last three years much more enjoyable and kept me sane and smiling throughout the entire process. I wish all of them the best in their scientific careers and personal lives.

Lastly, I express my deepest gratitude to my fiancé Leonardo, for his invaluable support and for standing by my side, accepting both the good and the bad in me every day.

A huge thank you to my mother, Paolo, my brothers Antonio and Anna, and all my family who have always been my solid foundation upon which I have built my life day by day.

I dedicate the entire work and these three years of experience to my dear dad, who could not personally support me but has always been with me in spirit.

This project has received funding from the European Union's Horizon 2020 research and innovation programme under the Marie Skłodowska-Curie grant agreement No 956154.

INNOTARGETS